AD-A172 111 STUDY OF HELICOPTER ROLL CONTROL EFFECTIVENESS CRITERIA 1/3
(U) MANUDYNE SYSTEMS INC LOS ALTOS CA
R K HEFFLEY ET AL. APR 86 MANUDYNE-83-1
UNCLASSIFIED USAAVSCOM-TR-85-A-5 NAS2-11665 F/G 1/2 NL

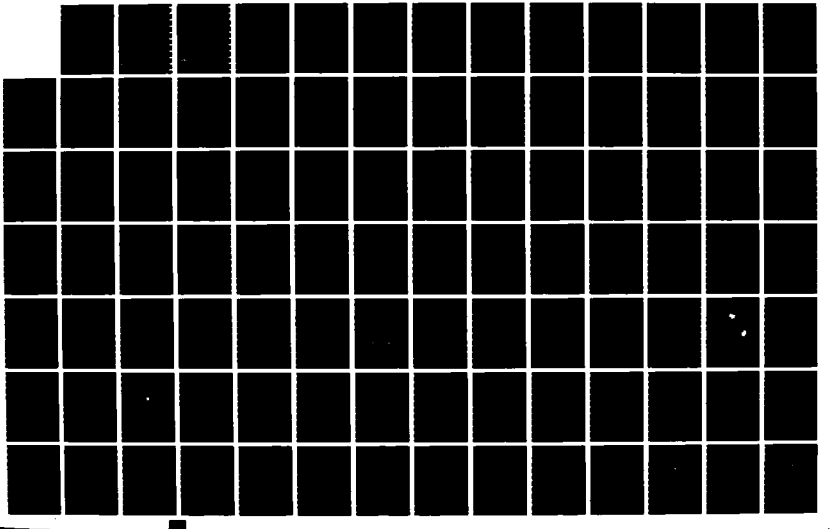

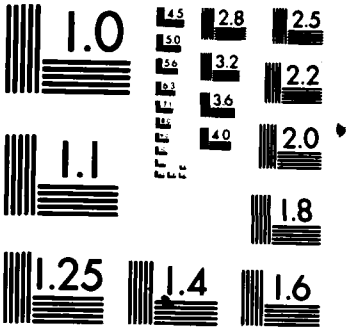

MICROCOPY RESOLUTION TEST CHART
NATIONAL BUREAU OF STANDARDS-1963-A

NASA CONTRACTOR REPORT 177404

USAAVSCOM TR 85-A-5

AD-A172 111

STUDY OF HELICOPTER ROLL CONTROL EFFECTIVENESS CRITERIA

Robert K. Heffley
Simon M. Bourne
Howard C. Curtiss, Jr.
William S. Hindson
Ronald A. Hess

DTIC
ELECTE
SEP 2 4 1986
S D
E

CONTRACT NAS2-11665
April 1986

NASA

US ARMY
AVIATION
SYSTEMS COMMAND
AVIATION R&T ACTIVITY

This document has been approved for public release and sale; its distribution is unlimited.

86 9 24 060

NASA CONTRACTOR REPORT 177404

USAAVSCOM TR 85-A-5

STUDY OF HELICOPTER ROLL CONTROL EFFECTIVENESS CRITERIA

Robert K. Heffley
Simon M. Bourne
Manudyne Systems, Inc.
Los Altos, California

Howard C. Curtiss, Jr.
Princeton University
Princeton, New Jersey

William S. Hindson
Stanford University
Stanford, California

Ronald A. Hess
University of California
Davis, California

QUALITY INSPECTED 1

Accession For	
NTIS GRA&I	☒
DTIC TAB	☐
Unannounced	☐
Justification	
By	
Distribution/	
Availability Codes	
Dist	Avail and/or Special
A-1	

Prepared for
Aeroflightdynamics Directorate
U.S. Army Research and Technology Activity (AVSCOM)
under Contract NAS2-11665

April 1986

National Aeronautics and Space Administration

Ames Research Center
Moffett Field, California 94035

Aeroflightdynamics Directorate
Moffett Field, California 94035

US ARMY AVIATION SYSTEMS COMMAND
AVIATION R&T ACTIVITY

This document has been approved for public release and sale; its distribution is unlimited.

Abstract

A study of helicopter roll control effectiveness based on closed-loop task performance measurement and modeling is presented. Roll Control criteria are based upon task margin, the excess of vehicle task performance capability over the pilot's task performance demand. Appropriate helicopter roll axis dynamic models are defined for use with analytic models for task performance. Both near-earth and up-and-away large-amplitude maneuvering phases are considered. The results of in-flight and moving-base simulation measurements are presented to support the roll control effectiveness criteria offered. Volume I contains the theoretical analysis, simulation results and criteria development. Volume II documents the simulation program hardware, software, protocol and data collection efforts.

This document has been approved for public release and sale; its distribution is unlimited.

Forward

This report was prepared by Manudyne Systems, Inc. for the Aeromechanics Laboratory, U. S. Army Research and Technology Laboratories (AVRADCOM) under NASA-Ames Research Center Contract NAS2-11665. Mr. Christopher L. Blanken supported the program as the contract monitor until October 1984 when Ms. Michelle M. Eshow took over the position.

Manudyne Systems, Inc., was assisted in the analysis of theoretical roll response dynamics by Professor Howard C. Curtiss. Mr. William S. Hindson aided in design of simulator flight tasks and served as simulator check-out pilot. Professor Ronald A. Hess performed analysis of several discrete maneuver flight tasks.

The following individuals provided invaluable support to the overall research program:

Evaluation Pilots: Major James Casler, U. S. Marine Corps.; CW2 James A. Elton, U. S. Army; Mr. William S. Hindson, Stanford University/NASA Ames; CW3 David Klindt, U. S. Army; Lt. Col. Patrick Morris, U.S. Army/NASA Ames; Mr. Manfred Roessing, DFVLR; CW4 Les Scott, U. S. Army; Mr. George Tucker, NASA Ames; Lt. Col. Grady Wilson, U. S. Army/NASA Ames.

Simulation Support: NASA; Mr. David L. Astill, Mr. Richard S. Bray, Mr. James A. Jeske, and Ms. Liza Tweton. U. S. Army; Mr. Mike S. Lewis. SYRE; Mr. Joseph Ogwell (Simulation Programmer), Mr. Matt Blake, Mr. Russ Sansom, and Mr. Greg Bookout.

TABLE OF CONTENTS

Section		Page
I.	Background and Introduction	1
	A. Purpose of Study	1
	1. Background	1
	2. Criteria and Specification Development	3
	3. New Approaches to Handling Qualities Research	4
	B. Views of Manufacturers and Users	5
	1. Needs of Military Users	6
	2. Concerns of Designers and Manufacturers	7
	C. Technical Approach	8
	1. Theoretical Development	9
	2. Task and Maneuver Analysis	11
	3. Experimental Simulator Investigation	12
	4. Criteria Development	13
II.	Theoretical Development	15
	A. Helicopter Roll-Axis Dynamics	15
	1. Important Considerations in Criteria Development	15
	2. Rotor-Body Models	16
	3. Primary Analysis Model	23
	4. Survey of Existing Helicopters	27
	B. Effects of the Pilot-in-the-Loop	35
	1. Inner-Loop Control and Regulation of Roll Attitude	35
	2. Outer-Loop Control of Velocity and Position	38
	C. Discrete Maneuver and Task Performance Capability Modeling	40
	1. Discrete Flight Maneuver Modeling	40
	2. Defining Maximum Task Performance Capability	49
	D. Lateral Control Effectiveness Criteria Review	52
	1. Purpose of Handling Criteria	52
	2. Summary of Roll Control Effectiveness Criteria	55
	3. Criteria Specification Philosophy	55
III.	Flight Task Analysis	61
	A. Classification and Description of Lateral Maneuvers	61
	1. Roll Attitude Regulation	61
	2. Bank-to-Turn Maneuvers	62
	3. Bank-to-Translate Maneuvers	63
	4. Ground Contact Flight Tasks	65

B. Flight Measurements 65
1. Measurement Techniques 66
2. Flight Data Obtained 66

C. Characteristics of Flight Data 92

D. Implications for Simulation Program Design 97

IV. Experimental Simulator Investigation 99

A. Simulation Objectives and Experimental Design 99
1. Objectives 99
2. Flight Tasks 101
3. Vehicle Configurations 109
4. Pilots 122
5. Environmental Conditions 122

B. Simulator Apparatus 122
1. Cockpit 122
2. Visual System 126
3. Motion System 128
4. Computer 129

C. Data Acquisition 129
1. Quantitative Data 129
2. *Qualitative Data* 132

D. Experimental Results 138
1. General 138
2. HUD Tracking Task 142
3. ACM Tasks 162
4. Sidestep Task 168
5. Turns 183
6. Slalom 189
7. Jink Maneuver 191
8. IFR Turns 195

E. Simulation Fidelity Issues 198

F. Task Performance Comparison between Simulator and Flight 202

V. Criteria Development 211

A. Task Performance Modeling 211
1. Aggressiveness Characteristics 212
2. Amplitude Characteristics 215
3. Maneuver Settling 215
4. Precision 217

B. Vehicle Capability 217

C. Pilot Centered Components 218

D. Control Effectiveness Criteria Development 219
1. Definition of Task Margin 219
2. Roll Axis Control Power 221
3. Roll Axis Short-Term Response 222
4. Roll Rate Sensitivity 229
5. Higher Augmentation System Types 231

E. Comparison With Proposed Control Power Criteria for MIL-H-8501A Update 231

F. Areas of Further Analysis 234
1. Theoretical 234
2. Experimental 238

VI. Conclusions 241

References 243

LIST OF ILLUSTRATIONS

Figure		Page
1-1	Block Diagram of Pilot-Vehicle-Task System	5
2-1	Rotor Flapping Response Modes	21
2-2	Rotor Body Coupling Effects on the Original Rotor Response Modes from Reference 34	25
2-3	Relationship Between Unaugmented Vehicle Bandwidth and Flapping Stiffness	29
2-4	Components of Flapping Stiffness for a Survey of Helicopters	34
2-5	Short-Term Eigenvalue Locations as a Function of Flapping Stiffness	37
2-6	Bank Angle Loop Closures for Various Roll Damping Values	39
2-7	A Timing Diagram for a Typical Helicopter Sidestep Maneuver	42
2-8	Analysis Technique for Discrete Roll Maneuver Data	43
2-9	Illustration of System Bandwidth Effects on the Maneuver Performance Diagram	46
2-10	Definition of "Task Signature" from Discrete Maneuver Time Histories	47
2-11	Quantification of Task Demand	48
2-12	Characteristics of Square Wave Input Response for a Second Order System	50
2-13	Typical Vehicle Capability Based Upon Square Wave Inputs	53
2-14	Comparison of Level 1 Iso-Opinion Curves of L_p vs L_{δ_A}	59
3-1	Runway Intersection and U Turns Flown at NALF Crow's Landing	68
3-2	Turn Maneuver Data	70

3-3	210 Deg. Turn Maneuver Data	73
3-4	Definition of In-Line Slalom and Sidestep Maneuvers Flown at NALF Crow's Landing	74
3-5	In-Line Slalom Maneuver Data	75
3-6	Lateral Jink Maneuver Data	77
3-7	Sidestep Maneuver Data	78
3-8	Outer-Loop Sidestep Maneuver Data	81
3-9	Definition of Tasks Used in the DFVLR Evaluations	83
3-10	"U.S. Slalom" Maneuver Data	84
3-11	"German Slalom" Maneuver Data	86
3-12	High-G Turn Maneuver Data for UH-1D and BO-105 Helicopters	88
3-13	Abstract of Scissors Maneuver from the Rotary Wing Air Combat Maneuvering Guide	89
3-14	Plan View of Flight Paths for Scissors Maneuver 23008 from the D-318 Data Base	90
3-15	Scissors Maneuver Data for a Variety of Aircraft	91
3-16	Typical X-22A Lateral Positioning Flight Data, Configuration 218F	93
3-17	X-22A Sidestep Maneuver Data	94
3-18	Corliss and Carico Maneuver Flight Data "U. S. Slalom" Results for L_p = -4.0	95
4-1	Primary Dimensions of the Experimental Matrix	101
4-2	Heading Turn Maneuver Description	103
4-3	Slalom Maneuver Descriptions	104
4-4	Jinking Maneuver Description	105
4-5	Sidestep Maneuver Description	106
4-6	HUD Tracking Task Description	107
4-7	Roll Attitude Command for the Roll Tracking Task	108

4-8	Basic Helicopter Configuration Parameters	112
4-9	Roll Mode Eigenvalue Locations for Basic Helicopter Configurations	113
4-10	Step Response for Basic Helicopter Configurations	114
4-11	Attitude-Command/Attitude-Hold Configurations	115
4-12	Lateral Response Characteristics for Attitude Configuration ATAT8	117
4-13	General Form for a Rate-Command/Attitude-Hold System	118
4-14	Response to Lateral Control Input for Rate-Command/ Attitude-Hold Configuration RAAT2	120
4-15	Saturation of Lateral Control Input for Control Power Investigations	121
4-16	NASA Ames Vertical Motion Simulator with RCAB Module	124
4-17	Cab Instrumentation	125
4-18	Effect of Cycle Time on Throughput Time Delay from Reference 49	127
4-19	Application of the Discrete Maneuver Analysis Algorithm to Slalom Maneuver Data	133
4-20	Lateral Stick Activity Data Obtained for Each Simulation Run	134
4-21	Guide to Pilot Commentary	135
4-22	Cooper-Harper Pilot Opinion Rating Scale	137
4-23	Typical Case Illustrating the Maximum Roll Rate Trend	140
4-24	Cooper-Harper Pilot Opinion Variation with Turbulence Level in the Sidestep and Precision Hover Tasks	141
4-25	Definition of the HUD Tracking Task Amplitude Characteristics	143
4-26	Effect of Control Power Saturation on the HUD Tracking Task	145
4-27	HUD Tracking Performance	146

4-28	Identified Closed-Loop Natural Frequency and Damping Ratio for the HUD Tracking Task	151
4-29	RMS Attitude Error and Percent Time on Target Metrics as a Function of Control Power Saturation	154
4-30	Pilot Opinion Variation with Vehicle Short Term Response in the HUD Tracking Task	156
4-31	HUD Task Performance	157
4-32	HUD Task Performance	160
4-33	ACM Tracking Performance	163
4-34	Pilot Opinion Variation in ACM Tracking Task with Control Power Saturation	166
4-35	Example of Air Combat Free Engagement Task Performance	169
4-36	Sidestep Task Performance	171
4-37	Variation in Pilot Opinion with Control Power Saturation in the Sidestep Task	172
4-38	Identified Closed-Loop Natural Frequency and Damping Ratio for Sidestep Maneuver	174
4-39	Pilot Opinion Variation in the Sidestep Maneuver with Attitude Command Configuration	177
4-40	Sidestep Task Performance	178
4-41	Typical Sidestep Task Performance for Attitude-Command/Attitude-Hold System	184
4-42	Typical Sidestep Task Performance for Rate-Command/ Attitude-Hold System	185
4-43	Heading Turn Maneuver Data for Basic Helicopter	187
4-44	Heading Turn Maneuver Data for Attitude Command Response Type	188
4-45	Task Performance for the Slalom Maneuver for Basic Helicopter Type Configuration	190
4-46	Task Performance for the Jink Maneuver for Basic Helicopter Type Configuration	193

4-47	Slalom Task Performance for Attitude Command Response Type	194
4-48	Jink Task Performance for Attitude Command Response Type	196
4-49	IFR Heading Change Performance Data for Basic Helicopter Response Type	197
4-50	Anomalous Sideslip/Airspeed Response Seen in Large Amplitude Maneuvering with Attitude Systems	200
4-51	Slalom and Jink Maneuver Performance for Pilot X	203
4-52	Slalom and Jink Maneuver Performance for Pilot Y	205
4-53	Comparison of Sidestep Performance Between Flight and Simulation	207
4-54	Comparison of Air Combat Maneuvering Performance Between Flight and Simulator	209
5-1	Aggressiveness Versus Attitude Change for the HUD Tracking Task	214
5-2	Characteristic Roll Rate Limiting for Large Amplitude Maneuvering	216
5-3	Definition of Task Margin for Handling Qualities Analyses	220
5-4	Summary of Task Performance and Pilot Opinion for Control Power Variation	222
5-5	Summary of Pilot Opinion Variation with Control Power Saturation	226
5-6	Pilot Opinion Data Plotted versus Control Power Factor	227
5-7	Summary of Task Performance and Pilot Opinion for Short-Term Response Variation	228
5-8	Comparison of HUD Tracking Task Performance with Vehicle Short-Term Reponse Variation	230
5-9	Comparison of Task Requirements and Helicopter Capability for Vehicles Satisfying Current t_{30} Criteria	232

5-10 Pilot Model for the Triple Bend Maneuver 236

5-11 Comparison of Predicted and Simulation Data for the Triple Bend Maneuver 237

LIST OF TABLES

Table		Page
2-1	Rotor Flapping Equations of Motion for Zero Pitch Flap Coupling, μ=o	18
2-2	Rotor Flapping Transfer Functions	20
2-3	Hub Rolling Moment and Sideforce Expressions from Reference 35	22
2-4	Simplified Model for Helicopter Lateral Dynamics	24
2-5	Definition of Primary Analysis Model Form	26
2-6	Approximate Factors for Primary Analysis Model	28
2-7	A Survey of Helicopter Lateral Stability and Control Data	30
2-8	Lateral Transfer Functions Containing High Order Flapping Effects	36
2-9	Relationship between Peak Rate/Attitude Change and Ideal Second Order System Parameters	45
2-10	Summary of Second Order System Response Characteristics to Square Wave Inputs	51
2-11	Limiting Characteristics for Square Wave Input Response for a Second Order System	54
2-12	A Summary of Roll Control Effectiveness Criteria	56
3-1	Roll-to-Translate Response for BO-105 for a Range of Airspeeds	64
3-2	Maneuver Flight Data Bases	67
3-3	Summary of Lateral Maneuver Flight Data Characteristics	96
4-1	Summary of Flight Tasks Chosen for Simulation	102
4-2	Sequence of Target Aircraft Heading Change and Bank Angle Commands	110
4-3	Classification of Simulated Vehicle Configurations	110

4-4	Basic Helicopter Configurations	112
4-5	Attitude Command System Parameters	116
4-6	Lateral Control System Parameters for Rate-Command/Attitude-Hold Configurations	119
4-7	Simulation Program Test Pilots	123
4-8	Controller Characteristics	126
4-9	Estimated Visual System Time Delay	126
4-10	VMS Motion System Limits	128
4-11	Definition of Motion System Washout Parameters	130
4-12	Roll Control Simulation Motion Gains	131
5-1	Catalog of Task Performance	213
5-2	Triple Bend Maneuver Model Parameters	237

LIST OF SYMBOLS

Symbol	Description
a	blade lift-curve slope, per rad
a_o	blade coning angle measured from hub plane, rad
a_1	longitudinal first-harmonic flapping coefficient measured from hub plane and in "wind-hub" system, rad
a_{1_s}	longitudinal first-harmonic flapping coefficient measured from hub plane and in "hub-body" system, rad
A	swashplate authority, deg
A_{1_c}	lateral cyclic pitch measured from hub plane and in "wind-hub" system, rad
A_{1_s}	lateral cyclic pitch measured from hub plane and in "hub-body" system, rad
b_1	lateral first-harmonic flapping coefficient measured from hub plane and in "wind-hub" system, rad
b_{1_s}	lateral first-harmonic flapping coefficient measured from hub plane and in hub-body system, rad
B_{1_c}	longitudinal cyclic pitch measured from hub plane and in "wind-hub" system, rad
B_{1_s}	longitudinal cyclic pitch measured from hub plane and in "hub-body" system, rad
c	blade chord, m (ft)
C_T	rotor thrust coefficient
e	flapping hinge offset, m (ft)
g	gravitational constant, m/sec^2 (ft/sec^2)
h	altitude, m (ft)
h_r	cg to hub vertical distance in body axis system, m (ft)
I_β	blade moment of inertia about flapping hinge, $kg\text{-}m^2$ ($slug\text{-}ft^2$)

I_x inertia about body roll axis, kg-m^2 (slugs-ft^2)

j complex operator

K_I integral feedforward gain

K_p lagged roll rate feedback gain, or proportional feedforward gain

$K_{()}$ gain

K_1 pitch-flap coupling ratio

K_β flapping hinge restraint, N-m/rad (ft-lb/rad)

$L_{b_{1_s}}$ lateral flapping stiffness, N-m/rad (ft-lb/rad)

$L_{()}$ rolling hub moment, N-m (ft-lb)

m vehicle mass, Kg (slugs)

M_β blade mass moment about the flapping hinge, Kg-m (slugs-ft)

n_b number of blades

p aircraft roll rate, deg/sec

p_{pk} peak roll rate, degs/sec

P ratio of flapping frequency to rotor system angular velocity

q aircraft pitch rate, deg/sec

R rotor radius, m (ft)

R_T turn radius, m (ft)

s Laplace operator

t_x time to x degees attitude change, secs

T main rotor thrust, N (lbf)

T_L lead time constant, sec

T_{max} time to maximum roll rate, secs

T_p lagged roll rate time constant, secs

T_0 time to maximum roll attitude change, secs

T_1 dwell time, secs

U Airspeed, m/sec (ft/sec)

v lateral velocity, m/sec (ft/sec)

W vehicle gross weight, N (lbf)

X longitudinal position, m (ft)

Y lateral position, m (ft)

$Y_{()}$ main rotor Y force, N (lbf)

α angle of attack, deg

β sideslip angle or visual flow-field angle, deg.

β_W rotor slideslip angle

γ Locks Number

$\delta_{()}$ control displacment

δ_3 pitch-flap coupling angle, degs

Λ transfer function denominator

ΔT time frame, secs

ΔT_0 throughput time delay, secs

$\Delta\phi$ bank angle change, degs

$\Delta\phi_{c_{max}}$ maximum commanded bank angle change, degs

ϵ $e/_R$, or stick gain modification factor

ζ damping ratio

η control power factor

θ pitch attitude, degs

θ_o blade-root collective pitch measured in hub plane, rad

θ_t total blade twist (tip with respect to root), rad

λ inflow ratio, or eigenvalue

μ advance ratio

ρ air density, kg/m^3 (slugs/ft^3)

σ settling frequency, or rotor solidity (blade area/disc area) ratio

σ_{u_g} gust standard deviation, m/sec (ft/sec)

τ preview time, secs

τ_b tip path plane lag, secs

ϕ roll attitude, degs

ψ heading, degs

ω frequency, rads/sec

ω_{bw} bandwidth for 45 deg phase margin, rads/sec

ω_c crossover frequency, rads/sec

ω_n natural frequency, rads/sec

Ω rotor system angular velocity, rad/sec

Subscripts:

A lateral control

C command

e error

E longitudinal control

f_a advancing flapping mode

f_c coning mode

f_r regressing flapping mode

g gust

H hub-wind axis system

max maximum value

P	yaw control
ss	steady state
TR	tail rotor
TRIM	trim value
v	lateral velocity
W	hub-wind axis system
Y	lateral position
θ	pitch
ϕ	roll
ψ	yaw

Superscripts:

h	hinge offset
s	*spring stiffness*
t	thrust

List of Abbreviations

ACM	Air Combat Maneuvering
AGL	Above Ground Level
ATAT	Attitude-Command/Attitude-Hold
CHR	Cooper-Harper Rating
HAC	Helicopter Air Combat
HQ	Handling Qualities
HUD	Head-Up Display
NADC	Naval Air Development Center
NASA	National Aeronautics and Space Administration
NATC	Naval Air Test Center
NOE	Nap-of-the-Earth
RAAT	Rate-Command/Attitude-Hold
V/STOL	Vertical/Short Take-Off and Landing

STUDY OF HELICOPTER ROLL CONTROL EFFECTIVENESS CRITERIA VOLUME I

I. BACKGROUND AND INTRODUCTION

This report describes the work conducted by Manudyne Systems, Inc., for the U. S. Army Aeromechanics Laboratory and NASA Ames Research Center under Contract NAS2-11665.

A. Purpose of Study

The purpose of this study is to determine a rational basis for helicopter handling qualities criteria with regard to roll control effectiveness for maneuvering. Such criteria are intended to be of use first to the military in specifying rotorcraft design requirements, second to the designers in tailoring a vehicle to its intended missions, and finally to both groups in the developmental testing phase.

A central theme in this effort is the establishment of the dependence of roll control effectiveness design criteria on given flight tasks and mission flight phases. Considerable effort was expended in defining closed-loop task performance characteristics for discrete maneuver flight tasks on a task-by-task basis.

1. Background

The present helicopter handling qualities specification, MIL-H-8501A (Reference 1), has been in use since 1952 with a revision in 1961. An analytical review of this specification was made in 1967 (Reference 2) but no changes were made. Presently the Army and Navy are underway with a systematic effort to develop a new general specification

for the handling qualities of military rotorcraft (References 3 and 4). The effort has built upon the ideas, techniques, and technology developed by the fixed-wing community, as well as utilizing the available experience with current helicopter specifications and V/STOL criteria (e.g., References 5-8).

In developing the new specification, the existing data base has been used to the maximum extent possible. It has also been necessary to supplement this data base by new data obtained under the auspices of this and other programs (such as References 9 and 10).

Roll control effectiveness has been recognized as an important and fundamental aspect of rotorcraft handling qualities, and the decision was made to support this study in order to gain better definition and understanding of design specification needs. However, the methodology applied here is not limited to the roll axis and can also be used to approach other axes of control and aspects of handling qualities.

Total control effectiveness required consists of the sum of control required to trim, suppress or recover from external upsets, and to maneuver. The amount of control required to trim is determined by the designer using analytical models of the design configuration and confirmed by flight test. The amount of control required to suppress or recover from upsets is not obtained as directly and requires a knowledge or estimate of the disturbance source. This aspect of control effectiveness is closely tied to small amplitude, short-term response. The amount of control required to perform given maneuvers has lacked methods for analytical definition but may be the driving factor in large-amplitude control usage.

This study has concentrated on examining the need for roll control effectiveness to support a variety of important helicopter maneuvers. This has been done in a manner which allows a degree of generalization

in approaching flight tasks and maneuvers beyond those studied directly. In fact it should be understood that the specific maneuvers which are considered in this study are intended only to be representative of general classes of flight tasks or maneuvers. There may be special cases where it is necessary to examine other specific flight tasks or flight conditions in order to extend or modify the results presented here.

2. Criteria and Specification Development

The handling qualities criteria and specification development process is a major issue in this study. There is a calculated effort to perform this process in a rational manner wherein the operational needs are quantified and serve as the basis for required vehicle capabilities.

Specification development has traditionally been carried out in two ways. One has been to simply take stock of the characteristics possessed by existing vehicles in order to set standards for new ones. This was apparent in early civil airworthiness standards and military specifications (e.g., References 11 and 12). A second more prevalent approach has been to perform systematic flight or simulation experiments wherein pilot opinion has been used to establish useful boundaries and criteria. This latter approach has formed the basis of refined versions of specifications such as References 5, 13, 14.

One notable handling qualities study was the flight-test based determination of armed-helicopter requirements cited in Reference 15. This involved the use of fairly realistic tactical flight maneuvers with existing flight vehicles. Boundaries were set for short-term response characteristics which seem to remain reasonably valid today.

Unfortunately, neither of the above approaches has resulted in a good analytic understanding of how mission performance factors really

may dictate design characteristics. This study has concentrated on improving this situation and establishing a general procedure for approaching handling qualities requirements in a more deliberate and rational manner than has been done heretofore.

3. New Approaches to Handling Qualities Research

A fundamental feature of this approach to specification development is in the quantification of flight task and maneuver performance in a form compatible with traditional analysis of vehicle flight dynamics. Thus handling qualities can be quantified in terms of the net difference between vehicle capability and task performance demands.

Manual control theory (as presently summarized by Reference 16) serves as an important basis for quantifying and explaining control effectiveness needs, but has traditionally been focused more on pilot control strategy than on defining the task, per se. The distinction between "task dynamics" and "pilot-" or "vehicle-dynamics" is important. As illustrated in Figure 1-1, "task dynamics" represent the overall, lumped, closed-loop pilot-vehicle combination. It appears useful to examine this aspect in contrast to either the pilot or vehicle individually because of the potential simplification and the relevance of the task itself.

In mathematically modeling the dynamics of flight task execution, one of the important features is the presence of "discrete maneuver" effects. This refers to the non-continuous behavior of the pilot in switching from one task to another or in performing one task via a series of several discrete commands. Discrete maneuver behavior is nearly analogous to sampled-data control operation. Reference 17 describes early work in addressing such effects in helicopters.

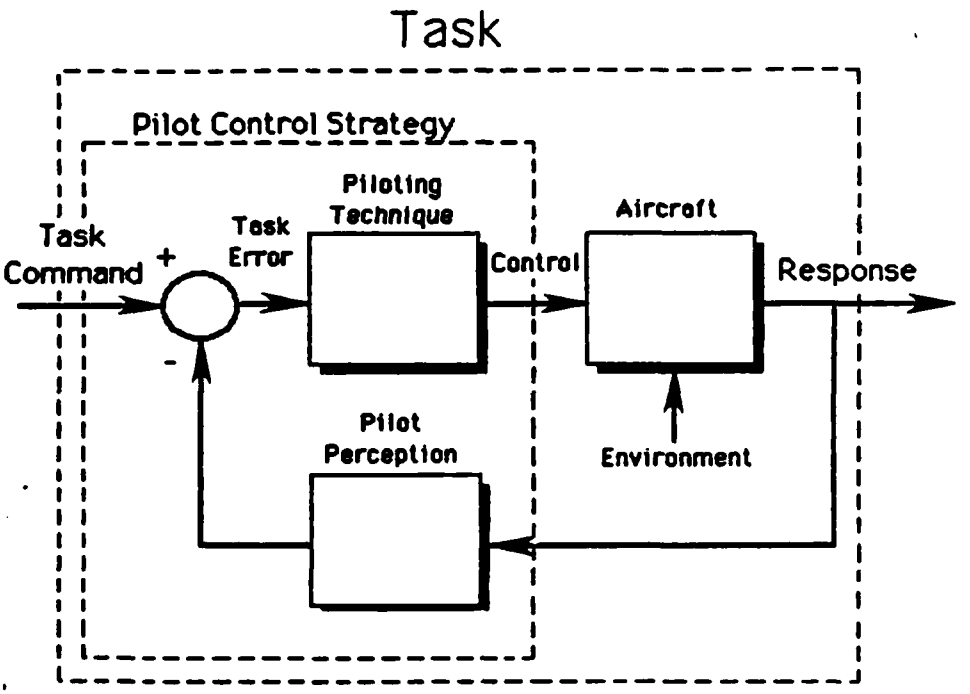

Figure 1-1. Block Diagram of Pilot-Vehicle-Task System.

The analysis of discrete maneuver tasks is not necessarily more difficult than continuous tasks. Discrete tasks can be portrayed using conventional feedback control block diagrams and Laplace transform operators. This will be discussed in considerable detail in connection with the pilot-in-the-loop theory presented in Section II. The methodology for the approach is based on applications to complex Navy flight tasks given in Reference 18.

B. Views of Manufacturers and Users

During the course of this study a number of individuals representing both helicopter manufacturers and helicopter users were contacted. Their respective views on helicopter handling criteria were

solicited along with requests for appropriate data and relevant experiences.

1. Needs of Military Users

Military users are concerned with procuring rotorcraft which are effective in carrying out their intended missions. This is a difficult process because each new aircraft development usually involves an advancement in vehicle performance, increased difficulty of missions, and use of new or improved pilot-assistance systems. In short, the lessons learned in a previous generation aircraft may not be sufficient for designing the next. Therefore, it appears valuable to establish a means for generalizing vehicle response requirements in terms of mission requirements to permit extrapolation to new flight conditions and mission performance requirements.

Reference 19 represents a good summary of how the military views the role of handling qualities specifications and the current status of helicopter specification. There is an emphasis on the use of handling qualities specifications as design guides and the usefulness of concentrating on characteristics that influence basic configuration design such as static and dynamic stability, and moment and thrust control power.

In the case of roll control effectiveness, the desire to incorporate the capability for air combat maneuvering (a relatively new mission for helicopters) in the next generation of attack and scout helicopters (e.g., the LHX family of light helicopters) raises questions about the adequacy of previous specifications. It seems unwise to base LHX requirements solely on the air combat flight experience with present aircraft such as OH-58, AH-1, and AH-64. Yet there is little to use as a basis for extrapolating to a new level of performance. Further, it is not known whether human limits exist even if the vehicle were to have

greatly enhanced capabilities.

While there is an interest in air combat by the Marine Corps, the Navy regards shipboard operation as a critical mission. Reference 20 states that hover control power criteria are inadequate for variations in both mission and vehicle configuration.

2. Concerns of Designers and Manufacturers

Rotorcraft designers and manufacturers are concerned with successfully producing flight vehicles capable of their intended missions but doing so with sufficient latitude in choosing design solutions. There is a fear of over-specification or unnecessarily ruling out viable system designs.

In general, the design of roll-axis control for flight is based on consideration of trim and maneuver requirements. The cross-slope takeoff and landing maneuver is seen as a particularly critical design point. There is considerable attention being devoted to the control power requirements for aerobatic maneuvers associated with air-to-air combat.

One designer points out that combinations of flight conditions can present especially interesting and difficult demands on the level of control available. For example, in one design no roll control deficiencies appeared until a flight in which the pilot performed simultaneously a decelerating, turning flare through transition airspeed in a cross wind. All available roll control was used in this case.

Another designer believes that it is the maximum effort collision avoidance maneuver which, if planned for, would set the most conservative standards for overall control effectiveness. Other views on this are that under such conditions, a pilot would simply use all the

control that is available and that there is no set value for such a maneuver anyway.

Reference 21 addresses helicopter large-amplitude maneuvering from a manufacturer's viewpoint. There is a major concern over how the customer defines maneuvering flight performance and thus sets requirements.

The use of equivalent systems models for expressing aircraft characteristics has been applied to fixed-wing aircraft (References 22 and 23). Some manufacturers believe that such an approach for helicopter handling qualities is not appropriate, however. The main shortcoming cited is the lack of important rotor-related dynamics. For example, the traditional first-order lag roll response transfer function (which may be useful for fixed-wing airplanes) does not include rotor tip-path-plane lags which are normally visible in helicopter roll response. Other dynamic effects which can play a role in handling qualities are rotor lag modes and possibly pylon structural modes.

C. Technical Approach

This study addresses the roll control requirements for maneuvering. The need for basic design criteria is recognized, but there is also a belief that the process of criteria development should be improved and made more rational than in the past. Thus the resulting technical approach contains three major elements:

(1) Theoretical treatment of the dynamics of the vehicle and the pilot.

(2) Analytical examination of the flight tasks and maneuvers involving roll control effectiveness.

(3) Experimental study of vehicle and task features and parameters.

The purpose of this approach is to provide a broad rational foundation for the criteria, the quantitative definition which is needed for ongoing specification development, and a means for analytically approaching new situations and design needs in the future.

1. Theoretical Development

The vehicle-related theoretical development portion of this study is concerned with understanding those features of helicopters which are involved in providing or detracting from roll control effectiveness. The contributions of the rotor, fuselage, and flight controls are examined starting with detailed models and ending with concise models which summarize the fundamental system dynamics. One aspect of the technical approach is to work with math models which are simple enough to provide insight into cause and effect relationships while at the same time sufficiently complete to provide a reasonable level of accuracy in predicting handling qualities effects.

For example, it is shown that the main contribution of the high frequency rotor dynamics to roll axis handling qualities effects can be effectively modeled using only a first order flapping equation. Such a model adequately represents a traditional second order regressing flapping mode but ignores the coning and advancing flapping modes which are usually outside the frequency ranges of interest.

Aerodynamic effects involve a combination of rotor hub dynamics and coupling with the fuselage. In forward flight the major aerodynamic contributions to roll control are the vertical position of the hub relative to the center of gravity, the amount of flapping hinge offset, and any direct flapping restraints such as a spring or rigid hub design. In sideward flight the dihedral effect of the rotor system can become

significant but can also be modeled in a simple and concise manner.

Following an examination of the primary vehicle dynamics, the second area of theoretical development is concerned with the pilot-in-the-loop effects. This is studied using manual control theory and discrete maneuver modeling techniques. This accomplishes two things, first the roles of the individual vehicle dynamics are put into the proper operating context and second a methodology is defined for the flight task analysis part of this study which is presented in Section III.

The most fundamental pilot-in-the-loop effect is the control and regulation of bank angle using lateral cyclic control. This loop is the most effective in revealing potential handling qualities problems. The relative success in applying a manual cross-over model in this loop can reveal PIO tendencies, the need for lead compensation and the potential destabilizing effects of higher frequency vehicle dynamics.

The next aspect of the manual control theoretical analysis is the outer-loop control, and is closely associated with the particular flight task being analyzed. Outer-loop control determines whether the side velocity degree of freedom of the helicopter is important. Further the outer-loop control sets the basic bandwidth requirements for inner-loop bank angle management.

A methodology is then proposed for the analysis of task performance in discrete maneuvers. For each task a "task signature" is defined by plotting maneuver data in terms of peak roll rate versus attitude change. The features of this signature are then quantitatively defined in terms of amplitude and aggressiveness parameters. A clear audit trail is then established between the key lateral vehicle design parameters, swash-plate authority and rotor hub type, and closed-loop task performance capability.

Finally, a review of past and current handling qualities criteria is presented. The philosophy behind criteria such as time to x degrees and roll attitude change after x seconds is detailed.

2. Task and Maneuver Analysis

The main purpose of analyzing flight tasks is to obtain a methodology for quantifying operationally useful flight tasks and maneuvers. Further, flight task analysis plays a crucial role in the development of roll control effectiveness criteria. The approach to flight task analysis is aimed at the quantification of flight task and maneuver performance features and the connection between those features and vehicle response characteristics.

Based on theoretical development of the methodology for describing flight tasks and maneuvers, a set of several lateral maneuvers are defined. Each of the maneuvers represents a condition where some level of lateral control effectiveness is required by the pilot. Collectively this set of maneuvers covers the range of performance demanded by the pilot in carrying out mission and flight phase objectives.

As part of this program several flight data bases were reviewed to define pilot-vehicle performance characteristics representative of operational missions. These closed-loop task performance characteristics can be generally considered to be independent of individual pilot or helicopter open-loop dynamics. A spectrum of mission scenarios were analyzed ranging from Nap-of-the Earth (NOE) to Air Combat Maneuvering (ACM). Several of these data bases were generated under the auspices of this program using a UH-1H helicopter and two experienced research pilots. Other flight data bases examined include data from the Deutsche Forschungs- and Versuchsanstalt fur Luft- and Raumfahrt e.V. (DFVLR) involving a UH-1 and BO-105 (Reference 24).

These data are presented to define possible task performance differences due to rotor hub types. Particularly valuable data from the Army-sponsored evasive maneuvering flight test program (Reference 25) are presented to indicate levels of aggressiveness and maneuver amplitudes in air combat situations. Other data include X-22 sidestep maneuver performance (Reference 26) and NASA variable stability UH-1H flights through a runway slalom course (Reference 27).

3. Experimental Simulator Investigation

An experimental program was conducted using the NASA Ames large amplitude Vertical Motion Simulator (VMS) in order to extend criteria development efforts under controlled conditions. The simulation was run using a number of pilots with various backgrounds, a variety of helicopter configurations and control system types, and a wide range of flight tasks and maneuvers.

The basis of the experimental design is to examine the levels of helicopter roll control effectiveness needed to perform realistic and crucial flight tasks and maneuvers. The fundamental element of the experimental design is performance of a given flight task or maneuver in a manner considered realistic by the pilot. No artificial test procedures are introduced and all measurements made of the pilot are non-intrusive.

A review of roll control simulation experiments prior to this showed a wide variation in results. These variations may be connected with motion and visual system fidelity as well as task features. An example of the effects of motion are given in References 27, 28, 29. The effects of narrow field of view are considerable also (Reference 30). Other simulation effects regarded as potentially damaging include effective lags and delays associated with digital computation and digital visual systems (Reference 31).

There is a calculated balance between the number of pilots, configurations, and maneuvers run and the general quality of the results obtained. The most important overall concern is to gain a good perspective view of the factors involved in piloting, vehicle response, and task performance.

A variety of data were acquired in the simulator. Qualitative or subjective data include transcribed pilot commentary as well as Cooper/Harper ratings (Reference 32). Pilot commentary is standardized and structured in a manner to lead the pilot into the Cooper/Harper rating scale.

Many forms of quantitative data have been gathered. These include stored time histories of all of the variables involved in the helicopter math model as well as a range of performance measurements for the closed-loop pilot vehicle system. These quantitative data were expected to reveal the relationship between task performance and roll control effectiveness criteria parameters. A special algorithm was designed to measure specific task performance parameters, namely the size of discrete maneuver excursions and the peak rates developed during each excursion. Finally statistical data were obtained for lateral control excursions.

4. Criteria Development

The philosophy and fundamental objectives of lateral control effectiveness criteria are addressed. The closed-loop task performance modeling structure is proposed as the unifying approach to all past and present lateral handling qualities data bases.

Task margin, the excess capability of the closed-loop pilot/vehicle system over the task demand is proposed as the fundamental handling

qualities parameter. This closed-loop performance modeling approach unifies the concepts of short-term response and control power requirements and clearly establishes the relationship between key vehicle design parameters and task performance capability.

Data from the simulation program are used to define closed-loop amplitude and aggressiveness characteristics on a task-by-task basis. Control power results from the simulation are presented in terms of the task margin parameter. This approach enables a control power (maximum roll rate) criteria specification to be made independent of the specific task in question. The same philosophy is applied to the short-term response issue. However, in this case the limited data available from the simulation did not allow quantitative definition of a criteria.

Finally, the current open-loop specification criteria are reviewed in comparison with the task margin approach. Limitations of the current criteria are discussed, and tasks which cannot be accommodated within the current Level 1 boundaries are identified.

II. THEORETICAL DEVELOPMENT

The purpose of this section is to provide a broad understanding of the aircraft and pilot dynamics connected with helicopter roll control effectiveness. Four general areas are discussed. First the helicopter roll axis dynamics are described at various levels of modeling complexity. Second the effects of the pilot-in-the-loop are derived using conventional pilot modeling techniques. Third the methodology for discrete maneuver analysis is presented together with an approach to clearly define the audit trail between key vehicle design parameters and task performance capability. Finally, a review of handling qualities criteria and the philosophy behind criteria development is given.

A. Helicopter Roll-Axis Dynamics

The purpose of the following pages is to derive the equations of motion pertinent to roll axis stability and control for a helicopter vehicle and to expose the essential parameters which describe vehicle performance. The material presented is based on standard forms of equations of motion. These basic relationships are then simplified into a general model form which lends itself to roll-axis handling qualities analysis. Finally a survey is made of roll-axis stability and control characteristics for existing helicopters.

1. Important Considerations in Criteria Development

There are at least two main concerns in choosing or developing vehicle math models. First is understanding the role of the math model in criteria development. The second concern is how to appropriately tailor the level of model complexity.

Here the role of the vehicle math model is to provide an understanding of the effect of individual design features on roll-axis

handling qualities. Hence there must be a reasonably explicit "audit trail" connecting identifiable handling characteristics to physically understandable vehicle features.

Another role of the vehicle model is its use in pilot-in-the-loop analyses. Hence the model must contain those features involved in manual control and reflect response characteristics over the spectral range important to the pilot.

The third role of the model is to serve as a framework for identification of system parameters.

The issue of model complexity is crucial. Most model forms of helicopter equations of motion or stability and control characteristics are too complex to allow a good understanding of design features. It is necessary to strike a balance in model complexity in order to adequately represent important effects and yet not inhibit reasonable understanding of those effects. Also, it should be recognized that model complexity alone does not provide the panacea for model fidelity and validity. In fact, model complexity in a simulator application can precipitate unwanted side effects such as excessive computational delays and lags.

2. Rotor-Body Models

A variety of model forms are available to describe helicopter flight dynamics, but in view of the above considerations, some forms are more appealing and useful.

The purpose here is to show the evolution of an appropriate model form starting with a comprehensive but overly-complex form for most purposes in examining roll-axis handling qualities. The discussion indicates modeling alternatives leading to the choice of a streamlined primary analysis model used for subsequent flight task and maneuver

analysis.

The chief determinant of in-flight rotorcraft roll-axis dynamics is the rotor-body combination. Motion involves the combined rotor flapping and coning response modes along with coupled roll-rate damping and side-velocity damping modes.

Rotor-Alone Response. The first step in examining the rotor-body combination is to view the rotor alone. This aids in understanding where the rotor response modes occur with respect to the general spectral range of interest.

Reference 33 provides a comprehensive derivation of rotor tip-path-plane equations of motion and the components of the response with respect to various rotor system design features. These include hinge placement, hinge compliance, pitch-flap coupling, and the proportion of aerodynamic to blade inertial forces (Lock number).

The general assumptions made in Reference 33 are:

(1) Rigid blades in bending and torsion.
(2) Small flapping and inflow angles applied to strip theory.
(3) Reverse flow ignored, compressibility and stall disregarded.
(4) Uniform inflow and zero tip loss.

Each of these assumptions is permissible for the purpose of gaining an understanding of general response features.

The complete set of tip-path-plane equations of motion are given in Reference 34. For the special case of hover and zero pitch-flap coupling the equations of motion are summarized in Table 2-1. Note that frequency is normalized with respect to rotor angular velocity, Ω. The three degrees of freedom include coning, longitudinal flapping, and

Table 2-1

Rotor Flapping Equations of Motion for Zero Pitch Flap Coupling, $\mu=0$

$$\begin{bmatrix} \left[\left(\frac{s}{\Omega}\right)^2 + \frac{\gamma}{2}\left(\frac{1}{4} - \frac{2}{3}\epsilon + \frac{\epsilon^2}{2}\right)\frac{s}{\Omega} + p^2\right] & 0 & 0 \\ 0 & \left[\left(\frac{s}{\Omega}\right)^2 + \frac{\gamma}{2}\left(\frac{1}{4} - \frac{2}{3}\epsilon + \frac{\epsilon^2}{2}\right)\frac{s}{\Omega} + p^2 - 1\right] & \left[\frac{2s}{\Omega} + \frac{\gamma}{2}\left(\frac{1}{4} - \frac{2}{3}\epsilon + \frac{\epsilon^2}{2}\right)\right] \\ 0 & -\left[\frac{2s}{\Omega} + \frac{\gamma}{2}\left(\frac{1}{4} - \frac{2}{3}\epsilon + \frac{\epsilon^2}{2}\right)\right] & \left[\left(\frac{s}{\Omega}\right)^2 + \frac{\gamma}{2}\left(\frac{1}{4} - \frac{2}{3}\epsilon + \frac{\epsilon^2}{2}\right)\frac{s}{\Omega} + p^2 - 1\right] \end{bmatrix} \begin{bmatrix} a_0 \\ a_{1_s} \\ b_{1_s} \end{bmatrix}$$

$$= \begin{bmatrix} 0 & 0 \\ \frac{\gamma}{2}\left(\frac{1}{4} - \frac{\epsilon}{3}\right) & 2\left(1 + \frac{eM_\beta}{I_\beta}\right) \\ 0 & \left[\frac{s}{\Omega} + \frac{\gamma}{2}\left(\frac{1}{4} - \frac{\epsilon}{3}\right)\right] \end{bmatrix} \begin{bmatrix} A_{1_s} \\ \frac{p}{\Omega} \end{bmatrix}$$

lateral flapping. Finally the two input states are roll rate, p, and lateral swashplate deflection angle, A_{1_s}.

Important response features are summarized in Table 2-2 as partially factored numerator and denominator polynomials. Note that the second order root representing coning is:

$$\left(\frac{s}{\Omega}\right)^2 + \frac{\gamma}{2}\left(\frac{1}{4} - \frac{2\epsilon}{3} + \frac{\epsilon^2}{2}\right)\frac{s}{\Omega} + P^2$$

Flapping contains two sets of second order roots with the same settling frequency ($\sigma = -\zeta\omega_n$) as coning but substantially different natural frequencies. It can be shown that the poles lie on a circle with radius P. A set of second order zeros occurs at the coning poles. Finally, the remaining zero in the flapping response to lateral cyclic swashplate is very nearly equal to the common settling frequency.

Figure 2-1 summarizes the arrangement of flapping poles and zeros. Note that the regressing flapping which represents the lateral precession of the rotor is the dominant low frequency response mode and is very nearly first order. The advancing flapping is a nutational effect on the tip-path-plane orientation and occurs at about 2Ω. Finally the coning mode is essentially cancelled by a control zero.

It is important to conclude that the complete transfer function shown here closely resembles a simple first order lag to frequencies well beyond $\gamma\Omega/16$ rad/sec, i.e. about 10 rad/sec.

Coupling the Body to the Rotor. The next step is to demonstrate the effect of coupling the body to the rotor shaft. This involves considerable complication if fairly exact expressions are used to represent the applied forces and moments. Reference 35 describes the body-axis forces and moments acting at the hub based on the Reference 33 math model. Table 2-3 indicates just the hub side force and rolling

Table 2-2

Rotor Flapping Transfer Functions

$$\frac{b_{1_s}}{A_{1_s}}(s) = \frac{N_{A_{1_s}}^{b_{1_s}}}{\Delta}$$

$$N_{A_{1_s}}^{b_{1_s}} = \begin{vmatrix} \left[\left(\frac{s}{\Omega}\right)^2 + \frac{\gamma}{2}\left(\frac{1}{4} - \frac{2}{3}\epsilon + \frac{\epsilon^2}{2}\right)\frac{s}{\Omega} + p^2\right] & 0 & 0 \\ 0 & \left[\left(\frac{s}{\Omega}\right)^2 + \frac{\gamma}{2}\left(\frac{1}{4} - \frac{2}{3}\epsilon + \frac{\epsilon^2}{2}\right)\frac{s}{\Omega} + p^2 - 1\right] & \frac{\gamma}{2}\left(\frac{1}{4} - \frac{\epsilon}{3}\right) \\ 0 & -\left[\frac{2s}{\Omega} + \frac{\gamma}{2}\left(\frac{1}{4} - \frac{2}{3}\epsilon + \frac{\epsilon^2}{2}\right)\right] & 0 \end{vmatrix}$$

$$= \underbrace{\left[\left(\frac{s}{\Omega}\right)^2 + \frac{\gamma}{2}\left(\frac{1}{4} - \frac{2}{3}\epsilon + \frac{\epsilon^2}{2}\right)\frac{s}{\Omega} + p^2\right]}_{\text{Cancels Coning Mode}} \quad \underbrace{\frac{\gamma}{2}\left(\frac{1}{4} - \frac{\epsilon}{3}\right)\left[\frac{2s}{\Omega} + \frac{\gamma}{2}\left(\frac{1}{4} - \frac{2}{3}\epsilon + \frac{\epsilon^2}{2}\right)\right]}_{\text{Residual Zero on the Real Axis at:}}$$

$$\frac{\sigma}{\Omega} = \frac{\gamma}{16}\left(1 - \frac{8}{3}\epsilon + 2\epsilon^2\right)$$

$$\Delta = \overbrace{\left[\left(\frac{s}{\Omega}\right)^2 + \frac{\gamma}{2}\left(\frac{1}{4} - \frac{2\epsilon}{3} + \frac{\epsilon^2}{2}\right)\frac{s}{\Omega} + p^2\right]}^{\text{Coning}}\left\{\left[\left(\frac{s}{\Omega}\right)^2 + \frac{\gamma}{2}\left(\frac{1}{4} - \frac{2\epsilon}{3} + \frac{\epsilon^2}{2}\right)\frac{s}{\Omega} + p^2 - 1\right]^2 + \left[\frac{2s}{\Omega} + \frac{\gamma}{2}\left(\frac{1}{4} - \frac{2\epsilon}{3} + \frac{\epsilon^2}{2}\right)\right]^2\right\}$$

$$\frac{b_{1_s}}{A_{1_s}}(s)$$

Constellation of poles and zeros for the uncoupled rotor system with second-order flapping and coning degrees of freedom.

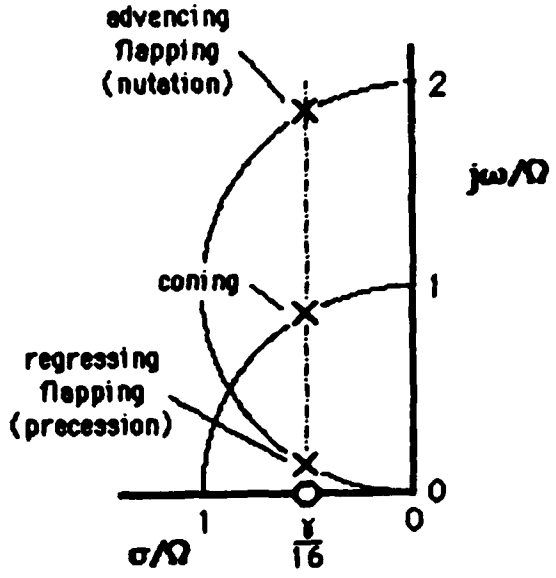

For normal ranges of rotor stiffness (i.e., P^2-1 appropriately small) then the rotor flapping roots can be estimated using the following approximation:

$$\left(\frac{\omega_{f_a}}{\Omega}\right)^2 \approx 2 + \sqrt{4 - \left(\frac{\gamma}{8}\right)^2}$$

$$\left(\frac{\omega_{f_c}}{\Omega}\right)^2 \approx P^2$$

$$\left(\frac{\omega_{f_r}}{\Omega}\right)^2 \approx 2 - \sqrt{4 - \left(\frac{\gamma}{8}\right)^2}$$

$$\zeta_{f_a}\omega_{f_a} = \zeta_{f_c}\omega_{f_c} = \zeta_{f_r}\omega_{f_r} = \frac{\Omega\gamma}{16}$$

Figure 2-1. Rotor Flapping Response Modes

Table 2-3

Hub Rolling Moment and Sideforce Expressions from Reference 35.

$$L_W = \frac{n_b}{2}\left[K_\beta b_1 - \frac{eM_\beta}{g}\left(\ddot{b}_1 - 2\dot{a}_1\Omega - b_1\Omega^2\right)\right] - \frac{n_b}{2} I_\beta \Omega^2 \gamma c \left\{\frac{\mu}{2}(1-\epsilon^2)(\theta_0 - K_1 a_0)\right.$$
$$-\left[\frac{1}{6} + \frac{3}{8}\mu^2(1-\epsilon)\right](B_{1c} - K_1 b_1) + \frac{\mu}{3}\theta_t + \frac{\mu}{2}(1-\epsilon)\lambda + \frac{\mu^2}{8}(1-\epsilon)a_1$$
$$\left. - \frac{\mu}{4}(1-\epsilon)^2\frac{\dot{a}_0}{\Omega} + \left(\frac{1}{6} - \frac{\epsilon}{4}\right)\left(\frac{\dot{b}_1}{\Omega} - a_1\right) + \frac{1}{6}\left(\frac{p_H}{\Omega}\cos\beta_w + \frac{q_H}{\Omega}\sin\beta_w\right)\right\}$$

$$Y_W = \frac{n_b}{2}\rho a c R(\Omega R)^2\left(-\frac{1}{4}(\theta_0 - K_1 a_0)\left\{\left[\left(\epsilon - \frac{2}{3}\right)\left(\frac{\dot{a}_1}{\Omega} + b_1\right) - \frac{2}{3}b_1\right] + 3a_0(1-\epsilon^2)\mu\right.$$
$$\left. - 2b_1(1-\epsilon)\mu^2 - \frac{2}{3}\left(-\frac{p_H}{\Omega}\sin\beta_w + \frac{q_H}{\Omega}\cos\beta_w\right)\right\} - \frac{\theta_t}{4}\left\{\left[\left(\frac{2\epsilon}{3} - \frac{1}{2}\right)\left(\frac{\dot{a}_1}{\Omega} + b_1\right) - \frac{b_1}{2}\right]\right.$$
$$\left. + 2a_0\mu - b_1(1-\epsilon^2)\mu^2 - \frac{1}{2}\left(-\frac{p_H}{\Omega}\sin\beta_w + \frac{q_H}{\Omega}\cos\beta_w\right)\right\}$$
$$- \frac{1}{4}(A_{1c} - K_1 a_1)\left\{\left[\left(\epsilon - \frac{2}{3}\right)\frac{\dot{a}_0}{\Omega} + \lambda(1-\epsilon^2)\right] + \mu\left[\frac{5a_1}{4}(1-\epsilon^2)\right.\right.$$
$$\left.\left. + \frac{1}{4}(1-\epsilon)^2\left(\frac{\dot{b}_1}{\Omega} - a_1\right)\right] + \frac{\mu}{4}(1-\epsilon^2)\left(\frac{p_H}{\Omega}\cos\beta_w + \frac{q_H}{\Omega}\sin\beta_w\right)\right\}$$
$$- \frac{1}{4}(B_{1c} - K_1 b_1)\left\{-\frac{2}{3}a_0 + \mu\left[\frac{7}{4}b_1(1-\epsilon^2) + \frac{1}{4}(1-\epsilon)^2\left(\frac{\dot{a}_1}{\Omega} + b_1\right)\right.\right.$$
$$\left.\left. + \frac{1}{4}\left(-\frac{p_H}{\Omega}\sin\beta_w + \frac{q_H}{\Omega}\cos\beta_w\right)\right] - \mu^2[2a_0(1-\epsilon)]\right\}$$
$$- \frac{1}{4}\left\{4\left(\frac{1}{3} - \epsilon + \epsilon^2\right)\frac{\dot{a}_0}{\Omega}\left(\frac{\dot{a}_1}{\Omega} + b_1\right) - 2\lambda(1-\epsilon)^2\left(\frac{\dot{a}_1}{\Omega} + b_1\right)\right.$$
$$+ \frac{2a_0}{3}\left(\frac{p_H}{\Omega}\cos\beta_w + \frac{q_H}{\Omega}\sin\beta_w\right) + 2a_0\left(\frac{1}{3} - \frac{\epsilon}{2}\right)\left(\frac{\dot{b}_1}{\Omega} - a_1\right) - 2b_1\left[\frac{\lambda}{2}(1-\epsilon^2)\right.$$
$$\left.\left. - \frac{\dot{a}_0}{\Omega}\left(\frac{1}{3} - \frac{\epsilon}{2}\right)\right] + \left[4\left(\frac{1}{3} - \frac{\epsilon}{2}\right)\frac{\dot{a}_0}{\Omega} - 2(1-\epsilon^2)\lambda\right]\left(-\frac{p_H}{\Omega}\sin\beta_w + \frac{q_H}{\Omega}\cos\beta_w\right)\right\}$$
$$- \frac{\mu}{4}\left[6a_0\lambda(1-\epsilon) - \frac{a_1 b_1}{2}(1-\epsilon^2) - 3(1-\epsilon)^2 a_0\frac{\dot{a}_0}{\Omega}\right.$$
$$- \frac{7}{4}(1-\epsilon)^2 a_1\left(\frac{\dot{a}_1}{\Omega} + b_1\right) - \frac{5}{4}b_1(1-\epsilon^2)\left(\frac{p_H}{\Omega}\cos\beta_w + \frac{q_H}{\Omega}\sin\beta_w\right)$$
$$\left. - \frac{7}{4}a_1(1-\epsilon^2)\left(-\frac{p_H}{\Omega}\sin\beta_w + \frac{q_H}{\Omega}\cos\beta_w\right) - \frac{5}{4}(1-\epsilon)^2 b_1\left(\frac{\dot{b}_1}{\Omega} - a_1\right)\right]$$
$$\left. - \mu^2[a_0 a_1(1-\epsilon)]\right)$$

moment expressions which are themselves formidable.

Some simplification is possible by considering only the effects of thrust acting normal the tip-path-plane and the applied rolling moment. Table 2-4 presents the overall equations of motion with this reduced number of coupling terms.

Figure 2-2 from Reference 34 illustrates how the rotor-body coupling affects the original rotor response modes. It is clear that the main effects are manifested in the regressing flapping response modes. Further, nearly the same effects would occur using an equivalent first-order lag to model the blade flapping.

Higher order and higher frequency coupling effects must be acknowledged, however. Instead of approximating the y-force as the thrust force tipped through the lateral flapping angle, b_{1_s}, the more complete form contains many more terms. A number of the additional terms represent direct aerodynamic feedbacks. Nevertheless, the dominance of the regressing flapping mode persists and all other tip-path-plane modes remain small.

3. Primary Analysis Model

The above discussion leads to the choice of the following model form to represent important roll-axis handling effects. This model spans a wide spectral range which includes classical hovering cubic effects in the low-frequency spectral range and rotor regressing flapping effects in the high-frequency range. This typically covers frequencies from 0.5 to 15 rad/sec--a range adequate for most handling qualities considerations not concerned with vibration.

The model equations of motion are summarized in Table 2-5. The state variables are lateral flapping angle, b_{1_s}; roll rate, p; and side

Table 2-4

Simplified Model for Helicopter Lateral Dynamics

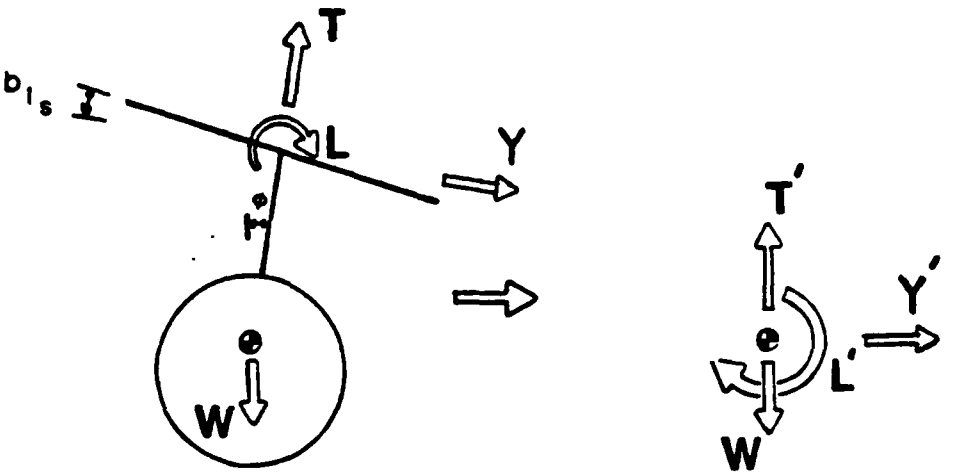

Linearized Equations of Motion

$$m\ddot{y} = Y'$$

$$I_x\dot{p} = L'$$

$$\dot{b}_{1_s} = -\frac{1}{\tau_b} b_{1_s} + \frac{1}{\tau_b}\frac{\partial b_{1_s}}{\partial p} p + \frac{1}{\tau_b}\frac{\partial b_{1_s}}{\partial v} v + \frac{1}{\tau_b} A_{1_s}$$

Rotor Forces and Moments

$$T = \frac{n_b}{2} \rho a c R^3 \Omega^2 \left[\frac{\theta_0}{3} + \frac{\lambda}{2} \right]$$

$$Y = \frac{n_b}{2} \rho a c R^3 \Omega^2 \left[\frac{\theta_0}{3} + \frac{\lambda}{4} \lambda \right] b_{1_s}$$

$$L = \frac{n_b}{2} \left[K_\beta + e M_\beta \Omega^2 \right] b_{1_s}$$

Stability Derivatives

$$\tau_b = \frac{16}{\gamma \Omega}$$

$$\frac{\partial b_{1_s}}{\partial p} = -\tau_b$$

$$\frac{\partial b_{1_s}}{\partial v} = \left[\frac{8\theta_0}{3} + 2\lambda \right]$$

In hover $\lambda = -\sqrt{\frac{C_T}{2}}$

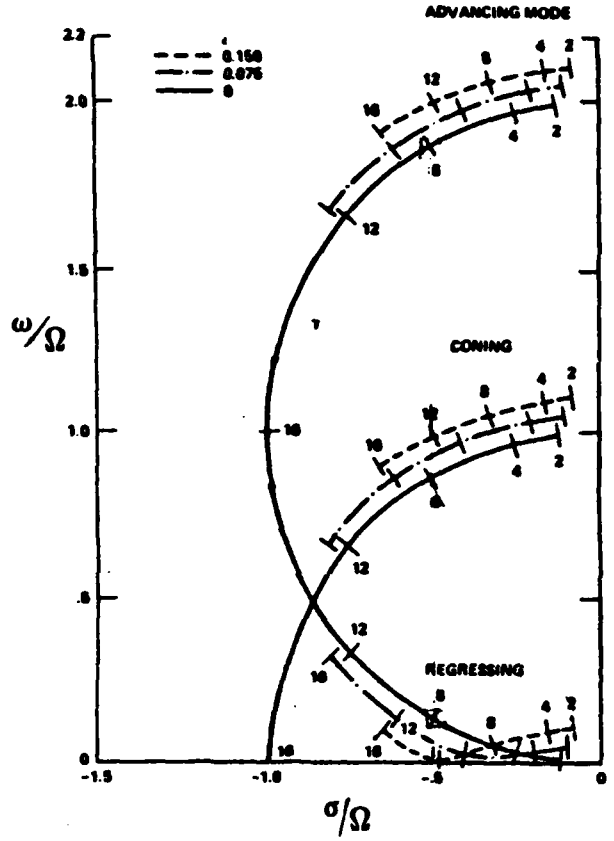

(a) Effect of Hinge Offset and Lock Number

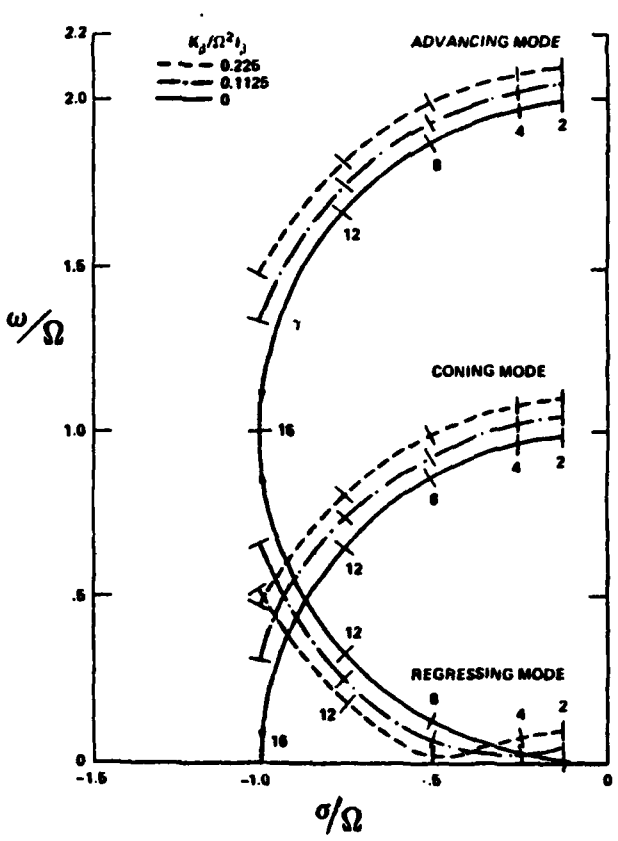

(b) Effect of Hinge Restraint and Lock Number

Figure 2-2. Rotor Body Coupling Effects on the Original Rotor Response Modes from Reference 35

Table 2-5

Definition of Primary Analysis Model Form

Equations of Motion

$$T_b(\dot{b}_{1_s} + p - p_g) + b_{1_s} + \frac{\partial b_{1_s}}{\partial v}(v - v_g) = A_{1_s} \quad \text{(flapping moment)}$$

$$\dot{p} = L_{b_{1_s}} b_{1_s} \quad \text{(hub moment)}$$

$$\dot{v} = g(\phi + b_{1_s}) \quad \text{(side force)}$$

Matrix Form

$$\begin{bmatrix} (T_b s + 1) & T_b & \frac{\partial b_{1_s}}{\partial v} \\ -L_{b_{1_s}} & s & 0 \\ -g & -g/s & s \end{bmatrix} \begin{bmatrix} b_{1_s} \\ p \\ v \end{bmatrix} = \begin{bmatrix} 1 & T_b & \frac{\partial b_{1_s}}{\partial v} \\ 0 & 0 & 0 \\ 0 & 0 & 0 \end{bmatrix} \begin{bmatrix} A_{1_s} \\ p_g \\ v_g \end{bmatrix}$$

Expanded Polynomials

$$\Delta = s^4 + 1/T_b\, s^3 + (L_{b_{1_s}} + \underbrace{\frac{g}{T_b}\frac{\partial b_{1_s}}{\partial v}}_{\text{small}})\, s^2 + \frac{g}{T_b} L_{b_{1_s}} \frac{\partial b_{1_s}}{\partial v}$$

$$N^{p}_{A_{1_s}} = L_{b_1}/T_b\, s^2$$

$$N^{b_{1_s}}_{A_{1_s}} = 1/T_b\, s^3$$

$$N^{v}_{A_{1_s}} = \frac{g}{T_b}(s^2 + L_{b_{1_s}})$$

Transfer Function

$$\frac{\beta}{A_{1_s}}(s) = \frac{[L_{b_{1_s}}/T_b]s}{\underbrace{[s^2 + 1/T_b s + L_{b_{1_s}}]}_{\pm} \quad \underbrace{[s^2 + \frac{g}{T_b}\frac{\partial b_{1_s}}{\partial v}]}_{\pm}}$$

$$\left[\frac{1}{2T_b\sqrt{L_{b_{1_s}}}}\,;\,\sqrt{L_{b_{1_s}}}\right] \quad \left[0\,;\,\sqrt{\frac{g}{T_b}\frac{\partial b_{1_s}}{\partial v}}\right]$$

Note: The factored roots are expressed in short-hand form:

$$(\zeta, \omega_n) \triangleq (s^2 + 2\zeta\omega_n s + \omega_n^2)$$

velocity, v. The four model coefficients include tip-path-plane lag, τ_b; the partial of flapping angle with respect to side velocity, $\frac{\partial b_{1_s}}{\partial v}$; flapping stiffness, $L_{b_{1_s}}$; and the gravity constant, g. Table 2-5 lists all basic transfer function numerator and denominator terms and important approximate factors relationships. Finally in Table 2-6 there is a breakdown of the vehicle configuration features which contribute to the equation of motion coefficients.

Several important features of helicopter roll response should be noted. First, the general response can be viewed as second order, not first order as implied by quasi-static models (i.e., as assumed in References 36 and 37). The effective rotor tip-path-plane lag, represents a kind of control actuator lag. For low flapping stiffness (e.g. teetering rotors) it contributes a control lag in series with the body roll dynamics; for high stiffness designs the flapping and body mode couple to give an oscillatory roll mode. Next, the effective roll rate sensitivity per unit swashplate deflection is a function of tip-path-plane lag and nearly equal to $\gamma\Omega/16$. Further, this relationship appears to be highly linear and, therefore, can be used to estimate maximum control power based on full-throw control authority.

An estimate of unaugmented vehicle bandwidth can be obtained from the above model and is plotted in Figure 2-3. Note that it is nearly linear to the square root of flapping stiffness, $\sqrt{L_{b_{1_s}}}$.

4. Survey of Existing Helicopters

It is instructive to view the characteristics of a variety of existing helicopters. This is done by systematically applying the model form and method for estimating coefficients presented previously.

Table 2-7 lists the basic characteristics for each vehicle followed by computed values of various factors. Although these are estimations,

Table 2-6

Approximate Factors for Primary Analysis Model

Stability Derivatives

$$1/\tau_b = \frac{\gamma\Omega}{16}\left(1 - \frac{8}{3}\frac{e}{R}\right) \qquad \text{(Tip path plane inverse lag)}$$

$$L_{b_{1_s}} = L_{b_{1_s}}^{(t)} + L_{b_{1_s}}^{(h)} + L_{b_{1_s}}^{(s)} \qquad \text{(Total flapping stiffness)}$$

$$L_{b_{1_s}}^{(t)} = \frac{W h_r}{I_x}\left(1 + \frac{\dot{h}}{\Omega R \frac{4C_T}{a\sigma}}\right) \qquad \text{(Thrust re cg)}$$

$$L_{b_{1_s}}^{(h)} = \frac{n_b M_\beta \Omega^2 e}{2 I_x} \qquad \text{(Hinge offset)}$$

$$L_{b_{1_s}}^{(s)} = \frac{n_b K_\beta}{2 I_x} \qquad \text{(Flapping spring)}$$

$$\frac{\partial b_{1_s}}{\partial v} = \frac{2}{\Omega R}\sqrt{\frac{8C_T}{a\sigma}} + \sqrt{\frac{C_T}{2}} \qquad \text{(Dihedral effect)}$$

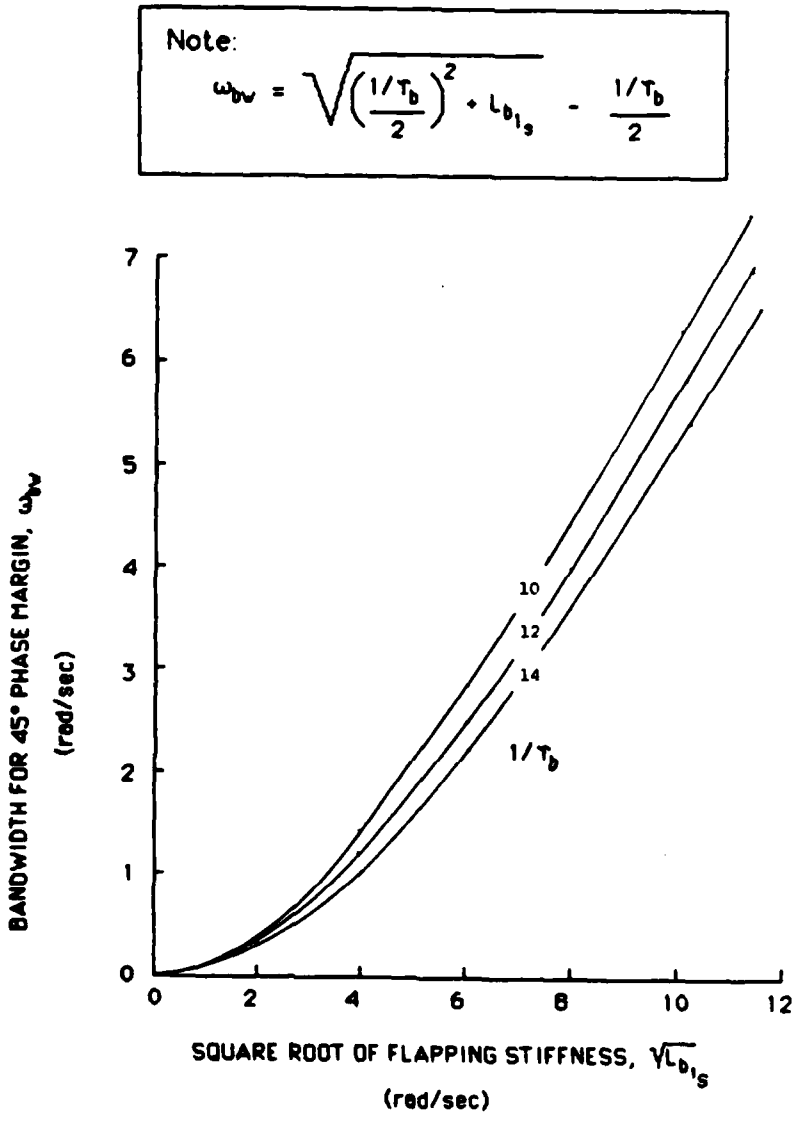

Note: The Definition of Bandwidth Used Throughout This Report is the Frequency at which the Bode Phase Response of the System in Question is 45 Degrees.

Figure 2-3. Relationship Between Unaugmented Vehicle Bandwidth and Flapping Stiffness

Table 2-7. A Survey of Helicopter Lateral Stability and Control Data

AIRCRAFT		Weight W		Roll Inertia I_x		Rotor Height, h_r Front		Rotor Height, h_r Rear		No. of Blades	Hub Type	Rotor Radius R		Rotor Chord c		Hinge Offset e	
		(lb)	(N)	(sl-ft²)	(kg-m²)	(ft)	(m)	(ft)	(m)			(ft)	(m)	(ft)	(m)	(ft)	(m)
Hughes	TH-55	1,600	7,117	207	280	4.4	1.35			3	articulated	12.65	3.86	0.56	0.17	0.18	0.05
Hughes	OH-6A	2,550	11,342	329	445	2.8	0.85			4	articulated	13.17	4.01	0.56	0.17	0.46	0.14
Bell	H-13	2,850	12,677							2	teetering	18.58	5.66	0.92	0.28	0.00	0.00
Bell	OH-58D	3,945	17,547	1,028	1,391	4.7	1.42			4	rigid	17.50	5.33	0.79	0.24	0.51	0.16
Lockheed	L-286	4,100	18,237	1,567	2,121	3.1	0.94			4	rigid	17.50	5.33	0.71	0.22		
Bolkow MBB	BO-105	4,620	20,550	1,330	1,800	5.0	1.52			4	rigid	16.11	4.91	0.89	0.27	1.92	0.59
Piesteki	HUP-1	5,550	24,686	971	1,314	5.3	1.60	8.83	2.082	3	articulated	17.60	5.36	1.085	0.33	0.17	0.05
Sikorsky	H-19	7,100	31,581	850	1,150	6.3	1.93			3	articulated	26.50	8.08	1.37	0.42	0.75	0.23
Bell	UH-1H	8,000	35,584	2,925	3,959	7.0	2.14			2	teetering	24.00	7.32	1.75	0.53	0.00	0.00
Bell	AH-1G	8,000	35,584	2,700	3,654	6.7	2.03			2	teetering	22.00	6.71	2.25	0.69	0.00	0.00
Kaman	SH-2F	11,250	50,040	6,481	8,772	5.4	1.65			4	articulated	22.00	6.71	1.80	0.55	0.69	0.21
Sikorsky	H-34	11,867	52,784	5,895	7,979	8.0	2.44			4	articulated	28.00	8.53	1.37	0.42	1.00	0.30
Aerospatiale	SA 330	12,600	56,045	6,380	8,635	7.1	2.15			4	articulated	24.61	7.50	1.75	0.53		
Hughes	AH-64	15,000	66,720	5,930	8,026	6.0	1.84			4	articulated	24.00	7.32	1.75	0.53	0.92	0.28
Sikorsky	UH-60A	16,400	72,947	5,629	7,619	5.7	1.72			4	articulated	26.83	8.18	1.73	0.53	1.25	0.38
Boeing-Vertol	YUH-61A	15,157	67,418		0					4	rigid	49.00	14.94		0.00		
Sikorsky	SH-3	17,640	78,463	13,480	18,245	7.5	2.28			5	articulated	31.00	9.45	1.52	0.46	1.05	0.32
Boeing-Vertol	CH-46E	20,800	92,518	16,211	21,942	5.6	1.70	10.2	3.097	3	articulated	25.50	7.77	1.56	0.48	0.43	0.13
Sikorsky	CH-54	25,000	111,200	17,100	23,145	5.2	1.59			6	articulated	36.00	10.97	1.97	0.60	2.00	0.61
Boeing-Vertol	CH-47B	33,000	146,784	34,000	46,019	7.5	2.28	12.2	3.706	3	articulated	30.00	9.14	2.10	0.64	0.67	0.20
Sikorsky	CH-53D	35,000	155,680	36,116	48,883	7.8	2.37			6	articulated	36.12	11.01	2.17	0.66	2.00	0.61
Boeing-Vertol	XCH-62A	120,000	533,760	266,820	361,141	8.2	2.50	18.8	5.721	4	articulated	46.32	14.12	3.36	1.02	2.18	0.67

Table 2-7 Continued.

Aircraft	Flapping Inertia I_β		Mass Moment M_β		Flapping Stiffness K_β		Delta 3 δ_3	Swashplate Front	Swashplate Rear	Lateral Stick Throw		RPM	Omega Ω	Locke No. γ	Swashplate Gearing		$\frac{\gamma\Omega}{16}$
	(sl-ft^2)	(kg-m^2)	(sl-ft)	(kg-m)	(ft-lb/r)	(N-m/r)	(deg)	(deg)		(in)	(cm)		(rad/s)		(deg/in)	(deg/cm)	(1/sec)
TH-55	44	60	4.6	21.3	0	0	0	-7.0	5.0	12.0	30.5	477	50.0	4.4	1.00	0.39	13.8
OH-6A	47	63	5.9	26.4	0	0	0	-7.3	6.3	11.5	29.2	483	50.6	4.9	1.17	0.46	15.5
H-13					0	0	0				0.0	355	37.2				
OH-58D	143	194	12.3	54.5	11,290	15,309	28	-8.4	8.4	12.0	30.5	238	24.9	7.0	1.40	0.55	10.9
L-286	231	313					0			7.0	17.8	355	37.2	3.9			9.0
BO-105	142	192	10.3	45.6	6,900	12,088	-5	-5.7	4.3	8.7	22.0	424	44.4	5.7	1.16	0.46	15.8
HUP-1	164	222	12.0	52.9	0	0	0					270	28.3	8.6	0.71	0.71	15.2
H-19	923	1,259	54.1	239.7	0	0	3	11.0	11.0			210	22.0	9.9			13.6
UH-1H	1,211	1,641	76.0	336.0	0	0	0	-10.0	10.0	12.6	32.1	324	33.9	8.5	1.58	0.62	13.8
AH-1G	1,382	1,873	94.0	416.0	0	0	0	-9.0	9.0	10.8	27.5	324	33.9	5.2	1.66	0.65	11.0
SH-2F	1,148	1,556	76.3	339.1	0	0	0			11.2	28.4	300	31.4	5.0			9.8
H-34	1,145	1,552	63.0	280.2	0	0	0	-8.0	8.0	14.0	35.6	222	23.2	9.9	1.14	0.45	14.4
SA 330	1,112	1,507	68.0	302.4	0	0	0					265	27.8	7.8			13.6
AH-64	952	1,290	64.0	284.6	0	0	0	-10.5	7.0	9.0	22.9	289	30.3	8.3	1.94	0.77	15.6
UH-60A	1,490	2,020	83.0	369.1	0	0	0	-8.0	8.0	10.0	25.4	258	27.0	8.2	1.60	0.63	13.8
YUH-61A																	
SH-3	1,706	2,312	89.5	398.0	0	0	0	-9.1	6.9	14.0	35.6	203	21.3	11.2	1.14	0.45	14.8
CH-46E	1,174	1,591	74.3	330.4	0	0	0	-8.8	8.8	9.2	23.4	264	27.6	7.6	1.91	0.75	13.2
CH-54	3,500	4,744	160.6	714.2	0	0	0					185	19.3	12.8		0.00	15.5
CH-47B	2,700	3,660	144.7	643.5	0	0	0	-8.0	8.0	8.4	21.2	230	24.1	8.8	1.91	0.75	12.9
CH-53D	4,046	5,484	184.3	819.6	0	0	0	-7.8	4.7	8.9	22.6	185	19.4	12.3	1.38	0.54	14.9
XCH-62A	16,932	22,951	578.0	2,570.4	0	0	0					155	19.4	12.4			15.0

Table 2-7 Continued

Aircraft	$\frac{1}{\tau_b}$	$L_{b_{1_s}}$ (a)	$L_{b_{1_s}}$ (a)	$L_{b_{1_s}}$ (a)	$L_{b_{1_s}}$	L_p (b)	L_p	Solidity σ	C_T	$\frac{C_T}{\sigma}$	$\frac{\partial b_{1_s}}{\partial v}$	L_v	ω_n Hover Cubic	Source
	(sec^{-1})	($1/s^2$)	($1/s^2$)	($1/s^2$)	($1/s^2$)	(rad/s)	(rad/s)				(rad/fps)	(rad/s/ft)	(rad/s)	
TH-55	13.3	34.2	15.6	0.0	49.8	-0.2	-3.91	0.043	0.0034	0.0789	0.000480	-0.0239	0.45	R. Prouty (Hughes data)
OH-6A	14.0	21.5	42.3	0.0	63.9	-0.4	-4.98	0.054	0.0044	0.0816	0.000485	-0.0310	0.47	NASA CR-3144 (Hughes data)
H-13								0.031	0.0023	0.0740	0.000400			Jane's
OH-58D	10.1	17.9	7.5	22.0	47.4	-0.2	-4.93	0.057	0.0091	0.1577	0.001323	-0.0627	0.66	C. Bivins, AVRADCOM (ARC Armcop)
L-286	9.0	8.1	0.0	0.0	8.1	0.0	-0.89	0.052	0.0042	0.0822	0.000496	-0.0040	0.38	Lockheed
BO-105	10.8	17.4	58.3	13.4	89.1	-1.1	-9.34	0.070	0.0047	0.0685	0.000396	-0.0353	0.37	NASA CR-3144, Pseudor DFVLR Fit ID update.
HUP-1	14.8	34.5	4.9	0.0	44.4	-0.1	-3.09	0.059	0.0097	0.1643	0.001205	-0.0535	0.76	STI TR 128, H. C. Curtiss data.
H-19	12.8	53.0	34.7	0.0	87.7	-1.7	-8.84	0.049	0.0040	0.0809	0.000542	-0.0476	0.47	STI TR 128, H. C. Curtiss, Princeton Rept 395, 1957.
UH-1H	13.8	19.2	0.0	0.0	19.2	0.0	-1.39	0.046	0.0028	0.0604	0.000300	-0.0058	0.36	NASA CR-3144 (C-81 estimate)
AH-1G	11.0	19.7	0.0	0.0	19.7	0.0	-1.6	0.065	0.0040	0.0610	0.000349	-0.0089	0.35	NASA CR-3144 (C-81 estimate)
SH-2F	9.0	9.4	16.0	0.0	25.4	-0.3	-3.12	0.104	0.0065	0.0625	0.000419	-0.0106	0.35	R. Nave, NADC
H-34	13.1	16.1	11.6	0.0	27.7	-0.5	-2.65	0.062	0.0048	0.0770	0.000482	-0.0133	0.45	Seckel, "Stability and Control of Aircraft"
SA 330	13.6	13.9	0.0	0.0	13.9	0.0	-1.03	0.091	0.0060	0.0660	0.000431	-0.0060	0.43	
AH-64	14.0	15.3	18.2	0.0	33.4	-0.5	-2.9	0.093	0.0066	0.0713	0.000434	-0.0145	0.44	R. Prouty (Hughes data)
UH-60A	12.0	16.5	26.9	0.0	43.3	-0.9	-4.5	0.082	0.0058	0.0708	0.000423	-0.0183	0.41	K. Hilbert, NASA (Armcop model)
YUH-61A									0.0000					
SH-3	13.5	9.8	7.9	0.0	17.7	-0.4	-1.71	0.078	0.0056	0.0723	0.000488	-0.0083	0.45	J. Phillips NASA ARC
CH-46E	12.6	10.1	4.5	0.0	14.6	-0.1	-1.29	0.058	0.0086	0.1476	0.000774	-0.0113	0.56	R. Nave, NADC
CH-54	13.2	7.8	21.1	0.0	28.7	-1.4	-3.58	0.105	0.0053	0.0510	0.000354	-0.0102	0.39	J. Phillips, NASA
CH-47B	12.1	9.5	4.9	0.0	14.5	-0.2	-1.38	0.067	0.0094	0.1404	0.000735	-0.0106	0.54	K. Hilbert, NASA (ARC simulator model)
CH-53D	12.7	7.5	11.5	0.0	19.0	-0.7	-2.23	0.115	0.0073	0.0641	0.000430	-0.0082	0.42	NASA CR-3144 (GEMHEL data)
XCH-62A	13.1	8.1	7.1	0.0	13.2	-0.5	-1.48	0.092	0.0093	0.1008	0.000467	-0.0061	0.44	AHS Preprint 843, 3U ton design point

they are nevertheless based on a consistent set of assumptions and computational methods. The following is a brief discussion of some of the more notable features of this survey.

Vehicle Size. A wide range of vehicle size is spanned from the light Hughes TH-55 (Model 269) to the Sikorsky CH-53D transport helicopter.

Rotor Hub Type. The designs represented include teetering, articulated, and rigid hubs. Both conventional single rotor designs as well as tandems are included. All are described in terms of the model previously presented. This requires that the rigid rotors be described in terms of an equivalent hinge offset and flapping spring.

Lock Number RPM Product. One notable feature of nearly all the designs is the narrow range of the Lock number-RPM product (all in the vicinity of 220). Since this is the main determinant of effective tip-path-plane lag, it can be concluded that wide experimental variations in this parameter are of little practical interest. An inspection of the estimated tip-path-plane break frequency shows a range of only 10 to 14 rad/sec.

Effective Flapping Stiffness. Three components of this are estimated: that due to the hub relative to the center of gravity $L^{(t)}_{b_{1_s}}$, that due to hinge offset $L^{(h)}_{b_{1_s}}$, and that due to an effective hinge flapping spring $L^{(s)}_{b_{1_s}}$. These components are plotted in Figure 2-4. The magnitudes vary substantially (from about 15 to 80) thus reflecting a wide range of vehicle short-term response. This suggests that flapping stiffness should be a primary experimental variable with regard to configuration.

Dihedral Effect. This feature varies over a large range, but when viewed in terms of the natural frequency of the hovering cubic there is a suprisingly narrow range. This represents another feature which, when viewed in terms of practical designs, appears to be of little interest

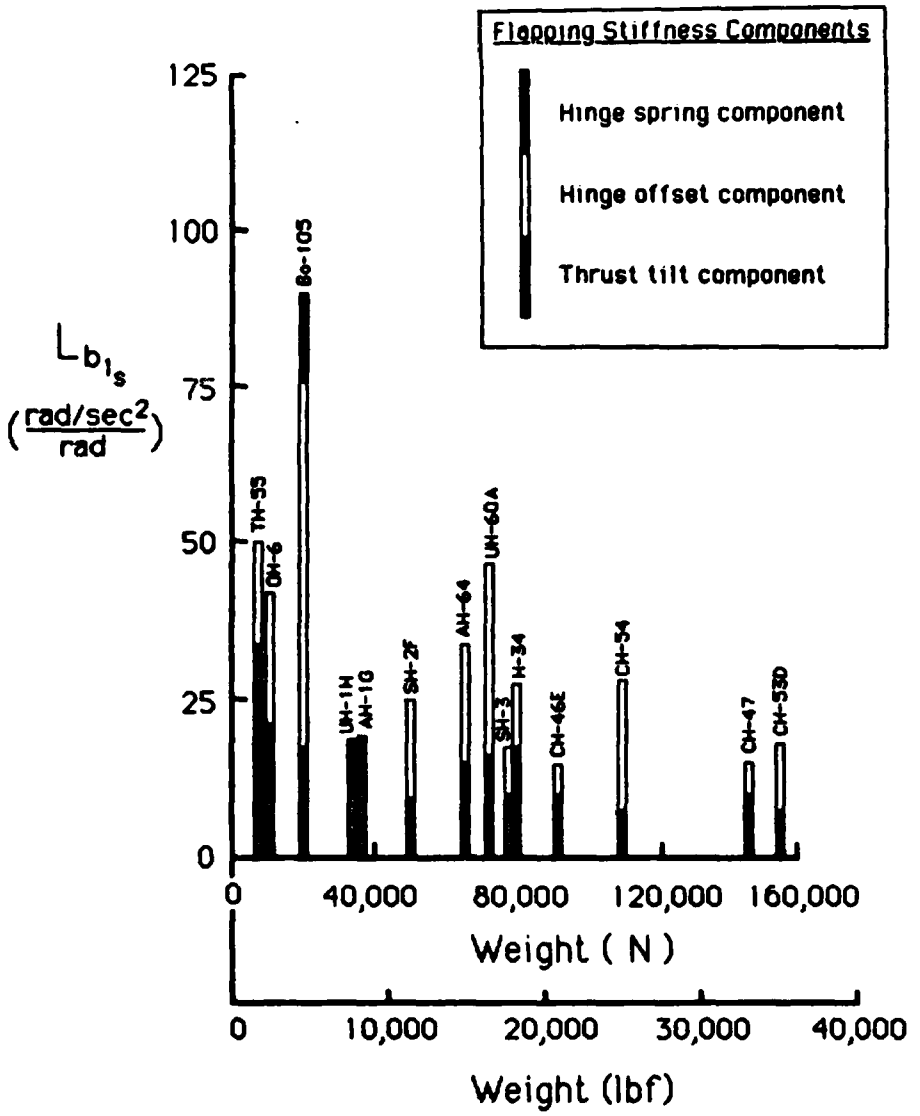

Figure 2-4. Components of Flapping Stiffness for a Survey of Helicopters

in terms of experimental variation.

Comparison with Higher Order Models. Table 2-8 lists a set of transfer functions computed for higher order flapping effects. This shows first that the advancing flapping mode is far above the range of interest to handling qualities. Next the table indicates the goodness of a simple approximation for the effective tip-path-plane lag.

Summary of Roll-Axis Response Trends. Figure 2-5a shows the locations of dominant short-term unaugmented response modes for a variety of helicopters. For low values of flapping stiffness, there is a conventional first-order roll damping mode. For large values of flapping stiffness the first-order pole joins with the tip-path-plane lag to form a dominant second order response mode. This trend is summarized in Figure 2-5b. An additional feature noted is loss of damping for roll-rate feedback augmentation systems where there is some significant lag or digital delay. This general effect is discussed in detail in Reference 38 and is backed up by actual flight measurements involving variable stability helicopters. The main implications of these trends for the study conducted here are the indication of vehicle response ranges that are of practical importance to helicopter design. This is reflected in the experimental simulator investigation as described in Section IV.

B. Effects of the Pilot-in-the-Loop

The following discussion describes the effects of basic pilot loop closures on the vehicle flight dynamics. This provides a theoretical basis for subsequent analysis of flight tasks and maneuvers.

1. Inner-Loop Control and Regulation of Roll Attitude

The most fundamental role of the pilot is to stabilize and control

Table 2-8

Lateral Transfer Functions Containing High Order Flapping Effects

Aircraft	$\frac{P(s)}{A_{1_s}(s)}$	$\left[\frac{P(s)}{A_{1_s}(s)}\right]_{SS}$	$\frac{\gamma\Omega}{16}\left[1-\frac{8\epsilon}{3}\right]$
TH-55	$\frac{468.0\ (13.5)\ (0.05,120.0)}{(0.94,7.4)\ (12.8)\ (0.13,99.0)}$	13.2	13.4
OH-6A	$\frac{325.0\ (14.2)\ (0.08,177.0)}{(0.84,8.5)\ (14.1)\ (0.14,102.0)}$	13.7	14.1
BO-105	$\frac{289.0\ (13.0)\ (-0.18,258.0)}{(0.43,13.9)\ (12.8)\ (0.13,93.0)}$	11.7	11.4
UH-1H	$\frac{265.0\ (14.5)\ (0.10,66.4)}{(1.5)\ (0.97,13.4)\ (0.21,66.4)}$	13.8	13.9
AH-1G	$\frac{217.0\ (11.3)\ (0.08,66.9)}{(2.2)\ (0.99,10.1)\ (0.16,66.9)}$	11.1	11.0
H-34	$\frac{227.0\ (13.8)\ (0.12,60.2)}{(2.9)\ (0.95,12.3)\ (0.29,45.1)}$	12.9	13.1
AH-64	$\frac{232.0\ (14.5)\ (0.11,90.0)}{(3.4)\ (0.98,12.7)\ (0.24,60.0)}$	13.8	14.1

Note: The factored numerator and denominator are shown in the short-hand form:

$$(\theta) = (s + \theta), \quad (\zeta, \omega_n) = (s^2 + 2\zeta\omega_n s + \omega_n^2)$$

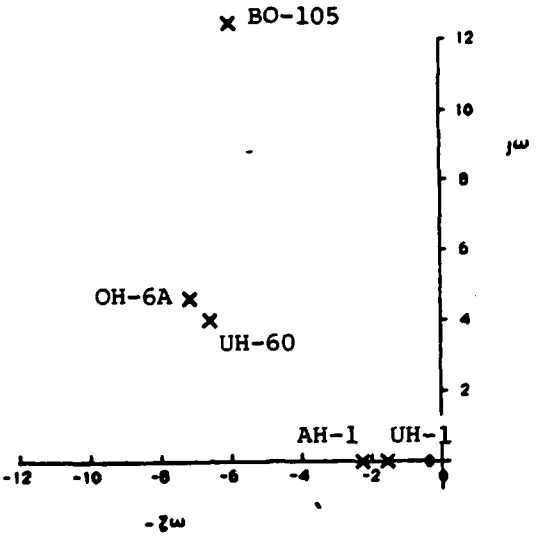

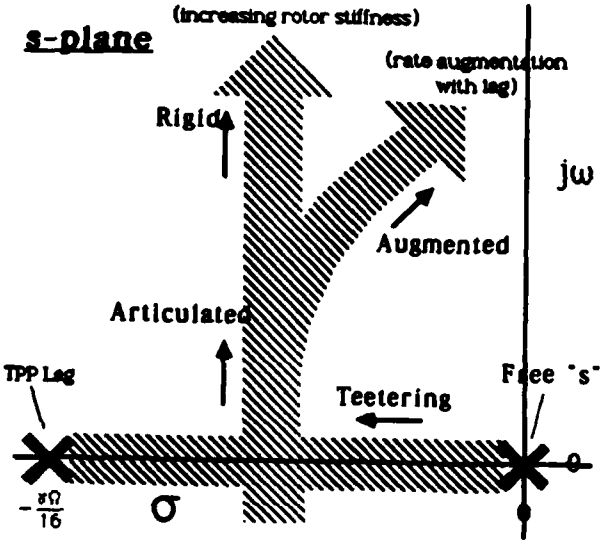

Figure 2-5. Short-Term Eigenvalue Locations as a Function of Flapping Stiffness.

roll attitude. Without an automatic roll stabilization system there is no natural roll attitude preference or restoring moment (except for very weak ground effects). Beyond that, roll attitude command is a basic supporting element for most lateral flight path tasks and maneuvers.

A generic view of bank-angle loop closures is shown in Figure 2-6 for two cases, one having a small amount of roll damping (flapping stiffness) and the other a large amount. Note that this includes both the short-term response (consisting of roll damping and tip-path-plane lag effects) and the low-frequency hovering cubic (phugoid-like effect).

The general effect of an attitude loop closure is to stabilize and damp all response modes within the bandwidth limitations of the aircraft. Where closed-loop response demands exceed the vehicle bandwidth as in Figure 2.6a, the pilot must begin to supply significant amounts of "lead compensation". This is equivalent to the inclusion of roll rate in the basic attitude feedback and normally has an associated cost in terms of pilot workload.

The net result of an attitude loop is to provide an attitude command support function for a number of basic flight tasks. The response of this command is determined by the tightness of the attitude loop and must be quick enough to satisfy the demands of the outer-loop flight task. This task might be control of position, side velocity, heading, or possibly lateral acceleration.

2. Outer-Loop Control of Velocity and Position

As indicated above, the control and regulation of lateral velocity and position should be viewed in the context of an inner roll attitude loop. This is not only realistic but also serves to simplify the essential equations of motion and response characteristics.

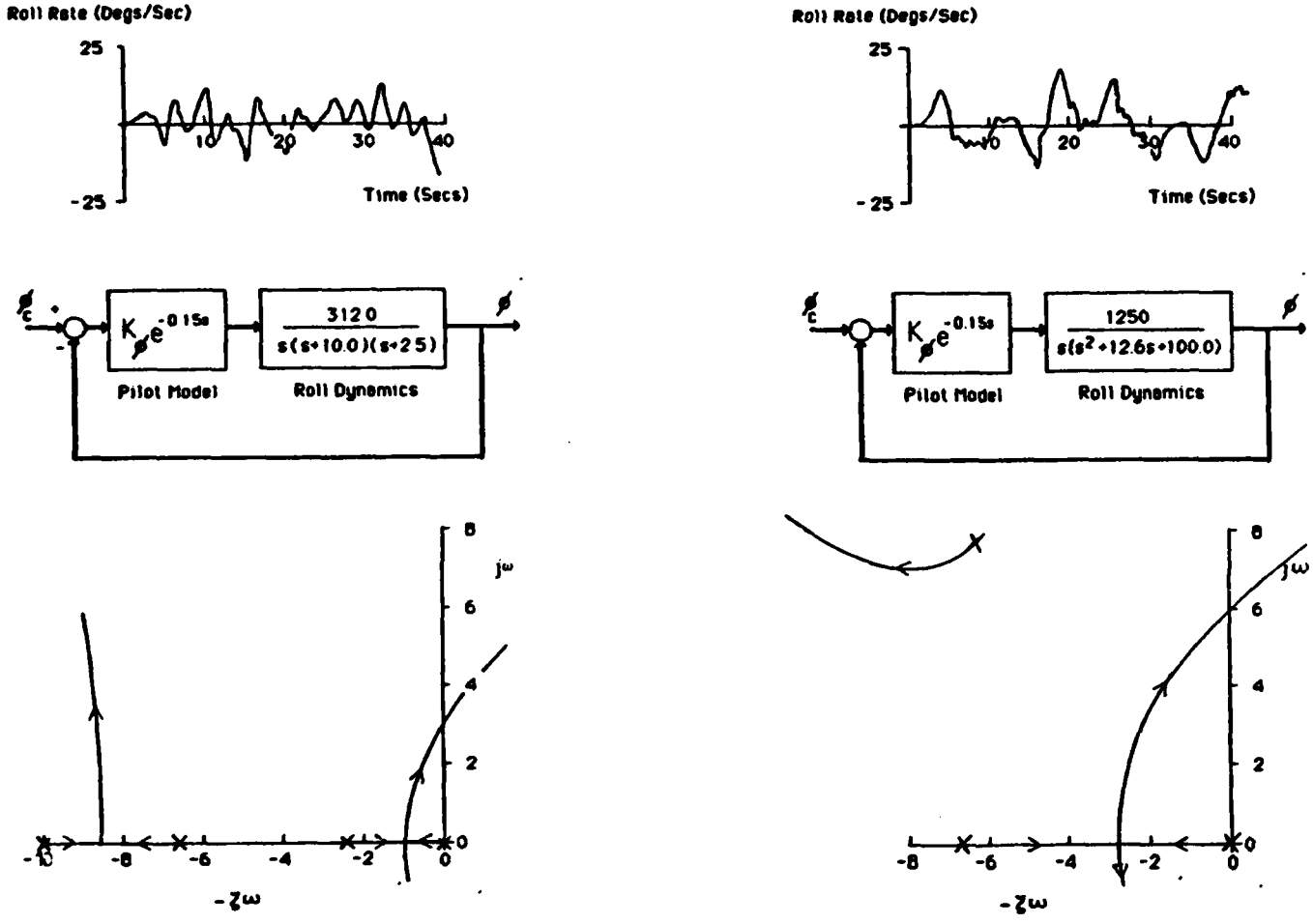

(a) Case $L_p = -2.0$

(b) Case $L_p = -8.0$

Figure 2-6. Inner Loop Attitude Closures for Various Roll Damping Values

The "control" for the outer-loop task should be viewed as the inner-loop bank angle command (not the lateral cyclic input, per se). The vehicle dynamics important to the outer loop are therefore represented by the "ratio of numerators" of the outer-loop task variable (e.g., y-position or turn rate) and bank angle. Frequently this is approximated well by simple kinematic relationships (see Reference 37).

The important implications are that the pilot demands on bank angle control (i.e., roll control effectiveness) depend heavily on the nature of the outer-loop task. If there is no outer loop task, roll control and regulation can be far less crucial than if there is a tight lateral position holding task. To be more general, roll control requirements are dependent upon the outer-loop task. Further the task should be well quantified if quantification of the roll characteristics are expected.

C. Discrete Maneuver and Task Performance Capability Modeling

1. Discrete Flight Maneuver Modeling

Pilot-in-the-loop analysis is made more relevant by consideration of discrete flight maneuvers rather than viewing only long-term continuous tracking tasks. The following discussion reviews some of the aspects of discrete-maneuver modeling and analysis techniques.

A discrete maneuver is one in which there is a single identifiable command. This applies not only to the outer-loop task, but also to the inner support loop. A lateral sidestep is an example of a discrete maneuver involving a distinct, identifiable command in lateral position. However, in the process of performing this, there will be a series of two or more discrete commands of bank angle. The first change in bank angle starts the lateral translation, and the second is usually a bank in the opposite direction to arrest the sideward velocity. A third bank-angle command to nearly level attitude might then be made in order

to maintain the new commanded position. Each command might typically occur every three or four seconds, and the closed-loop response to a command need be only about one half cycle of the dominant mode of the bank angle task. Finally, bank angle commands may not be very periodic. Some of these features are illustrated in a timing diagram of an actual sidestep maneuver as shown in Figure 2-7. The term "timing diagram" is used because of the resemblance to the sequence of commands of a digital computer software timing sequence. The outer-loop lateral position commands correspond to a kind of slow duty cycle while the inner-loop bank angle commands occur much more frequently. However, a typical flight task may involve only a few cycles of commands, and it is therefore necessary to use response identification techniques which will work over a fairly short sample.

Discrete maneuver behavior can be better analyzed as a "sampled-data" system than as a traditional continuous control system. However, the analysis of any single discrete maneuver occurrence can still be done in conventional continuous control terms.

One of the benefits of viewing manual control as a series of discrete maneuvers is that each maneuver element can be considered separately. There is not the need to treat long sequences of control activity in order to achieve an identification of system parameters and performance. In fact, assuming a series of discrete maneuver activity to be continuous behavior can lead to significant distortions and obscure or average out important events. This is especially true if there are dwell periods during one flight task when the pilot is perhaps attending to another flight task.

The analysis of discrete maneuver activity can be a relatively simple process. One method for handling individual short-term discrete maneuvers is illustrated in Figure 2-8. If the features of a roll maneuver are to be studied, the first step is simply to obtain time

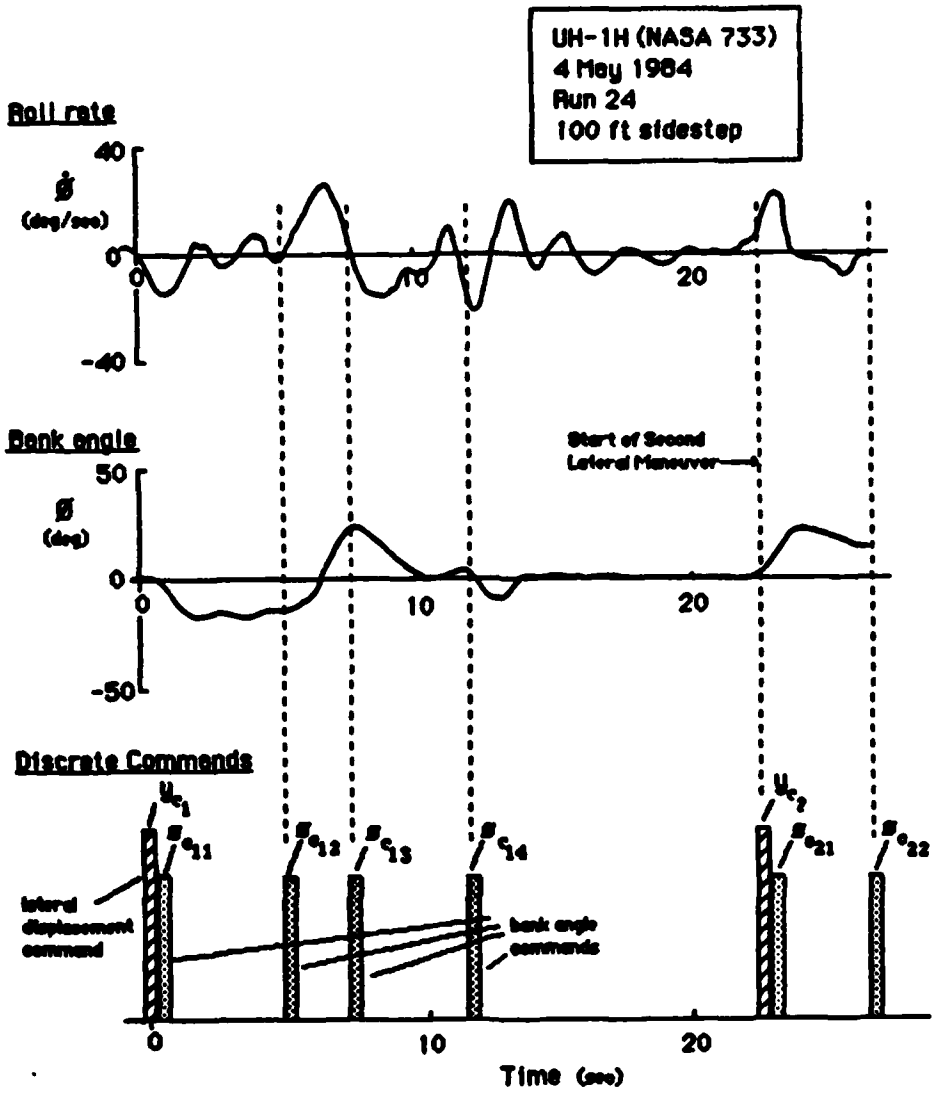

Figure 2-7. A timing Diagram for a Typical Helicopter Sidestep Maneuver.

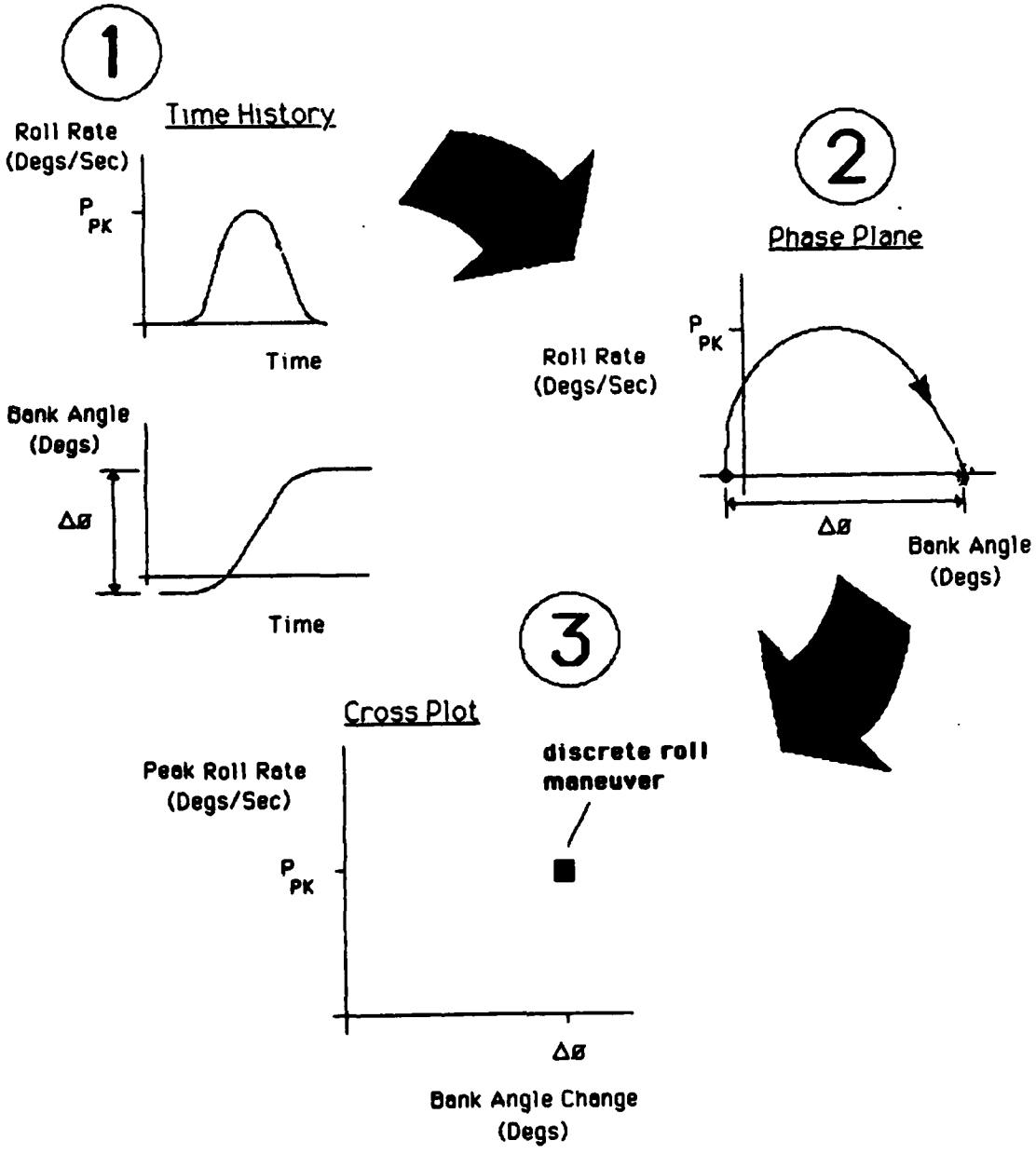

Figure 2-8. Analysis Technique for Discrete Roll Maneuver Data.

history information which indicates the magnitudes of roll rate and corresponding bank angle change. Alternatively, this can be expressed on a phase-plane portrait in which case two important features can be clearly seen: (1) The net bank angle change and (2) the peak roll rate during that change. Finally, these two features can be cross-plotted in a discrete maneuver performance diagram to yield a concise summary of a single discrete maneuver task execution.

Roll rate versus net bank angle change can be interpreted in at least two ways. First, as explained in Reference 17, the proportion of peak rate to the net change in displacement is proportional to closed-loop natural frequency or approximate bandwidth. For a broad range of closed-loop damping ratios, the bandwidth is about twice the ratio of peak rate to the net command. Table 2-9 defines this relationship for an ideal second order system. Reference 39 provides a further discussion of this relationship. The implications of system closed-loop bandwidth on the discrete maneuver performance diagram are clearly illustrated in Figure 2-9.

Using this method a unique task signature can be constructed for each maneuver. The maneuver time history data is examined and for each attitude change identified the associated peak roll rate is determined. These discrete maneuver data point pairs are then plotted on the discrete maneuver performance (peak roll rate versus attitude change) diagram to form the task signature. Figure 2-10 illustrates this process for an air combat tracking task.

To quantify the task signature two metrics have been chosen: the amplitude and the aggressiveness. The amplitude is represented by two parameters the maximum peak roll rate, p_{PK}, and the maximum commanded bank angle change, $\Delta\phi_{c_{max}}$; both parameters are shown in Figure 2-11. The aggressiveness parameter is a measure of the maximum closed-loop bandwidth sought, by the pilot in making precision attitude control.

Table 2-9. Relationship Between Peak Rate/ Attitude Change and Ideal Second Order System Parameters

Ideal Second Order System

$$\frac{\phi}{\delta_\phi}(s) = \frac{K}{S^2 + 2\zeta\omega_n S + \omega_n^2}$$

Response Characteristics to a Step Input

$$\frac{\omega_n}{p_{PK}/\Delta\phi} = \frac{\sqrt{1-\zeta^2} - \exp\left(\frac{-\zeta\pi}{\sqrt{1-\zeta^2}}\right)\cos(\pi-\theta)}{\exp\left(\frac{-\zeta\pi}{\sqrt{1-\zeta^2}}(0.5-\theta)\right)\sin(\pi(0.5-\theta))}$$

$$\frac{\omega_{bw}}{p_{PK}/\Delta\phi} = \left\{\zeta + \sqrt{1-\zeta^2}\right\}\frac{\omega_n}{p_{PK}/\Delta\phi}$$

$$\theta = \tan^{-1}\left\{\frac{-\zeta\pi}{\sqrt{1-\zeta^2}}\right\}$$

Note: ω_{bw} is the frequency at which the phase margin of the second order system is 45 degrees

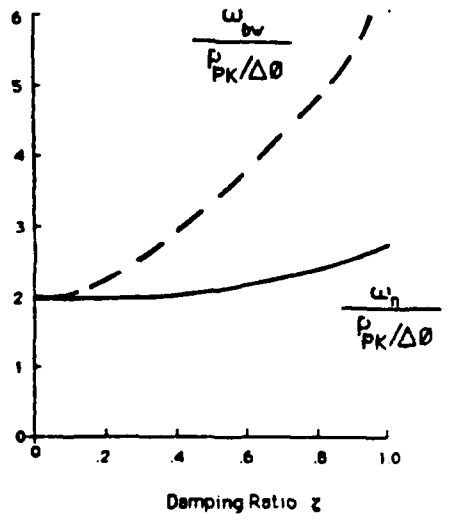

Ideal Second Order System

$$G(s) = \frac{\phi}{\delta_A}(s) = \frac{\omega_n^2}{S^2 + 2\zeta\omega_n S + \omega_n^2} \qquad \zeta = 0.707$$

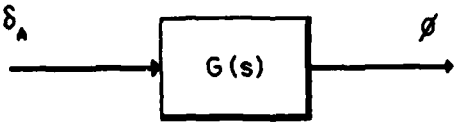

Phase Characteristics for ω_n = 1.0, 2.0 and 4.0 rads/sec ζ = 0.707

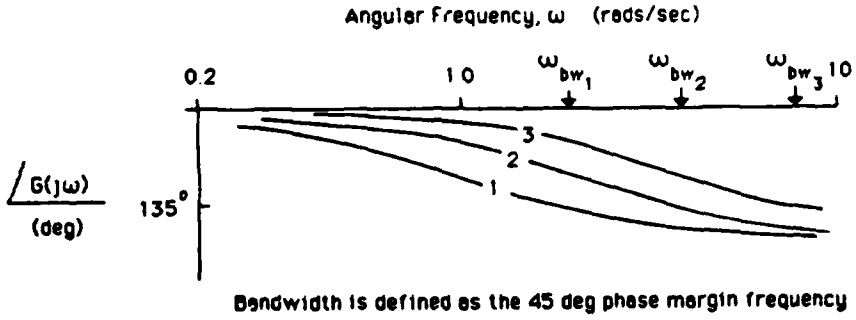

System Maneuver Performance Characteristics

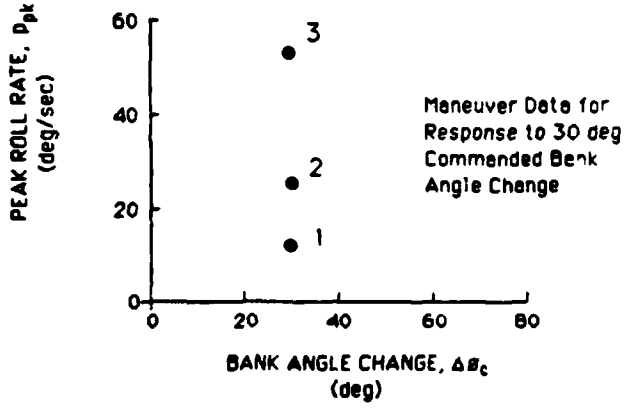

Figure 2-9. Illustration of System Bandwidth Effects on the Maneuver Performance Diagram

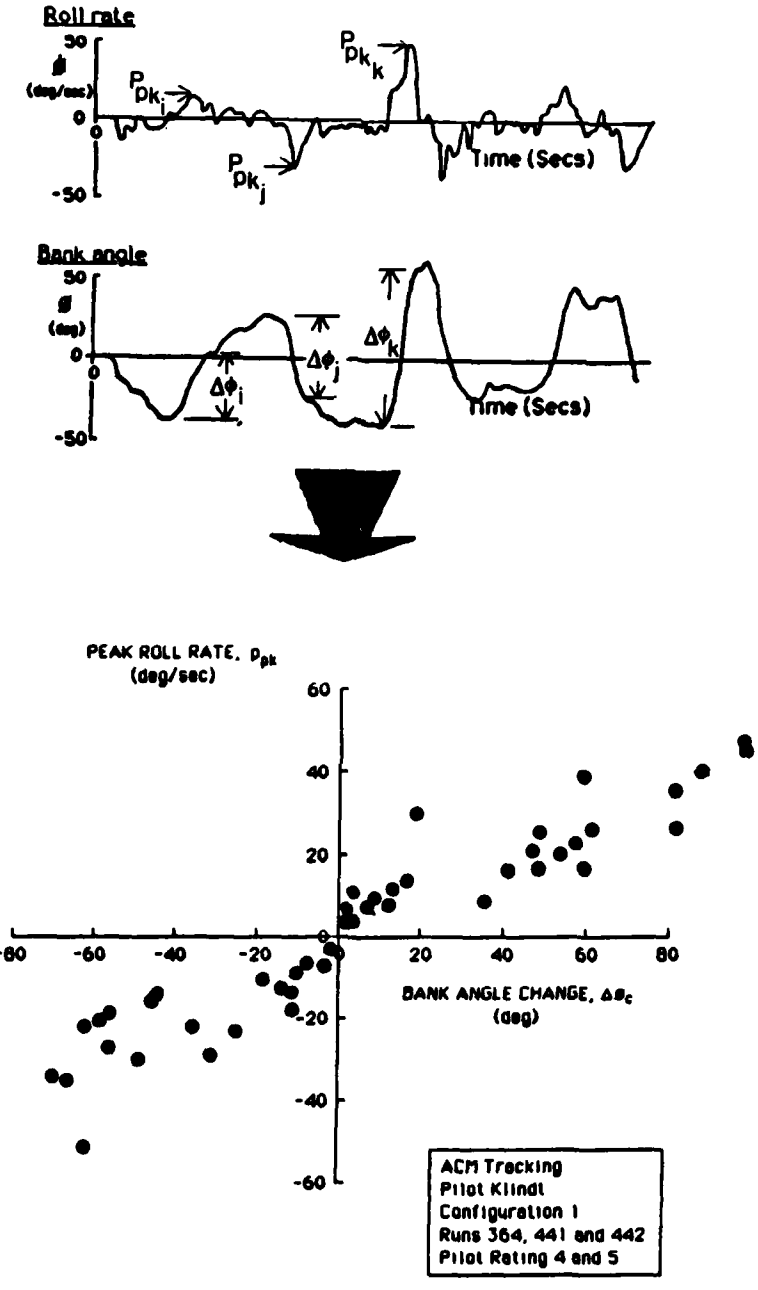

Figure 2-10. Definition of the "Task Signature" from Discrete Maneuver Time Histories

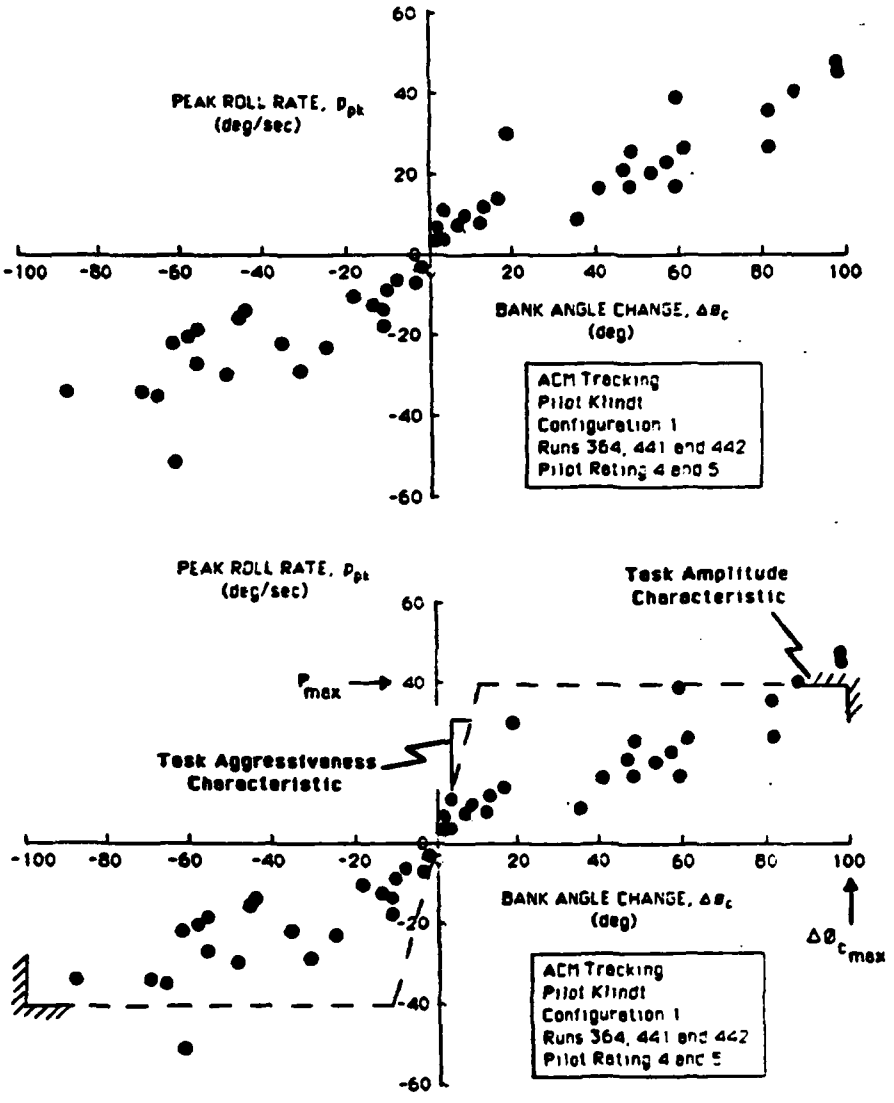

Task Performance Characteristics

Amplitude: P_{max} , $\Delta\phi_{c_{max}}$

Aggressiveness: Identified natural frequency and damping ratio for precision attitude control data point pairs

Figure 2-11. Quantification of Task Demand

This is quantified through identification of an equivalent second order model for small attitude changes; the resulting parameters are the identified natural frequency and damping ratio. This approach allows definition of a limit of task demands unique to each maneuver. This is illustrated in Figure 2-11.

2. Defining Maximum Task Performance Capability

The objective is to define an upper bound on closed-loop task performance capability for given vehicle dynamics. In helicopter lateral control the key design parameters are: swashplate authority, A_{1_s}, and rotor stiffness, $L_{b_{1_s}}$.

The maximum task performance capability is assumed to correspond to maximum bandwidth operation in the closed loop. This is associated with a switching control strategy on the part of the pilot. For the class of vehicle dynamics involved here it is proposed that the maximum (bandwidth) capability can be defined using a family of square wave inputs of different dwell times T_1 and amplitude equal to the swashplate authority, A .

The appropriate class of vehicle dynamics are:

$$\frac{p}{A_{1_s}}(s) = \frac{\frac{1}{\tau_b} L_{b_{1_s}}}{s^2 + \frac{1}{\tau_b} s + L_{b_{1_s}}} = \frac{K}{s^2 + 2\zeta\omega_n s + \omega_n^2}$$

The response characteristics to a square wave input are defined in Figure 2-12. Because the low order model involved closed-form solutions can be obtained for those characteristics, these are summarized in Table 2-10.

For an articulated rotor helicopter, with roll rate capability of approximately 17 deg/sec/stick inch, the appropriate dynamics are:

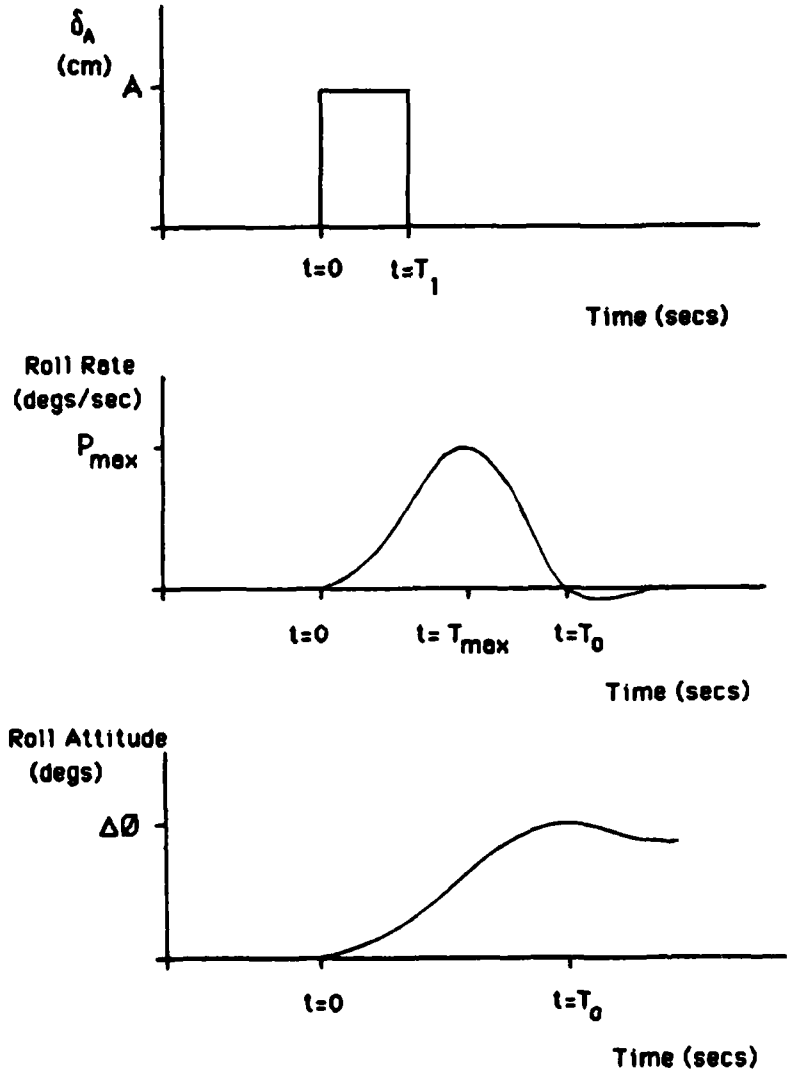

Figure 2-12. Characteristics of Square Wave Input Response for a Second Order System

Table 2-10

Summary of Second Order System Response Characteristics to Square Wave Inputs

Time to Maximum Roll Rate

If $T_{max} < P/2$ then

$$T_{max} = \tan^{-1}\left[\frac{\sin(\omega_d T_1)}{\cos(\omega_d T_1) - \exp(-\zeta\omega_n T_1)}\right] / \omega_d$$

else $T_{max} = P/2$

Time to Maximum Roll Attitude

$$T_O = \tan^{-1}\left[\frac{\cos(\omega_d T_1 + \theta) - \exp(-\zeta\omega_n T_1)\cos(\theta)}{\exp(-\zeta\omega_n T_1)\sin(\theta) - \sin(\omega_d T_1 + \theta)}\right] / \omega_d$$

where

$$\theta = \tan^{-1}\left(\frac{\zeta}{\sqrt{1-\zeta^2}}\right)$$

$$\omega_d = \omega_n\sqrt{1-\zeta^2}$$

$$P = 2\pi/\omega_d$$

Peak Roll Rate

$$P_{max} = \frac{AK}{\omega_n^2}\left[\exp(\zeta\omega_n T_1)\cos(\omega_d(T_{max} - T_1) - \theta) - \cos(\omega_d T_{max} - \theta)\right]\frac{\exp(-\zeta\omega_n T_{max})}{\sqrt{1-\zeta^2}}$$

Maximum Attitude Change

$$\Delta\theta = \frac{KA}{\omega_n^2}\left\{T_1 + \frac{\exp(-\zeta\omega_n T_O)}{\omega_d}\right.$$

$$\left\{2\zeta\left[\cos(\omega_d T_O + \theta) - \exp(\zeta\omega_n T_1)\cos(\omega_d(T_O - T_1) - \theta)\right]\right.$$

$$\left.\left.+\left[4\zeta^2 - 1\right]\left[\sin(\omega_d T_O) - \exp(\zeta\omega_n T_1)\sin(\omega_d(T_O - T_1))\right]\right]\right.$$

$$\frac{p}{A_{1_s}}(s) = \frac{736.0}{s^2 + 10.3\,s + 45}$$

The resulting maximum bandwidth capability (from Table 2-10) can be computed as a function of swashplate authority, A , the results appear in Figure 2-13.

It is noted that the highest bandwidth capability ($\sim p_{pK}/\Delta\phi$) is associated with precision attitude control. Analytical expressions for this feature can be obtained by application of limit theory to the relationships of Table 2-10. The resulting expressions are given in Table 2-11.

The above predicted maximum capability is based solely on roll dynamic response. The pilot can however augment or attenuate this response by using dihedral effect (via pedals). The pilot is thus able to exceed the above capability indicated when necessary to do so.

D. Lateral Control Effectiveness Criteria Review

1. Purposes of Handling Criteria

The purpose of handling criteria are to serve as specification standards, design guides, and demonstration objectives for desirable closed-loop handling qualities. They take the form of convenient metrics summarizing complicated characteristics which affect manual piloting tasks. They represent a specification of what constitutes good design practices based upon past design attempts. In general the body of information on which the specification is written provides inadequate coverage for the complete flight envelope and is not always consistent within itself.

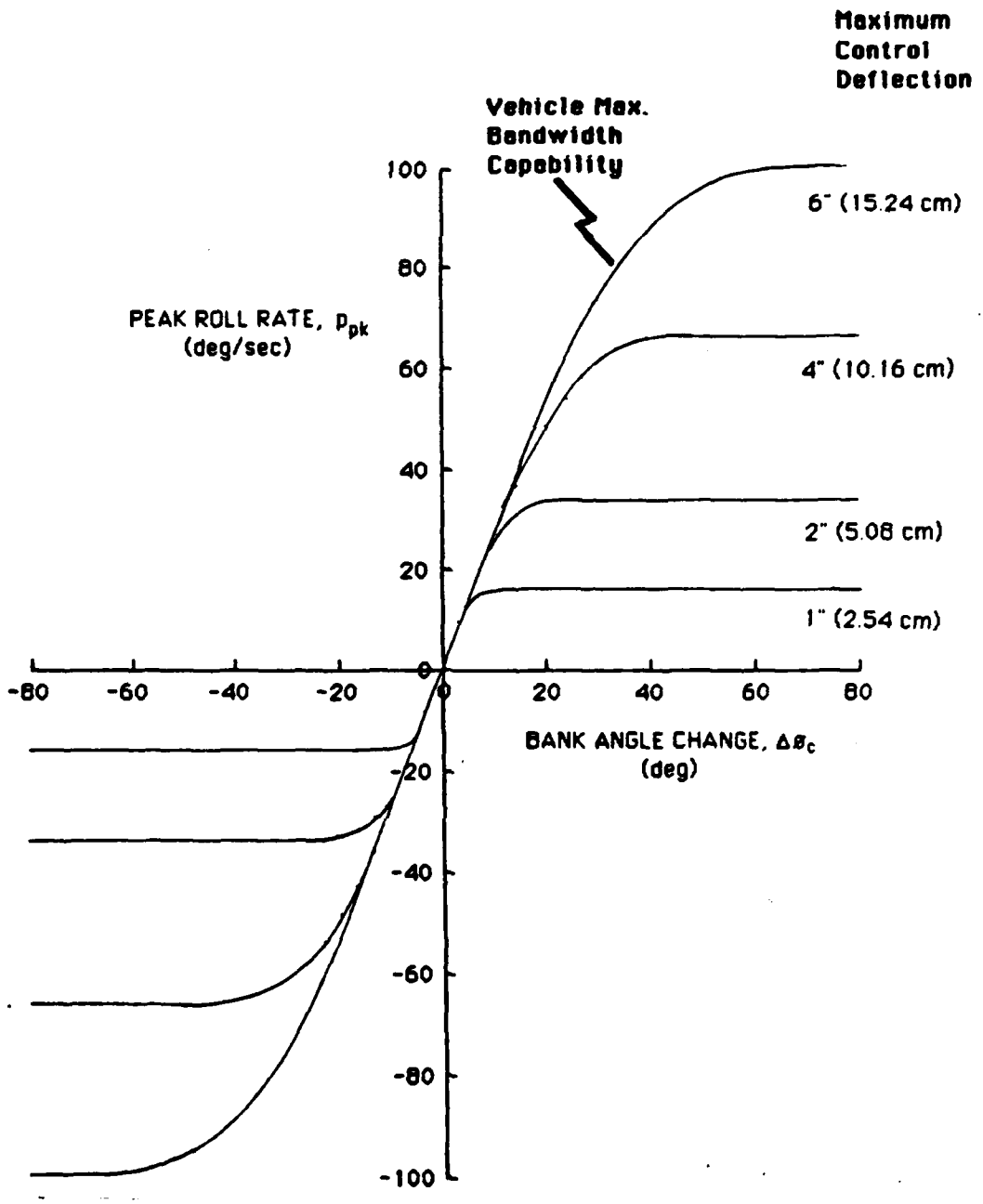

Figure 2-13. Typical Vehicle Capability Based Upon Square Wave Inputs

Table 2-11

Limiting Characteristics for Square Wave Input Response for a Second Order System

Time to Maximum Roll Rate

$$T_{max} = \frac{\frac{\pi}{2} - \tan^{-1}\left(\frac{\zeta}{\sqrt{1-\zeta^2}}\right)}{\omega_n\sqrt{1-\zeta^2}}$$

Time to Maximum Attitude Change

$$T_0 = \frac{\pi}{\omega_n\sqrt{1-\zeta^2}}$$

Peak Roll Rate/Attitude Change

$$\frac{P_{pk}}{\Delta\phi} = \frac{\omega_n \exp\left(\frac{-\zeta}{\sqrt{1-\zeta^2}}\left[\frac{\pi}{2} - \tan^{-1}\left(\frac{\zeta}{\sqrt{1-\zeta^2}}\right)\right]\right)}{1 + \exp\left(\frac{-\zeta\pi}{\sqrt{1-\zeta^2}}\right)}$$

Significant problems in specification re-definition are encountered when the vehicle role changes significantly from past applications. The evolution of the armed helicopter in nap-of-the-earth and air-to-air combat scenarios has provided a challenge to the present revision attempt of MIL-H-8501A which was last updated in 1962.

2. Summary of Roll Control Effectiveness Criteria

Handling qualities specifications and design guidelines pertinent to the operational requirements of helicopters have been reviewed. The six sources reviewed are: MIL-H-8501A, Helicopter Flying and Ground Handling Qualities (Reference 1); Edenborough and Wernicke, Control and Maneuver Requirements for Armed Helicopters (Reference 15); MIL-F-8785C, Flying Qualities of Piloted Airplanes (Reference 40); MIL-F-83300, Flying Qualities of Piloted V/STOL Aircraft (Reference 5); AGARD-R-577, V/STOL Handling (Reference 41); MIL-H-8501A Proposed Update, Mission Oriented Requirements (Reference 3). A summary of the lateral control effectiveness requirements appearing on these sources is given in Table 2-12.

3. Criteria Specification Philosophy

As noted in Table 2-12 there is a preference for open-loop handling criteria over closed-loop, this is because of the presumed vagueness and variability of pilot involvement. Most criteria are stated in terms of response to step inputs which is well suited for demonstration of compliance.

The criteria address the issues of long term and short term response, controller sensitivity and time delay issues. The time delay problem has become important through the widespread use of digital flight control systems. The response issue has been addressed primarily by a search in the control power, $\dot{p}_{max}$, versus roll damping, L_p, domain.

Table 2-12. A Summary of Roll Control Effectiveness Criteria.

FLIGHT REGIME	PARAMETER	MIL-H-8501A April 1962 Ref. 1		Edenborough & Wernicke Ref. 15	MIL-F-8785C Aug. 1969 Ref. 40 Class IV, CAT A Airspeed Range M
		VMC	IMC		
HOVER/ LOW SPEED	Roll Damping $\|L_p\|$ (1/sec)	$\geq 18\, I_x^{-.3}$	$\geq 27\, I_x^{-.3}$		
	Control Power $\phi(1)\|_1$ (deg)	$\geq \frac{27}{\sqrt[3]{W+1000}}$	$\geq \frac{32}{\sqrt[3]{W+1000}}$		
	$\phi(1)\|_{FA}$ FA-Full Authority	$\geq \frac{81}{\sqrt[3]{W+1000}}$	$\geq \frac{96}{\sqrt[3]{W+1000}}$		
	Roll Rate Sensitivity (degs/sec/in)	≤ 20.0			
FORWARD FLIGHT	Roll Damping $\|L_p\|$ (1/sec)			≥ 4.0	
	Control Power				$t_{90} \leq 1.3$ secs
	Roll Rate Sensitivity (degs/sec/in)	≤ 20		14-20	≤ 15
	Roll Control Sensitivity (degs/sec/sec/in)				
	Maximum Roll Rate (degs/sec)			≥ 70	
Specification		Helicopter HQ		Helicopter NOE HQ	Fixed Wing HQ
Comments		Uses the "Weight" rule to descriminate maneuver requirements. Does not address task or forward flight requirements		Based upon NOE flight data. Roll damping requirement somewhat subjective, maybe too restrictive	Spec. limited to forward flight. Time to 90 degs used as maneuver criterion & defined on a task-by-task basis

Table 2-12 Continued. Roll Control Effectiveness Summary

FLIGHT REGIME	PARAMETER	MIL-F-83300 March 1971 Ref. 5	AGARD 577 June 1973 Ref. 41	MIL-H-8501A Update Proposed Jan 1985 Ref. 3
HOVER/ LOW SPEED	Roll Damping $\|L_p\|$ (1/sec)		2 to 4	
	Control Power $\phi(1)\|_1$- (deg)	4 to 20	2 to 4	≥ 15
	Roll Control Sensitivity (degs/sec/sec/in)		8 to 17	
FORWARD FLIGHT	Roll Damping $\|L_p\|$ (1/sec)	≥ 0.71	0.5 to 3.0	
	Control Power	t_{30} ≤ 1.0 sec	$\phi(1)\|_1$- ϵ(2,4)	t_{30} ≤ 1.1 sec (Aggressive) t_{30} ≤ 1.5 sec (Moderate)
	Roll Control Sensitivity (degs/sec/sec/in)		3 to 14	
Specification		V/STOL HQ	V/STOL HQ	Mission Oriented HQ Spec.
Comments		No discrimination on the the basis of task or weight. Time to 30 deg used as the forward flight maneuver criteria	No discrimination on the basis of task or weight. Forward flight criteria based on STOL data bases	HQ specified on a task-by-task basis. Flight system type specified a function of task and visual conditions

Figure 2-14 illustrates the diversity of iso-opinion curves in such investigations as a function of task and investigation.

The long term response or control power criteria is usually specified in terms of time to x degrees, t_x , or attitude change in x seconds, $\phi(x)$, following maximum control input. The argument for adoption of these parameters is they provide a better "fit" to iso-opinion data boundaries than steady-state roll rate for example.

The short term response criteria address how quickly a commanded rolling motion can be obtained., The metric normally used is the first-order roll time constant, τ_R, or equivalently the roll damping derivative, $-L_p$. A lower bound exists on L_p due to the lead equalization limits of the pilot.

The proposed 8501A update (Reference 3) defines the maneuvering control power requirement for forward flight as time to 30 degrees bank (t_{30}). One major issue at the present time is the appropriateness of 30 deg to maneuvering requirments and whether a steady state roll rate requirement may be more appropriate. Fixed-wing maneuvering criteria for ground attack and air-to-air combat specifications use t_{30}, t_{50}, t_{90} and even t_{360} . These criteria based upon large attitude changes basically constitute a steady-state roll rate specification.

The utility of t_{30} versus steady-state roll rate will be discussed in depth in Section V following presentation of simulation results.

1. Corliss and Carico, UH-1H, Slalom, NASA TM-84376 , Ref. 27
2. Edenborough and Wernicke, NOE, Ref. 15.
3. Pausder, VSS 80-105, Slalom, Informal Transmittal to Manudyne Systems. Inc., from DFVLR
4. Faye, Hover, (θ,ϕ) Moving Base Simulation, NASA TN D-792
5. Tapscott and Sommer, IFR Hover, In-Flight, Large Single Rotor Helicopter, NASA TN D-3600

Note: Data for 4 and 5 above is taken from BUIG MIL-F-83300

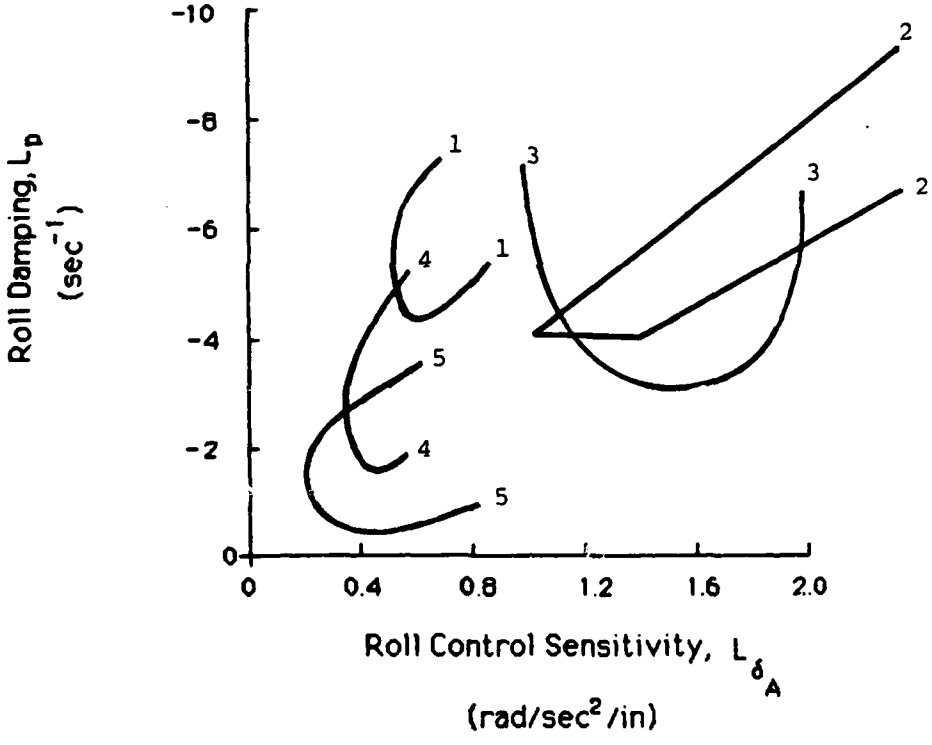

Figure 2-14. Comparison of Level 1 Iso-Opinion Curves of L_p versus L_{δ_A}.

III. FLIGHT TASK ANALYSIS

The purpose of this section is to provide an understanding of the operational context of the pilot-aircraft system. First, lateral maneuvers are classified and described in general terms. Next actual flight examples are analyzed and flight task analysis results are presented.

A. Classification and Description of Lateral Maneuvers

The fundamental classes of lateral flight tasks and maneuvers are defined in terms of:

- Roll attitude regulation.
- Bank-to-turn maneuvers.
- Bank-to-translate maneuvers.
- Ground contact flight tasks.

Each of these classes represents a different type of closed-loop response and influence of the vehicle dynamics.

1. Roll Attitude Regulation

This category of lateral task applies only to the task of basic bank angle control and regulation. It is assumed that there is no support role for an outer-loop task. As such the general utility of this task alone is limited and normally not crucial.

One example of this kind of task is manually controlled flight where course or heading is essentially unregulated. This particular example is not generally of interest, though, because only very loose roll attitude regulation is required. Namely, the objective is no more than remaining "right side up".

A more crucial variety of roll attitude regulation is the tracking of a lateral flight director command bar for the purpose of lateral guidance or weapon delivery. Here there can be sufficient urgency to induce fairly tight, aggressive tracking of commanded roll attitude.

This task was examined in the simulator experiment using a series of bank angle command steps and is discussed in Section IV. It is particularly interesting in terms of its distinction from tasks involving an outer lateral control loop.

The roll attitude task covers a wide spectral range. The high end is associated with the general level of aggressiveness, and the low end by the trimability or accommodation of unattended operation. In general the amplitude of roll attitude control and regulation tasks is small although, strictly speaking, barrel rolls or aileron rolls are included in this catagory.

2. Bank-to-Turn Maneuvers

In this maneuver the objective is to control or regulate heading or course using a bank-angle support loop and maintaining near-zero side velocity or lateral acceleration. The benefits are maintenance of a deck-level specific force vector and the use of normal acceleration to achieve a change in lateral flight path. In fact bank-to-turn maneuvers permit the use of the maximum available normal acceleration for turning. Where the turn is coordinated, the tightness of the turn is a direct function of commanded bank angle.

The bank-to-turn maneuver is useful only where there is a reasonable forward velocity component. Nevertheless pilots often exhibit coordinated banked turns even while taxiing at speeds of only about 25 kt. The reason for applying the technique at low speed may be

primarily comfort. At higher speeds the use of bank-to-turn maneuvering predominates with few exceptions.

3. Bank-to-Translate Maneuvers

In a bank-to-translate maneuver the lift vector is tilted to achieve a sideward acceleration component but without a significant change in heading. The maneuver is most common in hover but can also be effective in forward flight. In general the bank-to-translate maneuver does not involve (or permit) large increases in thrust. Thus it is essentially a 1g maneuver (unlike the bank-to-turn).

The most typical use of bank-to-translate is during precision hover above the ground. The counterpart longitudinal technique is simultaneously applied for fore-and-aft position. In this condition the chief rigid body dynamics are described by the classical "hover cubic" which involves a higher frequency roll time constant and a lower frequency oscillatory phugoid-like mode. In this study the effects of the tip-path-plane lag are added to the hover cubic (thus making it really a "hover quartic").

In forward flight the bank-to-translate maneuver can be used where there is a desire to maintain a steady heading. This could include a "wing-low" approach where line-up is regulated by bank angle and heading held constant or an air-to-ground gunnery task where heading is used to aim and bank angle used to control lateral position.

Even in forward flight, the roll-axis dynamics for bank-to-translate maneuvers are similar to those at hover including the lower frequency oscillatory mode. The "hover cubic" is not limited to just hover as demonstrated in Table 3-1 based on data from Reference 36.

Table 3-1

Roll-to-Translate Response for BO-105 for a Range of Airspeeds

AIRSPEED U(kt)	ROLL ATTITUDE RESPONSE TO LATERAL STICK (PITCH AND HEADING LOOP CLOSURES EFFECTED) $\frac{\phi}{\delta_A}\Big\vert_{\substack{\theta \rightarrow \delta_e \\ \Psi \rightarrow \delta_p}}$
0	$\frac{2.7\,(\,0.002)}{(\,-0.01;\ 0.44\,)\ (\,0.4;\ 14.\,)}$
60	$\frac{2.7\,(\,0.046)}{(0.04;\ 0.41\,)\ (\,9.9\,)}$
120	$\frac{2.7\,(\,0.09\,)}{(\,-0.07;\ 0.49\,)\ (\,9.4\,)}$
140	$\frac{2.8\ (\,0.11\,)}{(\,-0.26;\ 0.56\,)\ (\,9.2\,)}$

NOTE: Roll time constant, roll control sensitivity, and lateral phugoid frequency are all insensitive to airspeed.

Lateral phugoid damping and sway damping both change with speed but the effect is negligible.

The hovering cubic is present at all speeds - it is a function of piloting technique alone.

Note: The factored numerator and denominator roots are shown in the short hand form.

$$(a) = (s + a), \quad (\zeta, \omega_n) = (s^2 + 2\zeta\omega_n s + \omega_n^2)$$

4. Ground Contact Flight Tasks

This class of lateral maneuver includes cross-slope takeoff and landing and is radically different from the in-flight tasks described above. Here the pilot is more concerned with control of the rotor tip-path-plane attitude than with fuselage attitude. The main factor in ground contact tasks is that the motion of the vehicle is constrained by contact with a skid or wheel. In effect the essential center of rotation is about the landing gear rather than the center of gravity. As a result the dynamics of the controlled element are radically different.

Cross-slope takeoff and landing are considered crucial maneuvers but are hazardous and involve the same dynamic characteristics of the "dynamic rollover" condition. The execution of the task depends upon the amount of ground slope and is limited by the amount of lateral flapping available in the rotor system.

Statically, the roll control should be capable of producing a level tip-path-plane while the fuselage is aligned with the cross slope. In addition, there should be adequate margin of control to stabilize the statically unstable rotor-body system in the presence of any upsets during the transition from ground contact to airborne flight.

B. Flight Measurements

The maneuvers considered in this section represent those for which flight data are available as well as those which were studied in the simulator experiment. First, measurement techniques are described. This is followed by an examination of actual flight data obtained.

1. Measurement Techniques

Measurement techniques used in this study were limited to those which were "non-intrusive" to pilot performance. In general, flight data are limited to time history plots of state variables associated with lateral maneuvers including roll attitude, roll rate, lateral cyclic, and heading. In some cases lateral position data are available from radar tracking.

All the maneuvers studied were considered to be discrete, thus the discrete maneuver analysis method discussed in Section II is used.

2. Flight Data Obtained

The flight data bases listed in Table 3-2 have been analyzed in an effort to define lateral control usage requirements in operational flight phases. As shown an in-flight evaluation was conducted under the auspices of this program using a UH-1H helicopter. However, a diverse collection of data from other sources has also been reviewed. Each evaluation data base is detailed below.

NASA/Army UH-1H Flights (Manudyne Roll Control) Two experienced test pilots flew a NASA UH-1H through a series of aggressive turns, slalom courses, lateral sidesteps and lateral jinking maneuvers. The objective was to observe the magnitude and aggressiveness and possible variations in piloting technique among these various maneuvers. Each maneuver is described along with a summary of data obtained.

Turns of 50 deg, 130 deg, and 180 deg were performed at low altitude 30-40 ft (9-12 m) and at a speed of 60 Kt. The grass edges of the runway were used as visual cues, and both left and right turns were performed. Figure 3-1 illustrates the 130 deg and U-turn maneuvers as they were flown at NALF Crow's Landing.

Table 3-2. Maneuver Flight Data Bases

Source	Aircraft	Maneuver	Remarks
NASA/Army (Manudyne roll control)	UH-1H	50° and 130° Turns	60 Kt, 30-40' (9-12 m) AGL
		Low altitude U-turn	60 kt, 30-40' (9-12 m) AGL
		210° turn at altitude	60 kt, 1000' (305 m) AGL
		Sideward translation	Hover, 15-20' (4-6 m) AGL
		In-line slalom	450' (137 m) spacing, 60 & 80 kt
		Jinking maneuver	30 kt, 30-40' (9-12 m)AGL
DFVLR	UH-1D & BO-105	"U. S. slalom"	60 kt, 100' (30 m) AGL
		"German slalom" (jink)	
		High-g turn	
NATC/AVSCOM	OH-58, UH-60, S-76, & AH-1	Scissors maneuver	D-318 data base
NADC	X-22A	Lateral sidestep	No synthetic turbulence
NASA/Army (Corliss and Carico)	UH-1H (variable stability)	"U. S. slalom"	1000' (305 m) spacing, 60kt, L_p and $L_{\delta A}$ variations

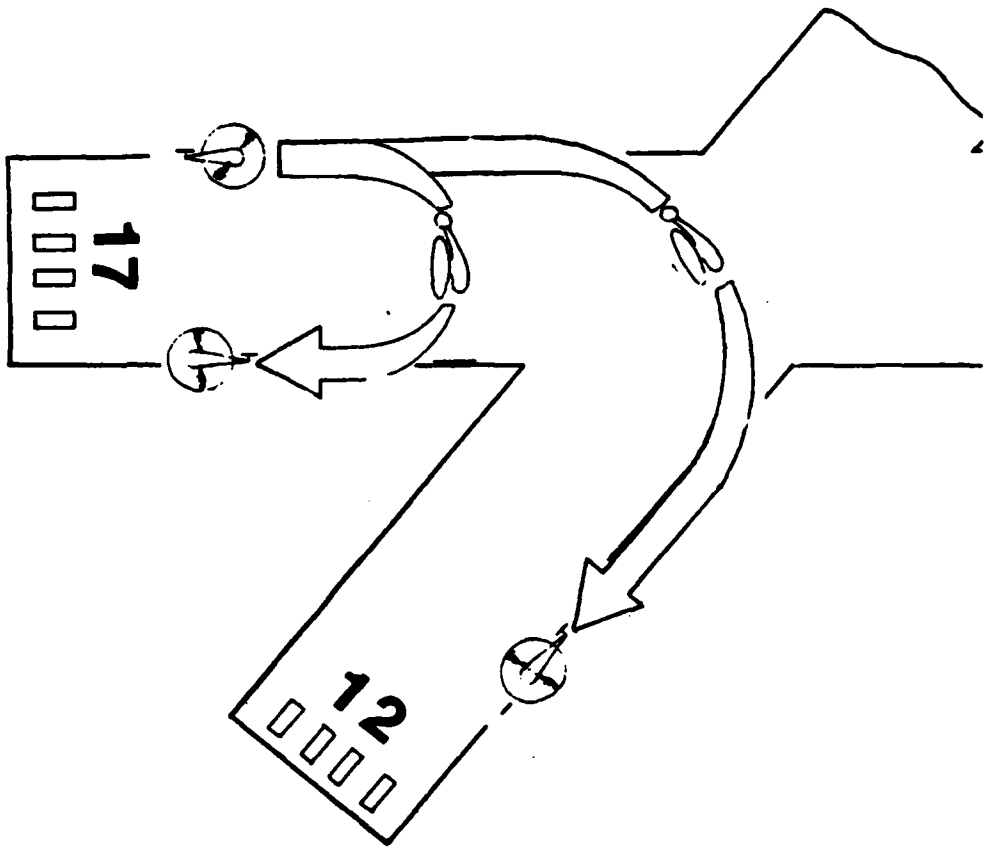

Figure 3-1. Runway Intersection and U-Turns Flown at NALF Crow's Landing

The data obtained for the turn maneuvers are summarized in the discrete maneuver performance plots in Figure 3-2.

A 210 degree turn was flown at an altitude of 1000 ft (305 m) and 60 Kt. The target bank angle was 45 deg, and both left and right turns were evaluated. These ara summarized in Figure 3-3.

An in-line slalom (Figure 3-4a) was performed along markers placed approximately 450 feet (137 m) apart along the side of the runway. Airspeeds of 60 and 80 kt were used, and the altitude was maintained at 30 to 40 ft (9-12 m) AGL. The results are plotted in Figure 3-5.

A lateral jinking maneuver defined by dimensions similar to the DFVLR "German Slalom" was flown around runway markers. The speed was approximately 30 Kt and the altitude 30 to 40 ft (9-12 m). Data are summarized in Figure 3-6.

A sideward translation (sidestep) maneuver was flown along a runway edge as shown in Figure 3-4b. The sidestep commands varied over 40, 80, and 160 ft (12, 24, and 48 m). A nearly constant heading was held and altitude was maintained at 15 to 20 ft (4-6 m). Data describing the agility are plotted in Figure 3-7. In addition, data describing the outer-loop lateral translation maneuver are given in Figure 3-8.

DFVLR Flight Data Two research pilots performed the following tasks using both the UH-1D teetering rotor helicopter (essentially identical to the UH-1H) and the BO-105 rigid rotor helicopter. Data from the flights described in Reference 24 were supplied by the DFVLR for analysis in this study.

A "U. S. slalom" maneuver (based on that flown in Reference 27) was flown around ground markers spaced 300 meters apart as shown in Figure

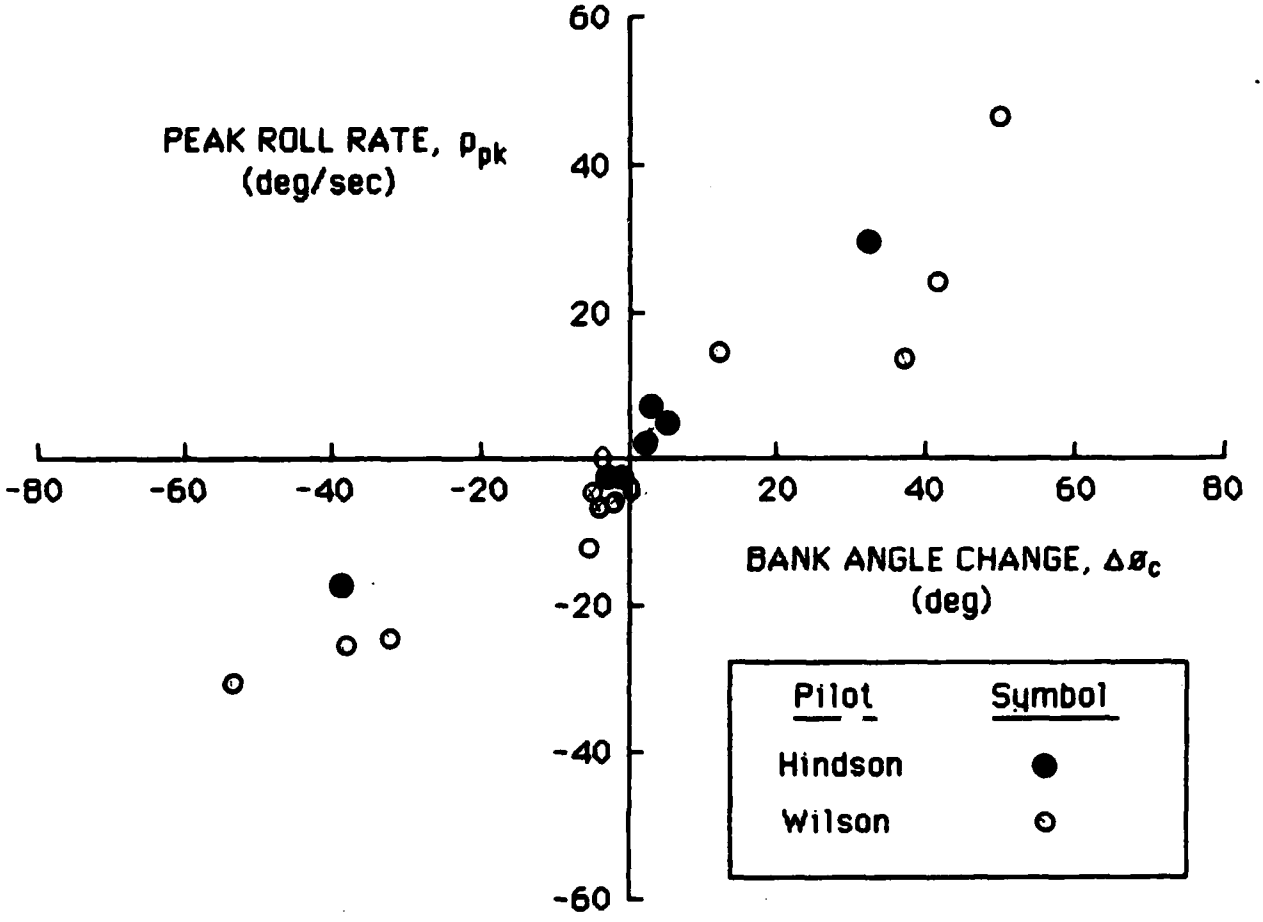

Figure 3-2a. 50 Degree Intersection Turn Maneuver Data

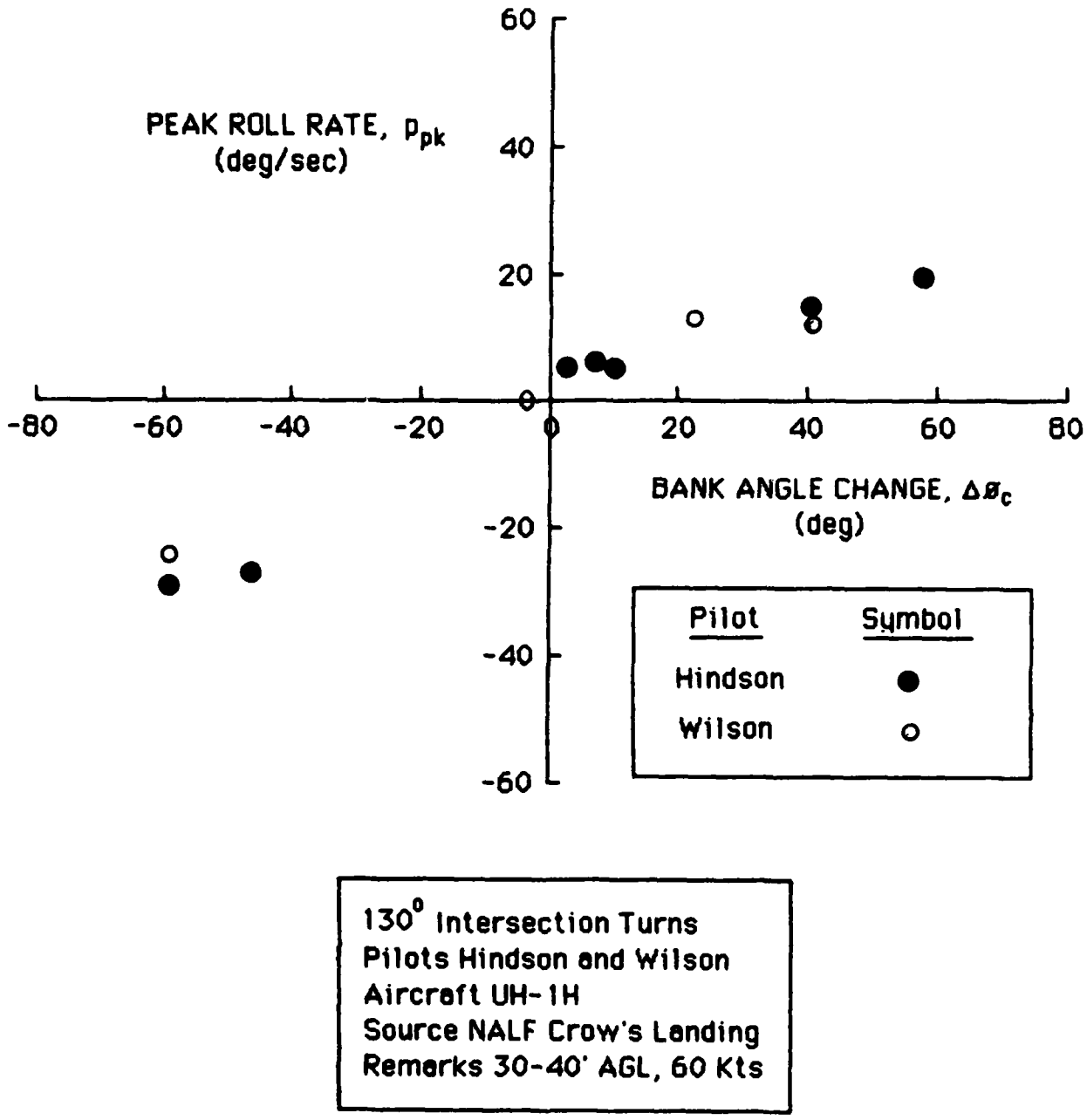

Figure 3-2b. 130 Degree Intersection Turn Maneuver Data

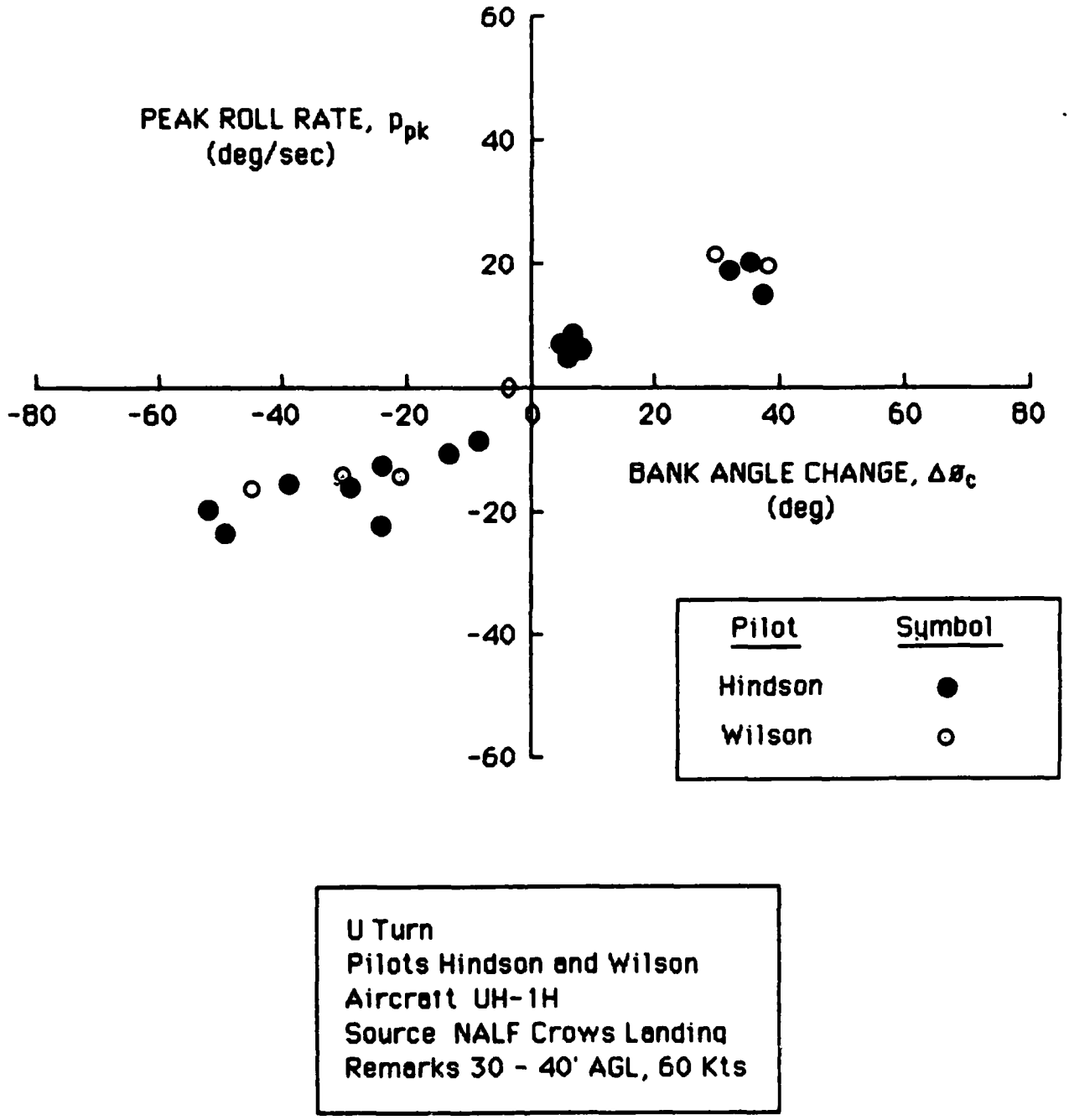

U Turn
Pilots Hindson and Wilson
Aircraft UH-1H
Source NALF Crows Landing
Remarks 30 - 40' AGL, 60 Kts

Figure 3-2c. U Turn Maneuver Data

AD-A172 111 STUDY OF HELICOPTER ROLL CONTROL EFFECTIVENESS CRITERIA 2/3
(U) MANUDYNE SYSTEMS INC LOS ALTOS CA
R K HEFFLEY ET AL. APR 86 MANUDYNE-83-1
UNCLASSIFIED USAAVSCOM-TR-85-A-5 NAS2-11665 F/G 1/2 NL

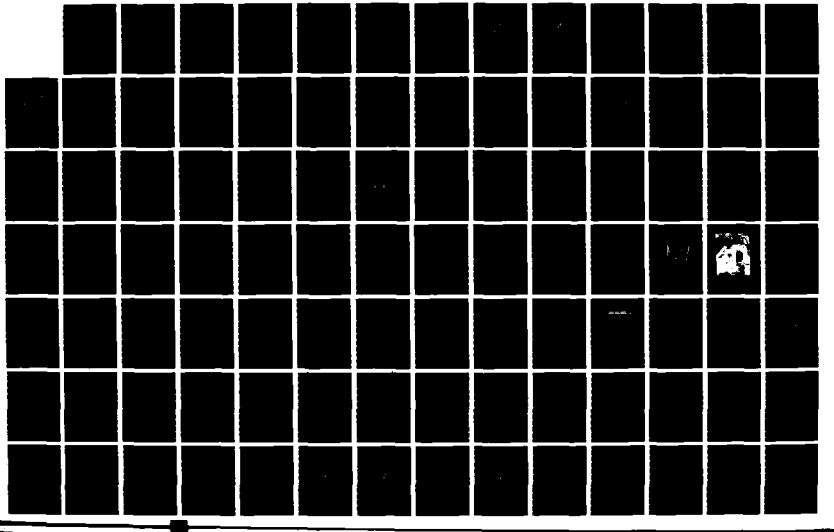

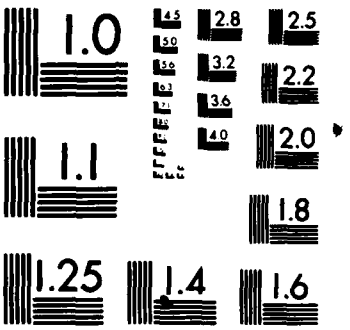

MICROCOPY RESOLUTION TEST CHART
NATIONAL BUREAU OF STANDARDS-1963-A

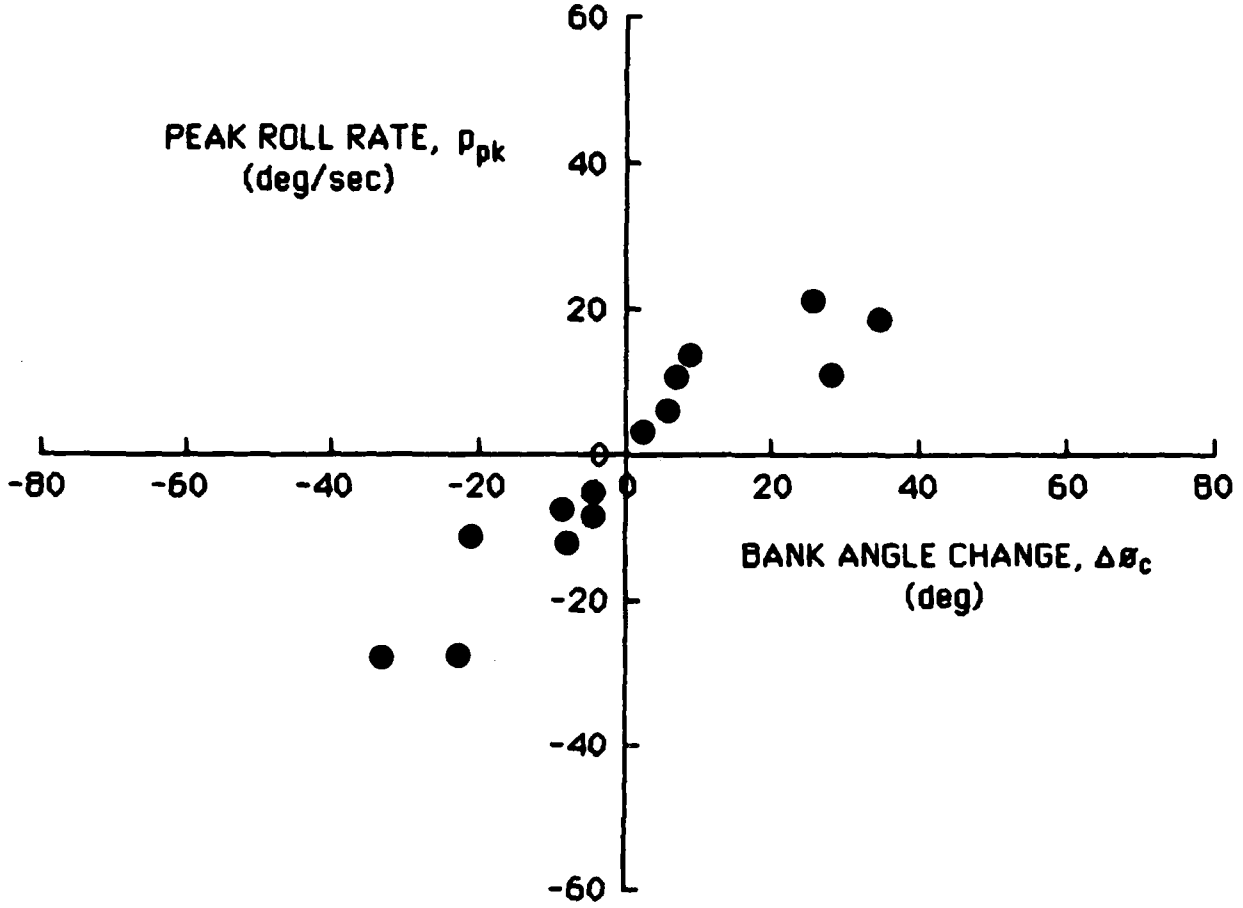

210° Turn
Pilots Hindson and Wilson
Aircraft UH-1H
Source NALF Crows Landing
Remarks 1000' AGL, 60 Kts

Figure 3-3. 210 Degree Turn Maneuver Data

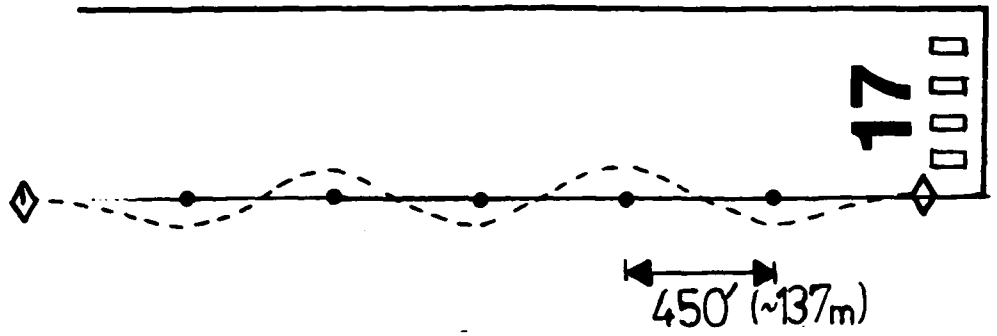

(a) In-Line Slalom

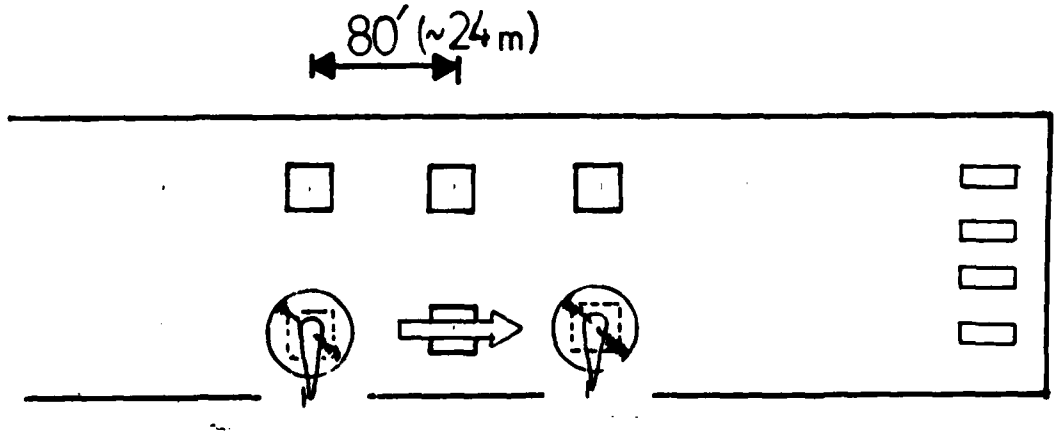

(b) Sidestep Task

Figure 3-4. Definition of In-Line Slalom and Sidestep Maneuvers Flown at NALF Crow's Landing

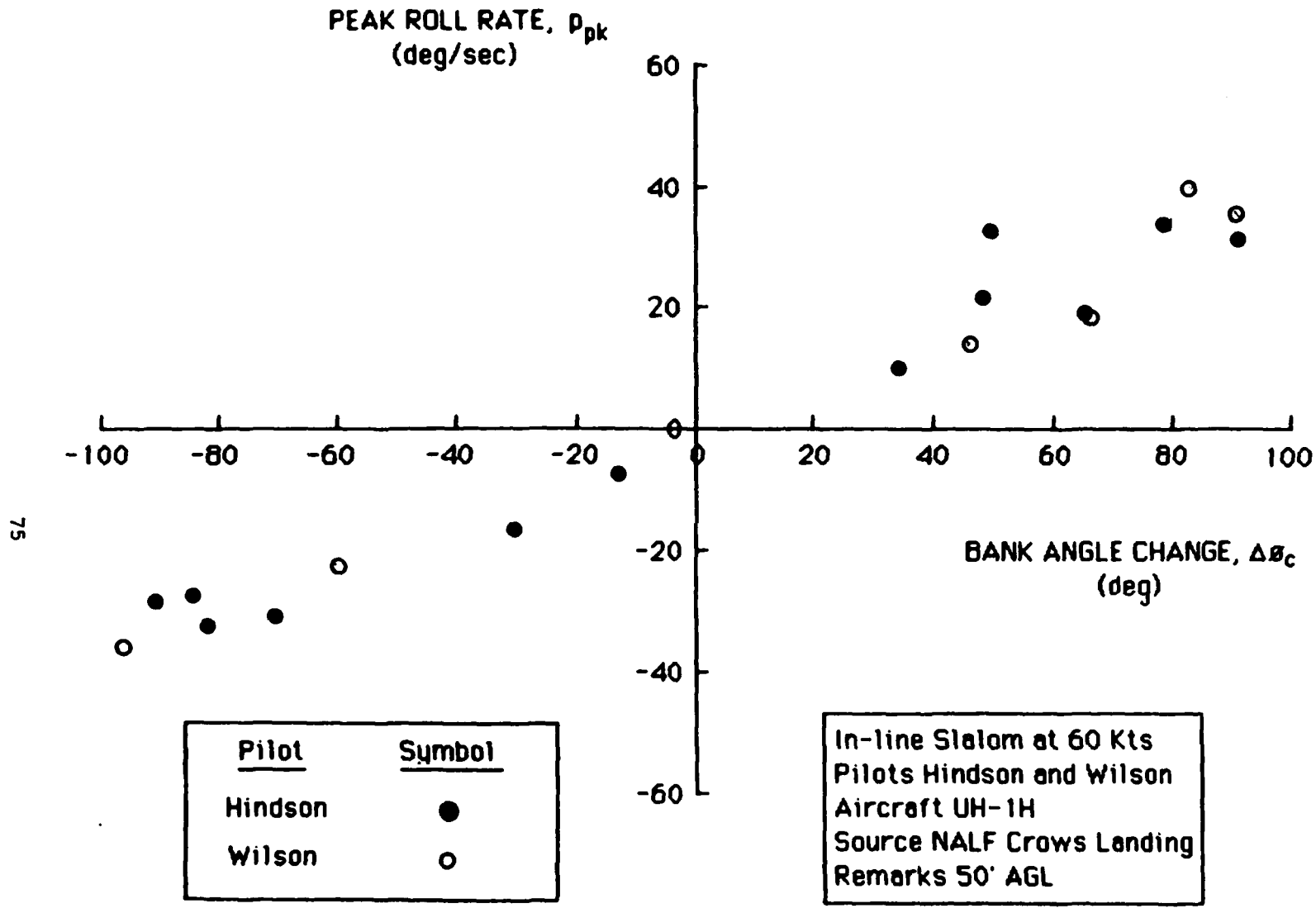

Figure 3-5a. In-Line Slalom Maneuver Data at 60 Kts Airspeed

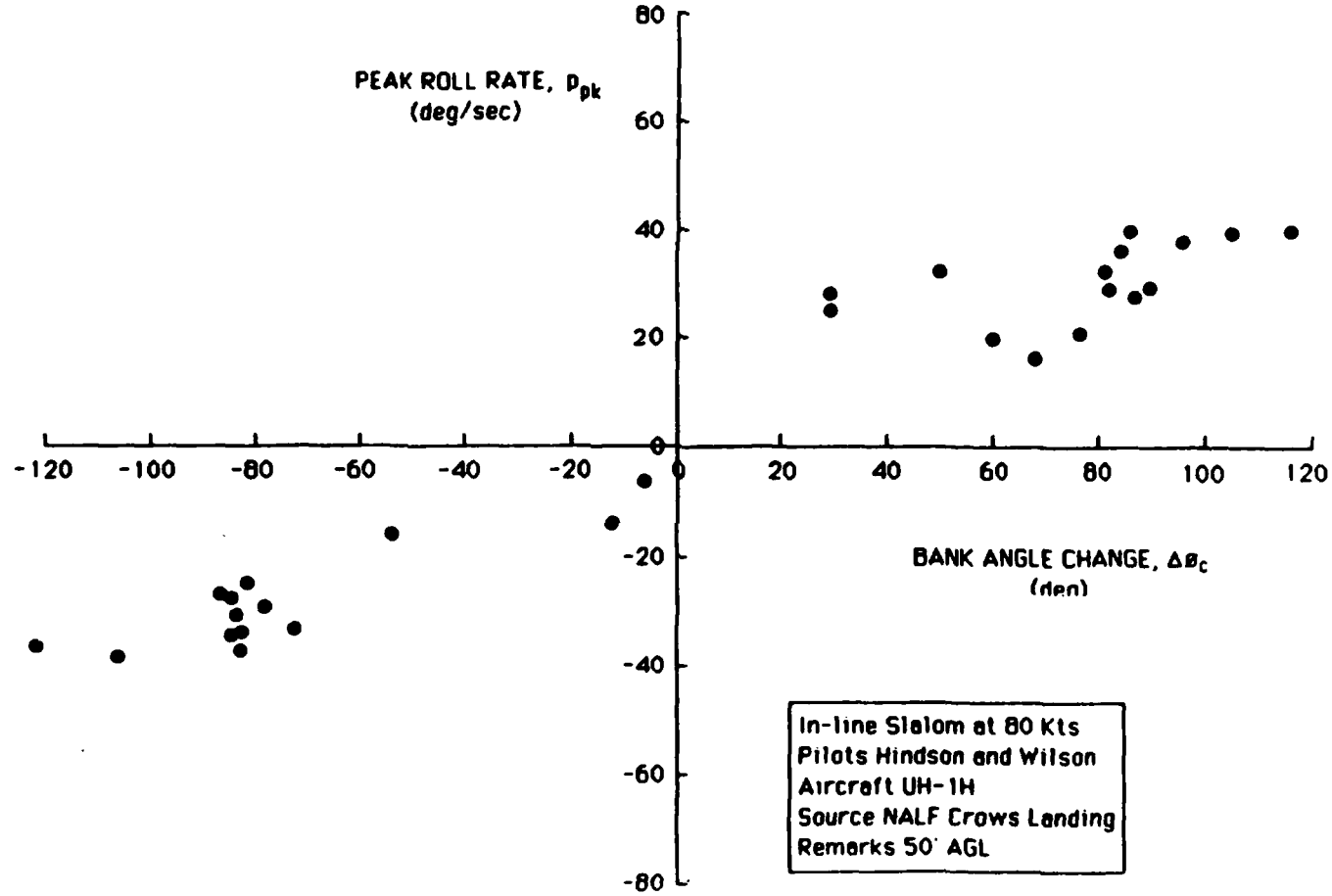

Figure 3-5b. In-Line Slalom Maneuver Data at 80 Kts Airspeed

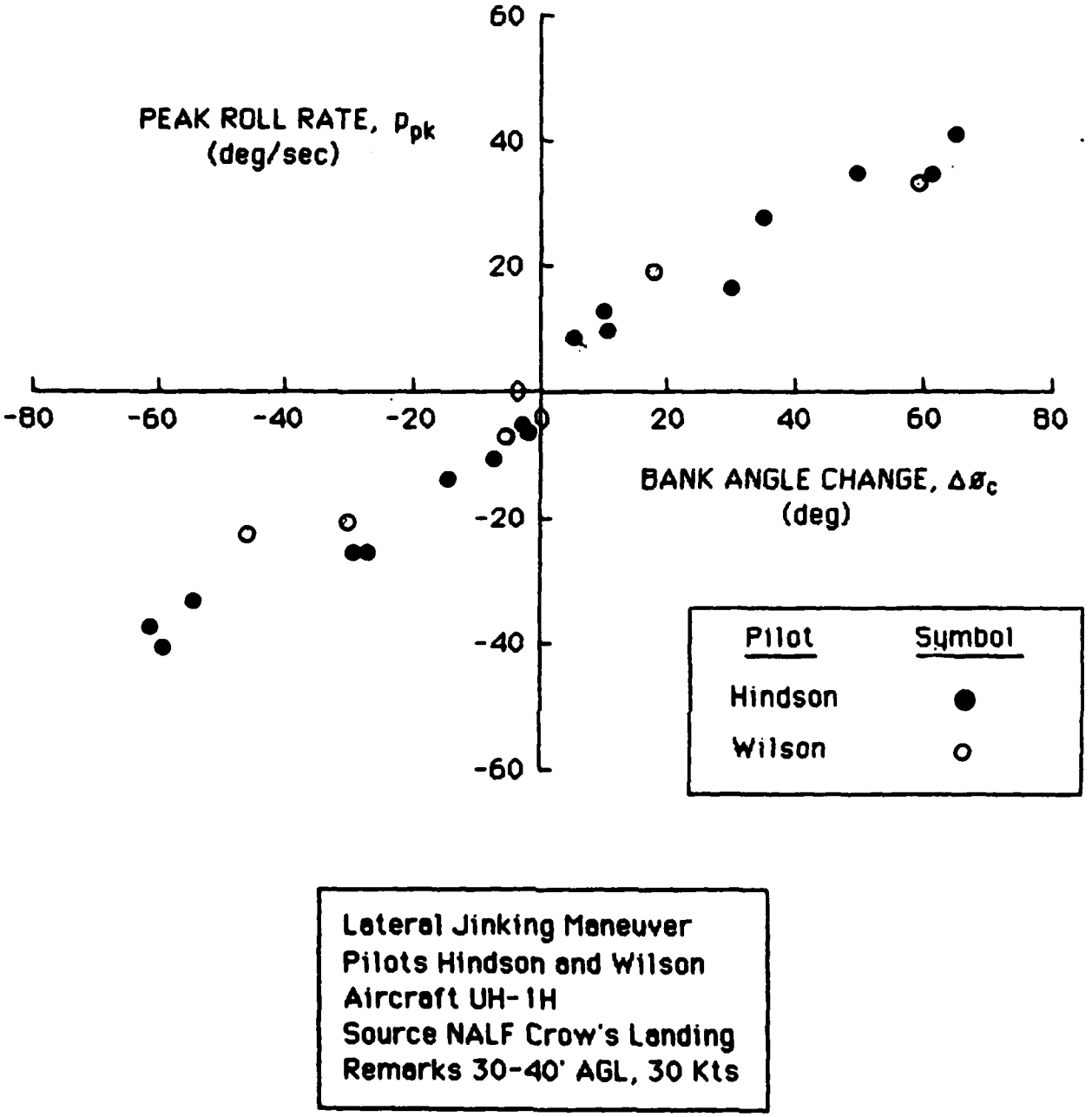

Figure 3-6. Lateral Jink Maneuver Data

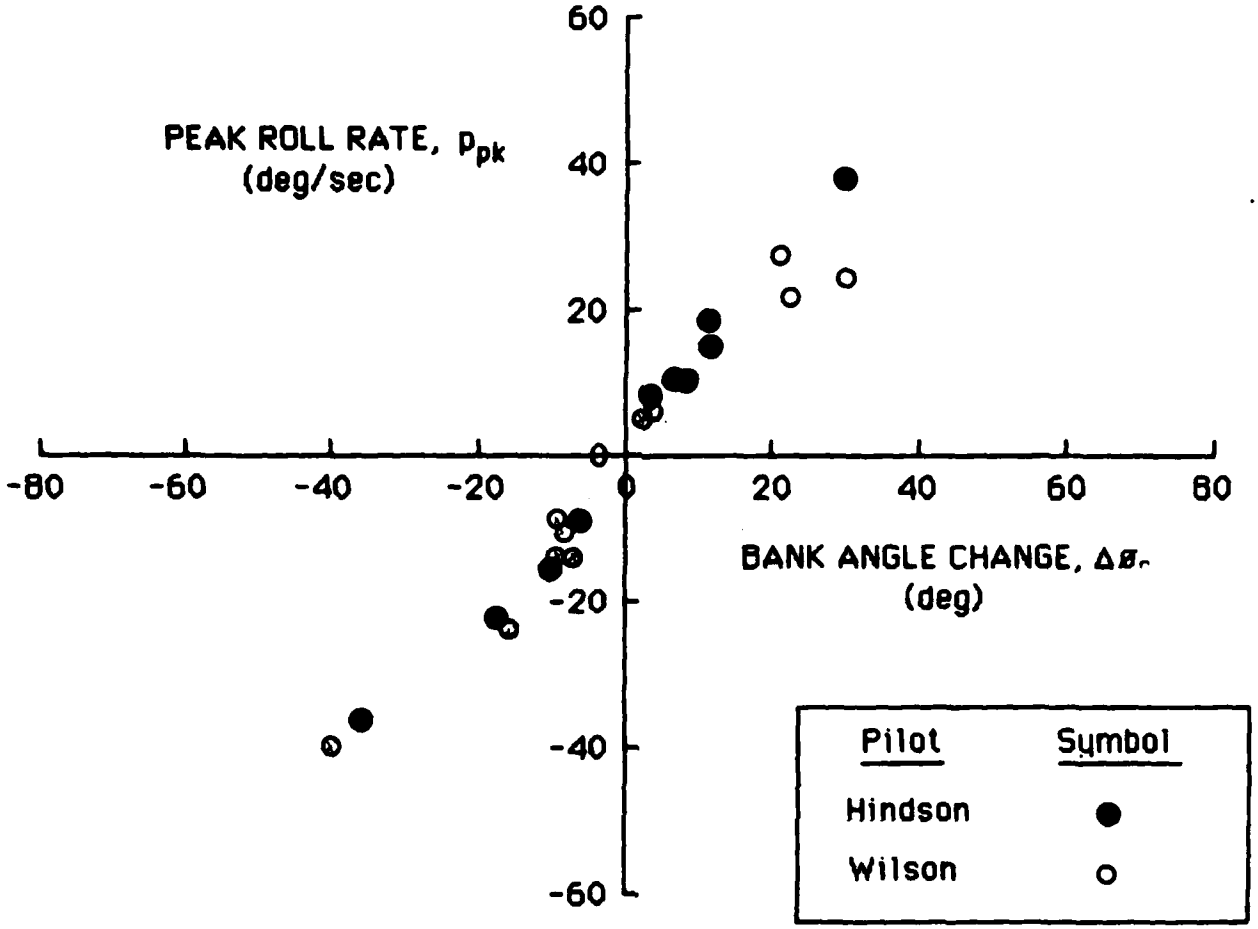

One Half Unit Sidestep (~ 40')
Pilots Hindson and Wilson
Aircraft UH-1H
Source NALF Crows Landing
Remarks Hover, 15-20' AGL

Figure 3-7a. One Half Unit (-40') Sidestep Maneuver Data

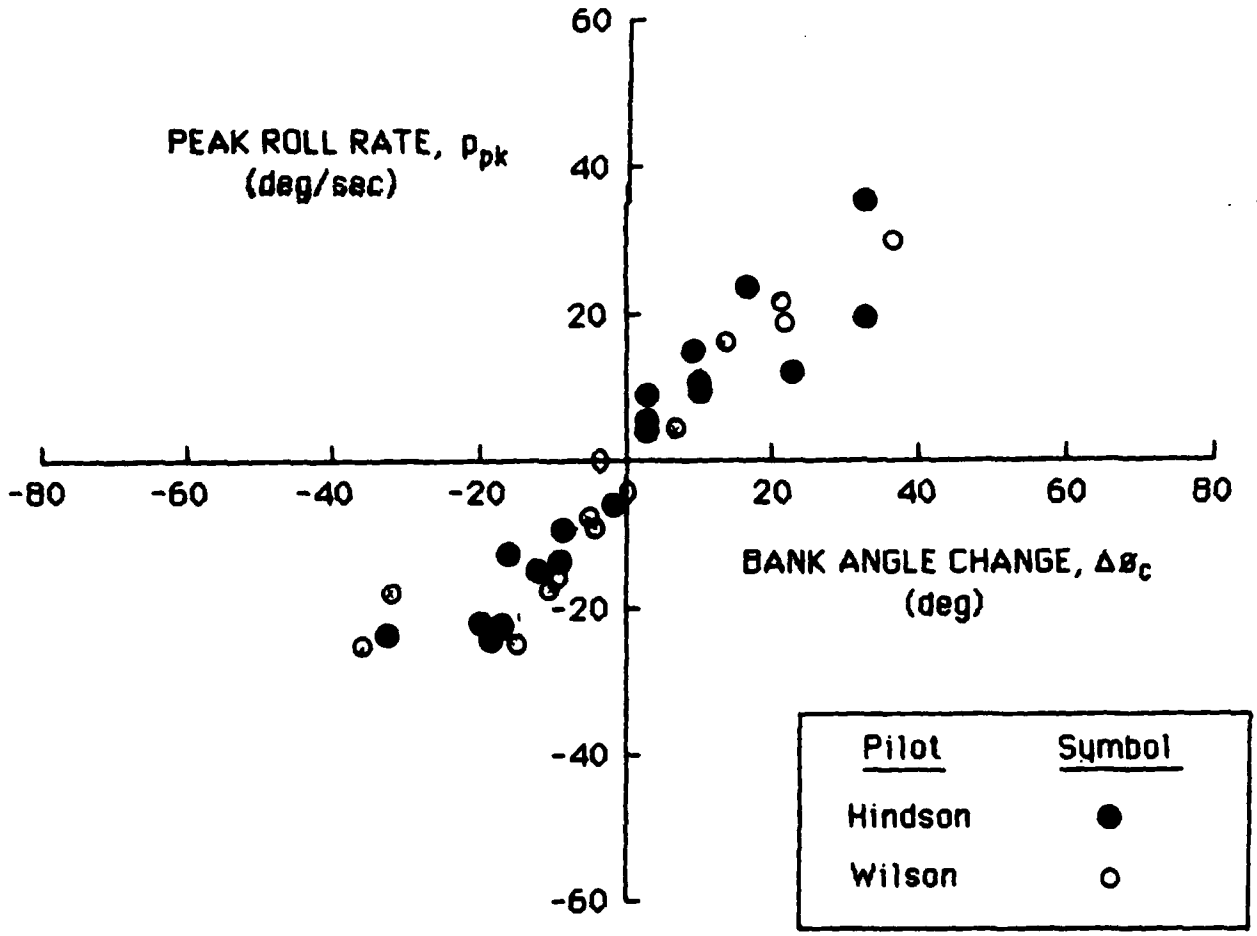

One Unit Sidestep (~ 80')
Pilots Hindson and Wilson
Aircraft UH-1H
Source NALF Crows Landing
Remarks Hover, 15-20' AGL

Figure 3-7b. One Unit (-80') Sidestep Maneuver Data

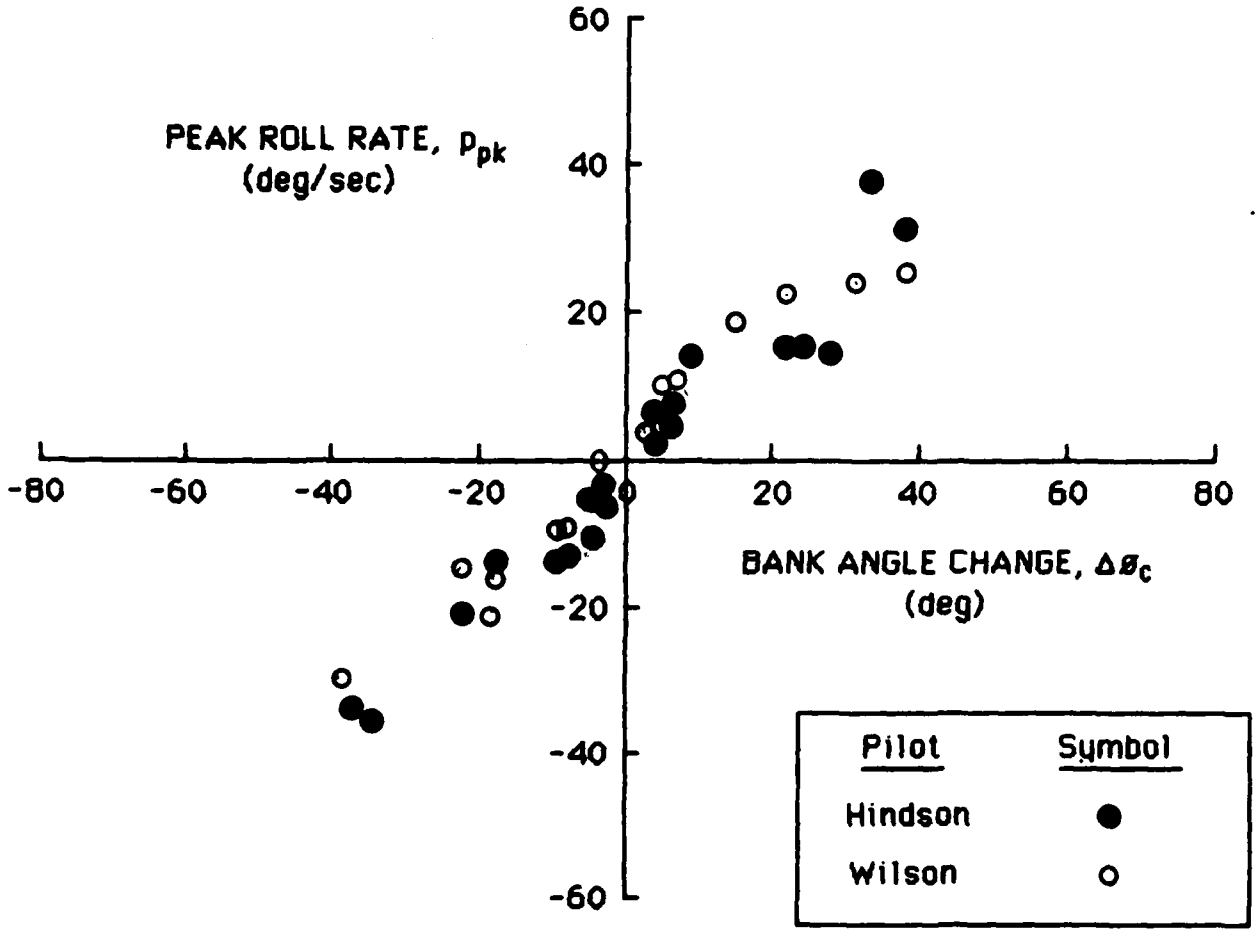

Two Unit Sidestep (~ 160')
Pilots Hindson and Wilson
Aircraft UH-1H
Source NALF Crows Landing
Remarks Hover, 15-20' AGL

Figure 3-7c. Two Unit (-160') Sidestep Maneuver Data

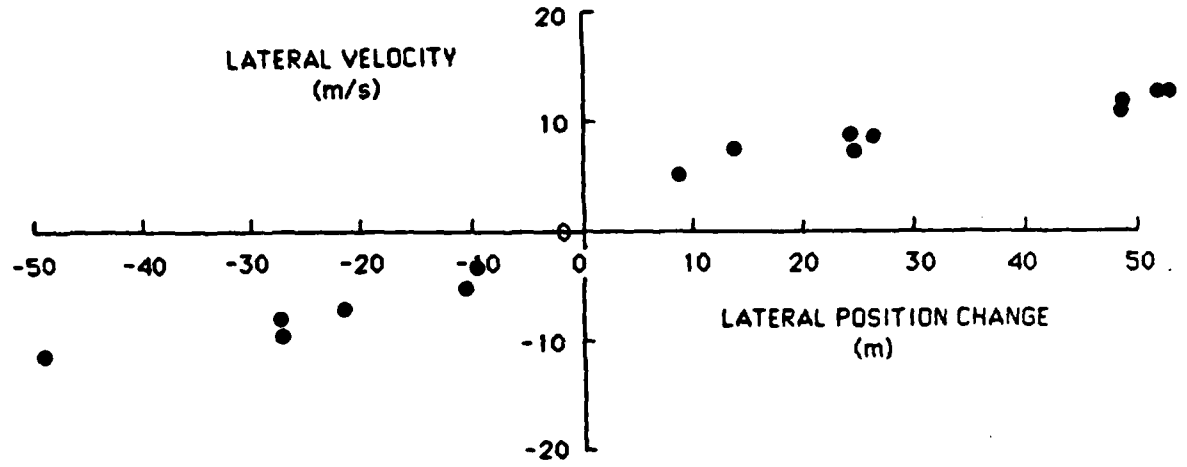

Figure 3-8. Outer Loop Sidestep Maneuver Data

3-9a. The pilot minimized the lateral displacement from imaginary poles located at the ground markers. During the task airspeed and altitude were maintained at 60 kt and 100 ft (30 m), respectivly. The results are plotted in Figure 3-10.

A "German Slalom", or lateral jinking maneuver, as shown in Figure 3-9b was flown around two ten meter high obstacles placed 350 meters apart and offset 10 meters from the course centerline. The pilot followed the course centerline as long as possible until forced to avoid the first obstacle. The second obstacle was then handled similarly. An airspeed of 60 kt and an altitude of 30 ft (9 m) were maintained. Data are shown in Figure 3-11.

High-g left turns were performed, and the data are shown in Figure 3-12.

NATC/AVSCOM D-318 Data Base As a result of the program described in Reference 25, flight data for maneuvers resembling "horizontal scissors" air combat maneuvers were obtained from the U. S. Navy Test Pilot School. The maneuver is described in Reference 42 and an abstract of this is shown in Figure 3-13 . An annotated plot of flight paths is shown in Figure 3-14 from data presented in Reference 25. Flight data for a variety of helicopters are shown in Figure 3-15.

NADC X-22A Data Base Reference 26 presents the results of an evaluation of a translational rate command control system for VTOL shipboard landing tasks using the X-22A ducted-fan VTOL aircraft.

One element of the evaluation required the pilot to track a pad which made discrete 25 ft (7.5 m) lateral jumps every 25 to 30 sec. The task was conducted at altitude with reference only to a head-up display. Most of the tests were conducted with the aircraft forced with synthetic turbulence representing wind-over-deck conditions in Sea State 5,

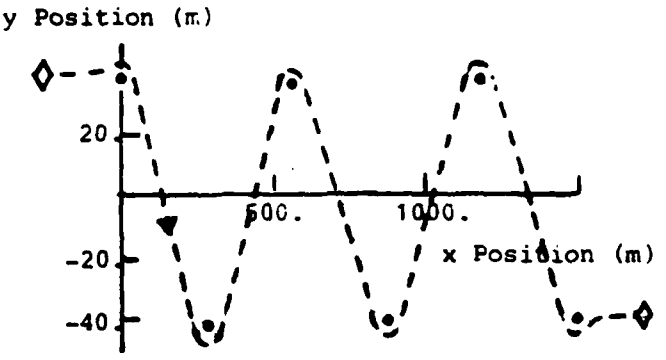

(a) 'U. S. Slalom' Course

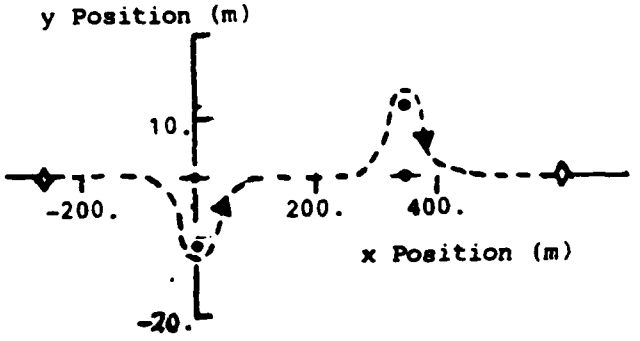

(b) 'German Slalom' Course

Figure 3-9. Definition of Tasks Used in the DFVLR Evaluations

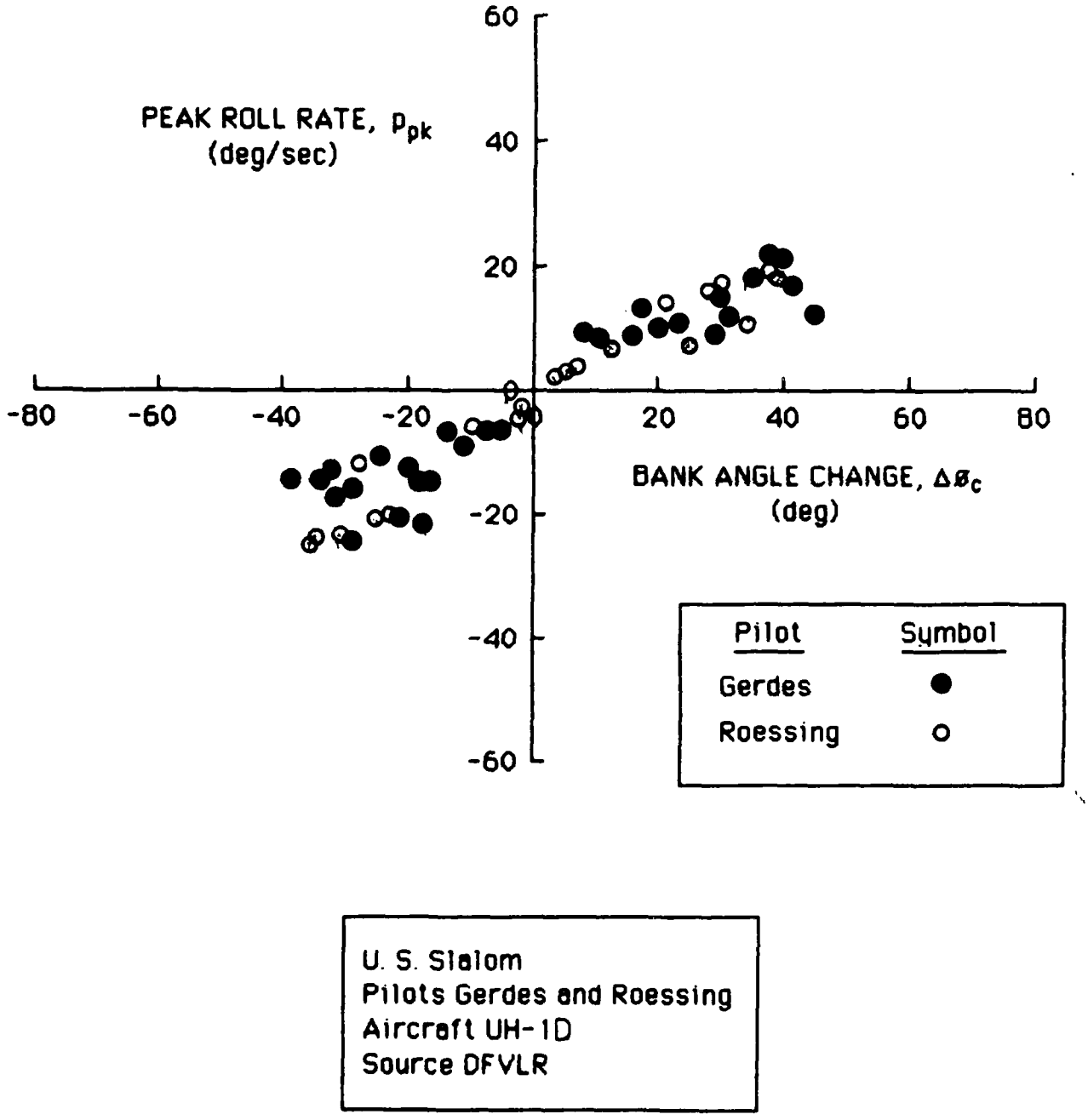

Figure 3-10a. 'U.S. Slalom' Maneuver Data for the UH-1D Helicopter

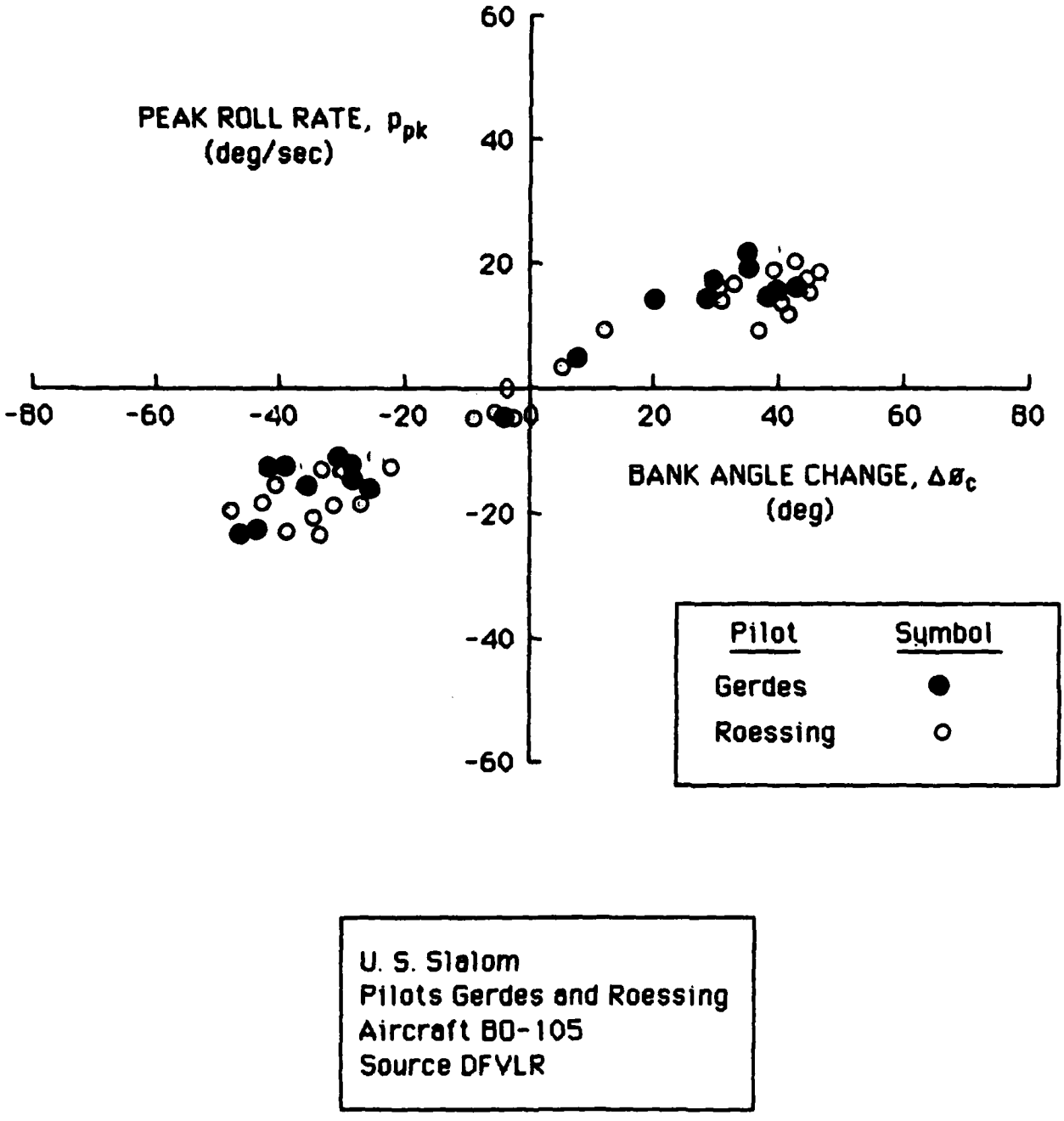

Figure 3-10b. 'U.S. Slalom' Maneuver Data for the BO-105 Helicopter

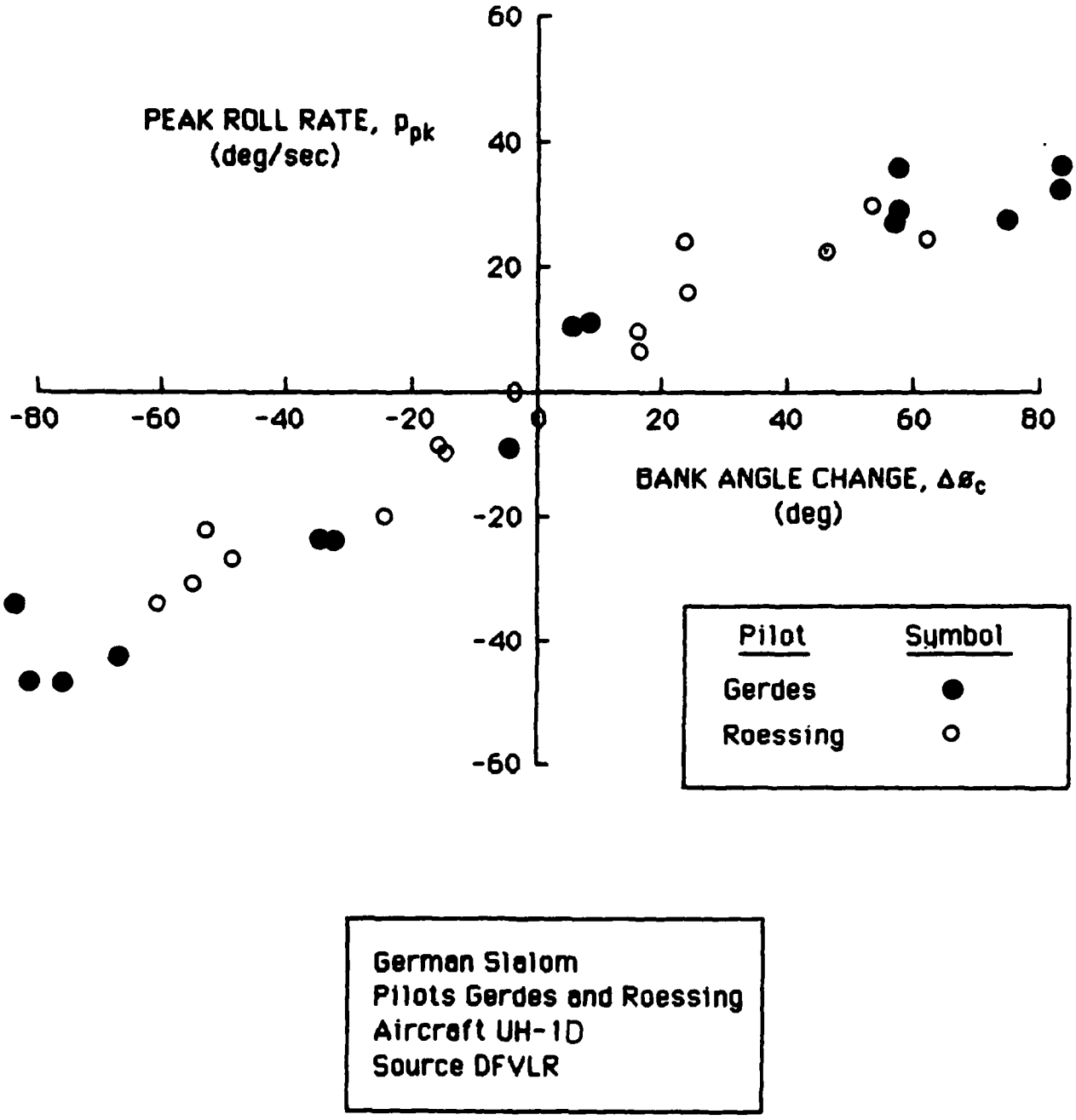

Figure 3-11a. 'German Slalom' Maneuver Data for the UH-1D Helicopter

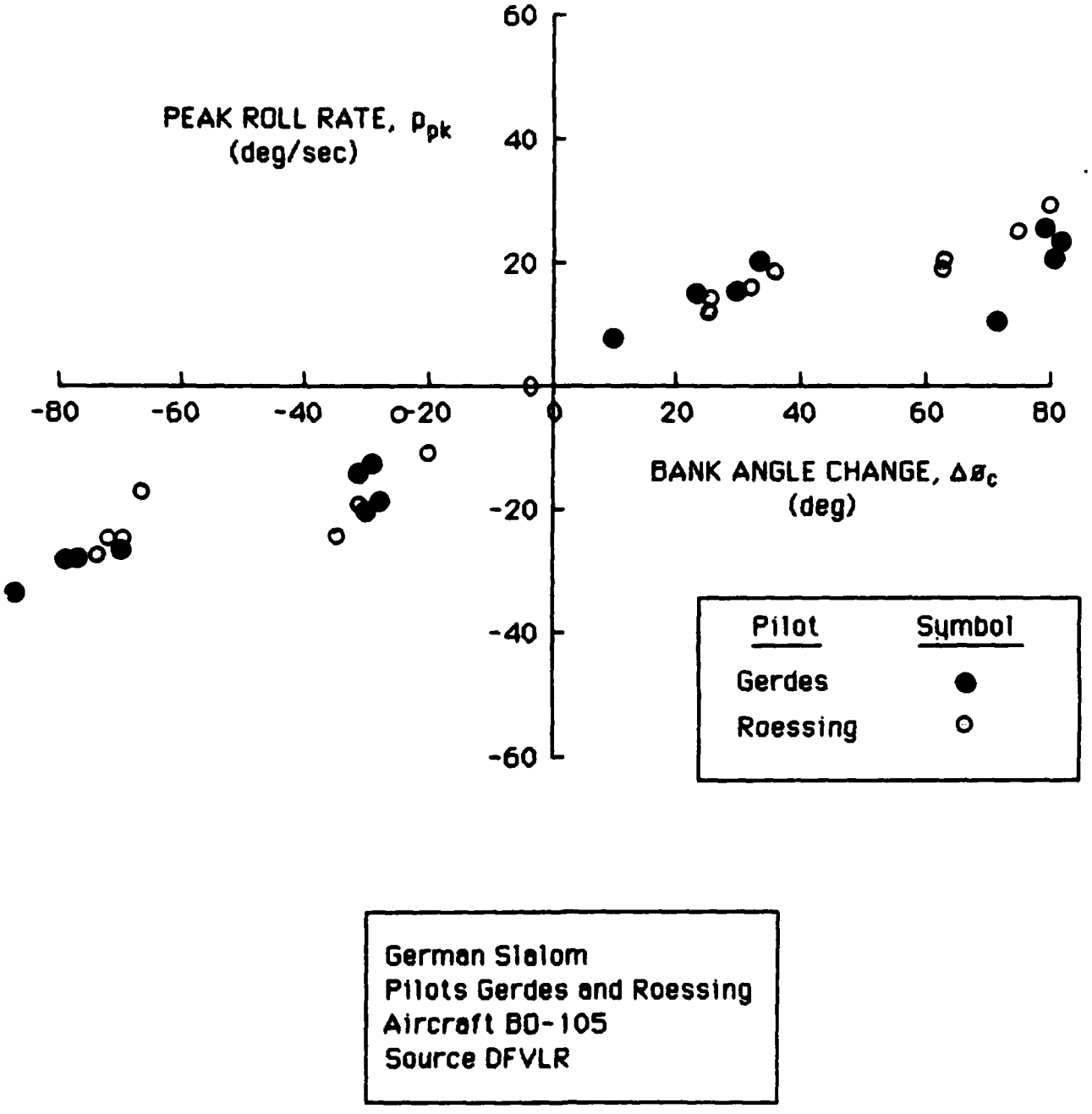

Figure 3-11b. 'German Slalom' Maneuver Data for the BO-105 Helicopter

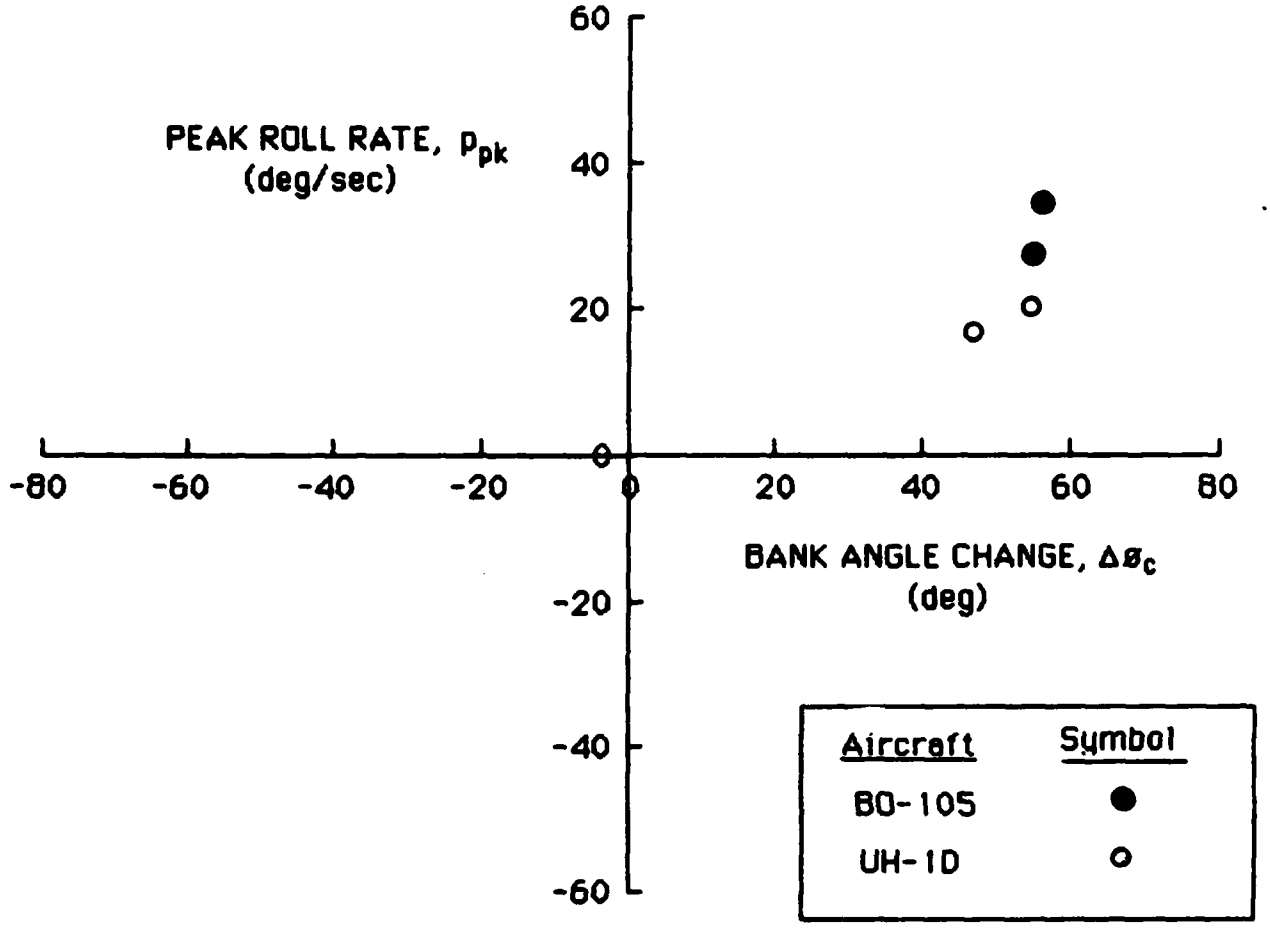

Figure 3-12. High-G Turn Maneuver Data for UH-1D and BO-105 Helicopters

TASK: Perform Horizontal Scissors

CONDITION: In an Army helicopter with an ACM IP/UT or ACM qualified pilot, VMC, at or above 100 ft AHO, with a designated bogey aircraft; perform horizontal scissors.

STANDARDS:

1. Clear the designated training area
2. Positive communications
3. Entry altitude as desired
4. Entry airspeed +/- 10 Knots
5. Maintain proper separation
6. Correct entry point
7. Bank angle not to exceed 60 degrees or -10 limits for aircraft configuration

DISCUSSION: The horizontal scissors is a defensive maneuver which normally should be avoided. It can be used if airspeed and nose-tail separation does not permit another maneuver.

DESCRIPTION:

1. BOGEY- in the tail chase position

2. FRIENDLY- Increase the rate of turn into the attacker until he overshoots or moves outside your turn. As he passes, execute a horizontal reversal (hard turn in the opposite direction). Repeat the reversal each time the opponent crosses your flight path to the outside of your turn. If you are behind the enemy, attempt to turn in phase with him and maneuver into the tail chase position.

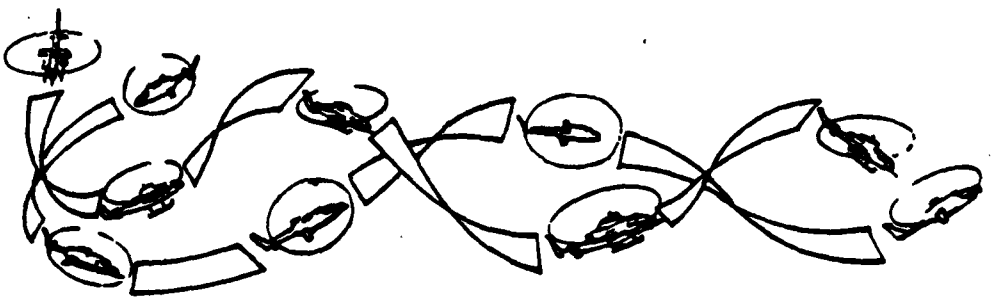

Figure 3-13. Abstract of Scissors Maneuver from the Rotary Wing Air Combat Maneuvering Guide

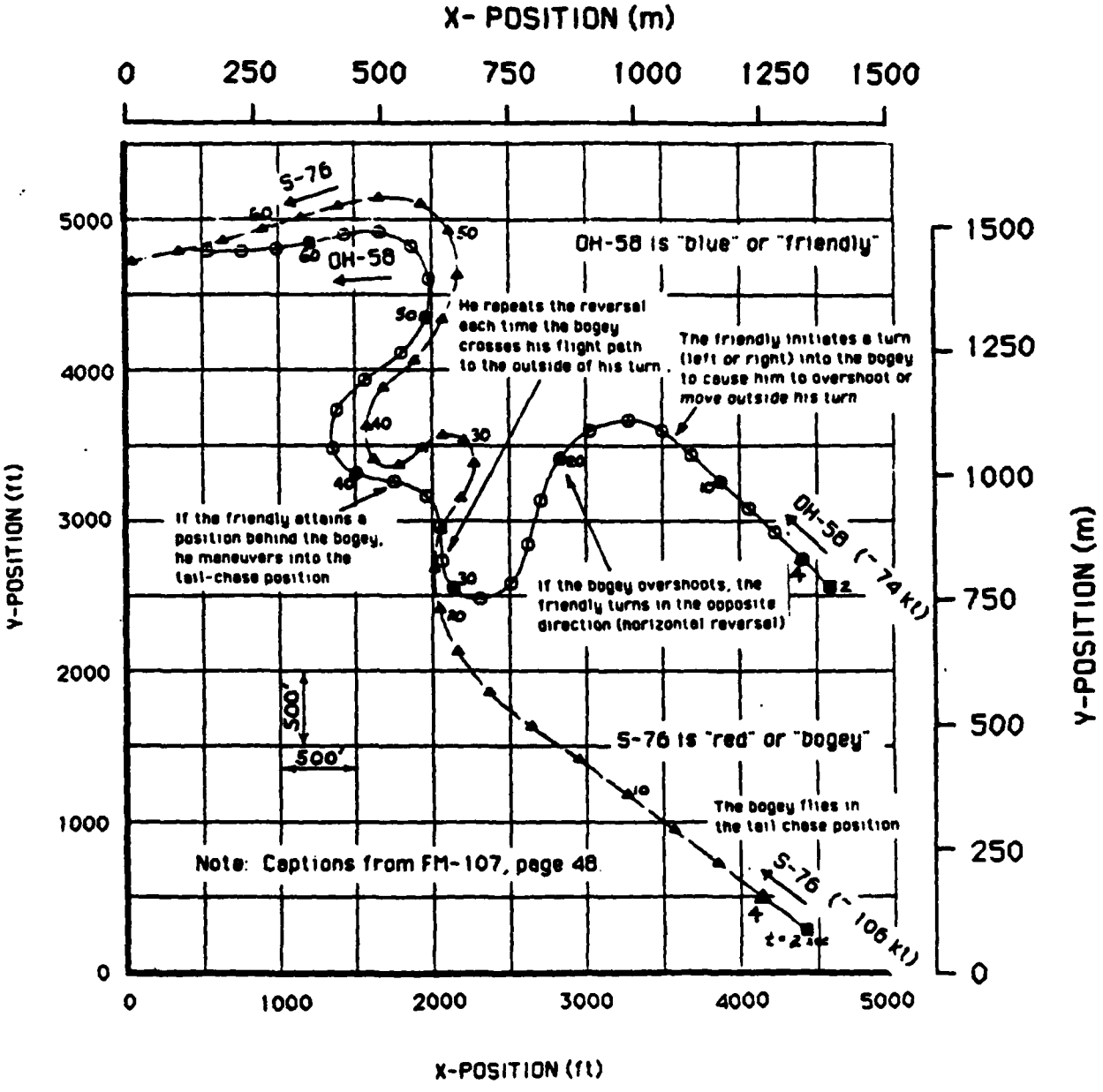

Figure 3-14. Planview of Flight Paths for Scissors Maneuver 23008 from the D-318 Data Base

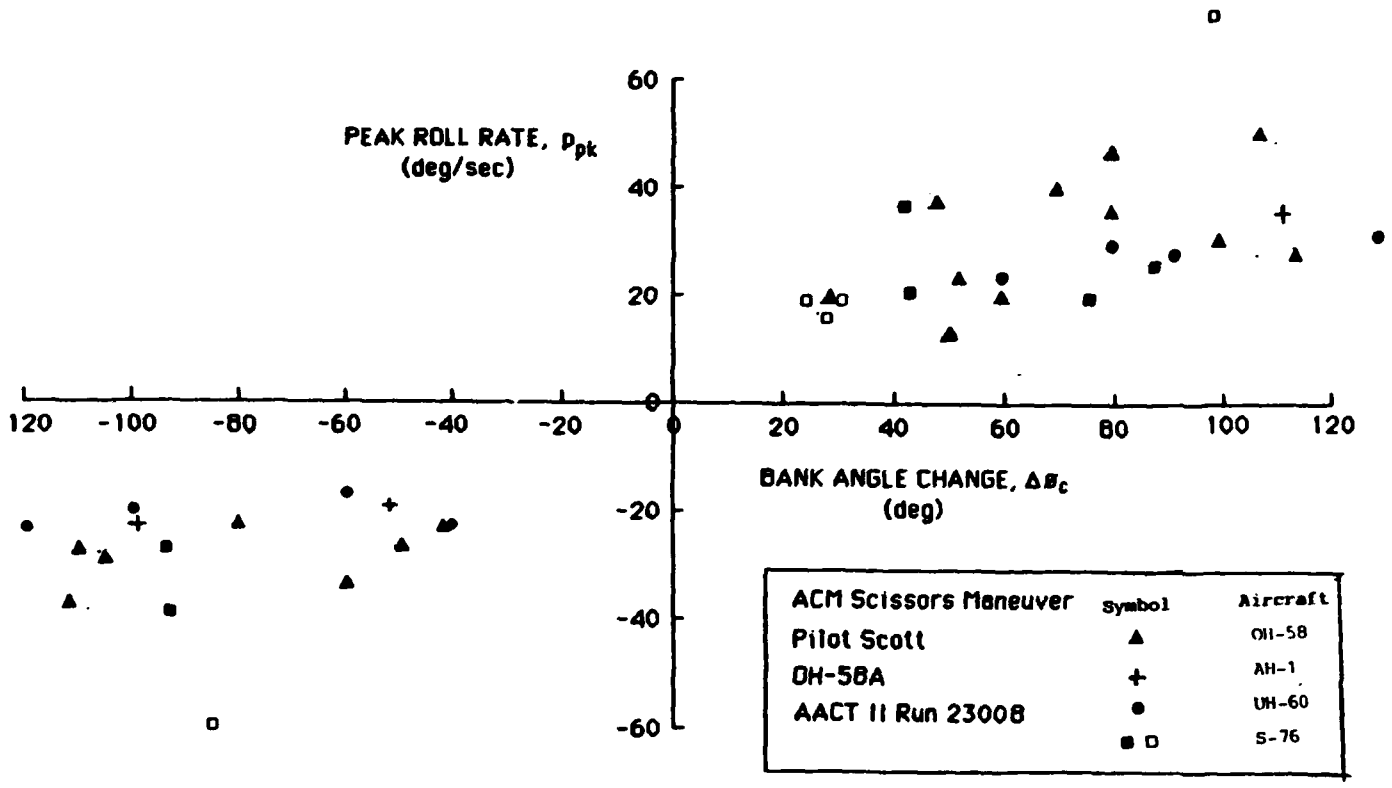

Figure 3-15. Scissors Maneuver Flight Data for a Variety of Helicopters

however data presented here were obtained without synthetic turbulence.

Figure 3-16 shows a typical time history for the pad tracking task, and Figure 3-17 shows a summary of the outer-loop and inner-loop performance. The maximum rates are significantly lower than those found in the UH-1H lateral positioning data, which was a product of the design goals for the translational rate control system.

NASA/Army (Corliss and Carico) Data Base A brief review of the results of the flight data from the roll damping and control sensitivity studies reported in Reference 27 was made. Typical maneuver performance data is shown in Figure 3-18.

C. Characteristics of Flight Data

The following observations are appropriate based upon the above flight data presentations:

Roll rate limiting is apparent in most maneuvers. The existence of a roll rate limit is clearly seen in the slalom maneuver (Figures 3-5 and 3-10) and the scissors air-to-air combat maneuver data (Figure 3-15). The lateral sidestep is the only maneuver where bandwidth requirements do not reduce with maneuver amplitude; a near straight-line relationship exists between peak rate and roll attitude change. It should be noted however that this maneuver is of small amplitude, less than 40 degrees roll attitude change.

Table 3-3 defines the peak roll rate characteristics for the flight data presented, most are limited to 40 degrees/second or less. The helicopter may be capable of substantially greater roll rates yet the pilot does not exploit them. In certain cases the roll rate limits

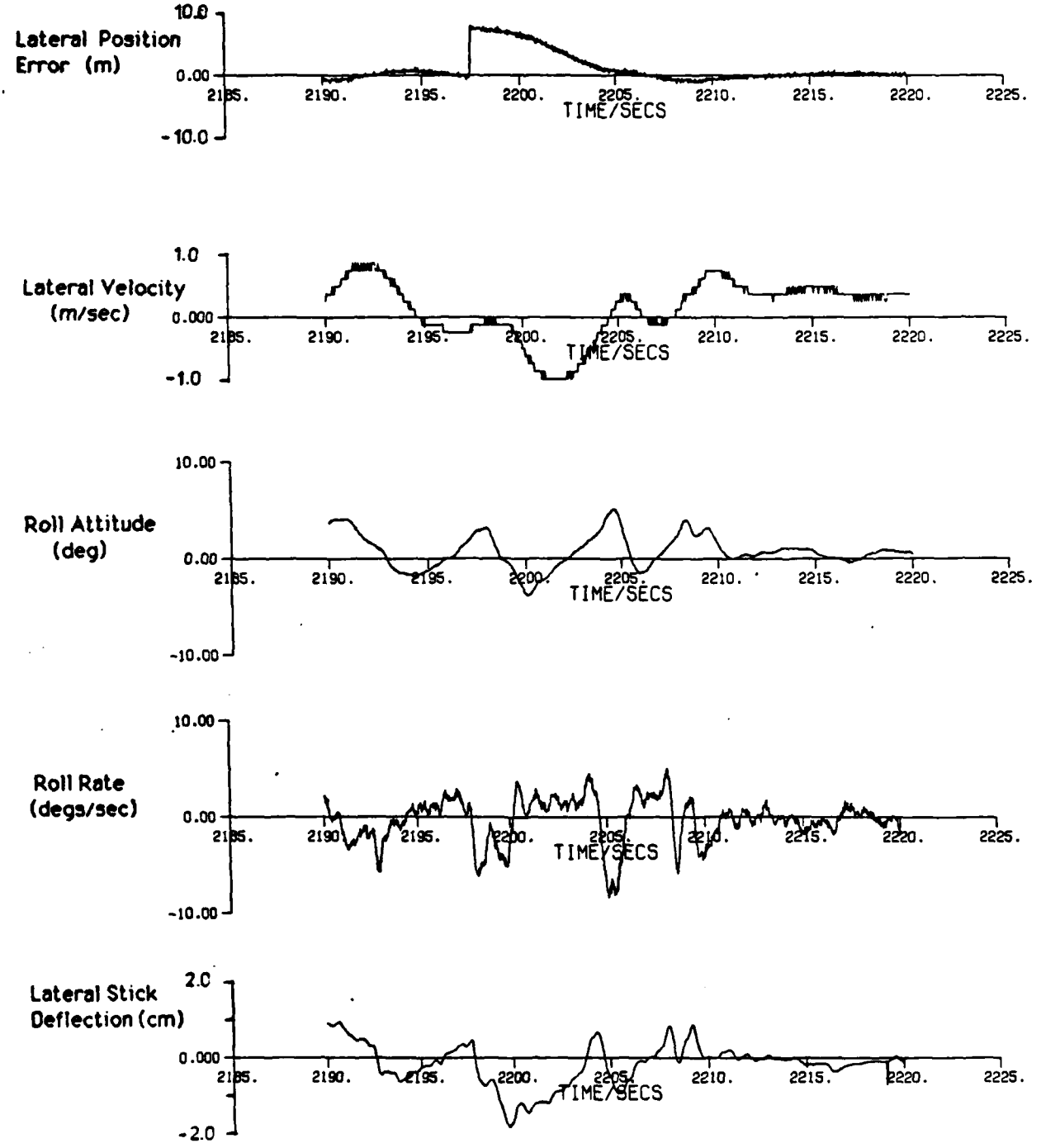

Figure 3-16. Typical X-22A Lateral Positioning Flight Data Configuration 218F

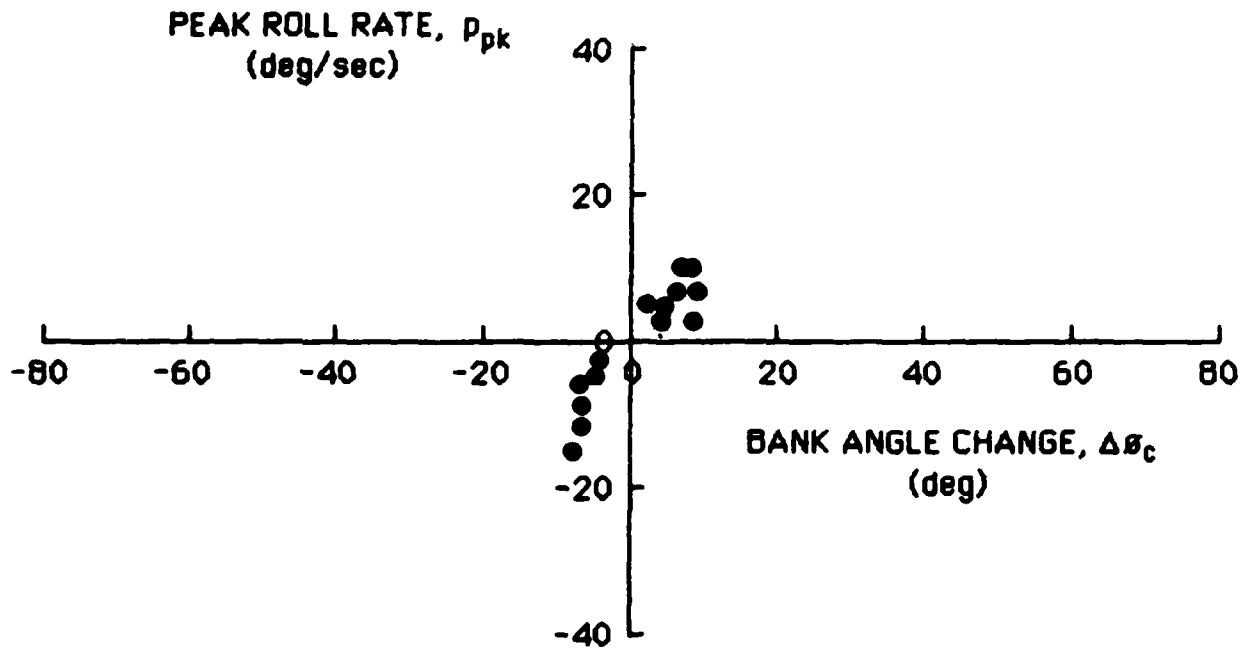

(a) Inner Loop Maneuver Data

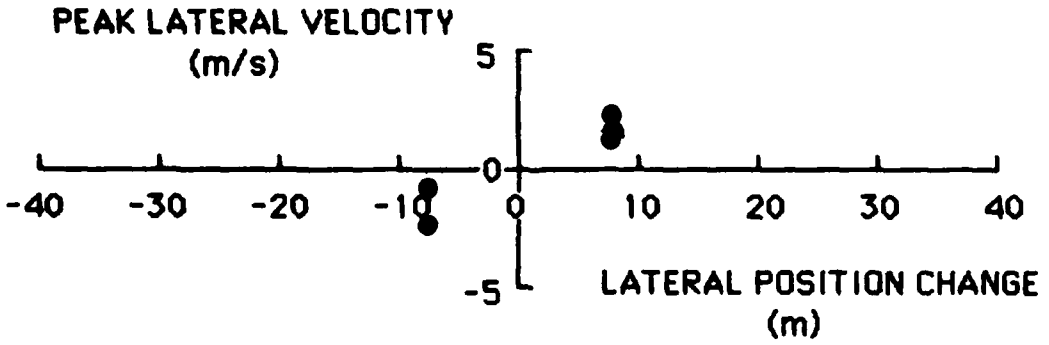

(b) Outer Loop Maneuver Data

Figure 3-17. X-22A Sidestep Maneuver Data

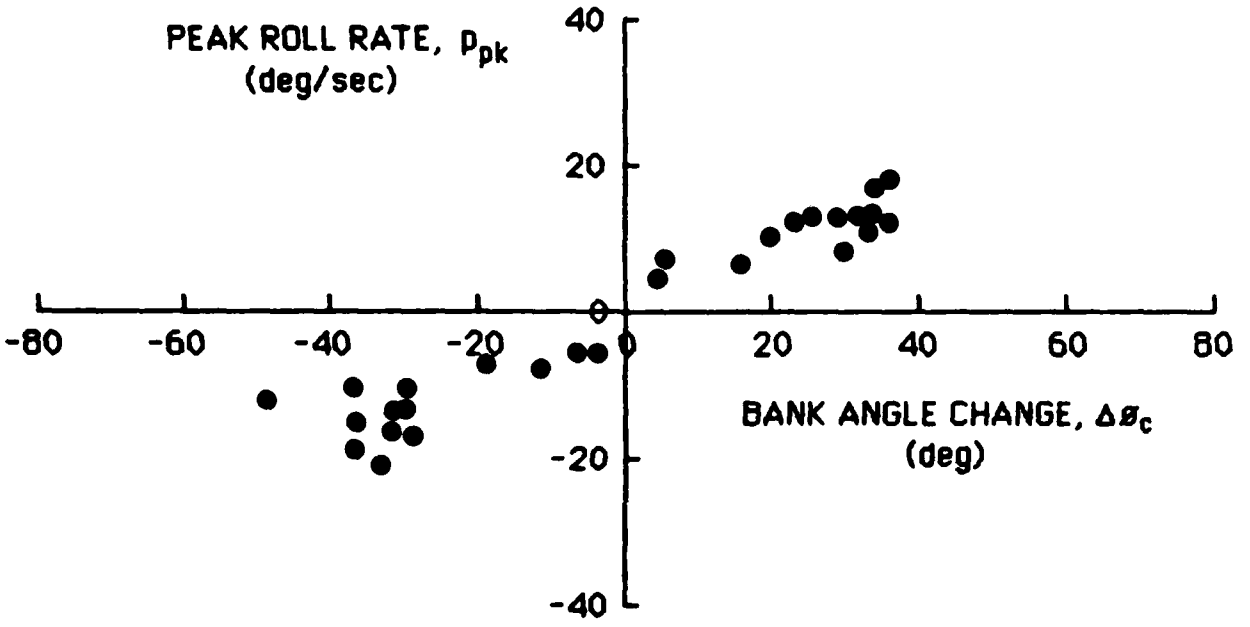

Corliss and Carico Flight Data (Reference 27)
Slalom Maneuver
Aircraft UH-1H (Variable Stability)

Figure 3-18. Corliss and Carico Maneuver Flight Data for the U. S. Slalom, L_p =-4.0

Table 3-3. Lateral Maneuver Flight Data Characteristics

Source	Aircraft	Maneuver	Airspeed (kt)	P_{MAX} (deg/sec)
NASA/Army (Manadyne Roll Control)	UH-1H	Straight-line slalom	60	40
		" " "	80	40
		50° intersection turn	60	46
		130° " "	60	30
		30 ft Lateral jink	30	40
		Sidestep	Hover	37
DFVLR	UH-1D	Straight-line slalom	60	25
	BO-105	" " "		23
	UH-1D	'German slalom'		47
	BO-105	" "		32
	UH-1D & BO-105	High-g turn		33
NATC/ AVSCOM		Scissors Maneuver (Various Helicopters)	-	40
NADC	X-22A	Sidestep	Hover	18
NASA/Army	UH-1H	Slalom (Corliss and Carico)	60	20

result from safety limitations imposed in the evaluation such as in the air-to-air combat engagements. However, this limiting characteristic is also seen in the absence of constraining safety restrictions such as in the slalom maneuver.

In section II the audit trail between the key lateral vehicle design parameters and closed-loop task performance capability was established. The phenomemon of roll rate limiting thus has significant implications on the swashplate and flapping stiffness required to achieve desired task performance.

Effects of Rotor Stiffness The DFVLR data comparing the UH-1D and BO-105 helicopters in the U.S. slalom (Figure 3-10) and the German slalom (Figure 3-11) are interesting. The UH-1D is characterized by a modest level of roll damping with some quickening provided by the mechanical stabilizer bar. The BO-105 has considerably faster short-term response as a result of the directly applied flapping moment at the rotor hub. The data indicates that the two helicopters were operated with comparable maneuver performance levels in the evaluations. The only significant difference was the peak roll rate demand of 40 degs/sec for the UH-1D in the German slalom while the BO-105 used 30 degs/sec. There may however be a difference in pilot technique in task execution between the BO-105 and UH-1D helicopters. This is suggested by the differences in relative clustering of the discrete maneuver data points between the two aircraft.

D. Implications for Simulation Program Design

The analysis of the flight data was effected prior to the simulation phase to provide a rational basis for maneuver and vehicle configuration selection. This analysis has provided the opportunity to define a collection of maneuvers which cover the range of performance demanded by the pilot in carrying out mission and flight phase objectives.

IV. EXPERIMENTAL SIMULATOR INVESTIGATION

A. Simulation Objectives and Experimental Design

1. Objectives

The analysis presented in Sections II and III provides a rational basis for a general approach to the lateral effectiveness issue on the simulator.

Section II of this report quantified closed-loop task performance characteristics in terms of the aggressiveness and amplitude parameters. The relationship between the key lateral design parameters and these closed-loop task performance characteristics was clearly established. The two parameters fundamental to this study are: maximum available roll rate (a control power issue) which affects the amplitude characteristic, and vehicle bandwidth, i.e.,rotor type (a short-term response issue) which affects the aggressiveness characteristics in the closed loop. These two aspects can be examined independently and under controlled conditions in the simulator.

The analysis of the flight data (Section III) provided a rational basis for the choice of tasks to be simulated, and most importantly provided a one-to-one comparison capability between flight and simulation. To achieve this objective the NASA/Army evaluation tasks flown at NALF Crow's Landing (see Section III) were used to construct a Computer Generated Imagery (CGI) data base for use in the simulation program.

Furthermore, the basic helicopter analysis of Section II showed flapping stiffness to be the sole determinant of response dynamics. This sensibly limited the number of configurations to be examined during

the program. The flight data analysis of the UH-1D and BO-105 helicopters provided specific configurations to be evaluated.

Up to this point there has been no mention of higher augmentation and response types such as rate and attitude command systems. Much of the structure of the proposed MIL-H-8501A update (Reference 3) addresses the requirements for higher order response types under high workload conditions requiring unattended operation. So a certain proportion of the simulation was set aside to look at the task performance capability of these higher order response types for the spectrum of flight tasks chosen.

Finally, there was an interest in studying the effects of pilot variation on task execution and the variety of pilot opinion with respect to vehicle configuration changes and task.

These ambitious and multifaceted objectives were at variance with the limited time devoted to simulation, however. An occupancy period of six weeks was allotted to this study of which about two were devoted mainly to checkout and refinement of test procedures. The remaining four weeks were divided between examination of near-earth, small-amplitude maneuvers and up-and-away, large amplitude maneuvers. The latter catagory was predominantly air combat maneuvering.

As illustrated in Figure 4-1, the main dimensions of the experimental design were the flight tasks and maneuvers, the vehicle configurations, and the pilots. Each of these plays a fundamental role in determination of the required levels of roll control effectiveness.

In order to provide a uniform guide to the conduct of the simulation an information package was prepared and distributed to participating pilots. This information package is documented in Volume II of this report.

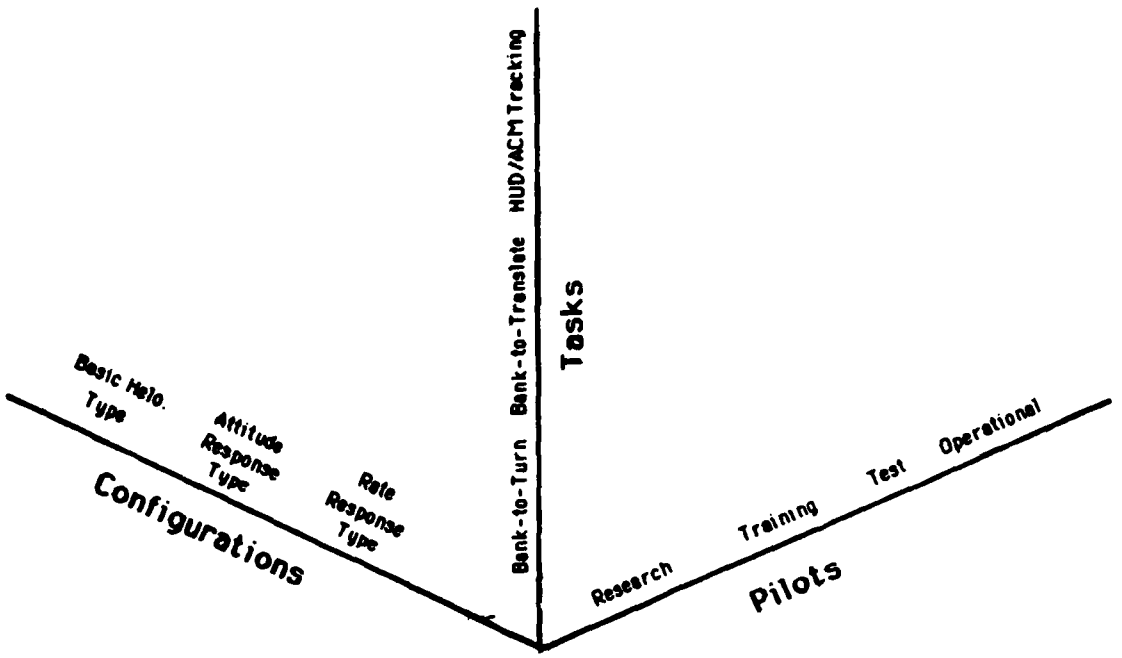

Figure 4-1. Primary Dimensions of the Experimental Matrix.

2. Flight Tasks

The array of flight tasks considered for the simulator experiment spanned the full spectrum of operational maneuvers, however not all were possible to execute in the simulator.

The tasks which were ultimately examined are listed in Table 4-1. These are classified as "near-earth, limited-amplitude" and "up-and-away, large-amplitude maneuvers". Most of these tasks were patterned after counterpart tasks already performed and analyzed in actual flight.

Table 4-1. Summary of Flight Tasks Chosen for Simulation.

Near-earth limited-amplitude maneuvers:

- Bank-to-turn
- In-line slalom turns
- Jinking (German slalom)
- Sidesteps
- Precision hover in gusts
- IFR heading change

Up-and-away large-amplitude maneuvers:

- Air combat tracking
- HUD bank angle tracking
- Air combat free engagement

The following set of figures reproduced from Volume II show the task definitions provided to each pilot participating in the simulation program. The versions shown here reflect refinements of the task descriptions and performance standards made by the pilots and engineers during the simulation period.

Bank-to-Turn Figure 4-2 shows the task description furnished for a bank-to-turn maneuver at a runway intersection. This maneuver was designed to closely approximate the corresponding task flown at NALF Crow's Landing with the UH-1H and discussed in the previous section.

Bank-to-turn maneuvers will be flown along the edges of intersecting runways. The pilot should wait until the last possible time to initiate the turn, then aggressively execute it, and roll out along the runway defining the new course. The turning maneuver should be level, coordinated, and flown at constant speed.

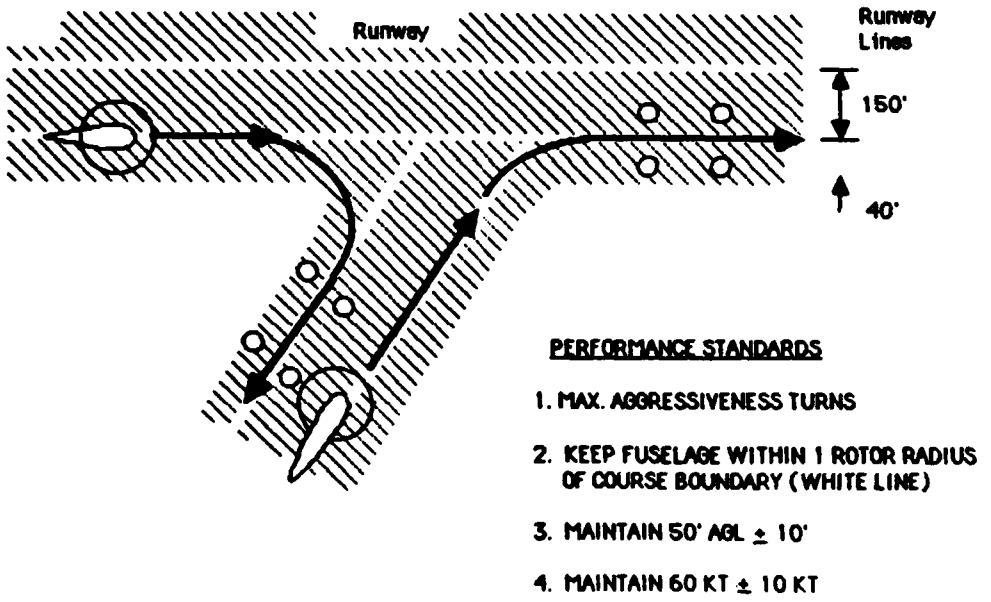

Figure 4-2. Heading Turn Maneuver Description

Slalom Turns. Figure 4-3 is the task description provided to pilots for the runway in-line slalom maneuver performed in the simulator. This also was patterned after the slalom flown at Crow's Landing.

Slalom turns will be flown, both at a nominal speed of 60 kt and at maximum possible speed, around pylons placed in the center of the runway every 600 ft. Minimum rotor clearance should be maintained while rounding pylons. Pilot's eye height should be at or below pylon height while maintaining level flight. The aircraft should not intrude beyond the runway white lines while negotiating the pylons.

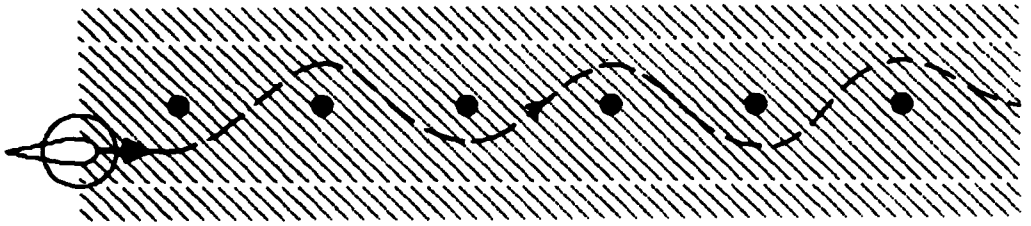

PERFORMANCE STANDARDS

1.. FUSELAGE INSIDE OF RUNWAY LINES

2a. FOR MAX. SPEED, CLEAR PYLONS BY TIP-PATH-PLANE

2b. FOR 60 KT, CLEAR PYLONS BY 10' ± ROTOR RADIUS

3. MAINTAIN 50' AGL ± 10'

Figure 4-3. Slalom Maneuver Description

Jinking Maneuvers. Figure 4-4 gives the task description for the lateral jink, a maneuver flown at Crow's Landing and similar to the "German slalom". The large obstacles placed in the computer-generated visual scene were a substantial difference from the markers used for the flight maneuvers.

Jinking maneuvers will be flown level at 40 kt around obstacles approximately 60 ft wide and 40 ft high. The nominal flight path is the runway centerline. NOE technique should be used keeping the longitudinal axis of the helicopter aligned with the ground track while clearing the pylons with the rotor at minimum distance. Maintain pilot eye height at or below obstacle height.

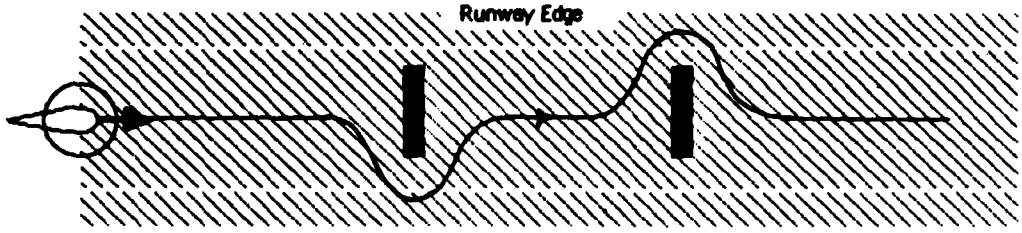

PERFORMANCE STANDARDS

1. CLEAR OBSTACLES BY AT LEAST ONE ROTOR DIAMETER, REMAINING WITHIN THE RUNWAY EDGES
2. MINIMIZE EXCURSIONS FROM THE CENTERLINE

Figure 4-4. Jinking Maneuver Description

Sidesteps. Figure 4-5 shows the sidestep task description. This also was flown at Crow's Landing but without the CGI trees which were used as position cues.

Sidesteps will be made aggressively starting in a hover condition and rapidly translating sideward to a specified position with minimal overshoot.

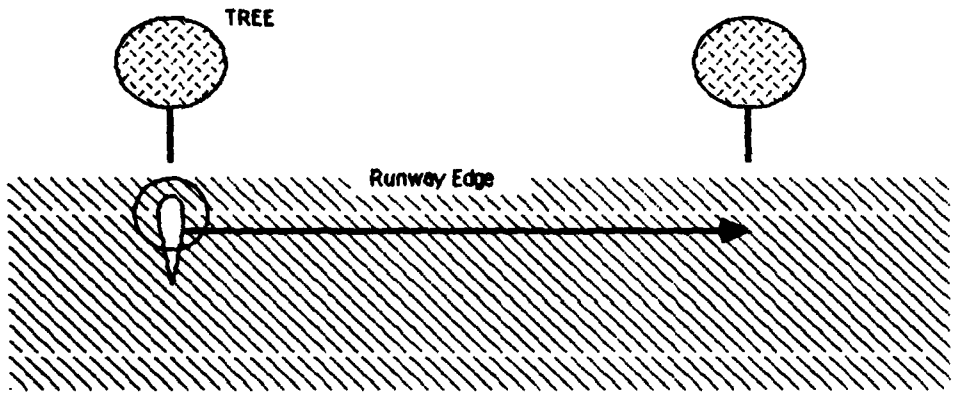

PERFORMANCE STANDARDS

1. MINIMIZE THE EXPOSURE TIME BETWEEN TREES
2. LIMIT OVERSHOOT TO LESS THAN 10' BEYOND TREE
3. MAINTAIN 25' AGL BUT REMAIN BELOW TREE-TOP LEVEL
4. MAINTAIN HEADING ± 15 DEG

Figure 4-5. Sidestep Maneuver Description

Bank Angle Tracking. This task consisted of the pilot aggressively following a Head-Up Display (HUD) command bar and only loosely controlling airspeed and altitude. Figure 4-6 describes the HUD format used. Figure 4-7 shows the sequence of roll commands. The roll attitude command signal was structured along the lines of the discrete bank angle tracking task used in the Lateral Higher Order System (LATHOS) fixed wing evaluations (Reference 44). The sequence used was the same throughout the program. Significant learning effects, i.e. precognitive pilot operation were not observed during the simulation.

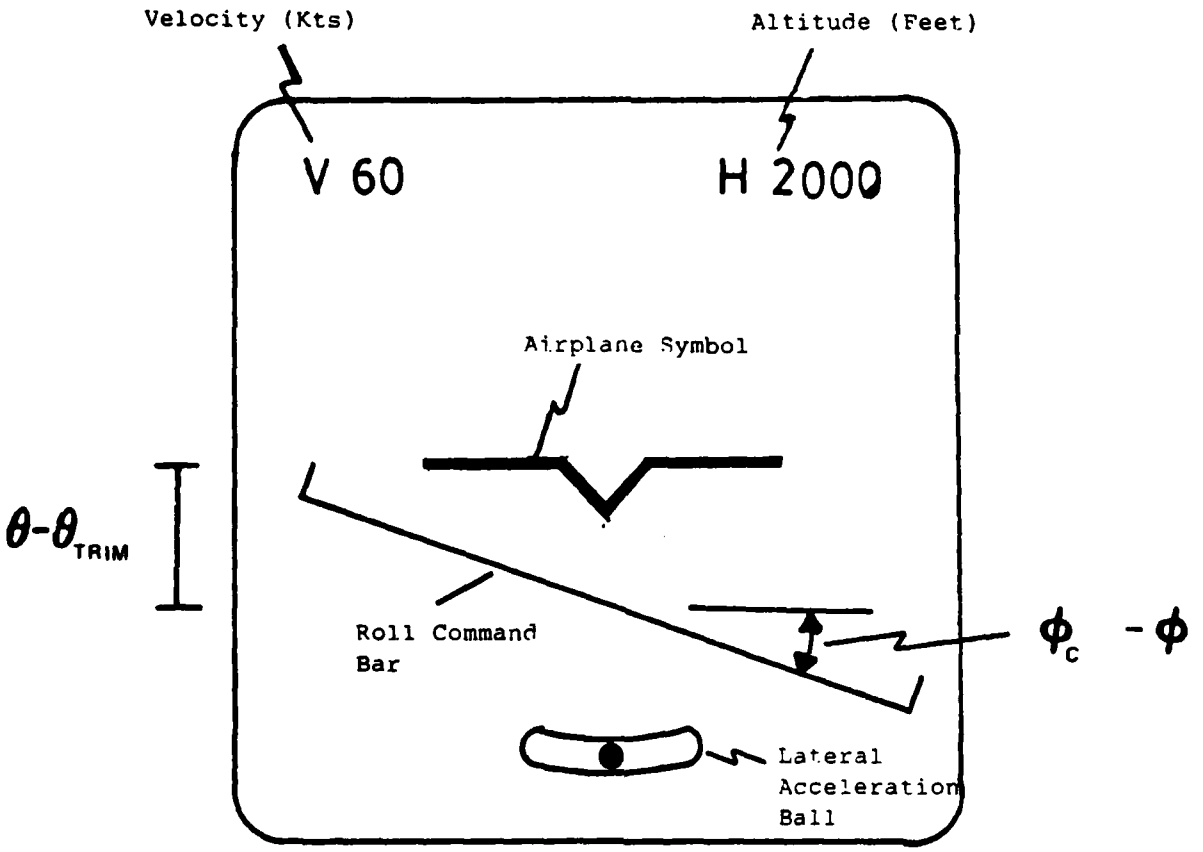

Figure 4-6. HUD Tracking Task Description

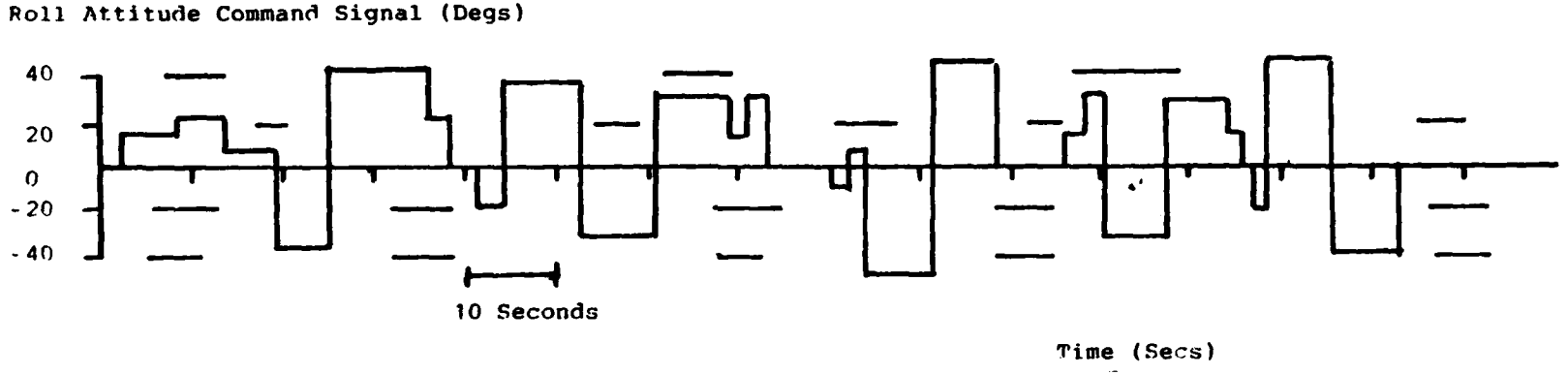

Figure 4-7. Roll Attitude Command for the Roll Tracking Task

IFR Heading Change. An IFR heading change task was conducted in order to examine and document a maneuver involving minimal agility. This was done strictly with reference to standard flight instruments.

Air Combat Tracking Maneuvers. The one-on-one Helicopter Air Combat (HAC) simulation developed by the U.S. Army Aeromechanics Laboratory, NASA Ames Research Center was used for this task. The details of the head-up displays, firing and scoring logic for both aircraft, the NOE data base developed for the simulation and visual characteristics are discussed in detail in Reference 45.

A modification to the HAC target (Red) aircraft allowed operation in either a manually controlled or automated mode. In the latter case the target was constrained to constant altitude and controlled by a series of command bank angles through a desired series of heading changes. Since the target aircraft is effecting co-ordinated turns through specified azimuth heading changes at specified bank angles the timing of the maneuver can be recovered easily using relationships for coordinated flight. Three automated turn schedules were used; the command bank angle and heading change schedules are shown in Table 4-2.

3. Vehicle Configurations

The vehicle configurations studied represent a wide range of basic helicopter rotor hub and airframe designs and flight control system types. It was intended to generally limit configurations to those which would be physically realizable and likely in view of anticipated design trends. The flight configurations used in the simulation program are documented thoroughly in terms of flight control system parameters, stability derivatives, trim conditions and dynamic checks in Volume II of this report. A summary of configuration types and response characteristics appear below. The classification of configurations is shown in Table 4-3.

Table 4-2. Sequence of Target Aircraft Heading Change and Bank Angle Commands.

Trajectory Element I	Trajectory 1		Trajectory 2		Trajectory 3	
	$\Delta\psi_{c_I}$ (deg)	ϕ_{c_I} (deg)	$\Delta\psi_{c_I}$ (deg)	ϕ_{c_I} (deg)	$\Delta\psi_{c_I}$ (deg)	ϕ_{c_I} (deg)
1	100	45	100	-45	120	45
2	90	-30	90	30	80	60
3	150	40	150	-40	90	-50
4	80	-50	80	50	30	20
5	60	20	60	-20	100	-40
6	100	-40	100	40	200	60
7	40	20	40	-20	120	-40
8	180	60	180	-60	60	20
9	210	-45	210	45	-	0

Table 4-3. Classification of Simulated Vehicle Configurations.

Basic Helicopter Type
Teetering Rotor
Teetering Rotor + Bell-Bar
Articulated Rotor
Rigid-Rotor

Rate-Command/ Attitude-Hold
with Turn Coordination Option

Attitude-Command/ Attitude-Hold
with Turn Coordination Option

The ARMCOP helicopter math model generally described in Reference 35, and particularized for the UH-60 Black Hawk (Reference 46), was the baseline vehicle used for evaluation. This helicopter was chosen because it represents a current generation design and has generally good roll control characteristics even without augmentation. Its articulated rotor hub represents a configuration intermediate to a teetering rotor and a rigid rotor.

Basic Helicopter Types. The basic unaugmented UH-60 has generally good roll control characteristics. The pitch and yaw axes, however, require augmentation to provide a suitable baseline evaluation model. The minimal complexity washed-out rate feedback design used on the YUH-60A and reported in Reference 47 was implemented in the pitch and yaw axes. The feedback transfer functions for this are:

$$\frac{b_{1_s}}{q} = 0.283 \frac{7s}{7s+1}$$

$$\frac{\theta_{TR}}{r} = 0.429 \frac{2s}{2s+1}$$

During the simulation significant problems were encountered in hover due to rapidly changing signs in side velocity and the consequence of solving flapping equations in the hub-wind axis system. A modification solved this problem by solution of the flapping equations in the hub-body axis system. This fix made by Mr. R. L. Fortenbaugh of Bell Helicopters, Textron is documented in Volume II of this report.

Basic helicopter types were created within the stucture shown in Figure 4-8. Rotor flapping stiffness variations were made varying the parameter L_{b1_s}, while the lag parameter T_L allowed variation of the

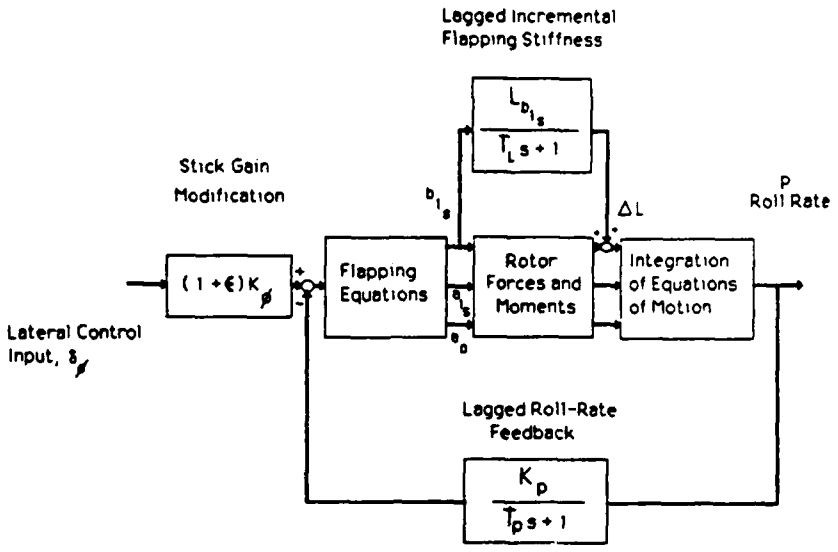

Figure 4-8. Basic Helicopter Configuration Parameters

amount of lag applied to the incremental stiffness. The lagged roll rate feedback loop (Figure 4-8) also allowed simulation of the Bell mechanical stabilizer bar (Bell-bar) found on the UH-1. Four basic helicopter configurations were constructed with steady-state roll rate sensitivity in the range 17-20 degs/sec/stick inch. The four configurations were representative of a teetering rotor, a teetering rotor plus a Bell-bar (UH-1 type), an articulated rotor (UH-60 type) and a rigid rotor (BO-105 type). Table 4-4 defines the parameters used to realize these configurations.

Table 4-4 Basic Helicopter Configurations

Configuration	Description	$\Delta L_{b_{1_s}}$	T_L	K_P	T_P	ϵ
1	Articulated Rotor (UH-60 Type)	0.0	0.0001	0.0	-	0.0
7	Rigid-Rotor (BO-105 Type)	100.0	0.0001	0.0	-	0.0
10	Teetering Rotor	-30.0	0.0001	0.0	-	0.0
15	Teetering Rotor + Bell-Bar (UH-1 Type)	-24.0	0.0001	0.16	3.0	0.44

The dominant roll response mode eigenvalues for the configurations are defined in Figure 4-9. Step input responses to lateral cyclic are shown for the configurations in Figure 4-10.

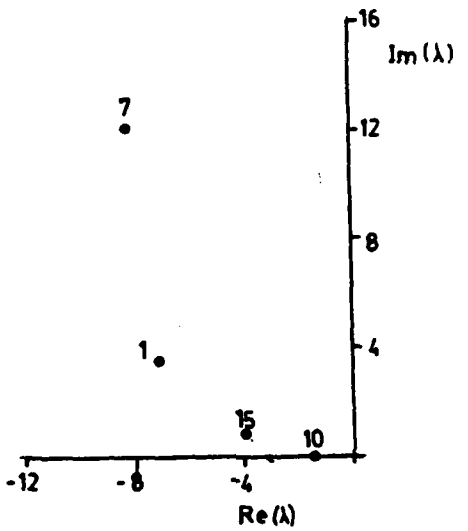

Figure 4-9. Roll Mode Eigenvalue Locations for Basic Helicopter Configurations

Attitude Command Response Types. One class of augmented response types investigated was the "attitude-command" or "attitude-command/-attitude-hold" system. This provides the pilot with automatic attitude maintenance during unattended operation and a change in attitude in proportion to lateral cyclic stick deflection.

These response types were obtained using a generic automatic flight control system structure developed under the Advanced Digital/Optical

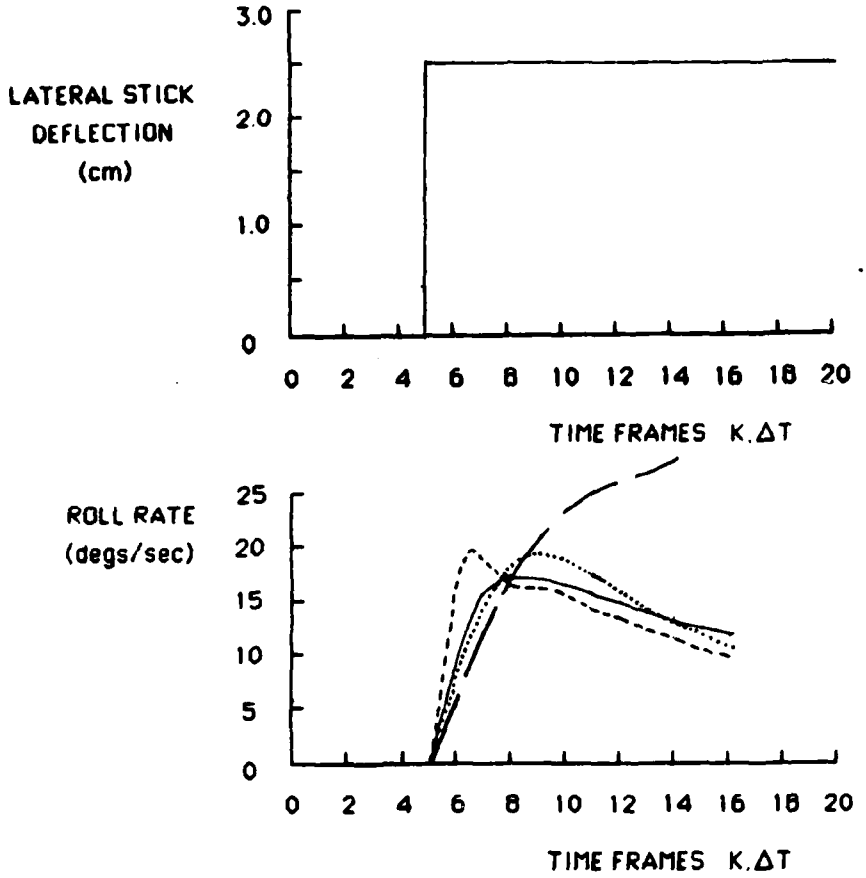

Figure 4-10. Step Response for Basic Helicopter Configurations

Flight Control System (ADOCS) work conducted by Boeing-Vertol (Reference 10). The structure consists of two main elements, stabilization feedback structure and feedforward command structure. Response-type variation was obtained by using the model-follower concept. The stabilization loops were closed around the vehicle to provide adequate stabilization characteristics with regard to disturbance. The feedforward structure was then used to effect any required pole/zero cancellation in the closed-loop model and to generate the required response-type command signal.

The parameters in the feedforward command generator structure were set to yield the configurations shown in Figure 4-11. The steady-state sensitivity for all configurations was set at 0.25 rads/stick inch in accordance with the data appearing in Reference 48 for Level 1 handling qualities. Table 4-5 defines the lateral feed-forward command generator stucture and the parameter values set for each configuration. A typical response to lateral control for the attitude-command/attitude-hold family is shown in Figure 4-12.

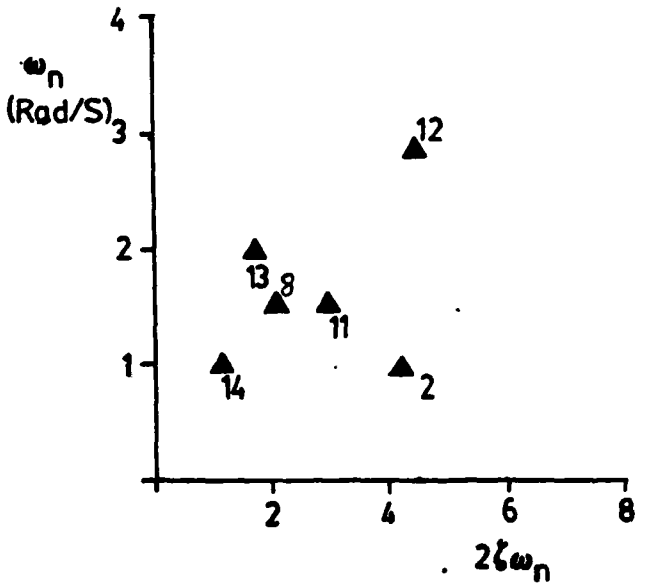

Figure 4-11 Attitude-Command/ Attitude-Hold Configurations

$$\frac{\phi(s)}{\delta_s(s)} = \frac{K}{s^2 + 2\zeta\omega_n s + \omega_n^2}$$

Table 4-5

Attitude Command System Parameters

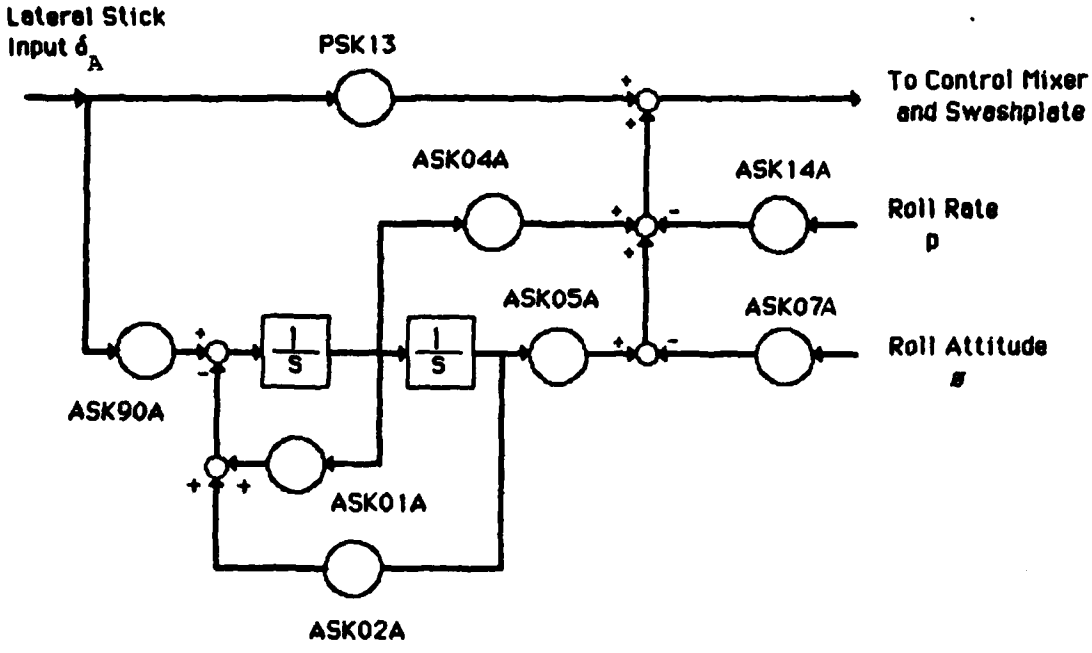

Config.	PSK13	ASK01A	ASK02A	ASK04A	ASK05A	ASK90A	ASK07A	ASK14A
2	0.48	4.0	1.0	0.70	2.8	1.65	20.0	6.0
8	0.53	2.0	2.25	2.50	5.63	1.83	20.0	6.0
11	0.53	3.0	2.25	2.50	5.63	1.83	20.0	6.0
12	0.48	4.5	9.0	7.2	25.2	1.65	20.0	6.0
13	0.48	1.75	4.0	4.48	11.2	1.65	20.0	6.0
14	0.0	1.0	1.0	0.93	2.80	1.65	20.0	6.0

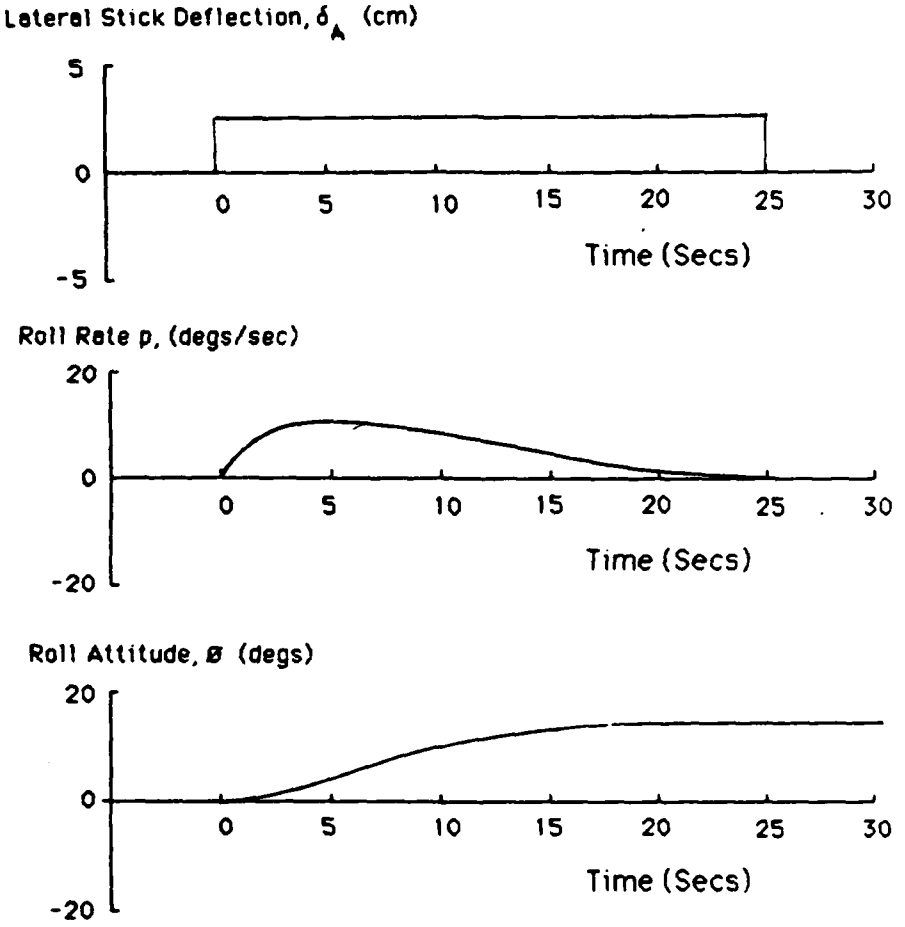

Figure 4-12. Lateral Control Response Characteristics for Attitude Configuration ATAT8

Rate-Command/Attitude-Hold Response Types. Another class of augmented response types implemented was the "rate-command/attitude-hold" system. The intent of this design was to provide a controlled element considered ideal for some kinds of flight tasks.

For this kind of response, a tight attitude stabilization loop was provided with a proportional plus integral feed-forward command path. This is illustrated in Figure 4-13.

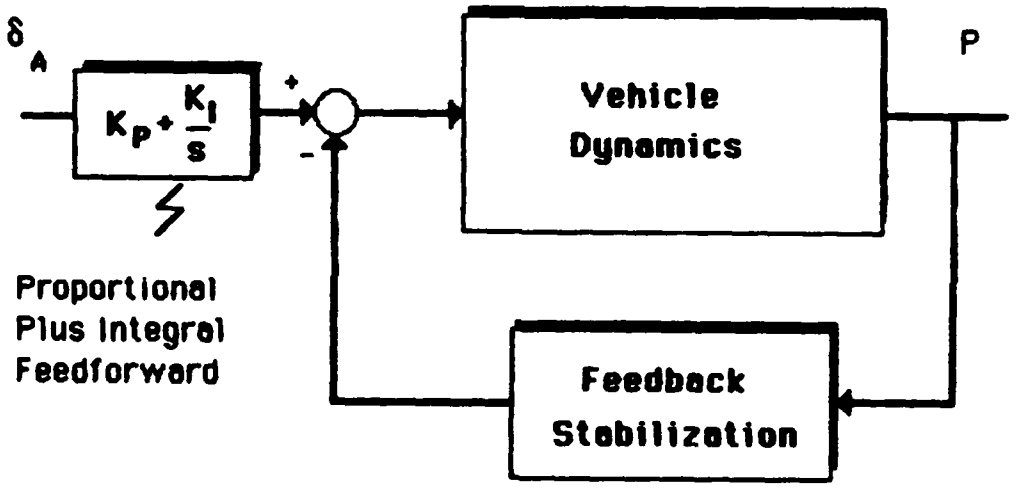

Figure 4-13. General Form for a Rate-Command/Attitude-Hold System.

Configurations were constructed having break frequencies at 1.0, 2.0 and 3.0 rads/sec in the roll rate response to lateral stick. The design roll rate sensitivity was 17 degs/sec/stick inch to provide comparable sensitivity to the basic helicopter types. The configuration parameters used in the ADOCS lateral control system are defined in Table 4-6. Figure 4-14 shows a typical response to lateral stick input.

Table 4-6

Lateral Control System Parameters for Rate-Command/Attitude-Hold Configurations

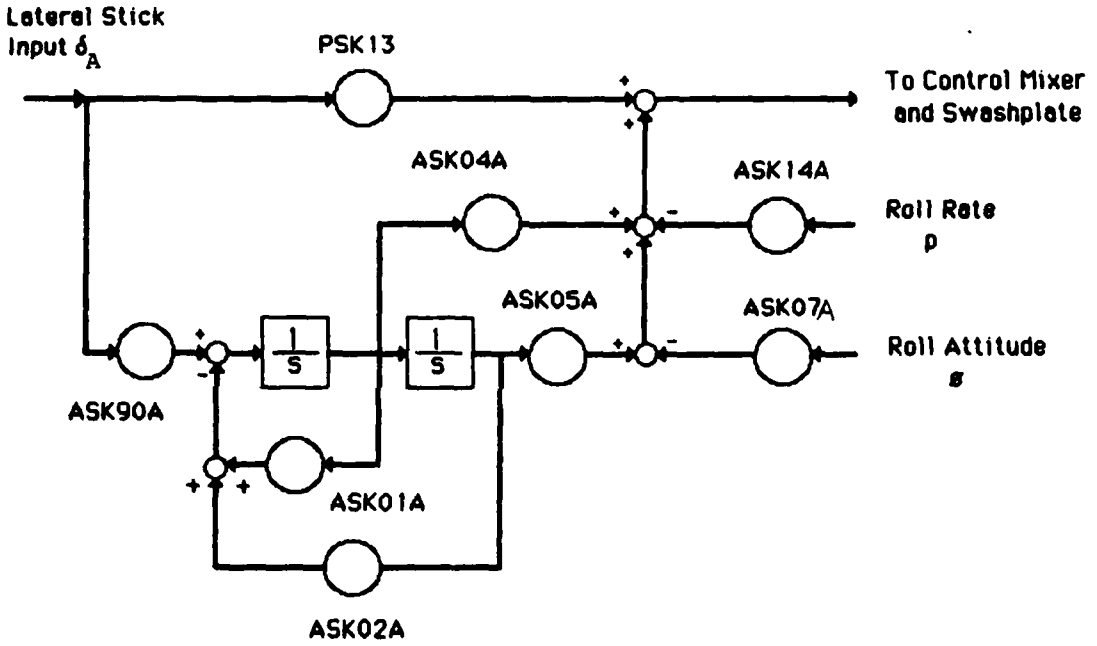

Config	PSK13	ASK01A	ASK02A	ASK04A	ASK05A	ASK90A	ASK07A	ASK14A
1	1.22	1.0	0.0	1.07	1.67	4.57	20.0	6.0
2	1.56	2.0	0.0	1.30	3.33	4.80	20.0	6.0
3	1.98	3.0	0.0	1.64	4.99	4.57	20.0	6.0

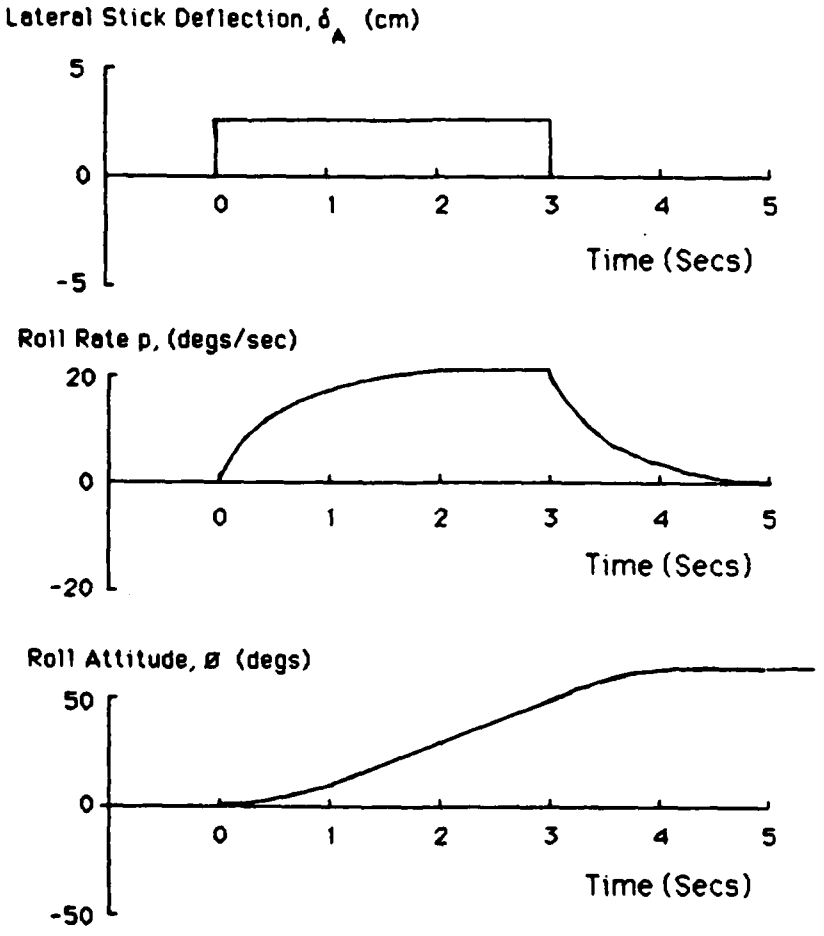

Figure 4-14. Response to Lateral Control For Rate-Command/-Attitude-Hold Configuration RAAT2

An objective of the simulation program was to define roll control power requirements in maneuvering tasks. Limitation of the roll control power available to the pilot was achieved in each vehicle configuration without the deleterious effects of hard stops (i.e. reducing control throw) by saturating the lateral control stick input as shown in Figure 4-15. The saturation point $\delta_{A_{max}}$ could be specified as desired.

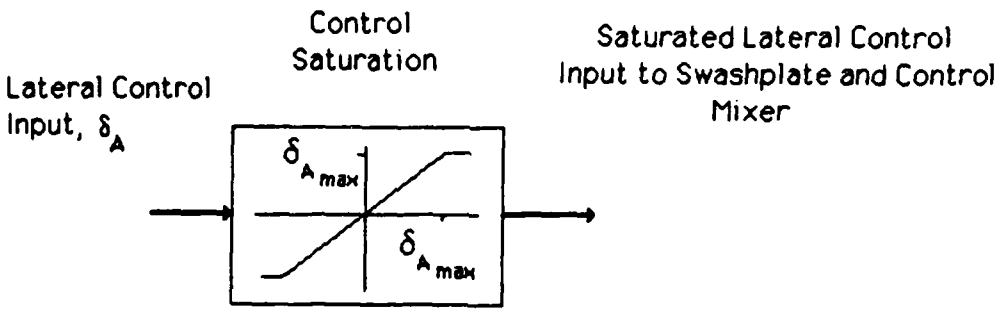

Figure 4-15. Saturation of Lateral Control Input for Control Power Investigations

4. Pilots

Pilots participating in the experimental program represented a variety of users and backgrounds. Each of the pilots are described in Table 4-7 in terms of their present affiliation, their qualifications, and their experience with various aircraft types and particular rotorcraft.

5. Environmental Conditions

The environmental conditions were not a primary variable in the test matrix. The normal operating conditions were unrestricted visibility and calm air. The flight maneuvers themselves provided the major "forcing function" to the pilot. In most cases visual cues were already substantially degraded because of the limitations of the visual system. A limited evaluation of the effects of turbulence on maneuvering was conducted. Turbulence environments characterized by root mean square lateral gust velocities of 3.0, 4.5 and 6.0 ft/sec were simulated. The specific turbulence parameters used in the simulation are documented in Volume II of this report.

B. Simulator Apparatus

This section on simulator hardware requirements is reproduced from Volume II of this report. The NASA Ames Vertical Motion Simulator with the RCAB module shown in Figure 4-16 was used in the simulation.

1. Cockpit

The cockpit was configured to represent a conventional helicopter in terms of instruments and controllers. A layout of cockpit instruments is shown in Figure 4-17. Controller characteristics are listed in Table 4-8.

Table 4-7

Simulation Program Test Pilots

Major James Casler U. S. Marine Corp.
Test Pilot, U. S. Navy Test Pilot School
Total Hours 3350 Hr
Total Rotary Wing Time 3100 Hr
Primary Rotary Wing Aircraft: CH-46, AH-1, UH-1
Evasive Maneuvering Time 30 Hr

CW2 James A. Elton, U. S. Army
ACM Instructor Pilot
Total Time 1000 Hr
Total Rotary Wing Time 950 Hr
Primary Rotary Wing Aircraft: OH-58, UH-1H, AH-1S
Evasive Maneuvering Time 75 Hr

Mr. William S. Hindson, Stanford University
Research Pilot NASA Ames
Total Time 4100 Hr
Total Rotary Wing Time 750 Hr
Primary Rotary Wing Aircraft: UH-1H, OH-58
Evasive Maneuvering Time 0 Hr

CW3 David Klindt, U.S. Army
ACM Instructor Pilot, Ft. Lewis , WA
Total Time 3000 Hr
Total Rotary Wing Time 3000 Hr
Primary Rotary Wing Aircraft: AH-1,UH-1,OH-58
Evasive Maneuvering Time 250 Hr

Mr. Manfred Roessing, DFVLR
Chief Test Pilot DFVLR
Total Time - Hr
Total Rotary Wing Time - Hr
Primary Rotary Wing Aircraft: UH-1, BO-105
Evasive Maneuvering Time 0 Hr

CW4 Les Scott, U. S. Army
Test Pilot, U. S. Navy Test Pilot School
Total Hours 5700 Hr
Total Rotary Wing Time 4700 Hr
Primary Rotary Wing Aircraft: AH-1, UH-1, UH-60
Evasive Maneuvering Time 30 Hr

Mr. George Tucker, NASA Ames
Research Pilot NASA Ames
Total Time 4740 Hr
Total Rotary Wing Time 1160 Hr
Primary Rotary Wing Aircraft: H-1, AH-1, SH-3, HH-3
CH-47, OH-58
Evasive Maneuvering Time - Hr

Lt. Col. Grady Wilson, U. S. Army
Research Pilot, Aeromechanics Laboratory NASA Ames
Total Time 6100 Hr
Total Rotary Wing Time 1507 Hr
Primary Rotary Wing Aircraft: UH-1H, CH-47, OH-58, AH-1
Evasive Maneuvering Time - Hr

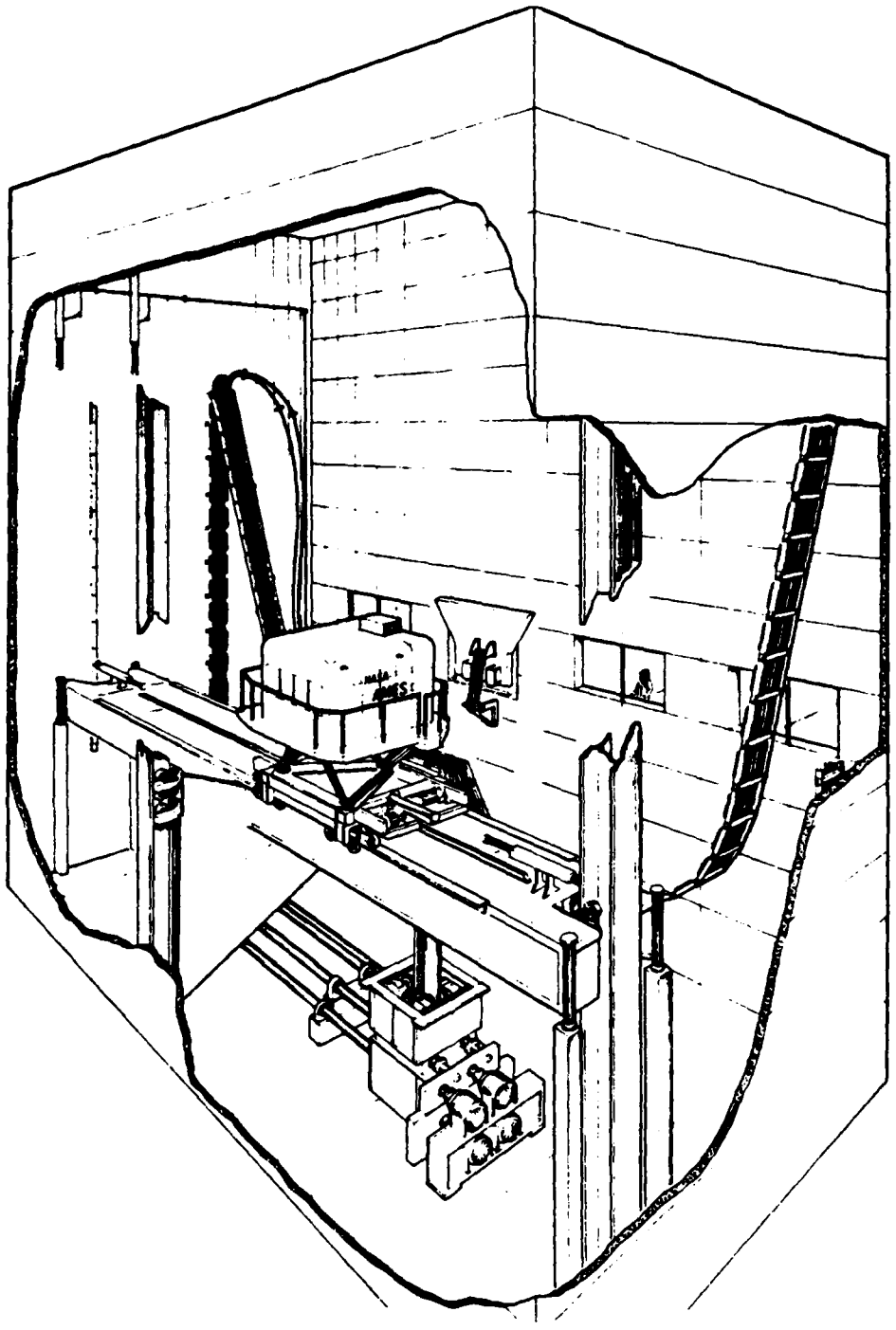

Figure 4-16. NASA Ames Vertical Motion Simulator with RCAB Module

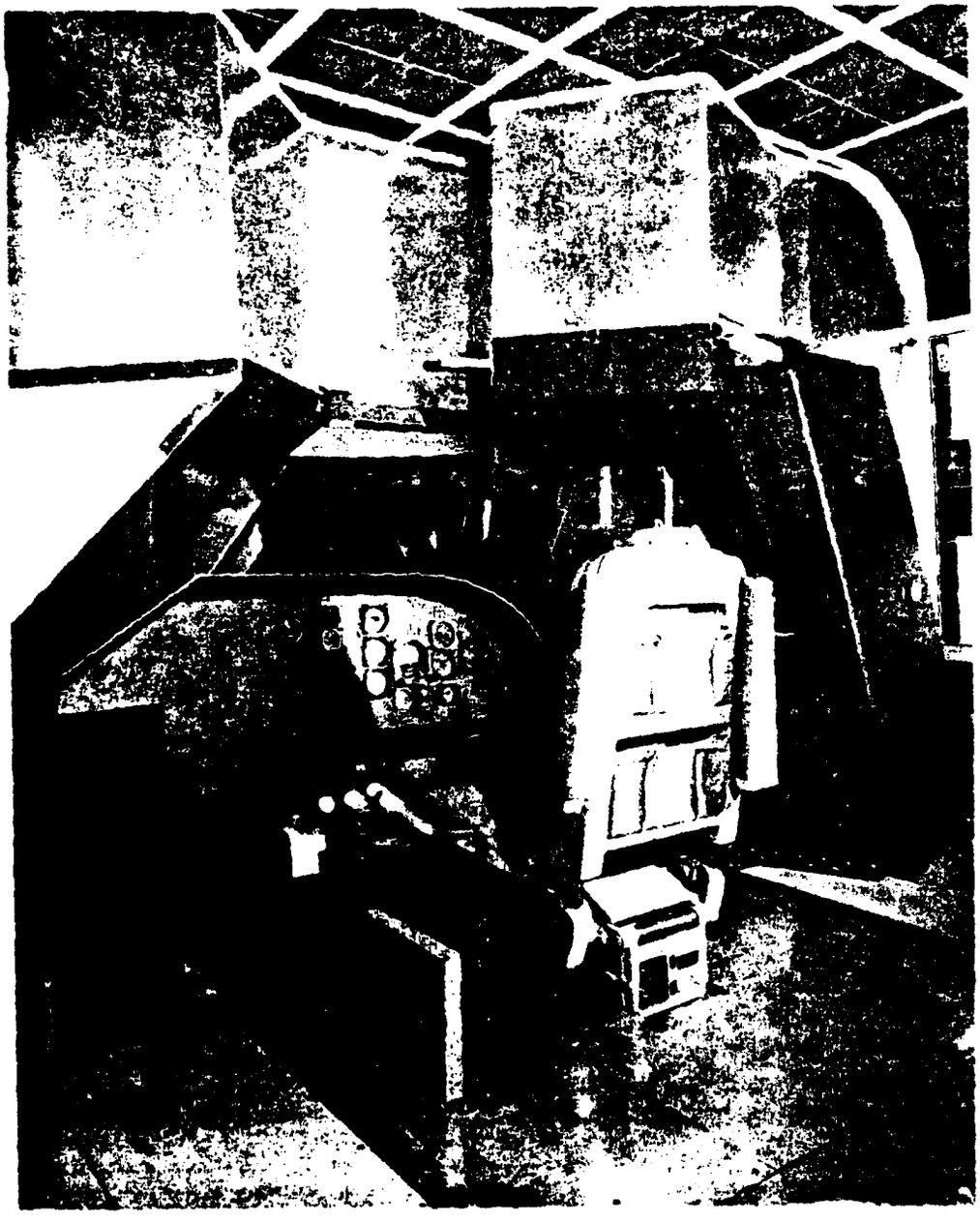

Figure 4-17. Cab Instrumentation

Table 4-8. Controller Characteristics.

Parameter	Longitudinal	Lateral	Rudder	Collective
Travel (cm)	± 15.2	± 15.2	± 7.6	0-25.4
Breakout Force (N)	4.45	4.45	13.35	0.0
Force Gradient (N/cm)	2.19	1.40	12.26	0.0
Coulomb Friction (N)	0.0	0.0	0.0	13.35

2. Visual System

A four window computer generated image (CGI) display was used in the performance of all flight tasks except for the IFR turns and the up-and-away large amplitude maneuvering phase. In the latter task the chin window had to be disabled in order to allow the target helicopter image to be added to the visual scene.

The visual system computation, interface, and refresh delays result in considerable time delay in addition to the basic time step for model integration. Figure 4-18 from Reference 49 defines the relationship between overall throughput time delay and cycle time. Cycle times were 64 and 72 msec for the near-earth and up-and-away maneuvering phases, respectively. This resulted in the estimates of the throughput time delay (control input to visual update) for the simulation shown in Table 4-9.

Table 4-9. Estimated Visual System Time Delay.

Simulation Phase	Cycle Time Delay (msec)	Throughput Time Delay (msec)
Near-Earth	64	189
Up-and-Away	72	202

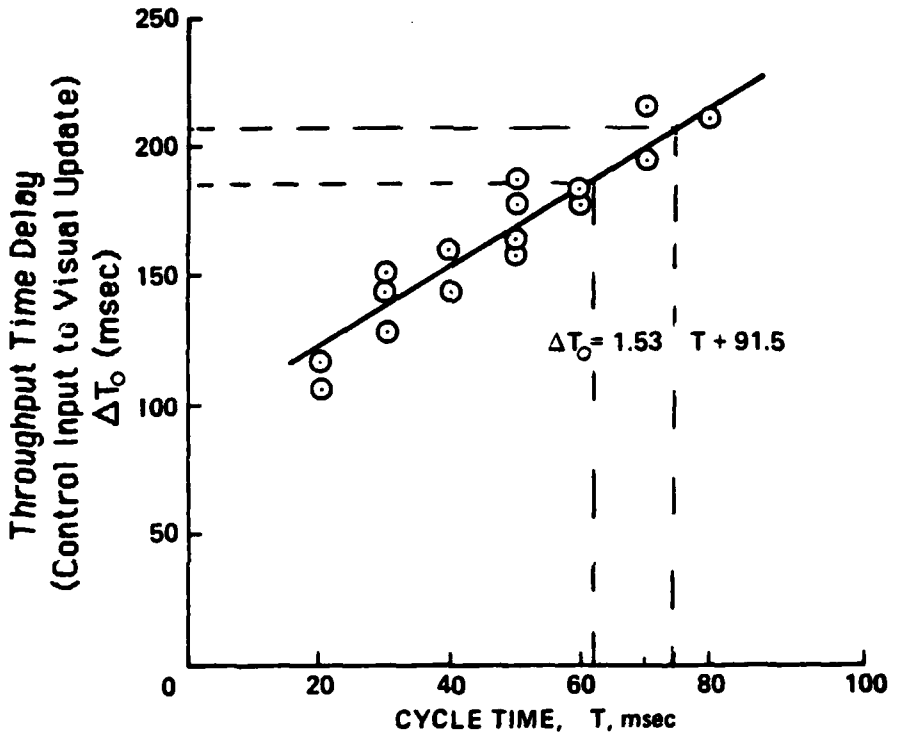

Figure 4-18. Effect of Cycle Time on Throughput Time Delay from Reference 49

The 12 msec increase in time frame from the near-earth to the up-and-away maneuvering phases is associated with the added software requirements for the adversary (Red) helicopter in the air combat maneuvering tasks.

To allow a one-on-one comparison of task execution between simulation and flight a Computer Generated Imagery (CGI) data base was built specifically for this simulation program. The data base modeled the NALF Crow's Landing area and tasks examined in the NASA/Army evaluations reported in Section III. Special concern was given to providing adequate relative velocity, position and height cues through the use of detail e.g. trees, markers, texture, etc. The other data base used during the simulation program was the HAC terrain for air combat and nap-of-the earth exercises.

3. Motion System

The motion system consisted of full travel (within electrical stops) of the NASA Ames Vertical Motion Simulator (VMS) shown in Figure 4-16. Nominal motion limits are given in Table 4-10 from Reference 49.

Table 4-10. VMS Motion System Limits.

Motion	Displacement	Velocity	Acceleration	Frequency at 30 Phase Lag Hz
Lateral	± 5.18 m	±2.44 m/s	$\pm 4.57\ m/s^2$	1.6
Vertical	± 7.62 m	±4.87 m/s	$\pm 7.31\ m/s^2$	1.1
Roll	$\pm 19.5^0$	$\pm 19.5^0/s$	$\pm 57.3^0/s^2$	1.2
Pitch	$+20.0^0, -24.5^0$	$\pm 19.5^0/s$	$\pm 57.3^0/s^2$	1.1
Yaw	$\pm 34.0^0$	$\pm 19.5^0/s$	$\pm 57.3^0/s^2$	1.1

Motion parameters defining the second-order washout scheme are shown in Table 4-11. These were adjusted individually for the near-earth maneuvers, air combat maneuvers, and the HUD tracking task. The values used appear in Table 4-12

4. Computer

The general-purpose simulator computer used for this experiment was a Xerox Sigma 8. The frame time used for the near-earth maneuvering phase was 62 msec and, for the up-and-away tasks, 74 msec. The larger frame times associated with up-and-away air combat maneuvering tasks results from the additional software requirements for the target aircraft. This was considered marginal and may have affected results for some vehicle configurations representing quick short-term response.

C. Data Acquisition

Data were acquired to provide both quantitative and qualitative definition of simulator results. A special emphasis was placed on on-line data acquisition although this was only partially successful because of limitations in computing and plotting facilities.

1. Quantitative Data

The primary purpose of quantitative data acquistion was to provide for on-line and post simulation analysis of task execution, pilot control usage, and vehicle response characteristics. State variables from most runs were stored on magnetic tape using RUNDUM format (Reference 50). Selected portions of these data were transfered to IBM PC floppy disk format for later analysis.

Automated recovery of discrete maneuver data. A discrete maneuver analysis algorithm was implemented to compute the time of maneuver

Table 4-11

Definition of Motion System Washout Parameters

Motion Washout Filter Form for all Six Axes:

$$\frac{\text{Motion Base Acceleration}}{\text{Model Acceleration}} = \frac{\ddot{X}_{Motion}}{\ddot{X}_{Model}}(s) = \frac{G\,s^2}{s^2 + 2\zeta\omega_n s + \omega_n^2}$$

ζ = 0.707 for all filters

The washout filter gains (G) and natural frequency (ω_n) are scheduled in the x degree of freedom with airspeed from low airspeed values of GxS and OMEGxS respectively to the higher airspeed values GxF and OMEGxF in accordance with the functional relationship:

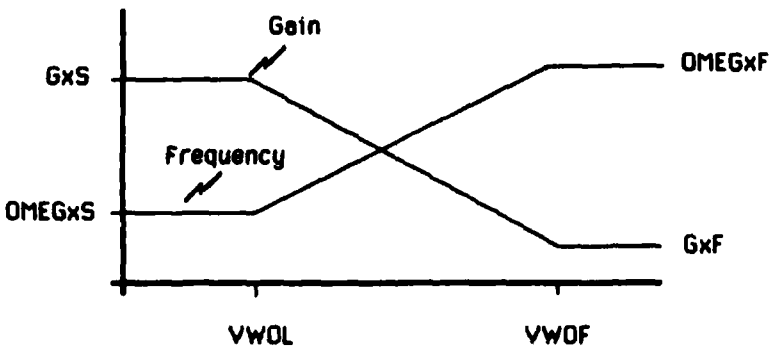

Scheduling the motion system parameters with airspeed allows optimization of motion fidelity subject to the system limits throughout the maneuver envelope, e.g. nap-of-the-earth and air combat maneuvering.

Table 4-12

Roll Control Simulation Motion Gains

Motion Filter Parameter	Low-Level Phase	Up-and-Away Phase
Low Speed		
GPS	0.4	0.7
GQS	0.7	0.7
GRS	0.3	0.3
GXS	1.0	1.0
GYS	0.5	1.0
GZS	0.8	1.0
OMEGPS	0.7	0.6
OMEGQS	0.5	0.5
OMEGRS	0.7	0.5
OMEGXS	0.6	0.6
OMEGYS	1.0	1.0
OMEGZS	0.2	0.2
YWOL	10.0	10.0
High Speed		
GPF	0.2	0.33
GQF	0.5	0.40
GRF	0.3	0.40
GXF	0.5	0.0
GYF	0.35	0.50
GZF	0.80	0.40
OMEGPF	0.65	0.80
OMEGQF	0.50	0.60
OMEGRF	0.50	0.60
OMEGXF	0.60	1.00
OMEGYF	0.70	0.70
OMEGZF	0.30	0.80
YWOF	20.00	20.00

Note: Parameters are defined in Table 4-11

initiation, peak roll rate, commanded bank angle change, time between bank angle changes and the bandwidth of the maneuver. Figure 4-19 shows an example of operation in the slalom maneuver task. Efforts were made to plot the peak roll rate versus amplitude change data on-line however the computer capability was found to be insufficient in the real time environment. This algorithm was applied to both inner- and outer- loop task variables.

Control usage data A histogram and probability of exceedence diagram for lateral stick activity was recovered for each run. Examples are shown in Figure 4-20.

2. Qualitative Data

Qualitative data consisted of recorded pilot comments following a carefully structured checklist and culminating in use of the standard Cooper-Harper pilot opinion rating scale (Reference 32). This provided a high degree of uniformity in the form of pilot commentary and a systematic means of addressing the topics of interest.

Pilot Commentary Checklist. This guide to pilot commentary is shown in Figure 4-21. It is divided into three topics which correspond to task, vehicle, and pilot issues, respectively. Each topic also is fundamentally related to the Cooper-Harper rating scale system. A numerical rating scheme (one to three) was established for each of the individual characteristics but was not used consistently throughout the experiment.

As shown in the above figure, flight task or maneuver objectives are classified in terms of the general task performance factors discussed earlier. The pilot was asked to comment on both the desired task objectives and those actually realized with a given configuration. This was intended to help the pilot determine a rational basis for

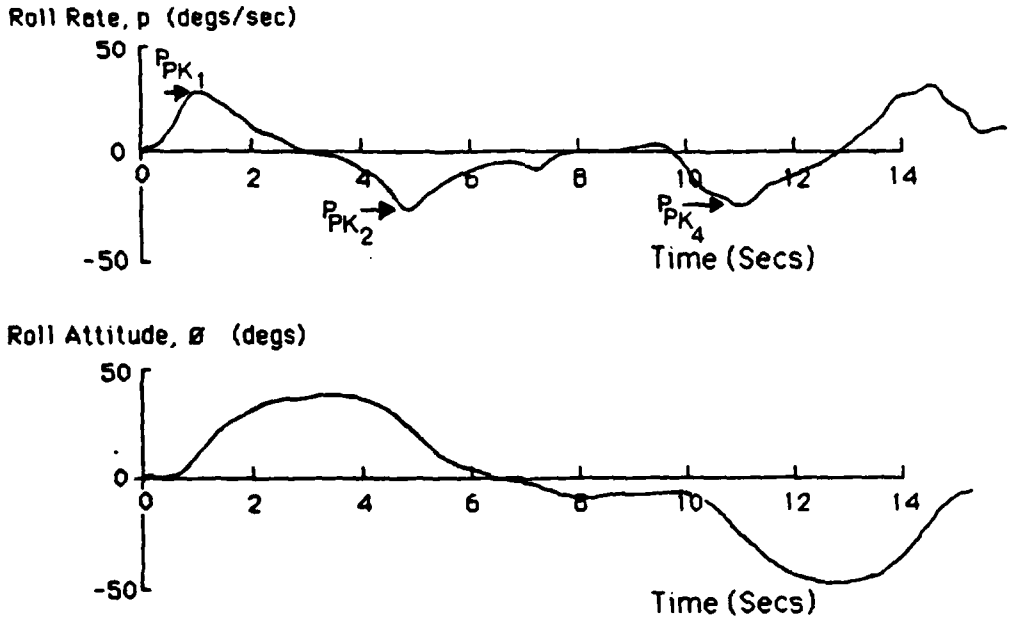

On-Line Inner Loop Performance Data

Maneuver Intiation (secs)	Commanded Attitude (deg)	Bank Angle Change $\Delta\phi_C$ (deg)	Peak Roll Rate P_{PK} (deg/sec)	Time Between Commands (secs)
0.0	38.94	38.94	27.36	-
3.02	-6.37	-45.31	-27.88	3.02
8.74	-5.65	0.72	4.52	5.71
9.29	-48.40	-42.74	-25.65	0.56
12.54	6.89	55.28	28.33	3.24

Figure 4-19. Application of the Discrete Maneuver Analysis Algorithm to Slalom Maneuver Data

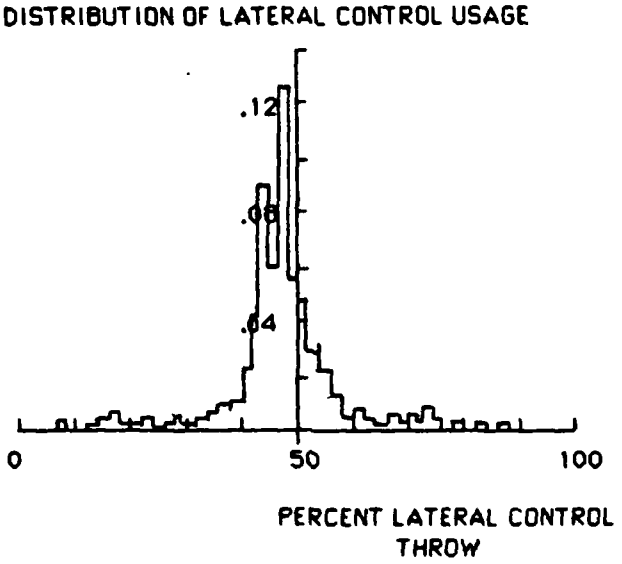

(a) Histogram of Stick Activity

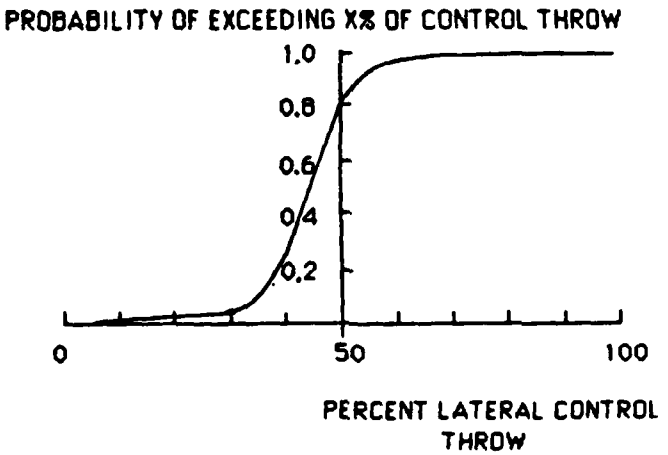

(b) Probability of Exceedence Diagram

Figure 4-20. Lateral Stick Activity Data Obtained for Each Simulation Run

PILOT COMMENTARY CHECKLIST

FLIGHT TASK OR MANEUVER OBJECTIVES

1. *Aggressiveness:* The quickness or speed of task execution (1= quick).
2. *Precision:* Fineness and exactness of task execution (1= high).
3. *Amplitude:* Size of maneuver or amount of motion (1= large).
4. *Overshoot:* Amount of damping or settling to a steady condition (1= none).
5. *Transition:* Gracefulness of ending a task segment and beginning next (1= easy).

AIRCRAFT CHARACTERISTICS

6. *Short term:* Immediateness of response with initial control input (1= fast).
7. *Control power:* Amount of response without saturation or limit (1= sufficient).
8. *Coupling:* Unwanted axis interactions as a result of control or motion (1= none).
9. *Oscillations:* Tendency for sustained nuisance motions (1= none).
10. *Forces:* Controller feel and sensitivity useful to obtaining response (1= good).

DEMANDS ON PILOT (TECHNIQUE OR STRATEGY)

11. *Compensation:* Amount of anticipation or lead required (1= none).
12. *Workload:* Mental and physical effort required to do task (1= low).

Manudyne Systems, Inc. December 1984

Figure 4-21. Guide to Pilot Commentary

expressing the "task or required operation" aspect of the Cooper-Harper rating scale.

Aircraft characteristics include those features of the vehicle which related to some aspect of roll control effectiveness. Each pilot was requested to discuss the specific configuration being examined within the framework of the features listed. This provided a basis for evaluating "aircraft characteristics" within the Cooper-Harper scale.

Demands on the pilot represented those features of pilot technique or control strategy to which the pilot should be sensitive. This was intended to provide a basis for the Cooper-Harper evaluation of "demands on the pilot", the last step in determining a pilot rating.

Cooper-Harper Rating Scale. A reproduction of the standard rating scale is shown in Figure 4-22. The Cooper-Harper scale was used to rate each task and vehicle configuration combination following a series of training or familiarization runs.

Figure 4-22. Cooper-Harper Pilot opinion Rating Scale

HANDLING QUALITIES RATING SCALE

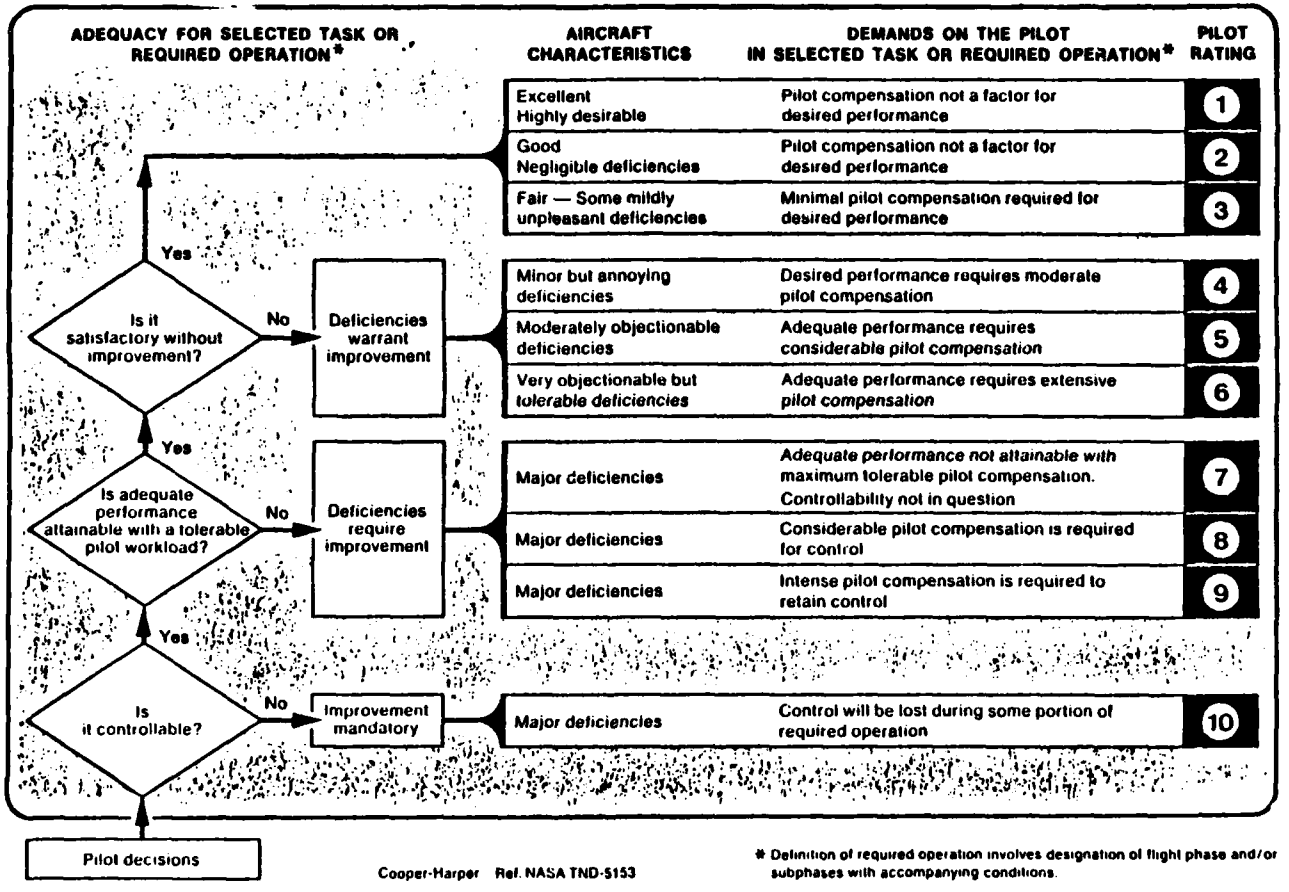

Cooper-Harper Ref. NASA TND-5153

* Definition of required operation involves designation of flight phase and/or subphases with accompanying conditions.

D. Experimental Results

The experimental results which are discussed here are divided into those pertaining, first, to the issues of roll control effectiveness criteria development and second, to the use of this particular flight simulator apparatus for accomplishing the previously stated objectives.

A complete summary of simulation usage and test matrix coverage is provided in Volume II of this report. Volume II also contains a catalog of raw pilot opinion rating data and commentary. The raw data compilation is limited to data runs taken after an extensive training period during which the pilot attained asymptotic performance.

1. General Results

The following results are presented in terms of first the general finding, next a detailed discussion of the finding, and finally the implication with regard to roll control effectiveness criteria development.

Maximum Roll Rate Feature

Finding: A maximum commanded roll rate is an obvious feature in nearly all discrete maneuver data.

Discussion: There is a consistent trend toward roll-rate limiting in all plots of peak roll rate versus bank angle command for each set of data examined. This applies to both simulator and flight results.

This feature is significant in that the peak roll rate limit appears to be usually imposed by the pilot rather than by a vehicle roll rate limit. The limit established is, however, a function of the particular task involved, and may be influenced by simulator

limitations. This latter topic will be discussed in Section IV-F. Figure 4-23 illustrates this phenomenon with a typical HUD tracking case. Note how the discrete maneuver points lie well below the boundary representing maximum vehicle capability.

Implication: The existence of this feature in discrete maneuver performance reflects a point of diminishing returns for provision of roll control effectiveness for a given flight task or maneuver capability.

Upset Caused by Maneuver vs Gusts

Finding: Performance of significant discrete maneuvers outweighs the effect of random atmospheric turbulence on pilot opinion rating.

Discussion: The execution of a significant discrete maneuver such as a sidestep does itself represent an upset from which the pilot must recover. The size of this maneuver "disturbance" was compared to the effect of random gusts.

The simulator experiment consisted of performing and rating a series of sidestep maneuvers in varying levels of random turbulence, rms lateral gust conditions of 3.0, 4.5 and 6.0 ft/sec were simulated. Ratings were also given for the task of hovering at one position in the presence of turbulence. The pilot ratings are summarized in Figure 4-24. The results show that where a significant maneuver is involved such as a sidestep, the pilot ratings are essentially unaffected by the gust disturbance.

Implication: The specification of an atmospheric disturbance level is probably unnecessary when specifying the control effectiveness needed for significant maneuvers, but is necessary where precise control of attitude is needed such as in gun tracking.

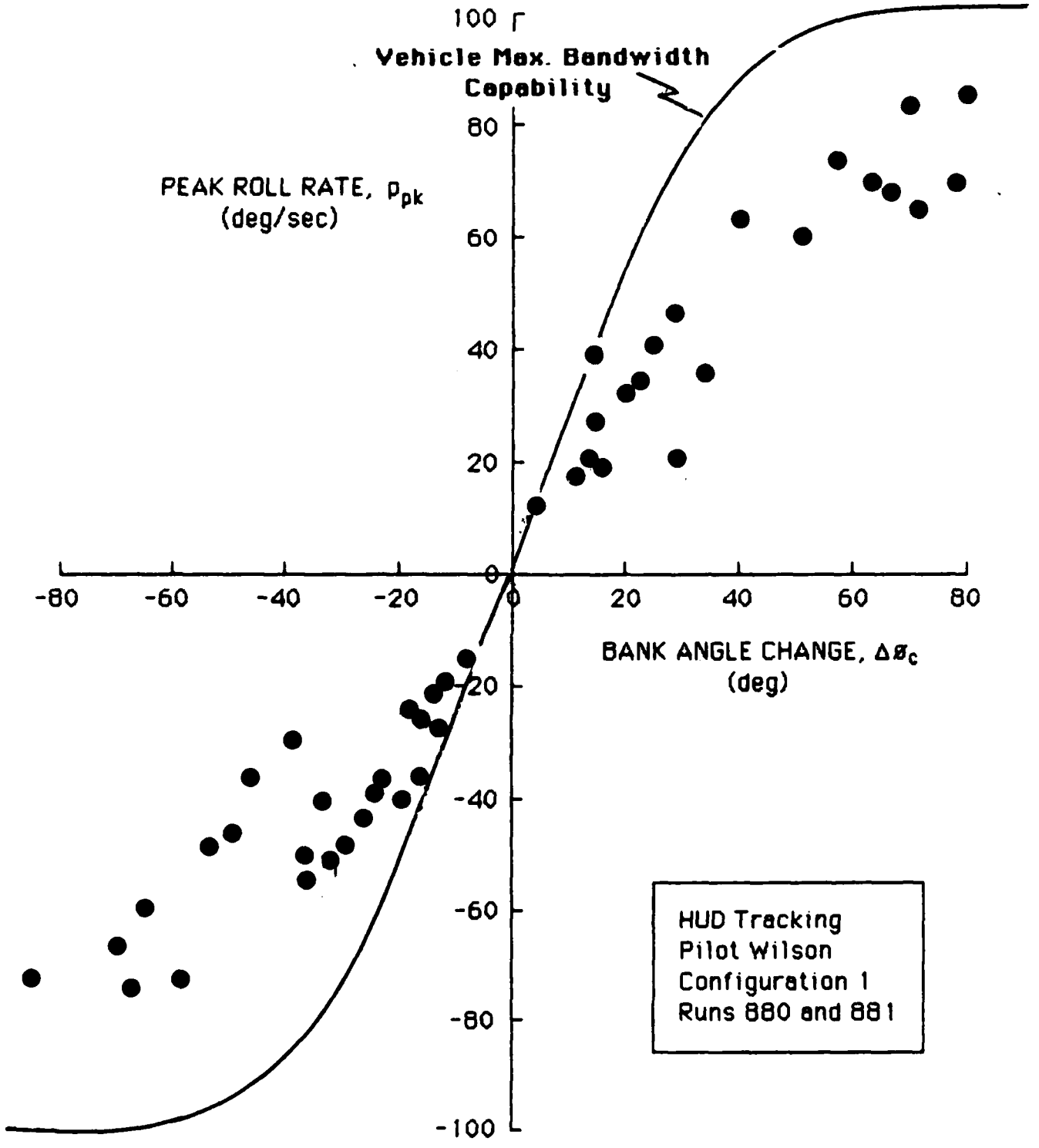

Figure 4-23. Typical Case Illustrating the Maximum Roll Rate Trend

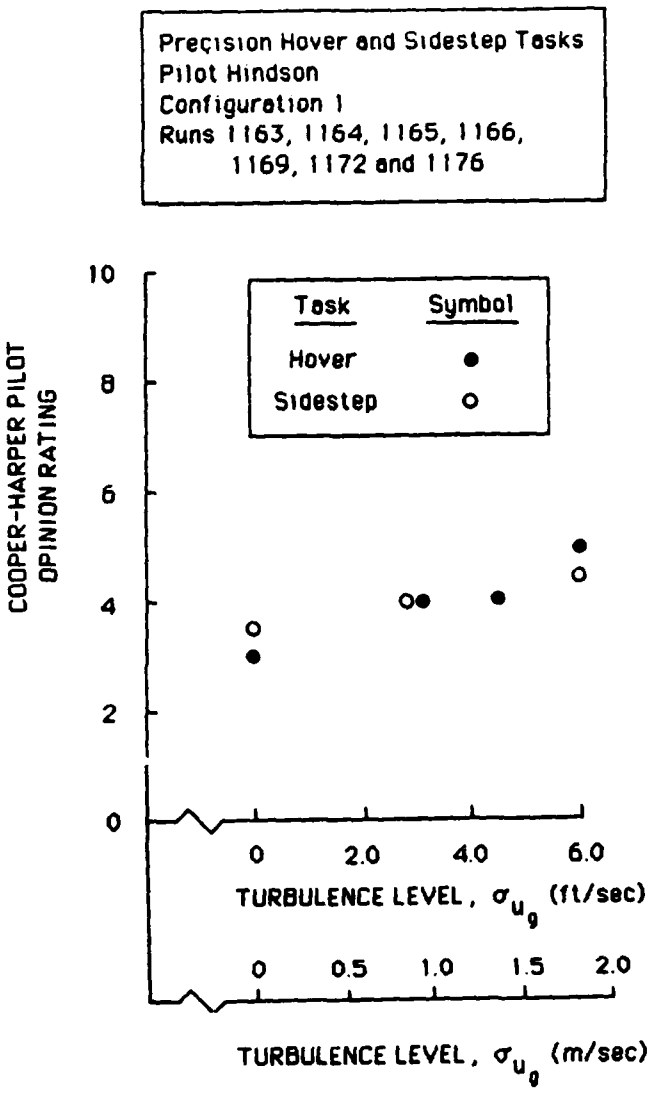

Figure 4-24. Cooper-Harper Pilot Opinion Variation with Turbulence Level in the Sidestep and Precision Hover Tasks

2. HUD Tracking Task Results

The HUD tracking task was found to be a useful laboratory means for studying roll control effectiveness requirements because it involves no lateral outer loop and its command sequence is precisely defined. Thus the results can be used to identify and map general characteristics and relationships among vehicle, pilot, and task. The HUD tracking task may also have an application to large evasive maneuvering such as collision avoidance.

Critical Aspects of the HUD Task

Finding: The HUD tracking task represents a critical design maneuver with respect to aggressiveness and amplitude of maneuver.

Discussion: For all of the tasks studied, including helicopter air combat, the HUD tracking task yielded the highest peak roll rates and at least matched levels of aggressiveness found elsewhere. The specific quantitative values representing task performance are indicated in Figure 4-25. These consist of a maximum roll rate of 90 deg/sec and a maximum commanded bank angle of 90 deg.

The HUD tracking task represents a fairly pure single loop task, i.e., there is not outer-loop control of flight path or heading. It may resemble a large-amplitude evasive or collision avoidance maneuver.

Implication: Where the HUD tracking task is representative of a useful mission-oriented maneuver, then it can be considered as a critical design point with respect to overall control effectiveness.

Control Power Saturation Effect on Pilot Rating

Finding: Pilot rating in the HUD tracking maneuver did not degrade

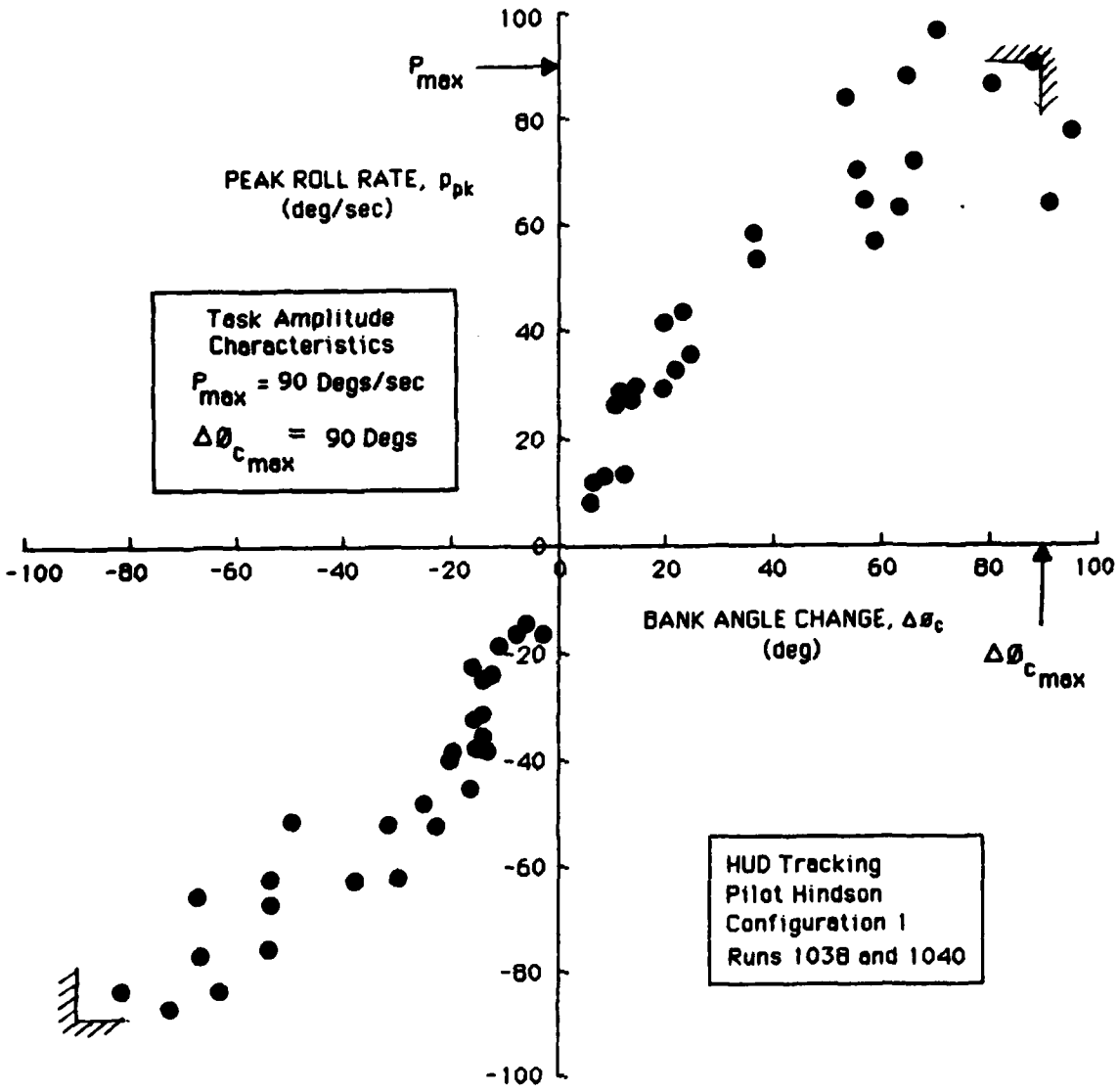

Figure 4-25. Definition of the HUD Task Amplitude Characteristics

significantly until available maximum roll rates were limited to 50-67 degs/seconds (equivalent cyclic deflection of 7.5 to 10.0 cms), see Figure 4-26.

Discussion: Lateral control power (maximum roll rate) limitation was achieved by saturation of the lateral stick input. The HUD tracking task was the most demanding task evaluated with regard to aggressiveness and amplitude demands. Pilot opinion degraded sharply when maximum available roll rate was limited to 66 degs/sec for Wilson and 50 degs/sec for Elton. In both cases the degradation represented a transition to Level 3 in terms of absolute Cooper-Harper rating.

The effect of progressive control power (maximum roll rate) reduction on maneuver performance can be seen in Figure 4-27. Figure 4-27a shows the nominal HUD tracking performance with maximum available roll rate of 100 degs/sec. Figure 4-27b through d shows the performance as the available control power is cut back through saturation of the lateral stick input. The limitation of the maximum bandwidth capability of the closed-loop system with control power reduction is apparent from these figures.

The effect of control power limitation is primarily on the larger amplitude commands. To an extent, the pilot can compensate by broadening the duration of the roll rate command (or control input). However, this lowers the effective closed-loop bandwidth and ultimately precipitates a short-term control effectiveness problem.

The pilot, however, has the capability to compensate for maximum roll rate deficiencies using dihedral effect (via pedals) to generate additional rolling moment. Thus it is possible to exceed the vehicle capability indicated by the maximum roll rate boundaries as seen in Figure 4-27b.

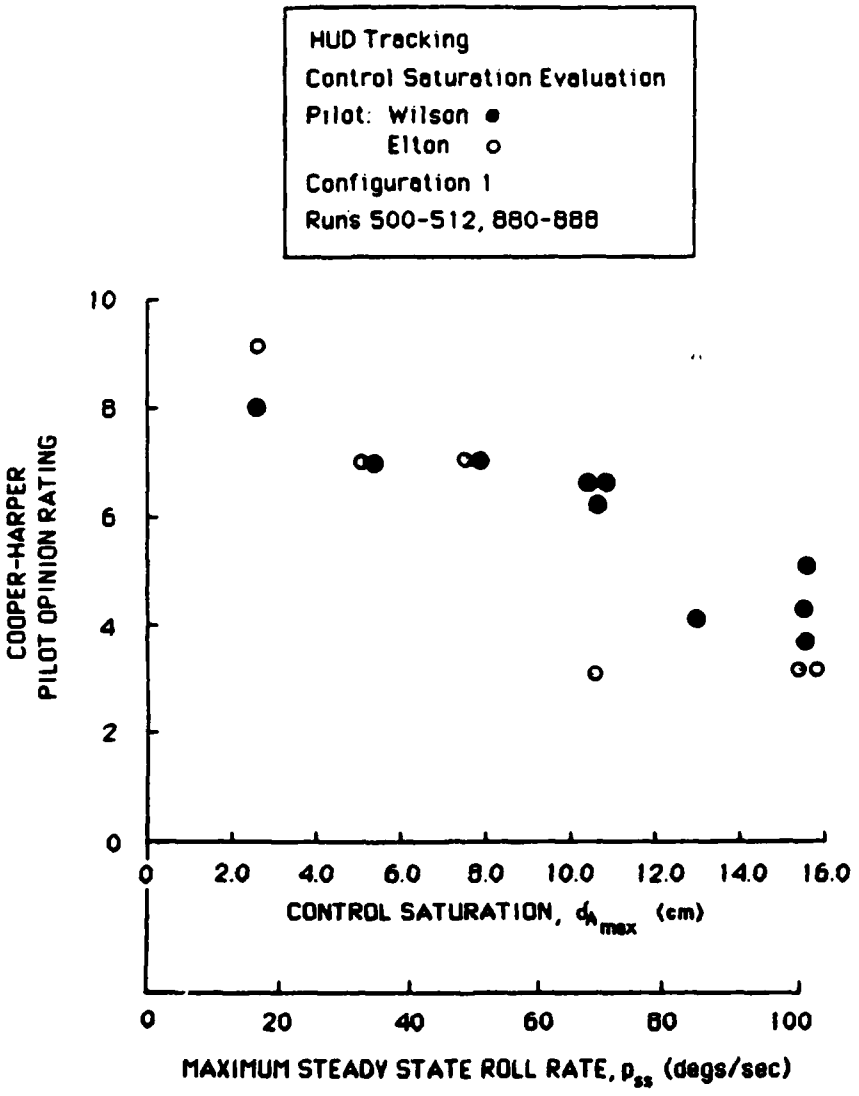

Figure 4-26. Effect of Control Power Saturation on HUD Tracking. Open-Loop Vehicle Bandwidth Unchanged

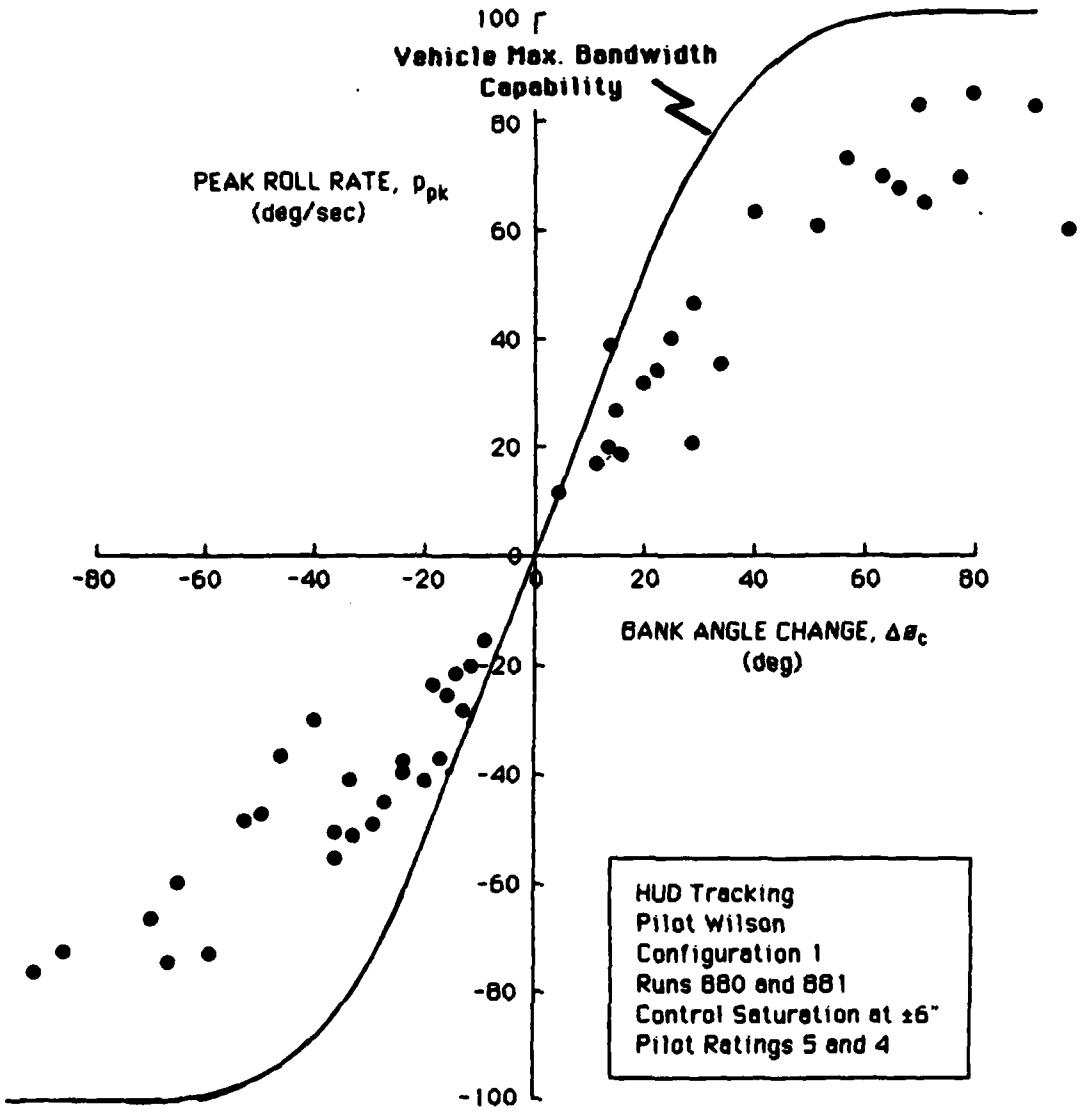

Figure 4-27a. Nominal HUD Tracking Performance

Vehicle Maximum Roll Rate Capability = 100 Degs/sec

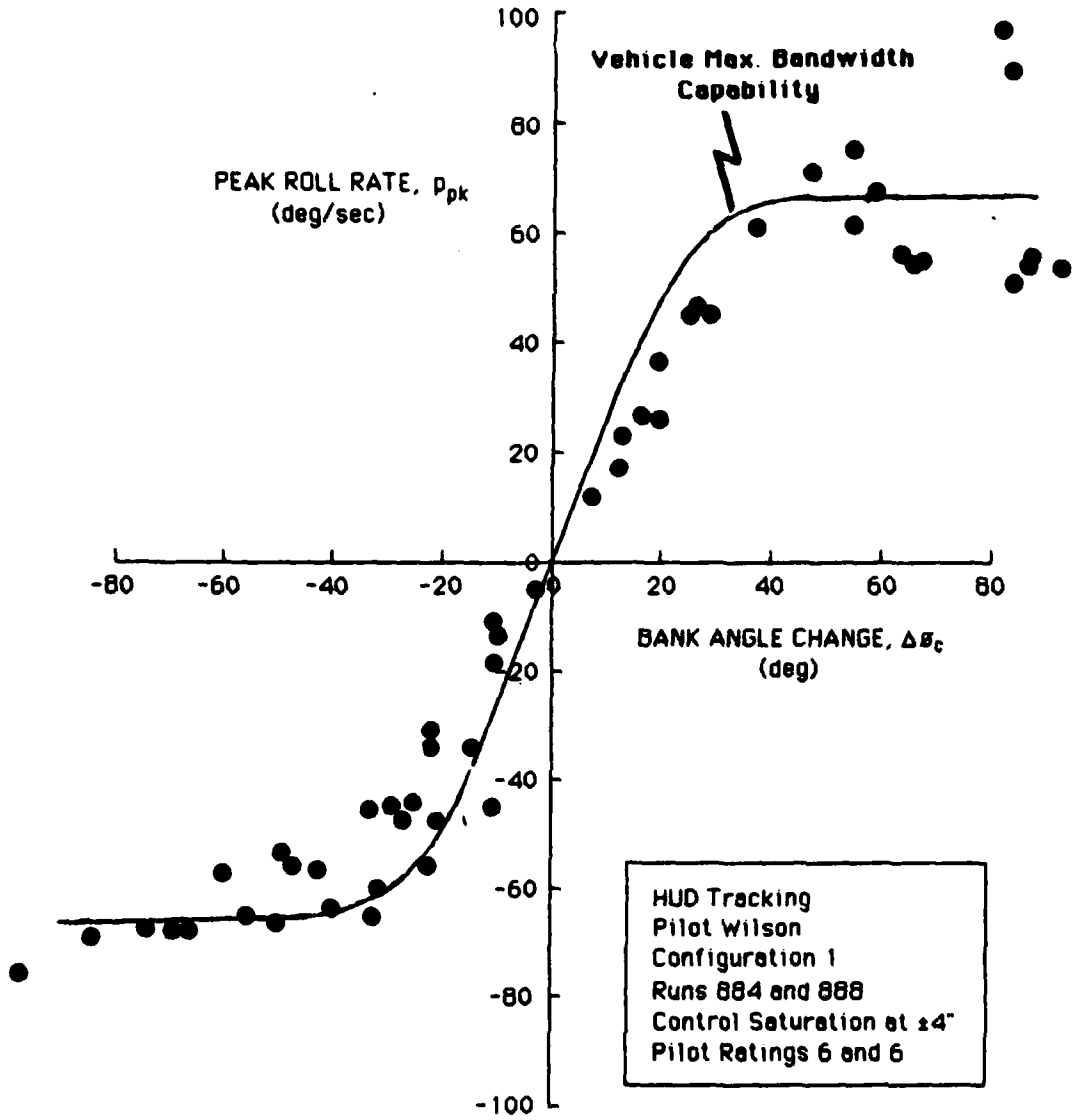

Figure 4-27b. HUD Tracking Performance With Control Power Saturation Vehicle Maximum Available Roll Rate = 67 Degs/sec

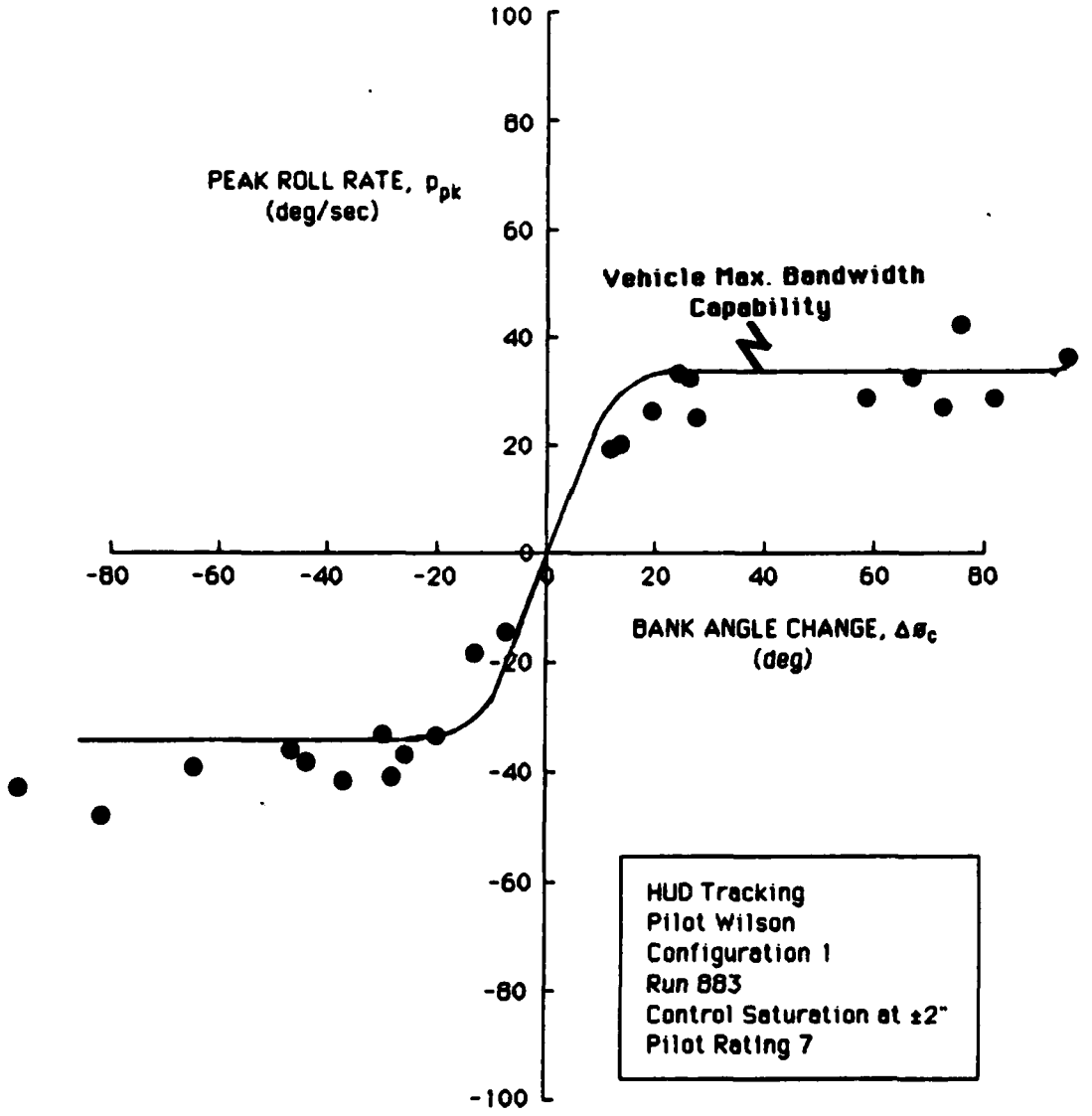

Figure 4-27c. HUD Tracking Performance With Control Power Saturation
Vehicle Maximum Roll Rate Capability = 33 Degs/sec

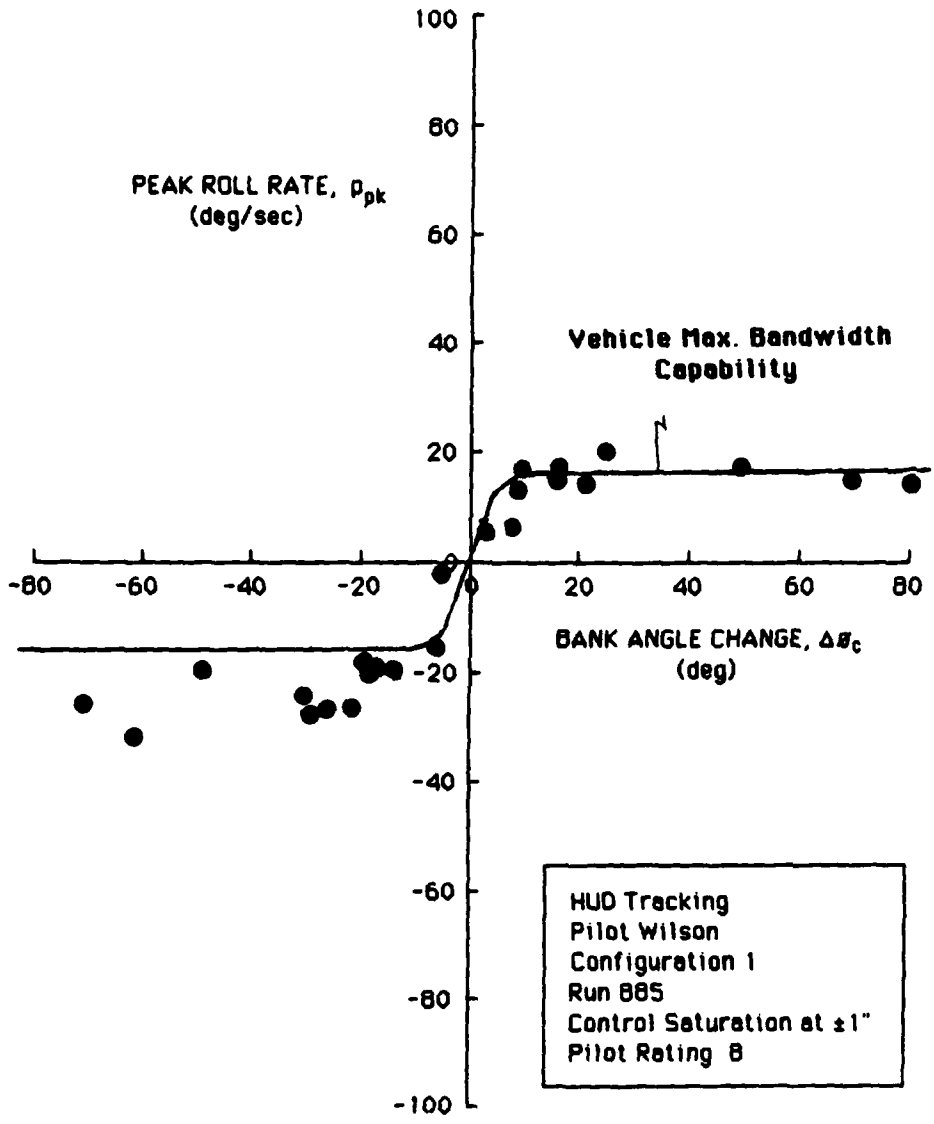

Figure 4-27d. HUD Tracking Performance With Control Power Saturation

Vehicle Maximum Roll Rate Capability = 17 Degs/sec

Implication: These data form a portion of the basis for a control power criterion based on a margin between vehicle capability and the nominal maneuver demand.

Maintenance of Closed-Loop Damping

Finding: With control power limitation in the HUD tracking task closed-loop damping levels are maintained, however there is an eventual loss of closed-loop natural frequency for large-amplitude maneuvers.

Discussion: Closed-loop natural frequency and damping information for an equivalent second order system were recovered for individual discrete roll maneuvers for different levels of available control power. These data are shown as a function of bank angle command amplitude in Figure 4-28. These correspond to the respective roll rate performance plots in Figure 4-27. Note that damping ratio is maintained even when the available roll rate is limited to 33 degs/sec (Pilot Rating 7). As predicted, however, natural frequency (i.e., aggressiveness) must ultimately suffer because of the reduced proportion of peak roll rate to bank angle change. This is shown in Figure 4-27c.

Maintenance of Tracking Precision

Finding: HUD tracking precision is maintained with control power degradation until the available roll rate is less than 33 deg/sec. This corresponds to the Level 3 control power boundary.

Discussion: This is not a new finding but is included here to again point out the fact that pilot rating degrades before precision. Figure 4-29 shows the degradation of tracking precision with limitation of available control power. The normalized rms attitude error and percent time on target metrics show insignificant variation until roll rate capability is limited to less than 33 degs/sec. Below this value the

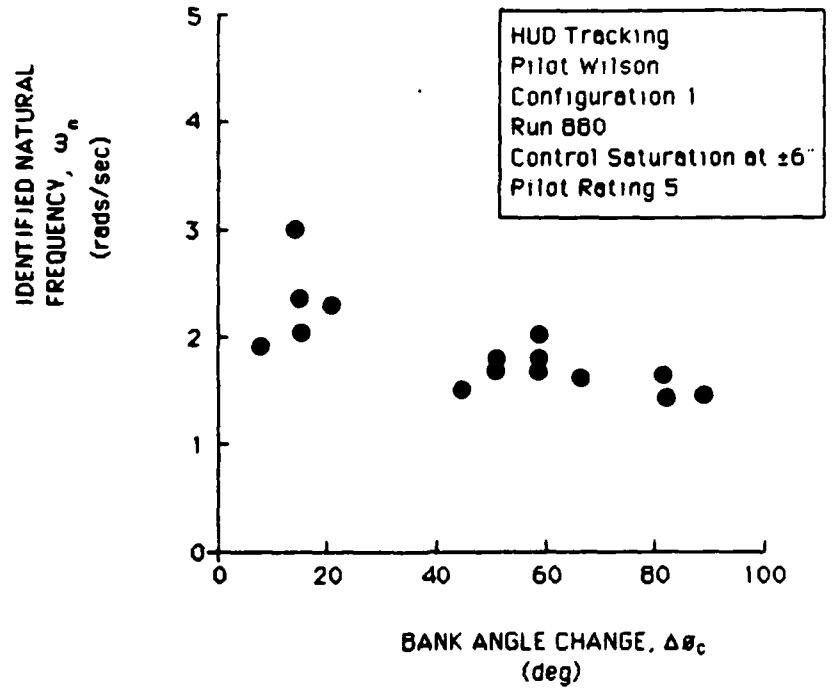

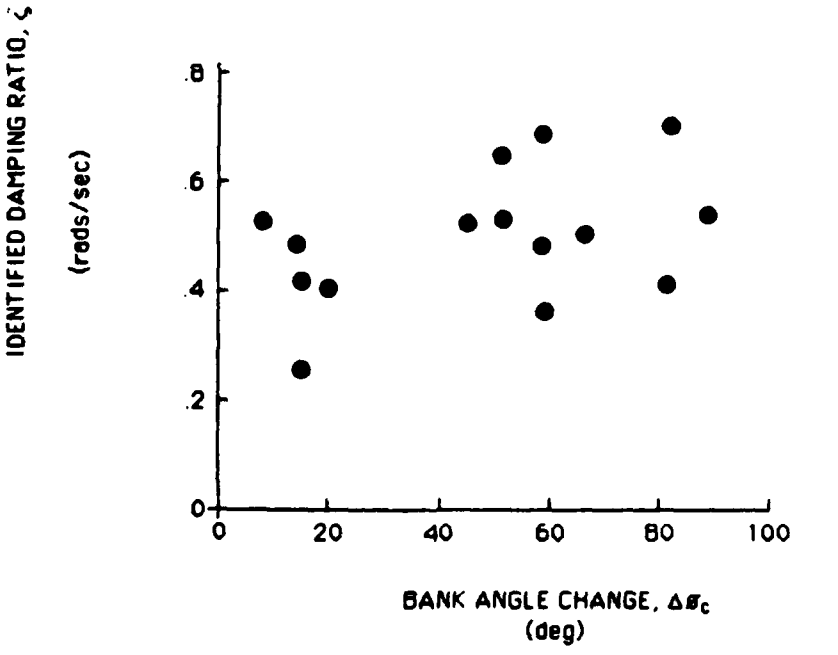

Figure 4-28a. Identified Closed-Loop Natural Frequency and Damping Ratio for HUD Tracking. p_{ss} = 100 Degs/sec

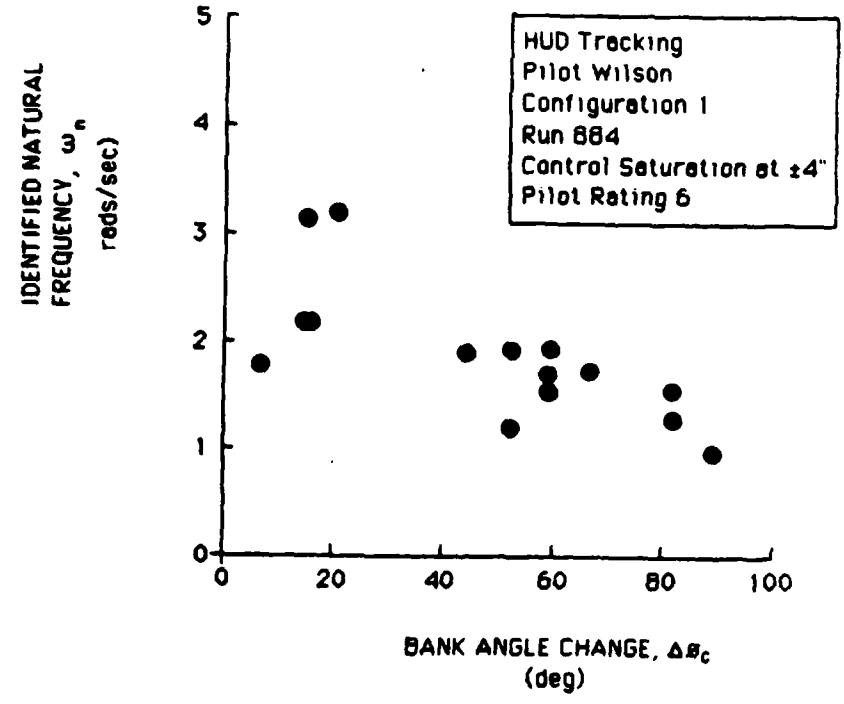

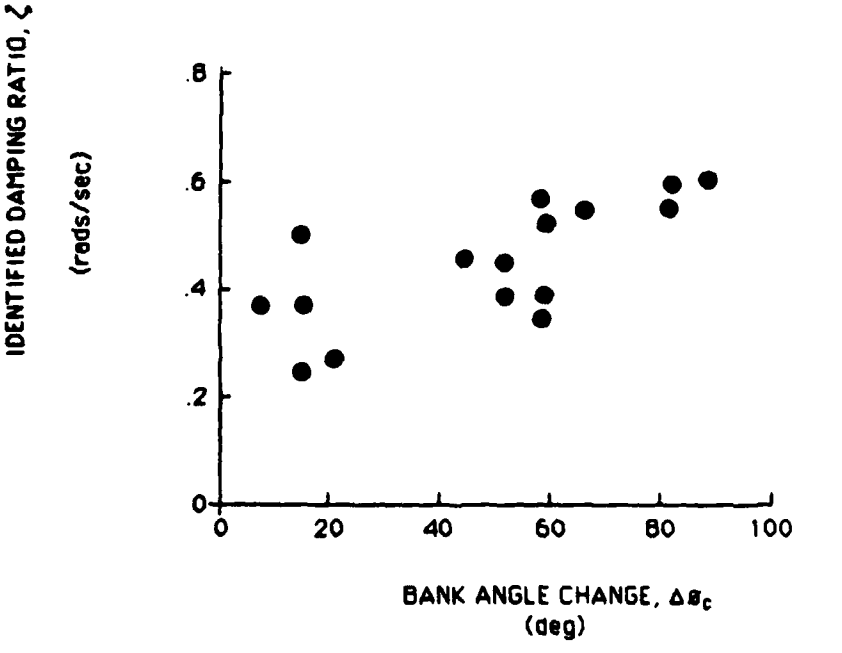

Figure 4-28b. Identified Closed-Loop Natural Frequency and Damping Ratio for HUD Tracking. p_{ss} = 67 Degs/sec

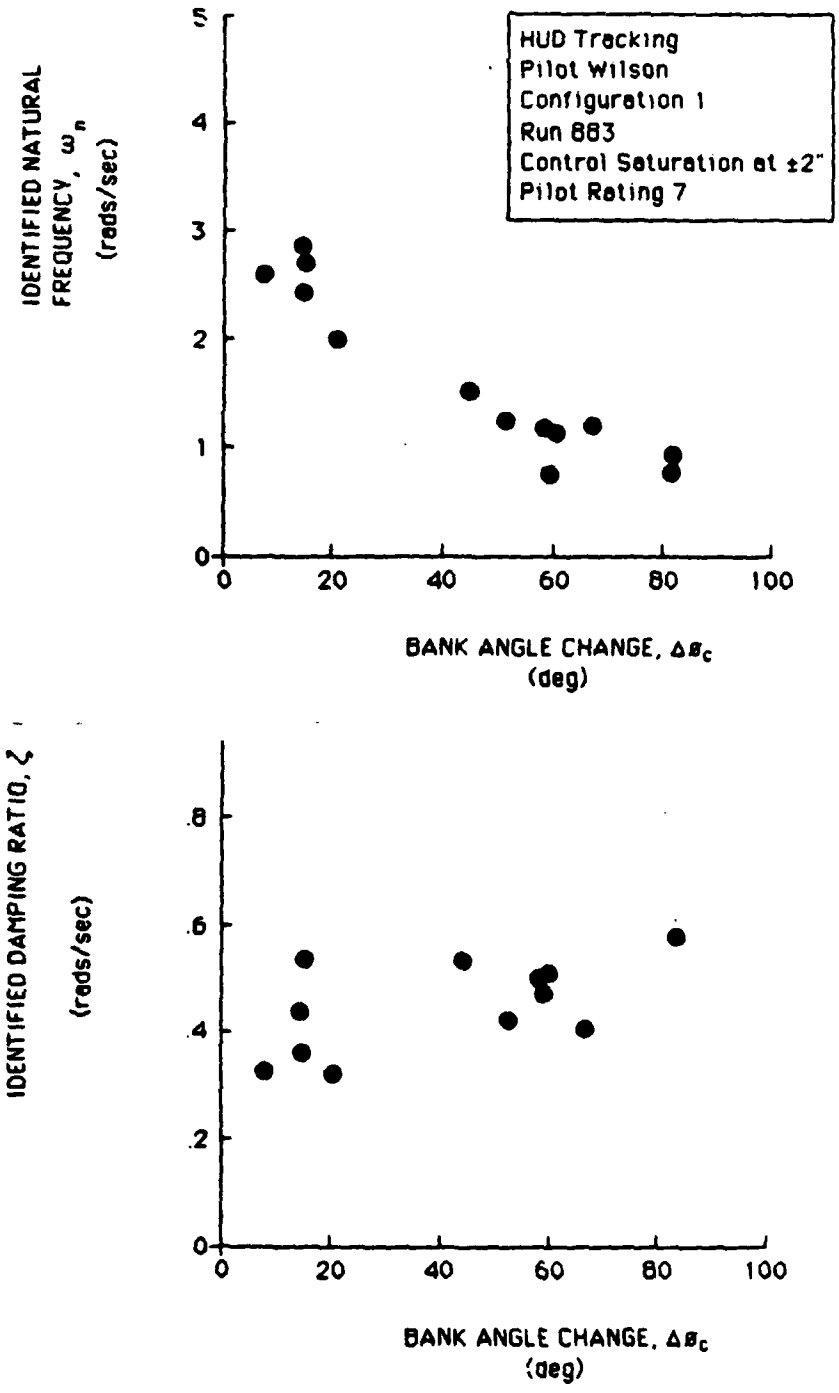

Figure 4-28c. Identified Closed-Loop Natural Frequency and Damping Ratio for HUD Tracking. p_{ss} = 33 Degs/sec

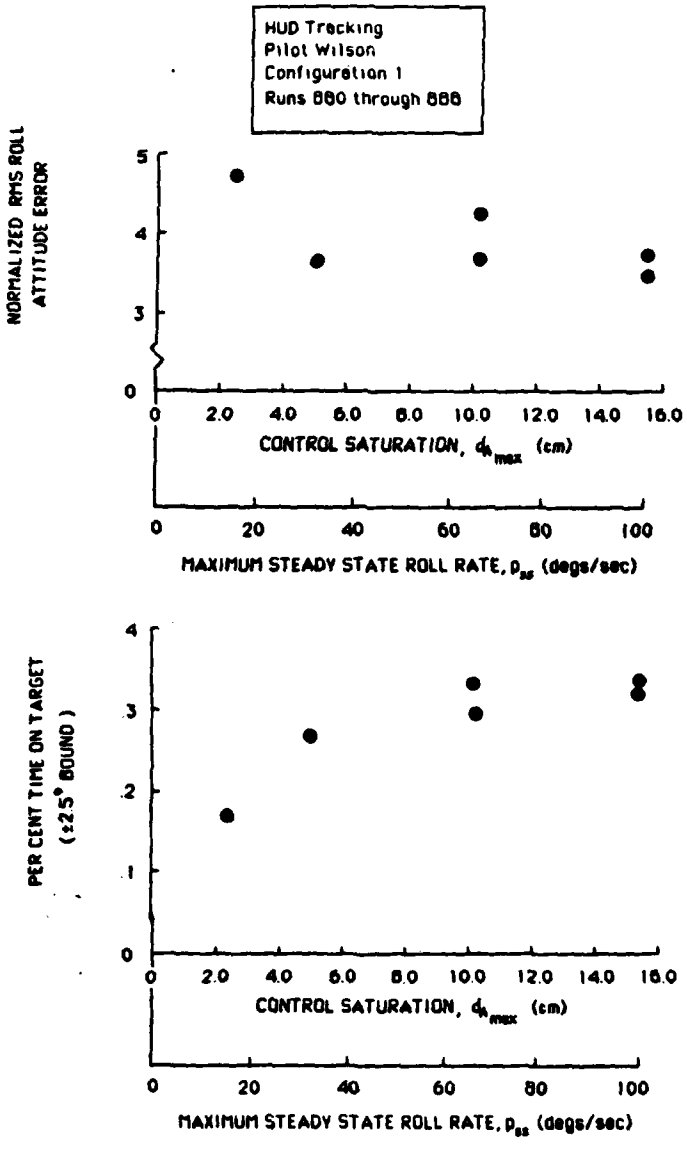

Figure 4-29. RMS Attitude Error and Percent Time-on-Target Metrics as a Function of Control Power Saturation

percent time on target appears to be the more sensitive performance metric with control power degradation.

Effect of Short-Term Response

Finding: Short-term response affected HUD tracking pilot opinion only in the case of Configuration 10.

Discussion: Figure 4-30 indicates that the configurations run resulted in no adverse pilot opinion effects for the HUD tracking task until the bandwidth was degraded to that of Configuration 10. The point of degradation generally corresponds to the level of task aggressiveness in terms of natural frequency.

Figure 4-31a through c illustrates the peak roll rate performance for the varying short-term response cases. There is only slight variation in the signature shown for Configuration 10 (Figure 4-31c). Thus there is fairly good evidence of pilot compensation for the degraded bandwidth just as there was in the cases of control saturation.

Unfortunately there was not sufficient usable data to define the nature of this effect with more precision. It is believed that the HUD tracking task demands a fairly high level of aggressiveness, thus this result is worthy of further investigation.

Essential Features of Attitude Command and Rate Command Systems

Finding: Use of an attitude command system produces essentially constant bandwidtn performance while a high gain rate system leads to the same type of performance seen for basic helicopter configurations.

Discussion: Typical HUD tracking results are presented in Figure 4-32. Results for an attitude command system are shown in Figure 4-32a and for

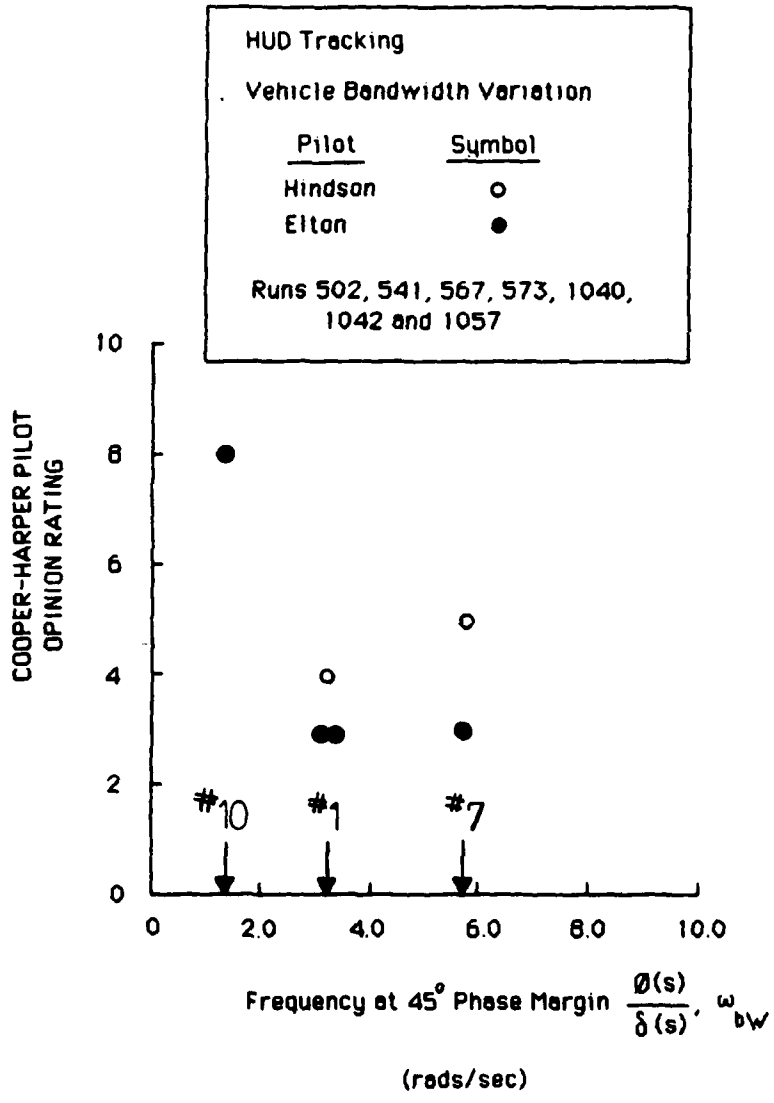

Figure 4-30. Pilot Opinion Variation with Vehicle Short-Term Response in the HUD Tracking Task

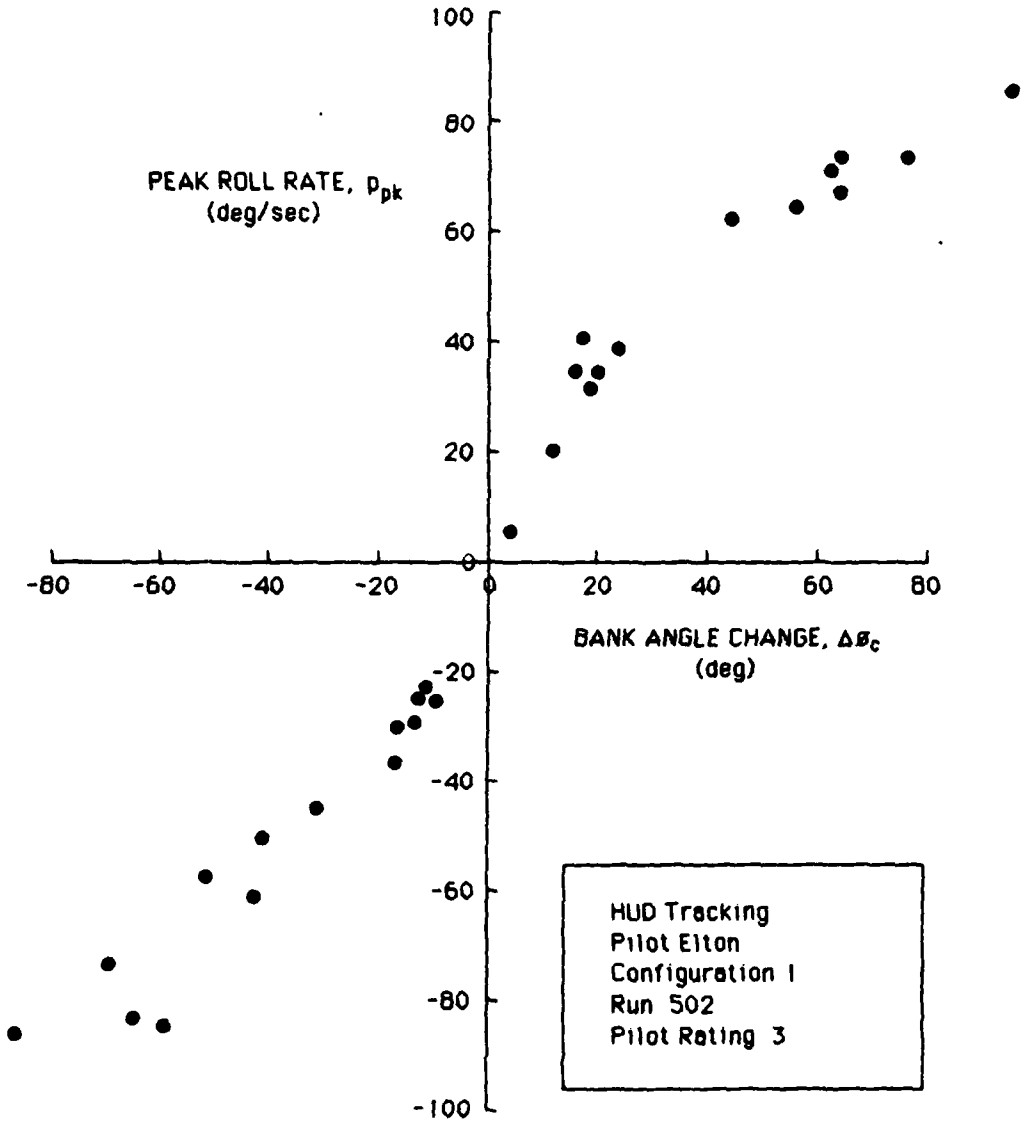

Figure 4-31a. HUD Task Performance for Basic Helicopter Configuration 1

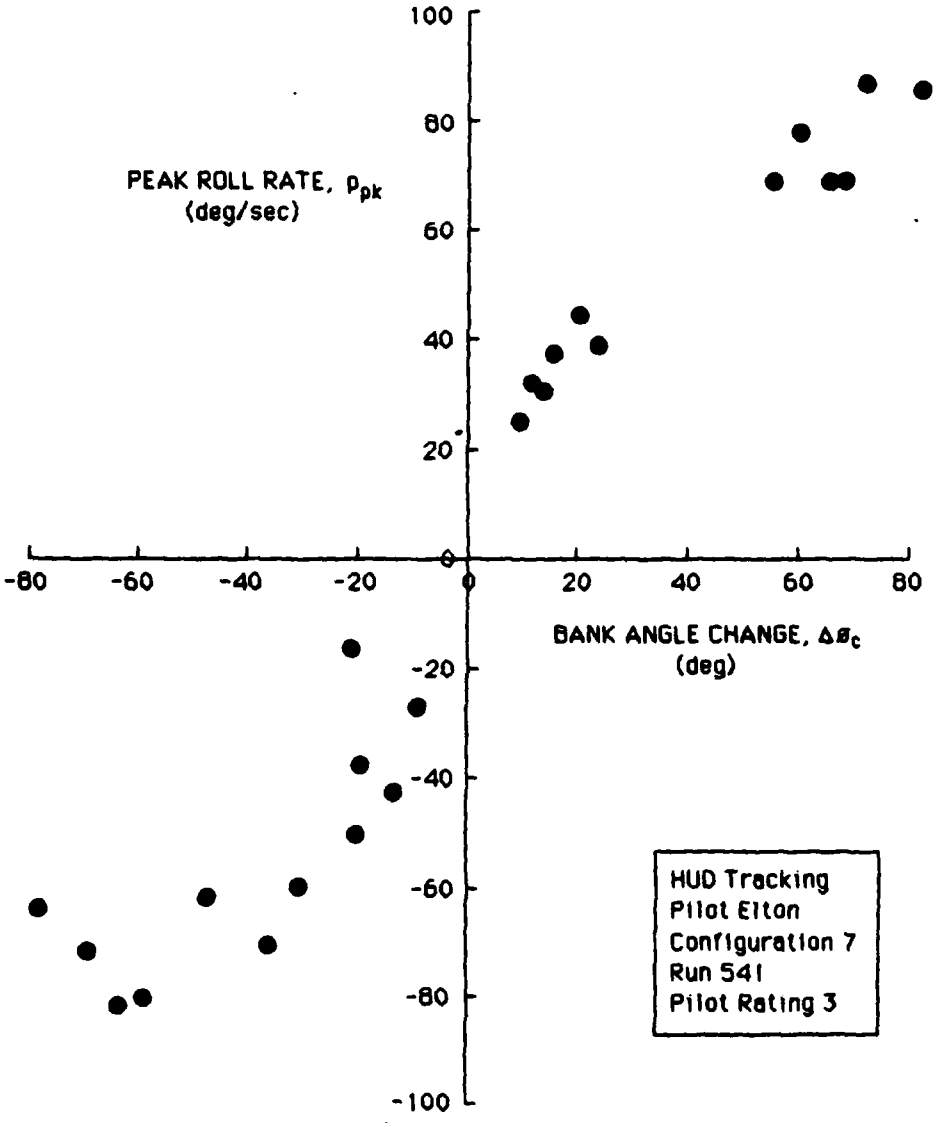

Figure 4-31b. HUD Task Performance for Basic Helicopter Configuration 7

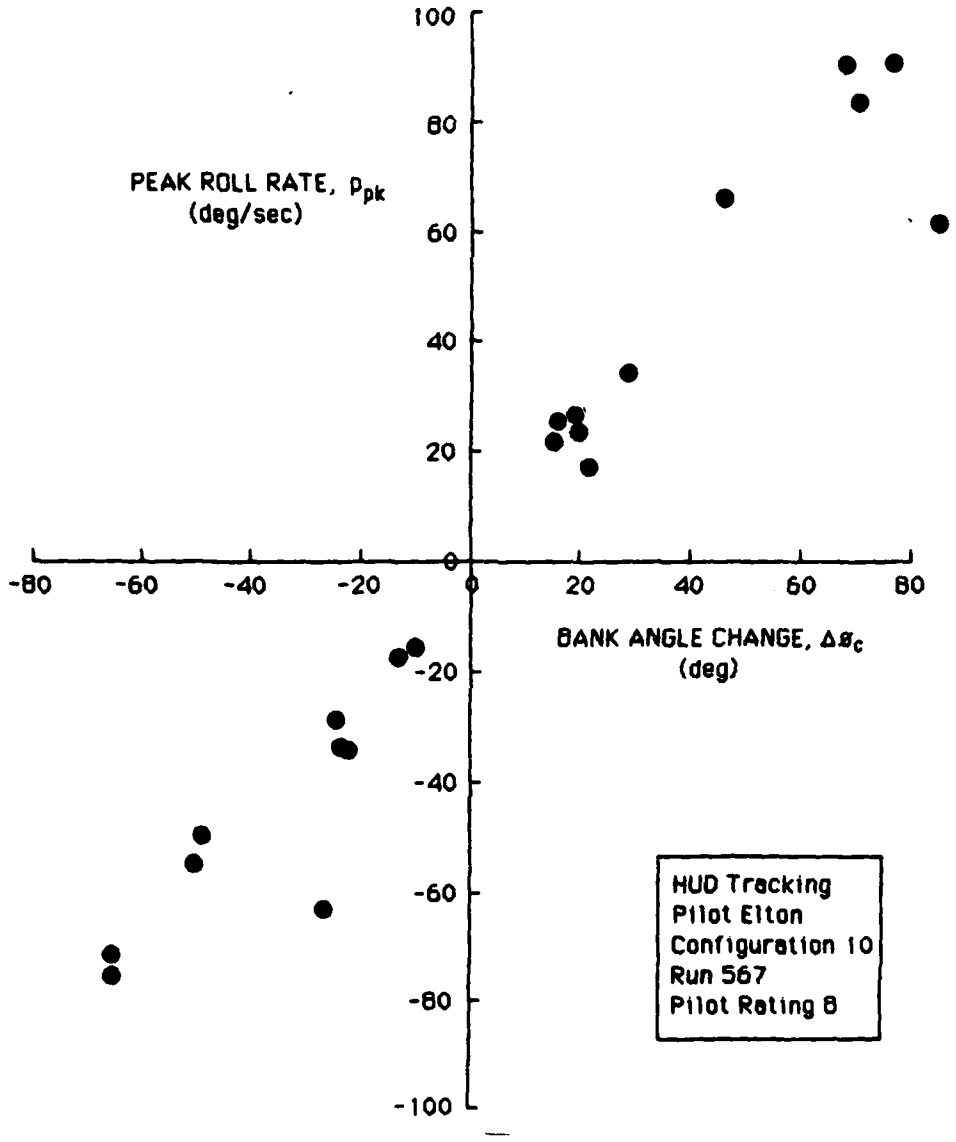

Figure 4-31c. HUD Task Performance for Basic Helicopter Configuration 10

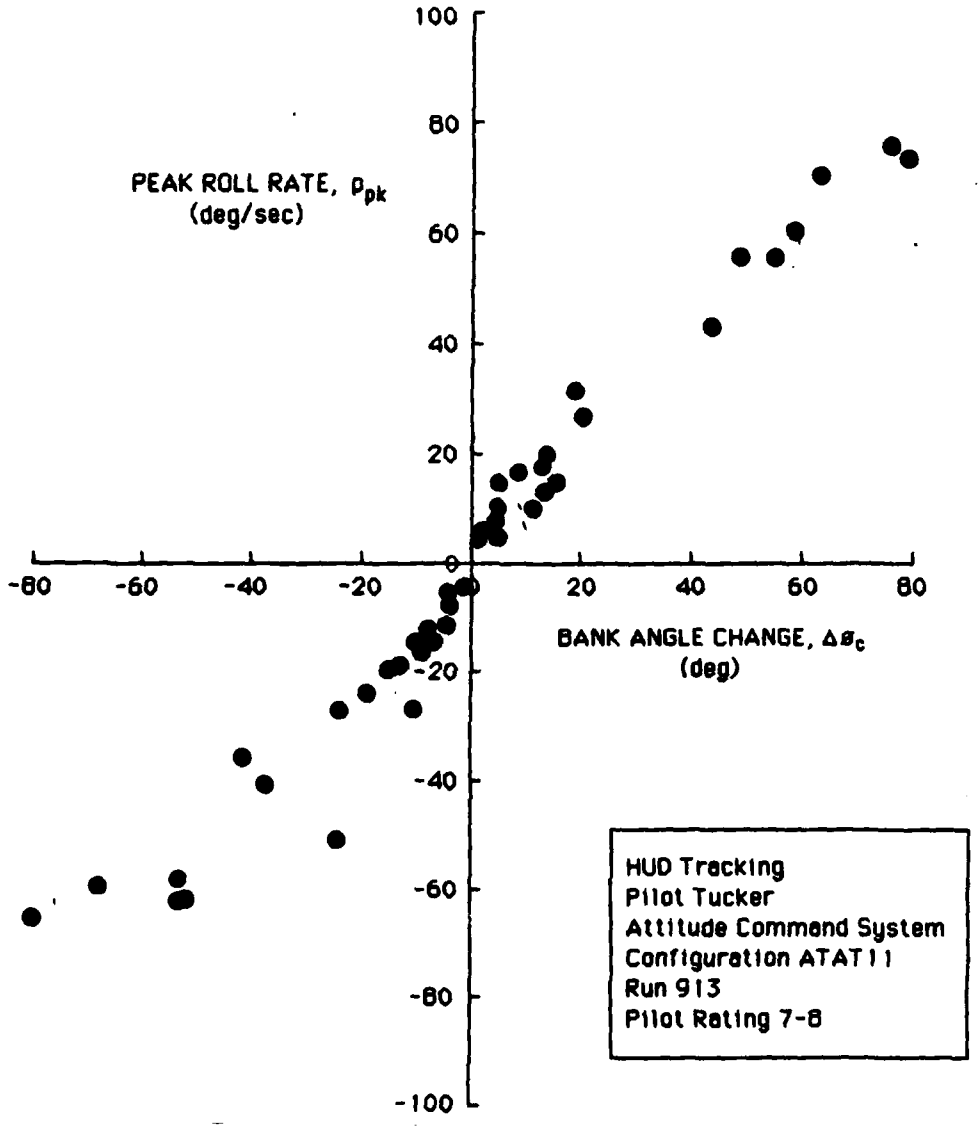

Figure 4-32a. HUD Task Performance Typical of Attitude Command Response Type

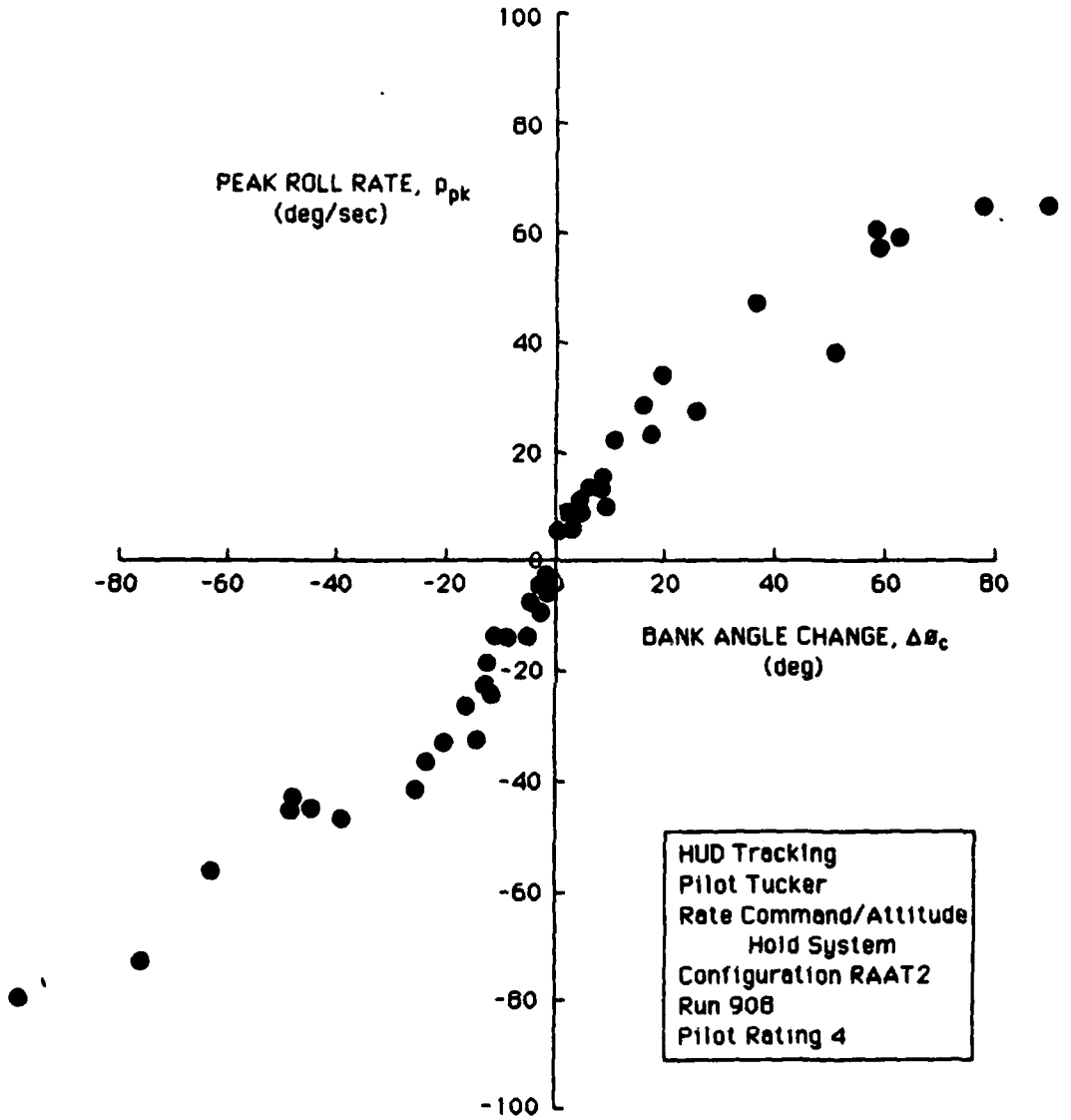

Figure 4-32b. HUD Task Performance Typical of Rate Command Response Type

a rate command system in 4-32b. Note that the proportion of peak roll rate to bank angle change is nearly constant for the attitude system while it is similar to previous cases for the rate system.

Unfortunately high angle of attack and sideslip difficulties in the basic math model led to poor pilot ratings and prevented a good assessment of the high gain SCAS characteristics in large amplitude maneuvers. Therefore the variations is SCAS dynamics could not be addressed fairly. This is an area which should be considered for future research.

3. Air Combat Maneuver Task Results

Two main types of air combat maneuvers were simulated. The "ACM tracking" task consisted of the simulator pilot tracking and firing a gun against an automatically controlled target flying at constant speed and altitude. The second type task was a "free engagement" wherein a manually controlled target was flown in response to the simulator pilot and configuration being studied.

Most of the analysis was performed on the ACM tracking task results because they were more structured and consistent, and important for examination of control saturation. The free engagement results were more random but were interesting insofar as any increase in maneuver amplitude performance parameters.

ACM Maneuver Amplitude

Finding: The ACM tracking task is characterized by a maximum roll rate range of 40 to 60 deg/sec and a maximum commanded bank angle of 100 deg.

Discussion: Figure 4-33 shows six sets of air combat tracking performance data. These are typical of results obtained and show some

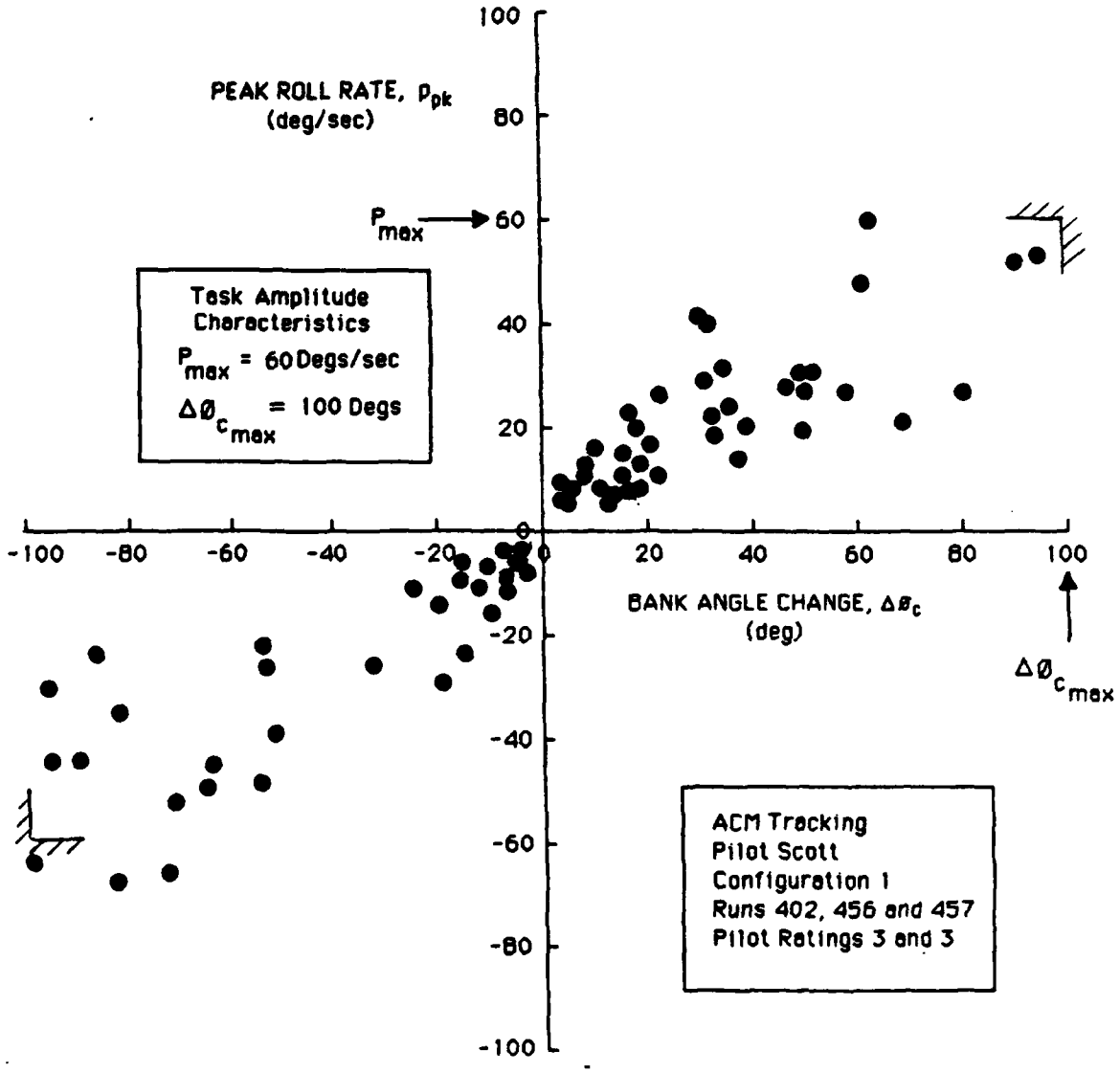

Figure 4-33a. Air Combat Tracking Performance Signature for Pilot Scott

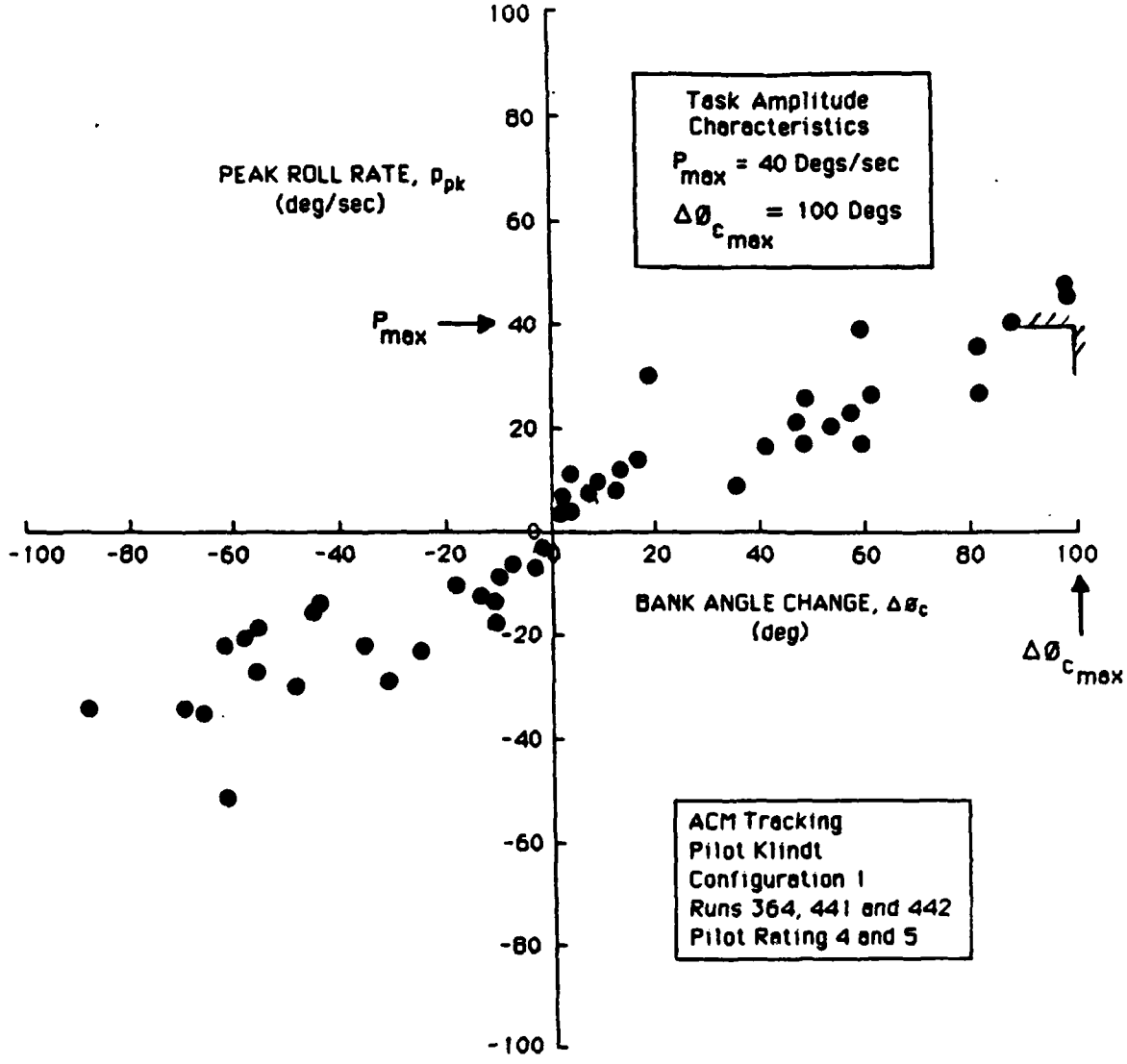

Figure 4-33b. Air Combat Tracking Performance Signature for Pilot Klindt

variation in the maximum peak roll rates.

The task is a combination of large-amplitude maneuvering and precision tracking, therefore there are fairly large values of peak roll rates along with high aggressiveness. The variation in maneuver amplitude will be discussed next and requires special attention when analyzing control power saturation results.

Finding: The ACM tracking task depends upon the distance maintained from the target.

Discussion: The data for Scott (Figure 4-33a) show generally higher peak roll rates than for Klindt (Figure 4-33b). This was found to be a strong function of the distance maintained from the target. The former set of data are representative of those obtained by moving within 500 ft of the target while the latter correspond to a distance of 500 to 750 ft. This factor represents an important dimension to the ACM task. More generally, this is a good example of the value of highly quantitative task performance measurements when studying a specific maneuver or class of maneuvers.

Finding: Pilot rating in the ACM tracking task does not degrade until steady state roll rate capability is limited to less than 35 deg/sec.

Discussion: The results of control power limitation in the ACM tracking task are presented in Figures 4-34a and -34b for the same two pilots discussed above.

Compared to the HUD tracking task, the ACM tracking task (for both of these pilots) permits considerably greater reduction of steady-state roll rate before pilot opinion is degraded. This lends support to the concept of weighting or conditioning handling qualities requirements to the type of task representative of a given mission or aircraft design

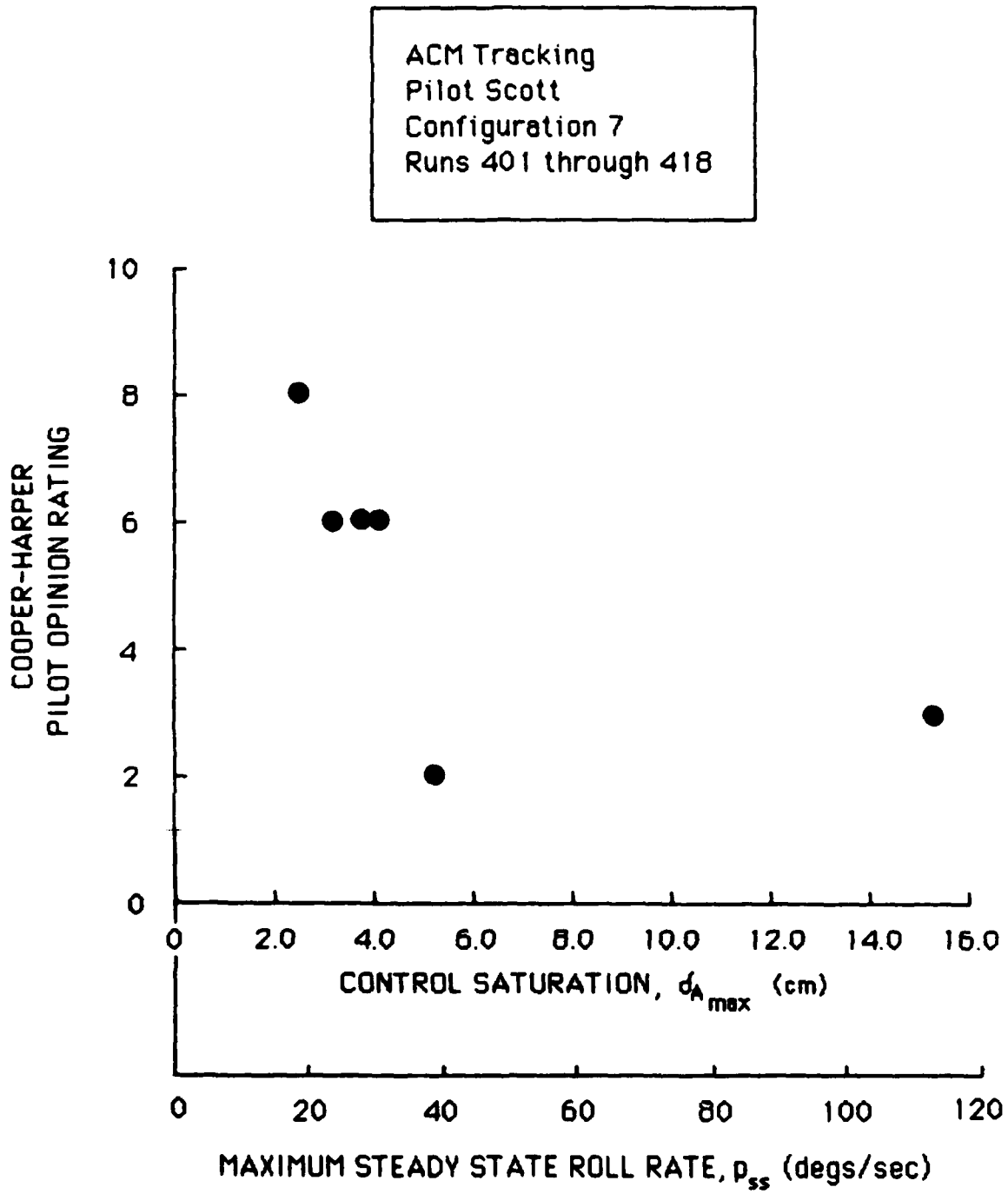

Figure 4-34a. Pilot Opinion Variation in ACM Tracking Task with Control Power Saturation for Pilot Scott

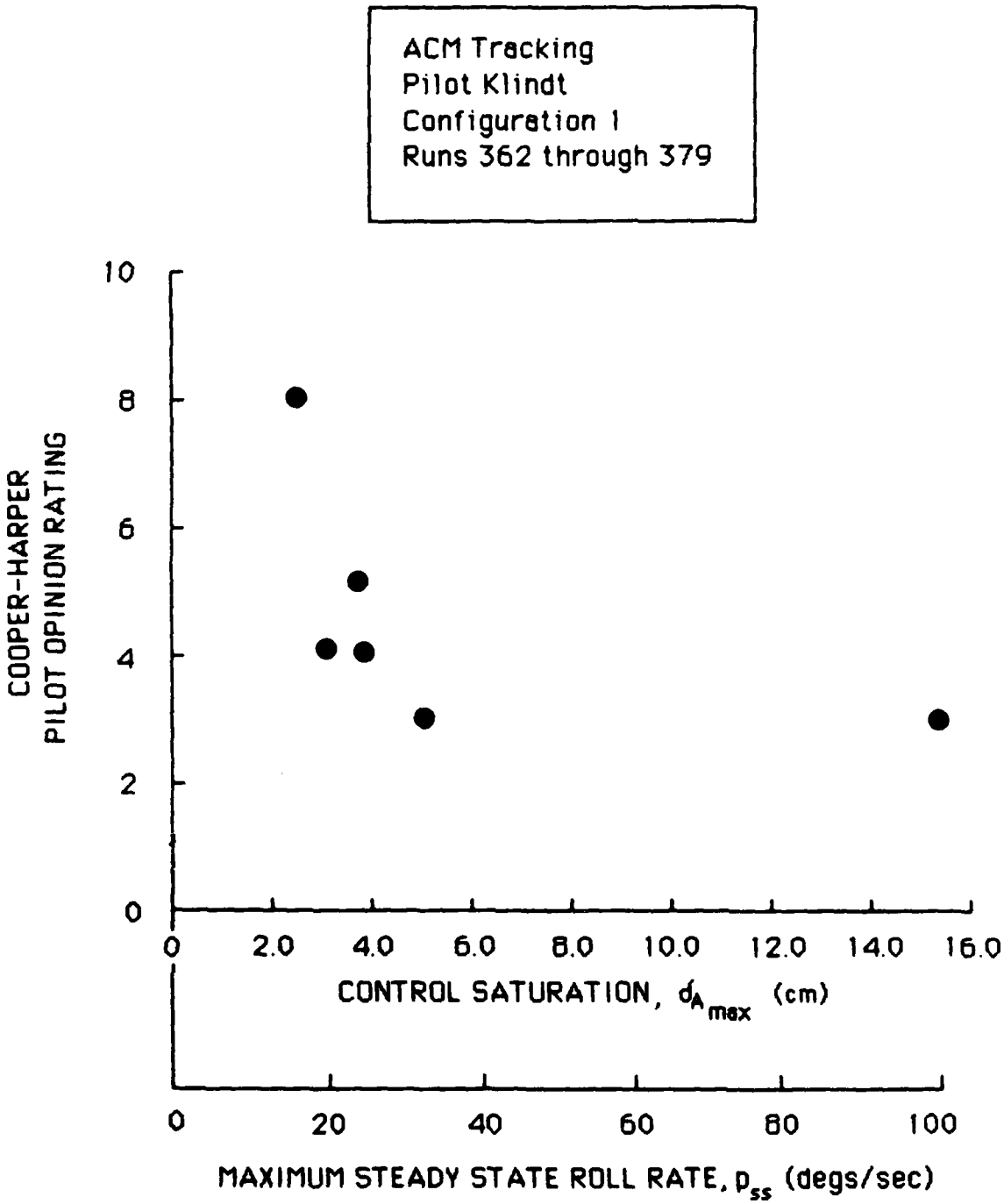

Figure 4-34b. Pilot Opinion Variation in ACM Tracking Task with Control Power Saturation for Pilot Klindt

objective.

ACM Free Engagement

Finding: ACM free engagements result in peak roll rates of 40 deg/sec and maximum command bank angle changes of 70 deg.

Discussion: The task signature for a typical free engagement is shown in Figure 4-35. This indicates that the ACM tracking task provides comparable task amplitude information with regard to roll rate demand. The tracking task has the advantage that the task structure is defined and repeatable for each run, a useful attribute for handling qualities evaluations.

Altitude and speed management is also a key element to the free engagement whereas the ACM tracking task used here was restricted to a horizontal plane. Simulator visual system limits restrict unlimited free engagment tactics.

ACM Maneuver Aggressiveness

Finding: Closed-loop natural frequency and damping ratio representative of fine attitude control are 2.5 rads/sec and 0.46 respectively, with associated standard deviation of 0.3 rads/sec and 0.11 respectively.

Discussion: Identification of these parameters was made on attitude changes less than 10 degrees. The sample was small, only three discrete attitude changes. Nevertheless, the data appear significant in view of the standard deviation of the sample set.

4. Sidestep Maneuver Results

The sidestep maneuver was a near-earth bank-to-translate task which

AD-A172 111 STUDY OF HELICOPTER ROLL CONTROL EFFECTIVENESS CRITERIA 3/3
(U) MANUDYNE SYSTEMS INC LOS ALTOS CA
R K HEFFLEY ET AL. APR 86 MANUDYNE-83-1
UNCLASSIFIED USAAVSCOM-TR-85-A-5 NAS2-11665 F/G 1/2 NL

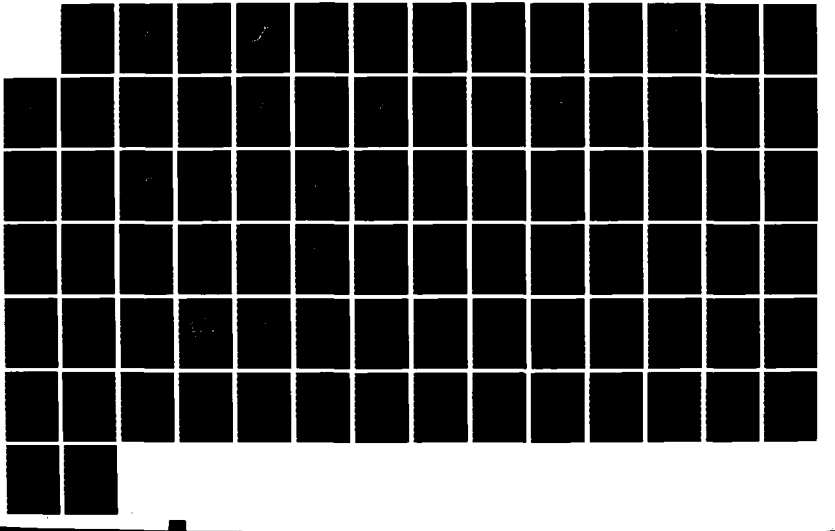

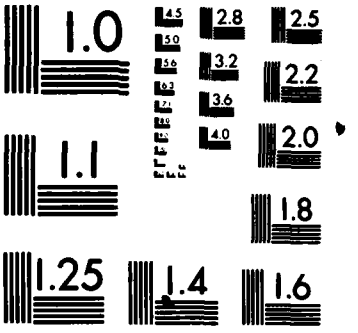

MICROCOPY RESOLUTION TEST CHART
NATIONAL BUREAU OF STANDARDS-1963-A

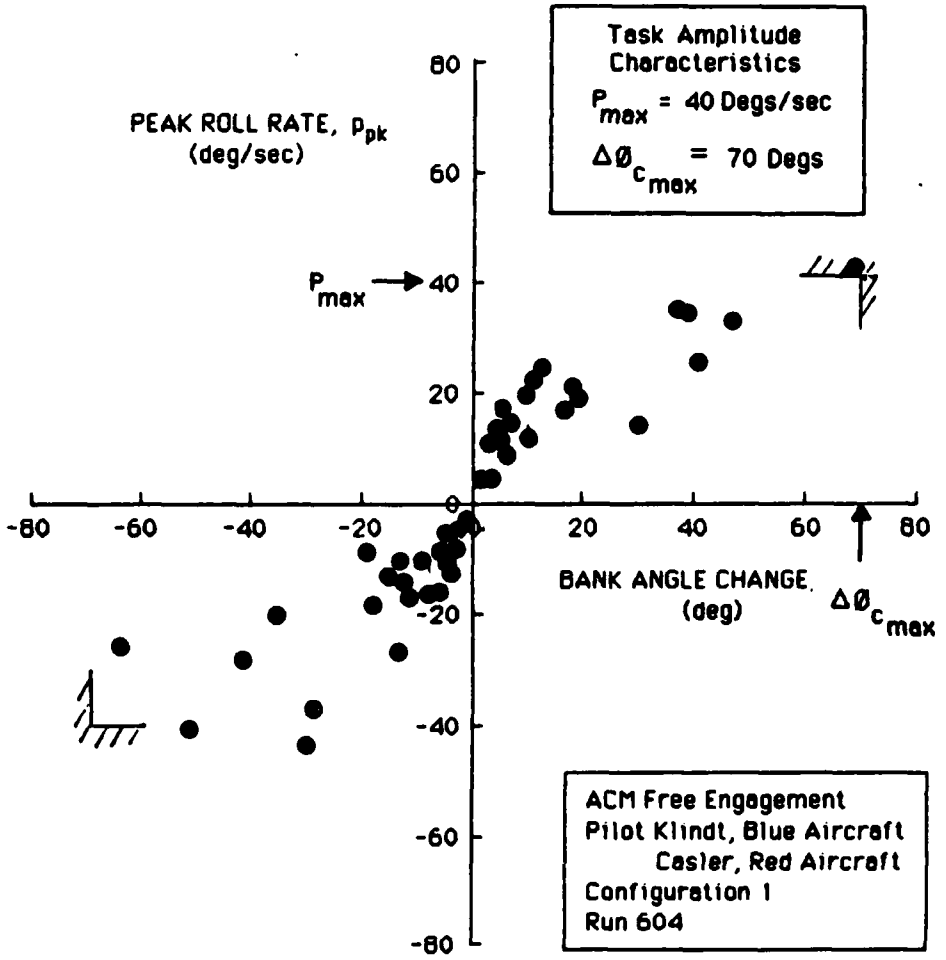

Figure 4-35. Example of Air Combat Free Engagement Task Performance

was found difficult as a result of CGI deficiencies. The primary visual difficulty was in the perception of depth and relative motion cues. Steps were taken to provide the highest texturing possible in the sidestep maneuver area yet fore and aft position cues were especially deficient. This resulted in the maneuver being very artificial from a task cue point of view.

Sidestep Maneuver Amplitude

Finding: The sidestep task is characterized by a peak roll rate of 50 degs/sec and a maximum commanded bank angle change of 60 deg.

Discussion: The characterizing amplitude data were derived from Figure 4-36. Again there is noted a reduction in closed-loop bandwidth for larger attitude changes. The large attitude changes are associated with roll reversals to decelerate the vehicle. Attitude changes of order 20 degrees indicate sidestep initiation and termination phases in the maneuver. There are however many points associated with small attitude changes which are made with high aggressiveness. These points represent precision attitude control in, for example, the hover phase. Many of these points lie on or close to the predicted maximum bandwidth capability of the vehicle. This suggests that short-term response requirements for the vehicle may be sized on precision control requirements alone.

Effects of Control Power Limitation in the Sidestep

Finding: Pilot opinion degraded sharply when steady state roll rate capability was limited to less than 25 degs/sec.

Discussion: Figure 4-37 defines the pilot opinion variation with control power limitation for the sidestep task. With available steady state roll rate limited to less that 25 deg/sec the pilot cannot quickly

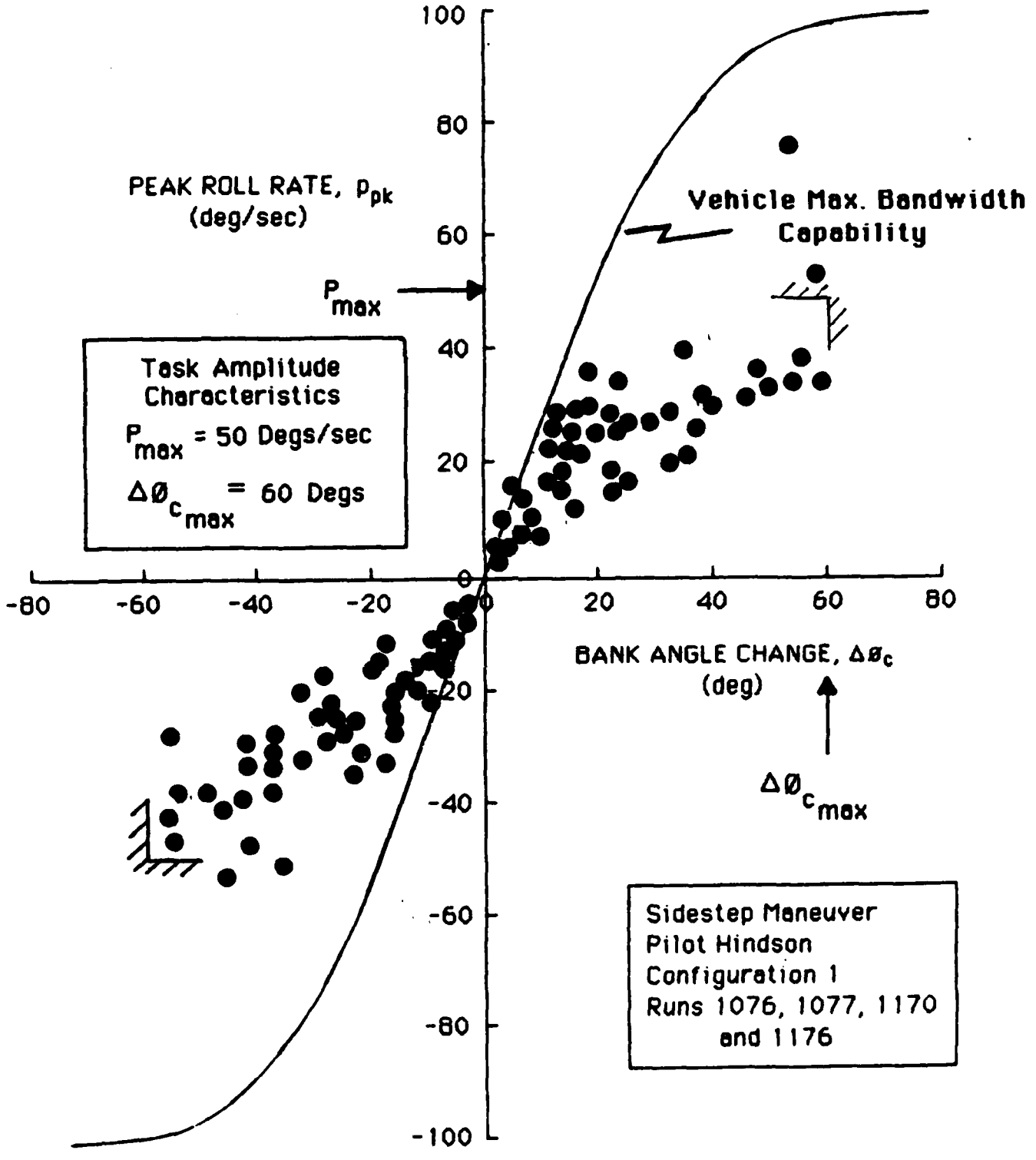

Figure 4-36. Sidestep Task Performance

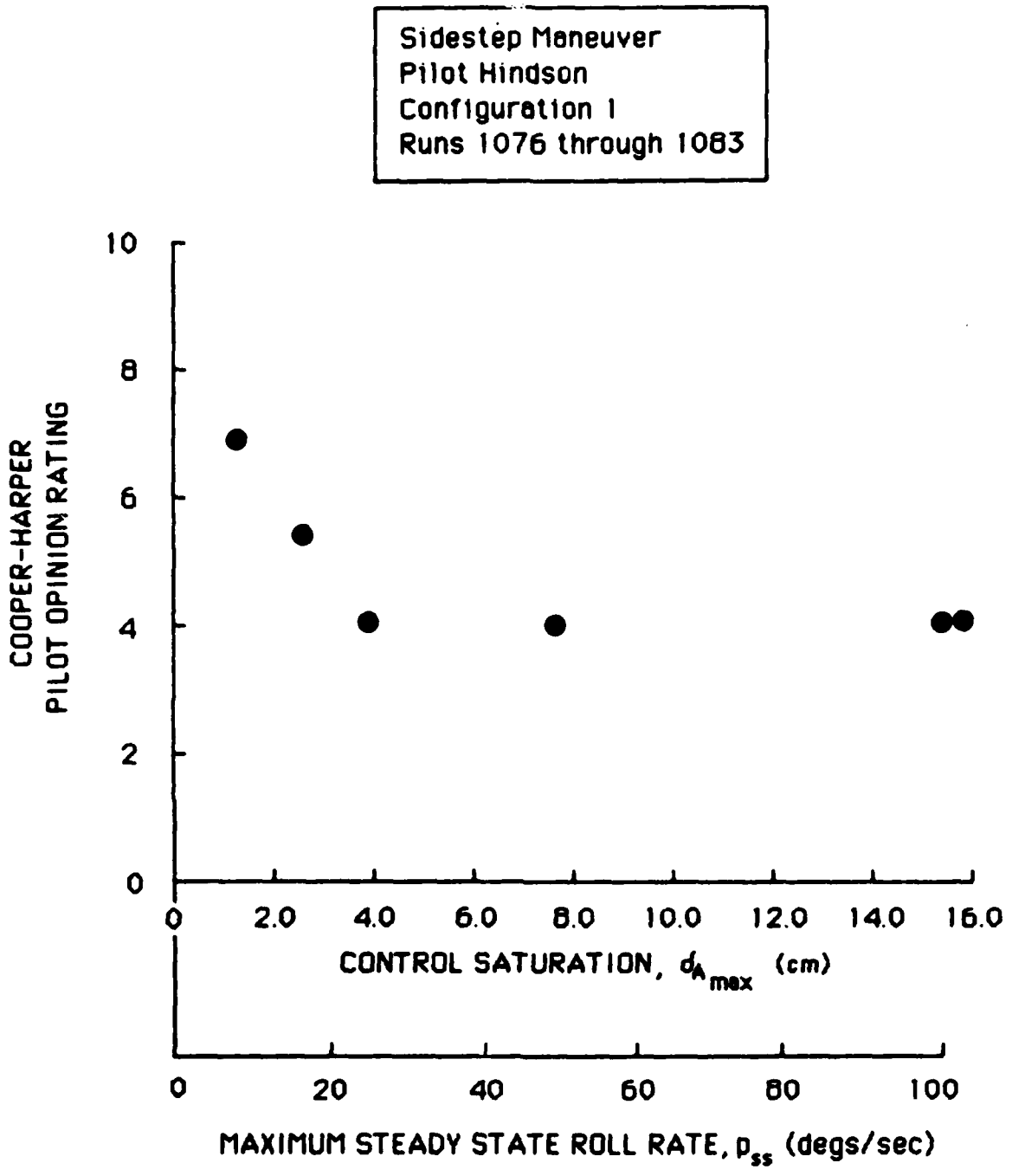

Figure 4-37. Variation in Pilot Opinion With Control Power Saturation in the Sidestep Task

establish lateral acceleration, being limited by the low bandwidth of the attitude dynamics. The degradation in authority appears to the pilot to be asymmetric. This arises from the beneficial effects of dihedral in the deceleration phase at high sideslip velocities. At 1.3 cm (0.5") saturation the pilot is essentially acting as a switching controller between the saturation limits. Time history data for this case suggests that the closed-loop system is in a limit cycle during the attempts to establish hover.

Performance degradation with control saturation is observed primarily in the outer position loop. Damping of the closed loop system reduces with saturation leading to large overshoots and long settling times.

Sidestep Maneuver Aggressiveness Effects

Finding: Closed-loop natural frequencies can be as high as 4.5 rads/sec for small attitude changes.

Discussion: The closed-loop roll dynamics were again identified within the second order equivalent structure using the least squares technique. The identified natural frequency and damping ratio as a function of commanded bank angle change are shown in Figure 4-38. As seen in previous closed-loop identification results the following trends are evident:

- Reduction of closed-loop natural frequency with amplitude of the maneuver
- Maximum natural frequencies in the range 4.0 to 5.0 rads/sec.
- Significant scatter in the natural frequency data but largest for fine attitude control
- Large scatter in the closed-loop damping ratio data.

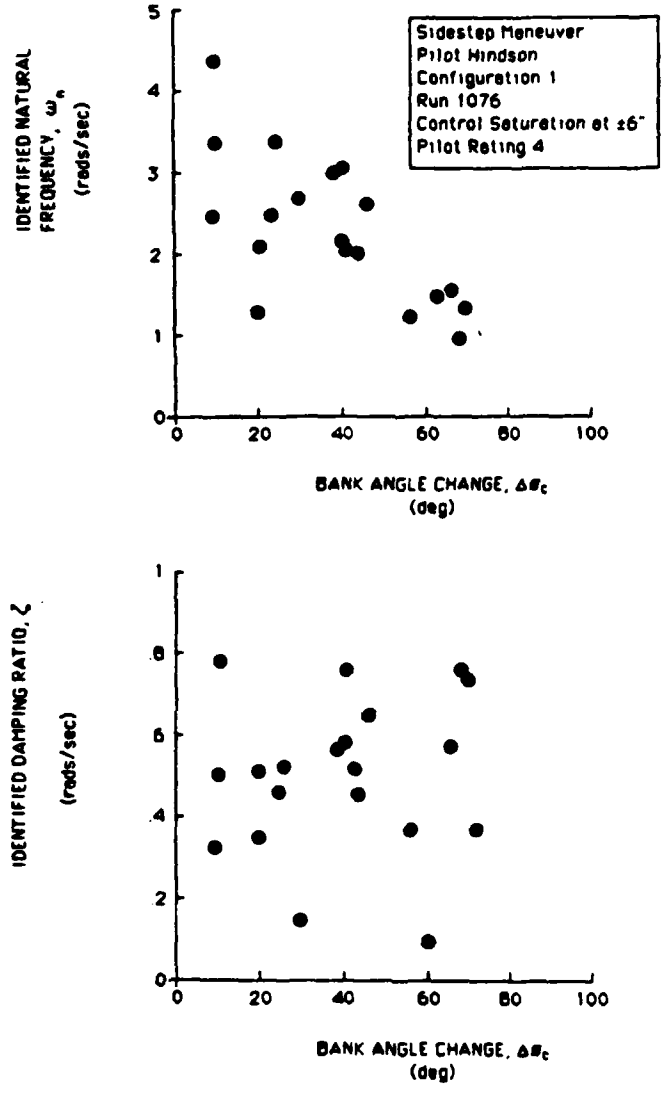

Figure 4-38. Identified Closed-Loop Natural Frequency and Damping Ratio for Nominal Performance in the Sidestep Maneuver Maximum Vehicle Roll Rate Capability = 100 Degs/sec

Rate and Attitude Command Response Types in the Sidestep Task

The attributes of vehicle stabilization and decoupled response associated with augmentation realizes an improvement over the basic helicopter response type for certain tasks. This is especially true for attitude systems with regard to unattended operation since they essentially relieve the pilot of inner-loop compensation duties. Baseline attitude systems show a 1.5 to 2 Cooper-Harper rating improvement over the baseline helicopter in hover and the sidestep task. The pure time delay inherent in simulation computation and the visual system tends to highlight the improvement between the two response types. Indeed, an attitude system is significantly easier to hover in simulation than the basic helicopter.

Analysis of the attitude and rate command response types was limited in scope and depth. The simulation provided adequate response fidelity in the low speed regime even though the high speed range was limited by the anomalous vehicle characteristics described in Section V-E. A bandwidth limitation was also encountered in simulation. Due to the relatively high cycle times (64 msec) augmentation system bandwidths could not be increased much beyond 3.5 rads/sec without encountering a stability boundary.

Finding: Level 1 handling qualities are assured in the sidestep task provided:

- o The closed-loop pilot compensated performance for attitude changes up to 30 degs. can satisfy the bandwidth requirement:

$$\frac{P_{PK}}{\Delta\phi} \geq 1.0$$

- o Adequate open loop damping exists in the vehicle.

Discussion Figure 4-39 shows pilot opinion variation with attitude system configuration in the sidestep task. Figure 4-40 defines the associated closed-loop performance characteristics. It is noted that the bandwidth relationship in the peak roll rate versus attitude change is typically linear. This linearity relates to the unquickened basic vehicle bandwidth capability which is linear and defined by:

$$\frac{P_{PK}}{\Delta\phi} = \frac{\omega_n \exp\left(\frac{-\zeta\pi}{\sqrt{1-\zeta^2}}\left[0.5 - \frac{\theta}{\pi}\right]\right)}{1 + \exp\left(\frac{-\zeta\pi}{\sqrt{1-\zeta^2}}\right)}$$

where $\frac{\phi}{\delta}(s) = \frac{K}{s^2 + 2\zeta\omega_n s + \omega_n^2}$

$$\theta = \tan^{-1}\left(\frac{\zeta}{\sqrt{1-\zeta^2}}\right)$$

This relationship is shown on Figure 4-40 for the configurations. It is observed that the pilot is quickening his input to enhance the closed-loop bandwidth in most cases. The closed-loop compensated bandwidth requirement specified above for Level 1 handling qualities is based upon the trends noted in Figure 4-40.

Implication This result re-emphasizes the requirement for tailoring of the vehicle capability to the closed-loop task requirements. In this case the objectives are to ensure adequate open-loop vehicle damping and minimze the quickening compensation required of the pilot to achieve desired performance.

Futher analysis should be made to quantify the quickening compensation versus task performance trade-off. Also the maximum task execution bandwidth available with pilot compensation should be defined theoretically. This can be approached in the same way as used to evaluate basic helicopter capability. This would provide a theoretical basis for a specification of handling qualities criteria for attitude response type vehicles.

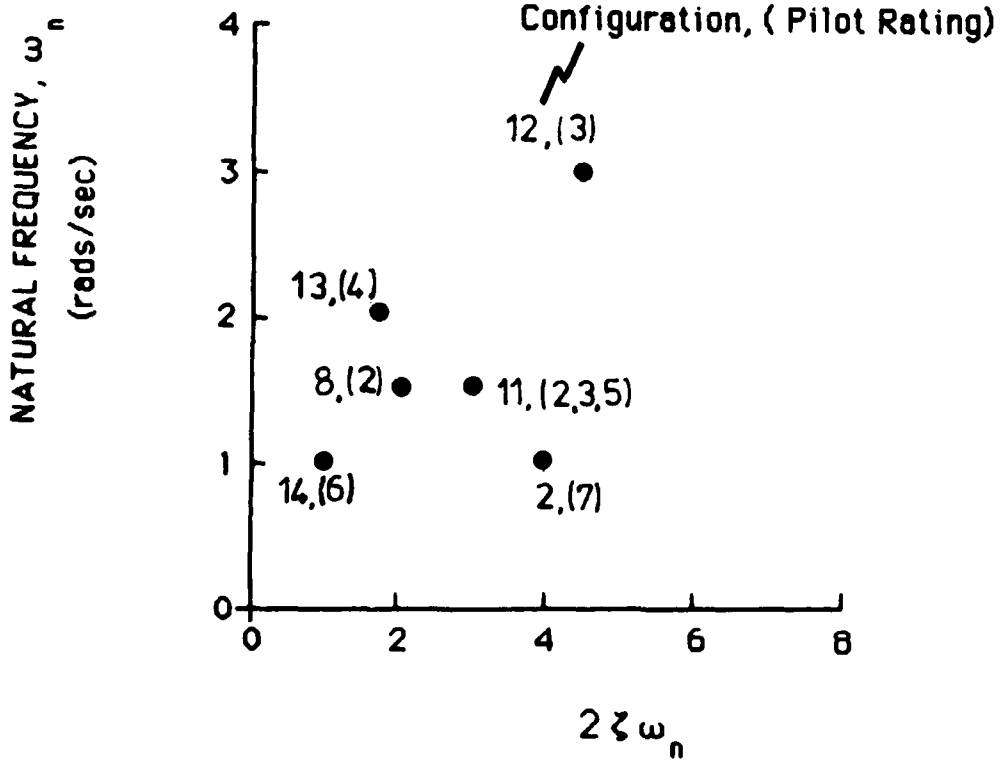

Sidestep Maneuver
Pilot Hindson
Attitude Command Response Types

Figure 4-39. Pilot Opinion Variation in the Sidestep Maneuver with Attitude Command Configuration

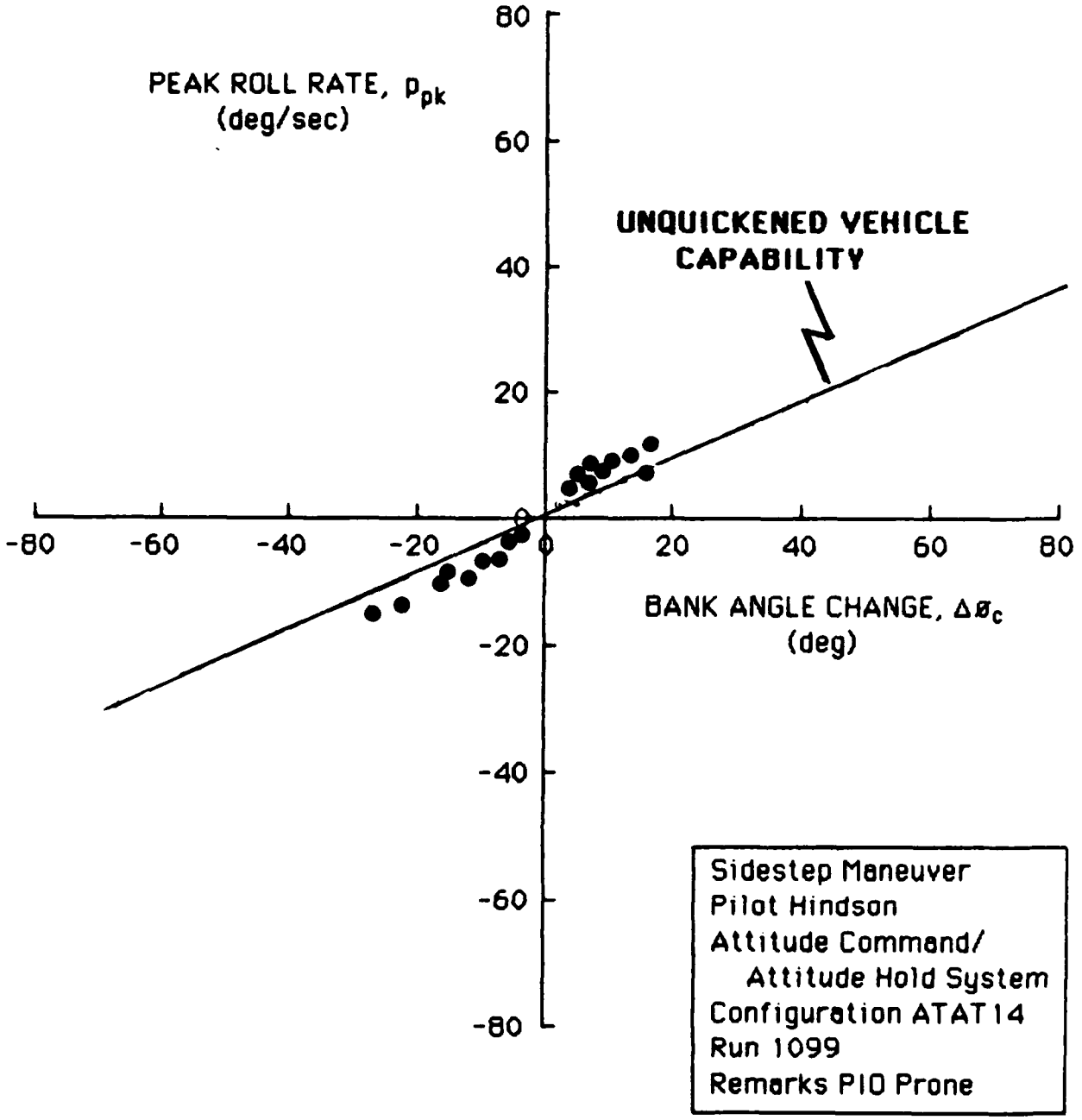

Figure 4-40a. Sidestep Task Performance for Attitude Command Configuration 14

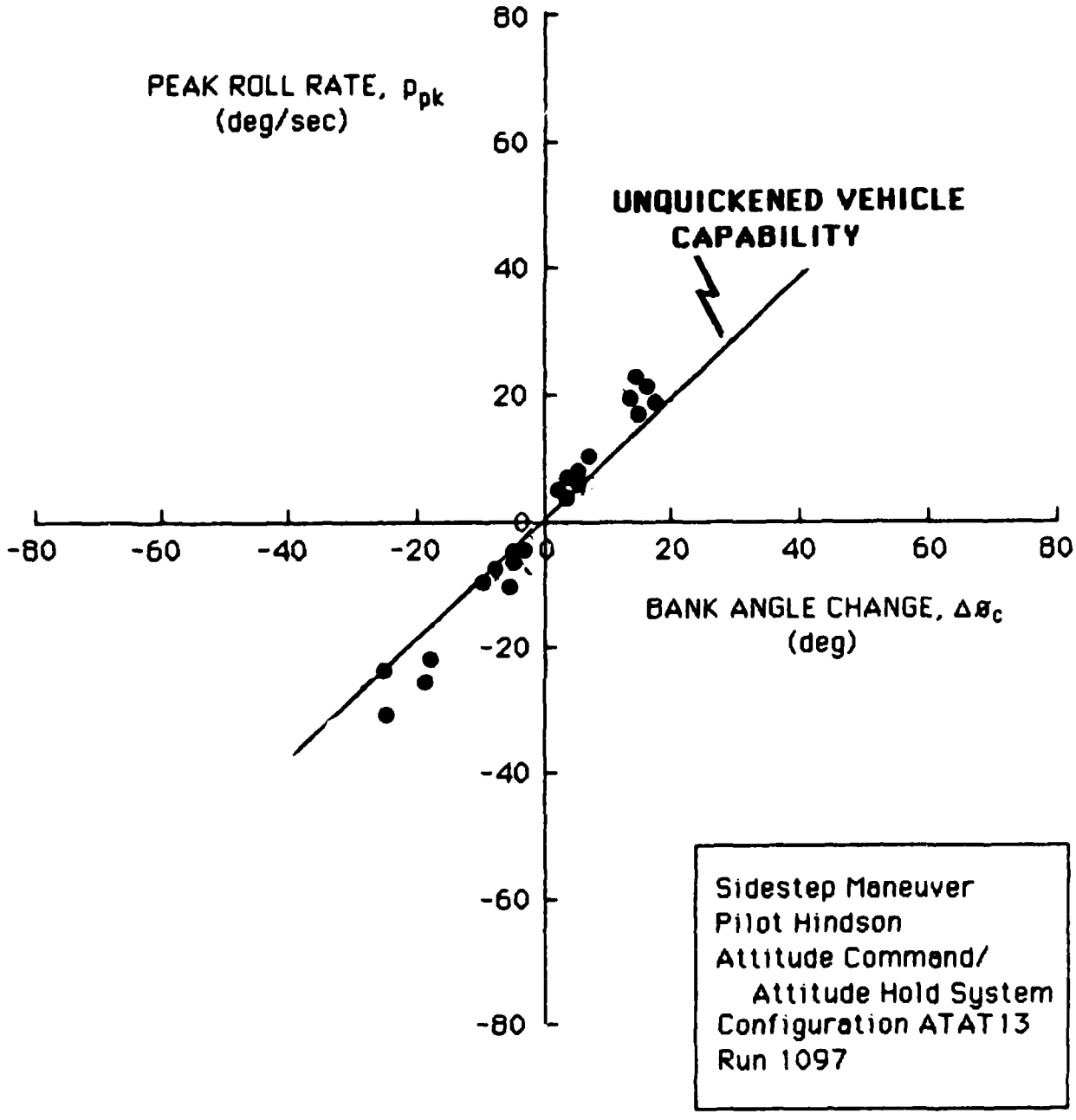

Figure 4-40b. Sidestep Task Performance for Attitude Command Configuration 13

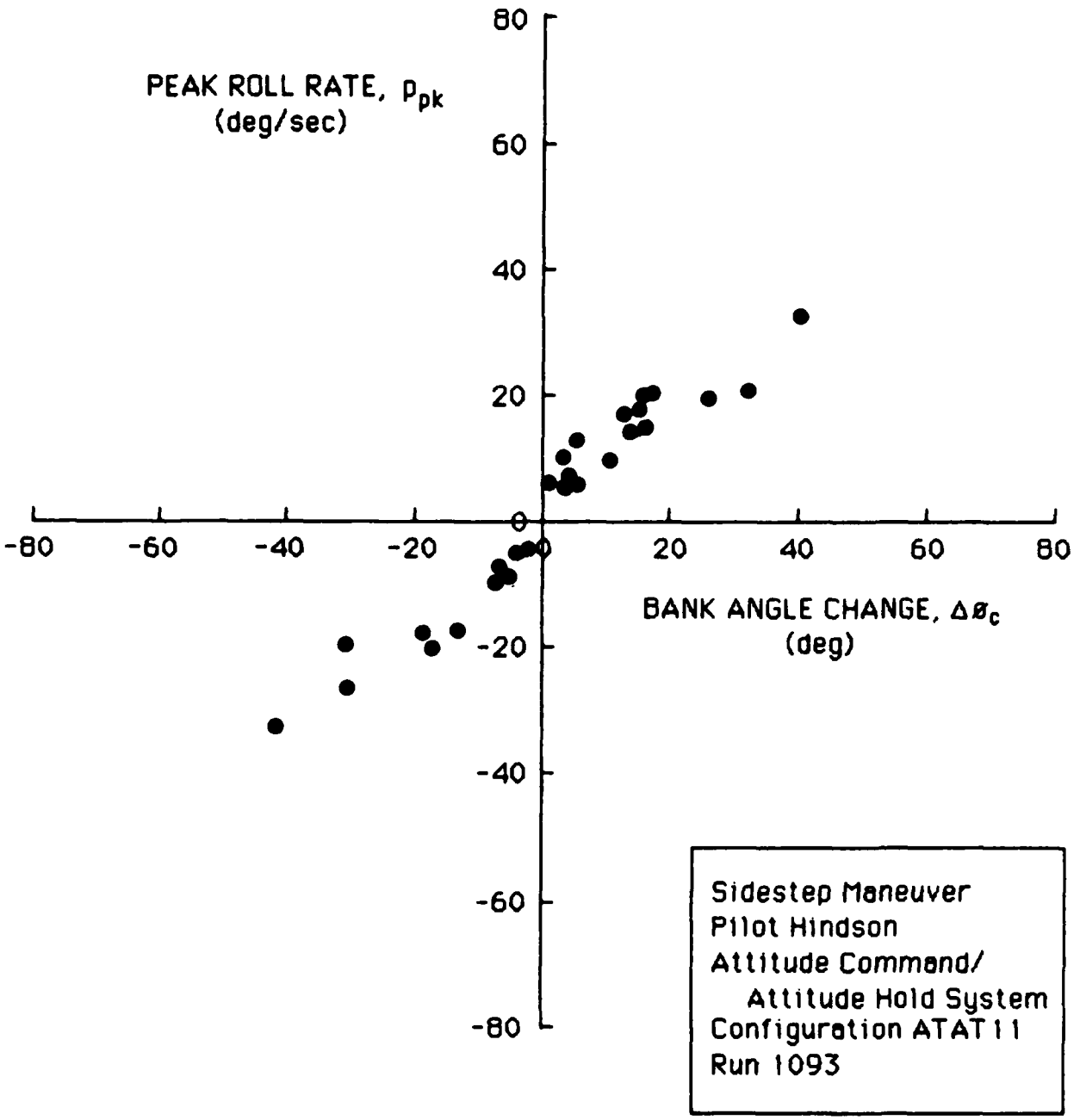

Figure 4-40c. Sidestep Task Performance for Attitude Command Configuration 11

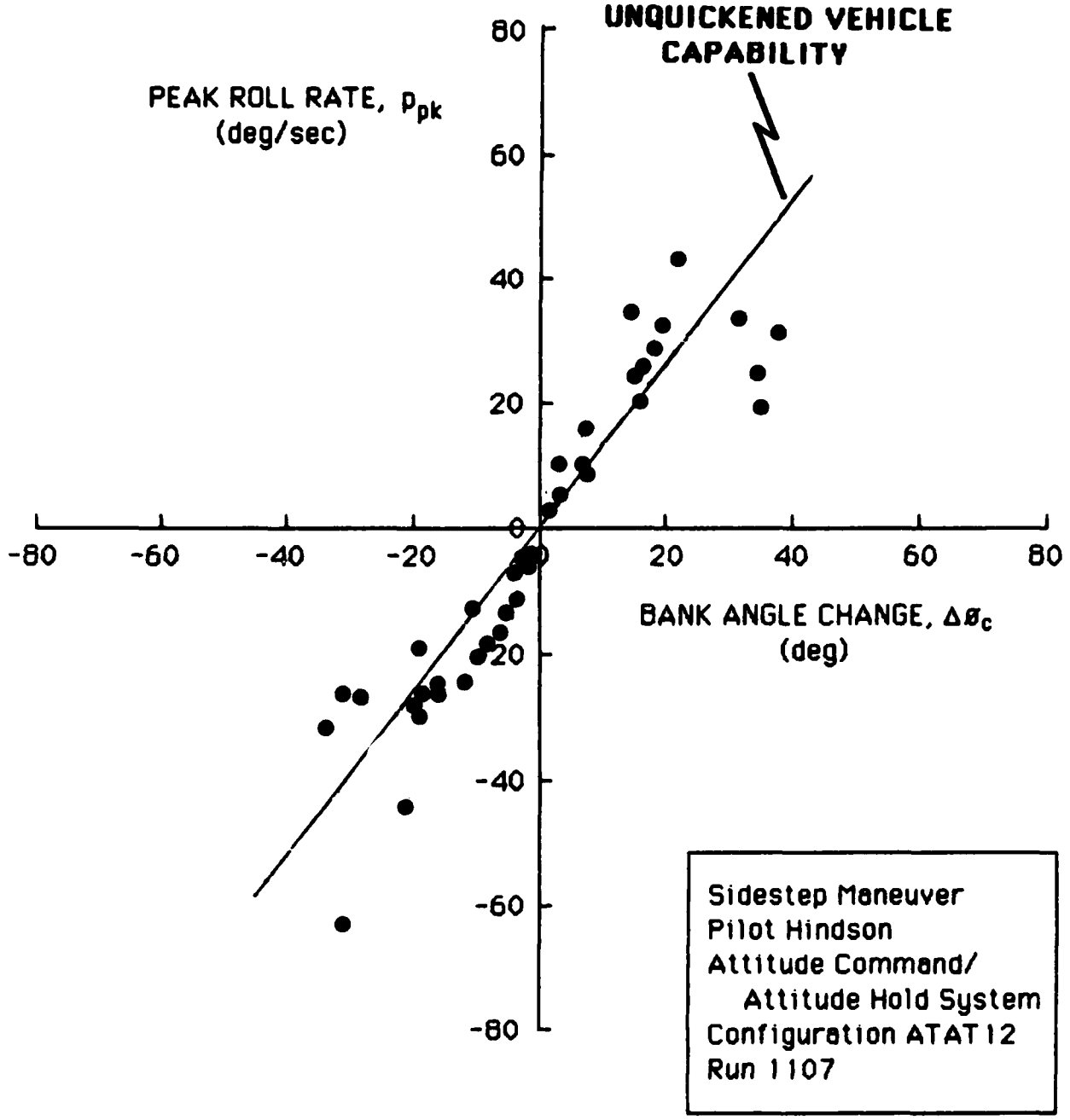

Figure 4-40d. Sidestep Task Performance for Attitude Command Configuration 12

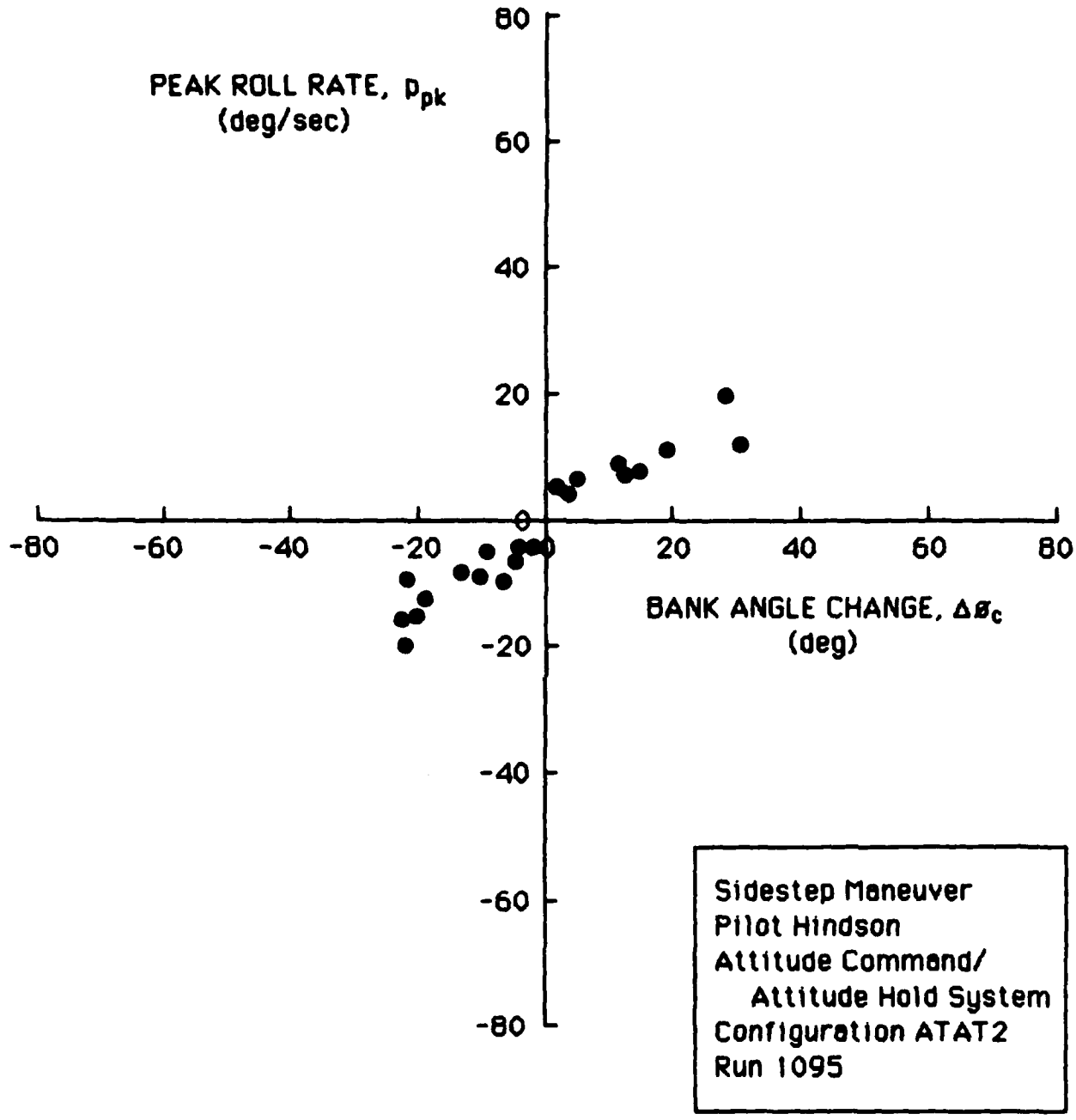

Figure 4-40e. Sidestep Task Performance for Attitude Command Configuration 2

Finding: Amplitude and aggressiveness characteristics of task performance are generally lower than those seen for the basic helicopter type.

Discussion: Figure 4-41 defines task performance for the attitude system in the sidestep task and compares it to the amplitude characteristics observed for the basic helicopter response type. The essentially lower closed-loop bandwidth is related to the uncompensated capabilty of the attitude system and the willingness of the pilot to increase closed-loop bandwidth by overdriving and leading the system. Futhermore, the augmentation of the vehicle to provide attitude command response negates any dihedral effect present in the vehicle. It has been observed in the HUD tracking task, for example, that the pilot will enhance his roll rate capability in the basic helicopter using dihedral effect to achieve desired task performance.

Finding: A high gain rate system leads to essentially the same performance as seen for basic helicopter types.

Discussion: This finding is based upon the task signature shown in Figure 4-42.

5. Turn Maneuver Results

This task is characterized by having both open- and closed-loop control policies, and by both heading and course control elements. The heading change element is basically effected using a co-ordinated turn. The airspeed and effective turn radius define apriori the attitude excursion required. The pilot rolls into the turn and holds the desired bank angle until roll-out. Since the task requires him to align with a certain course on roll-out he may have to effect a series of closed-loop course change maneuvers to satisfy desired performance.

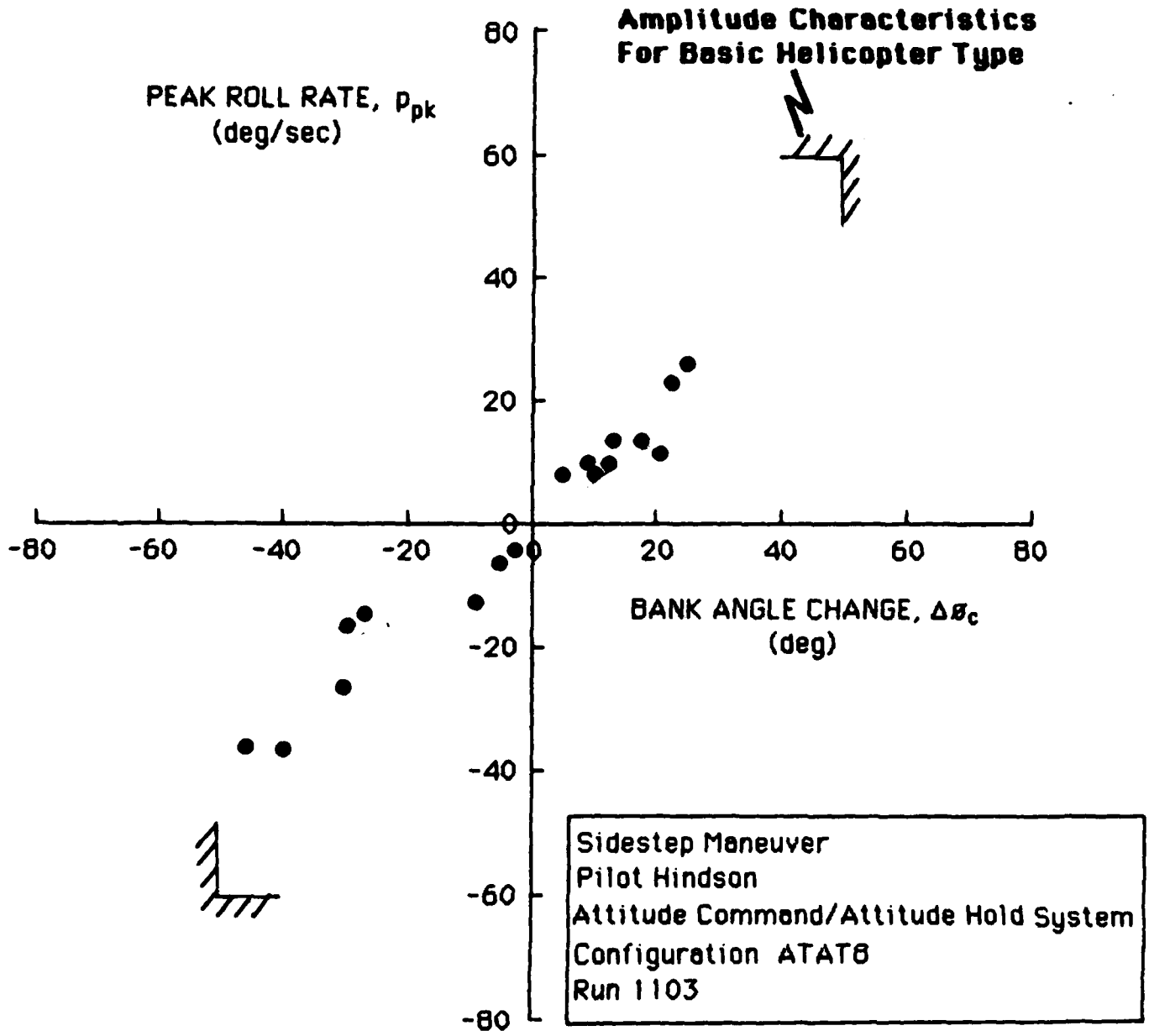

Figure 4-41. Typical Sidestep Task Performance for Attitude Command Response Type

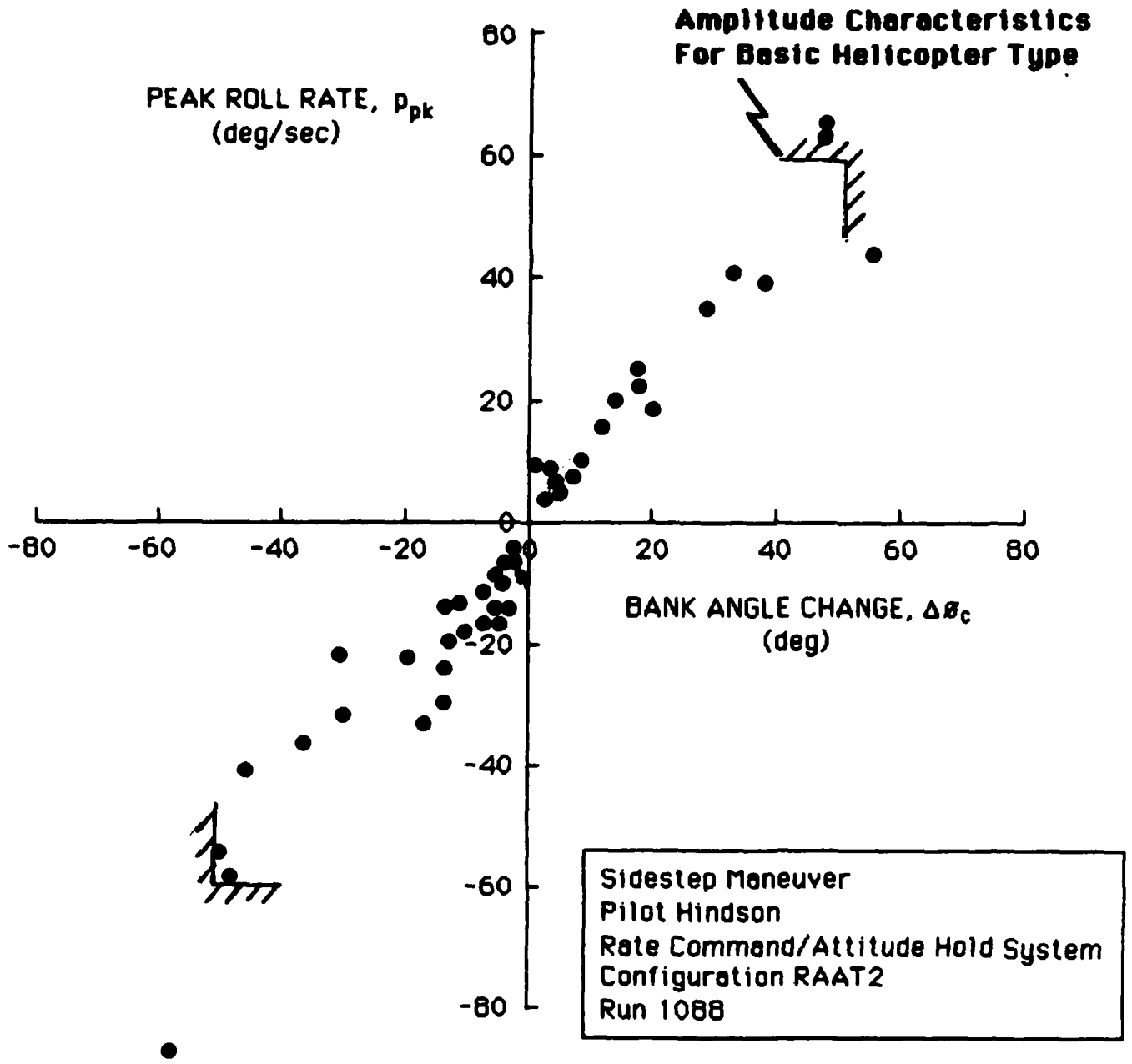

Figure 4-42. Typical Sidestep Task Performance for Rate-Command/ Attitude-Hold Configuration

Turn Maneuver Amplitude

Finding: The task performance signature is shown in Figure 4-43. The maneuver is characterized by a maximum roll rate of 40 degs/sec and a maximum commanded roll attitude change of 40 degs.

Discussion: Significant reduction in aggressiveness with amplitude is not apparent, although the attitude changes involved in this maneuver are relatively small.

Turn Maneuver Aggressiveness

Finding: Bandwidths comparable to the fine attitude control bandwidths seen in the HUD tracking data are observable. Significant scatter in the fine attitude control aggressiveness is again observed, consistent with previous data.

Discussion: The consistency between maximum observed bandwidths and aggressiveness between diverse tasks such as HUD and ACM tracking, sidestep and turn maneuvers gives support to the hypothesis that this mode of control is independent of the outer-loop task. This has some far reaching implications regarding definition of short-term response criteria. This concept will be discussed more thoroughly in Section V.

Other Control Response Types

Finding: The task performance for an attitude system is essentially the same as that defined for the basic helicopter type.

Discussion: The task signature is shown in Figure 4-44. The uncompensated vehicle capability is also shown. Since vehicle capability and task demand are comparable the observed result is not suprising. A provision needs to be added to the above finding. That

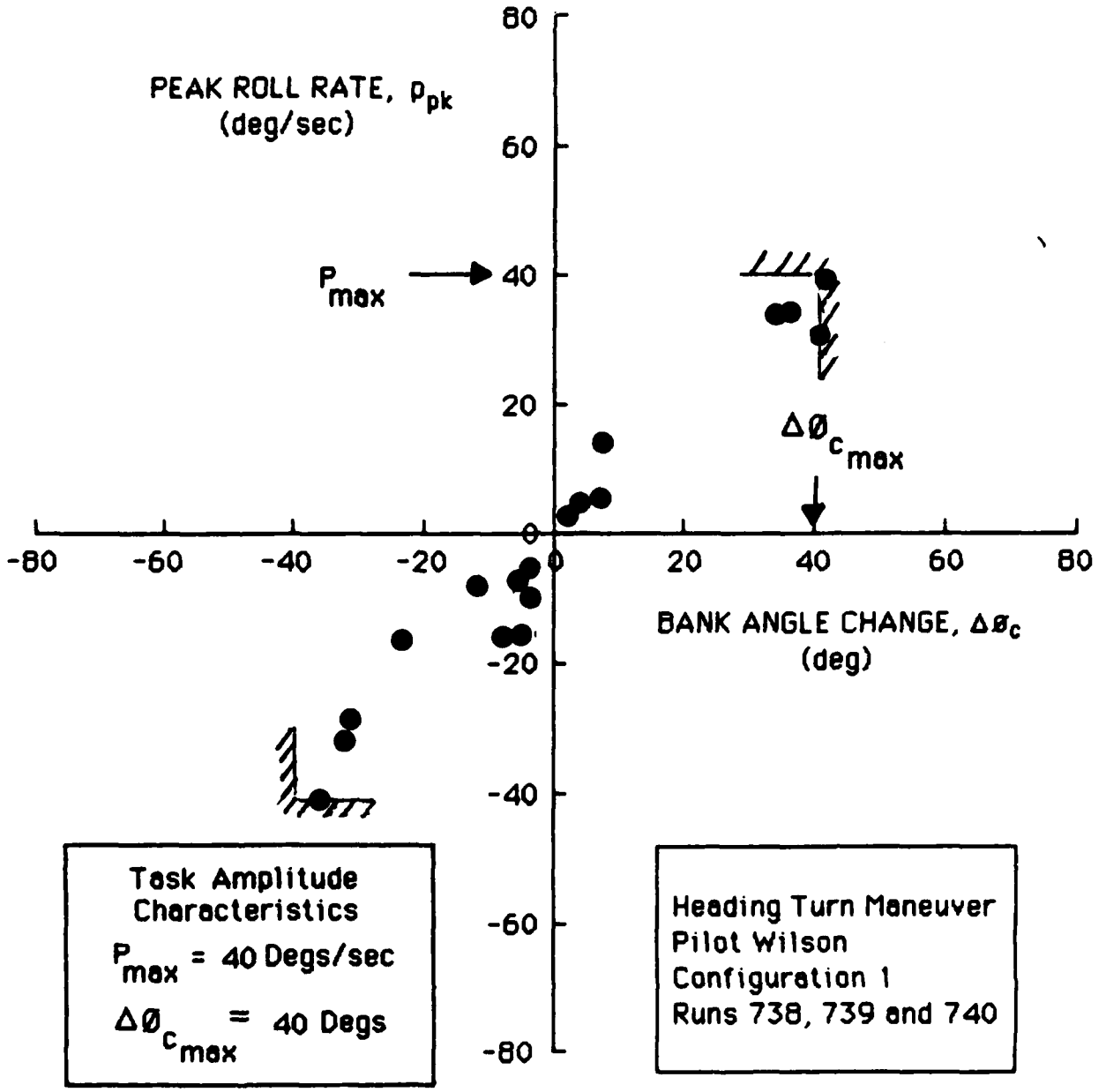

Figure 4-43. Heading Turn Maneuver Data for Basic Helicopter

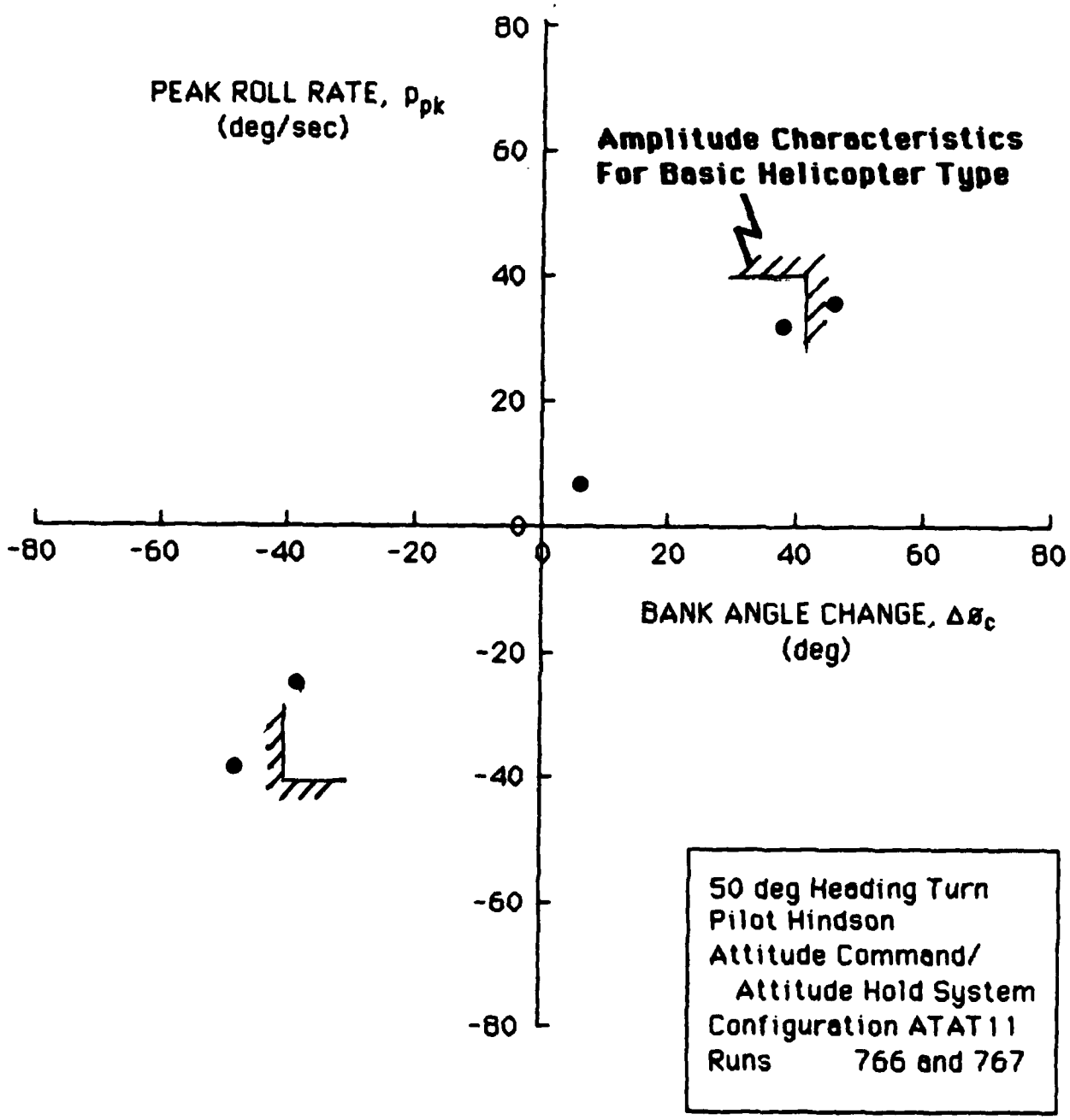

Figure 4-44. Heading Turn Maneuver Data for Attitude Command Response Type

is, task performance can be expected to be comparable between basic helicopter and attitude response types provided:

- Significant sideslip is not involved
- Vehicle uncompensated capability is not significantly less than task performance demands

6. Slalom Maneuver Results

The slalom maneuver is an interesting maneuver because of the likely presence of a primarily pursuit pilot control strategy. Roll commands tend to become well synchronized with the rounding of pylons. Thus, there is a modification in the usual partitioning of inner- and outer-loop control behavior.

A 60 Kt airspeed and 450' separation of the pylons results in a relatively low outer-loop bandwidth requirement for task execution. Furthermore, the relaxed preview times and no requirement on a precise ground track result in the maneuver having a characteristically low inner loop bandwidth and hence low peak roll rates.

Slalom Maneuver Amplitude

Finding: Amplitude characteristics for the task are a maximum roll rate of 30 degs/sec and a maximum commanded attitude change of 50 degs.

Discussion: These figures are based upon the task signature in Figure 4-45. Of all the data looked at to date the slalom task has the most pronounced roll rate limiting characteristic at large amplitudes. The data for fine attitude control are comparable to that seen in the HUD, ACM and sidestep tasks both in maximum bandwidths observed and the scatter noted. This again suggests that precise attitude control may be independent of the nature of the outer-loop task. The distinct roll

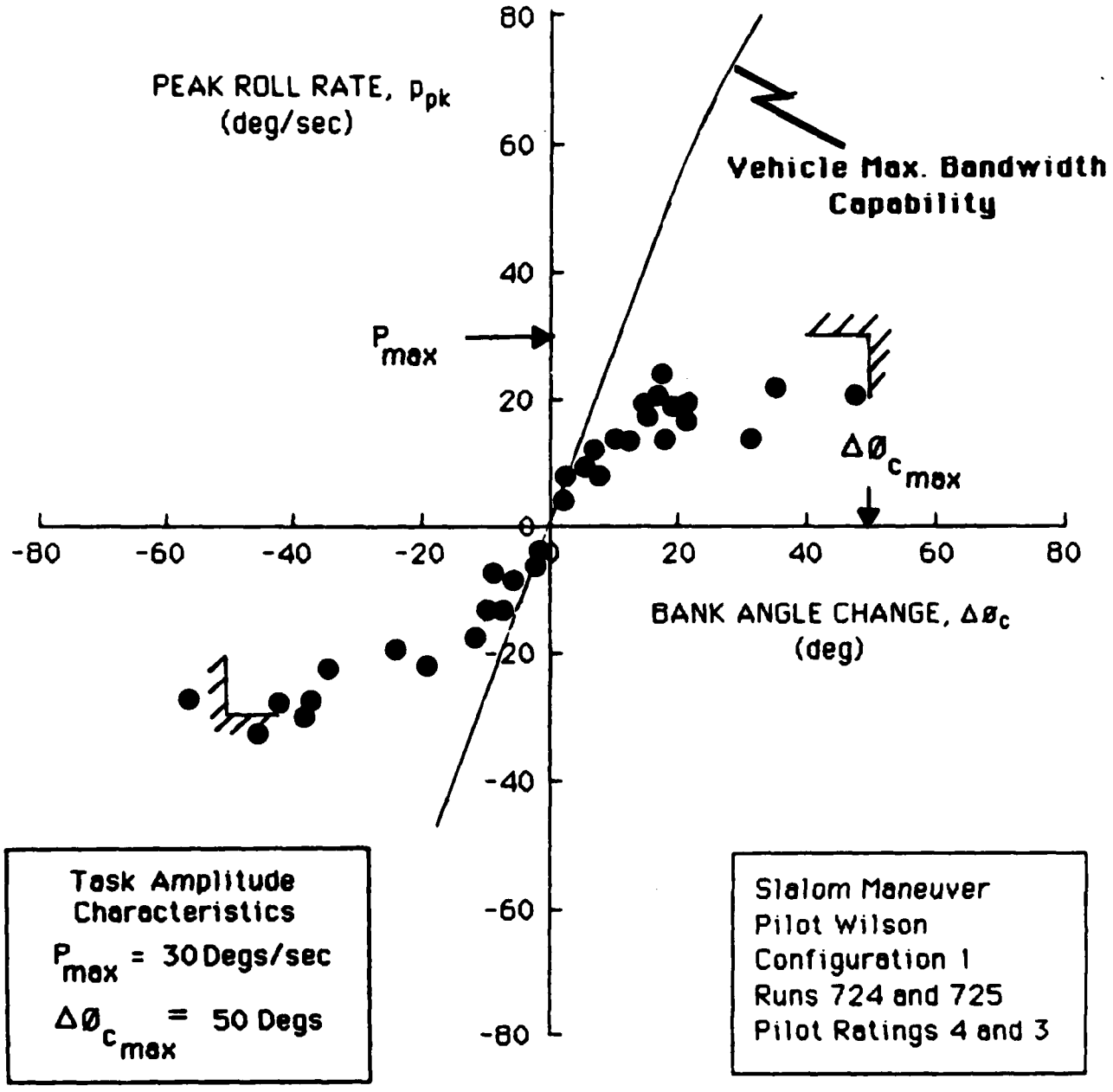

Figure 4-45. Task Performance for the Slalom Maneuver for Basic Helicopter Type Configuration

rate saturation feature may thus result from the relative bandwidth requirements between fine attitude control and mid- to large-amplitude requirements to support the outer-loop task.

Slalom Maneuver Aggressiveness

Finding: The peak roll rates and scatter in the fine attitude control aggressiveness data are comparable to those observed in the HUD, ACM and sidestep tasks.

Discussion: A limited sample of small bank angle commands (less than 20 degrees in amplitude) were identified within the second order equivalent system structure. The mean values realized were a natural frequency of 2.0 rads/sec and a damping ratio of 0.6. Obtaining identifiable precision attitude control data tends to be difficult for this task. The propensity of fine attitude command changes tends to be low because a precise ground track is not required. The identified sample are however consistent with the identification results for the HUD tracking task.

7. Jink Maneuver

This maneuver suffers from significant simulation fidelity limitations. Problems in depth perception on approach to the walls are encountered. Furthermore, the maneuver is characteristically un-coordinated involving large amounts of sideslip and extensive pedal activity. This degree of un-coordination leads to problems in motion fidelity and conflicting motion and visual cues are apparent.

Jink Maneuver Amplitude

Finding: The representative maneuver amplitude characteristics for the task are a maximum roll rate of 40 degs/sec and a maximum command

attitude change of 50 degs.

Discussion: The task amplitude characteristics are evaluated from the task signature in Figure 4-46. The limiting of roll rate is again apparent in the maneuver.

Jink Maneuver Aggressiveness

Finding: Small amplitude maneuver control for attitude changes of 15 degrees realize a closed-loop natural frequency of 2.0 rads/sec and a damping ratio of 0.6. For attitude changes of 5 degrees the natural frequency was identified at 4.5 rads/sec and damping ratio at 0.4.

Discussion: The data obtained from the second order equivalent system identification are again comparable with the data obtained in HUD, ACM and sidestep tasks for fine attitude control.

Attitude Command Performance Characteristics in the Slalom and Jink

Finding: Task performance with attitude systems is comparable to basic helicopter response types provided the pilot does not have to effect substantial compensation.

Discussion: Figure 4-47 compares attitude command system performance in the slalom task to performance characteristics required from a basic helicopter response type. Provided that the uncompensated vehicle bandwidth capability is not significantly deficient compared to the closed-loop task performance characteristics the pilot appears to demand very similar performance. This will only be true if the task does not require extensive use of sideslip dynamics.

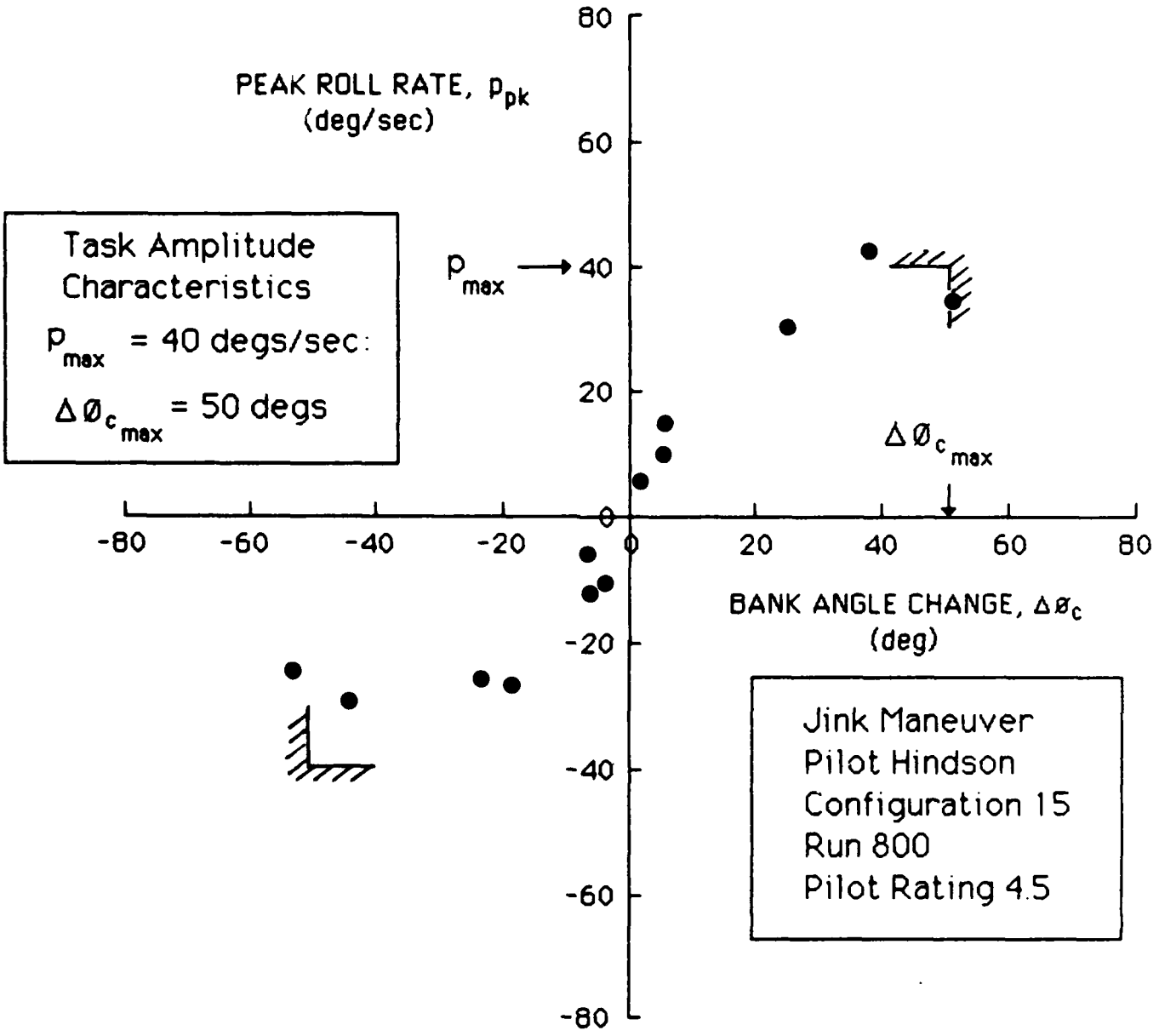

Figure 4-46. Task Performance for the Jink Maneuver for Basic Helicopter Type Configuration

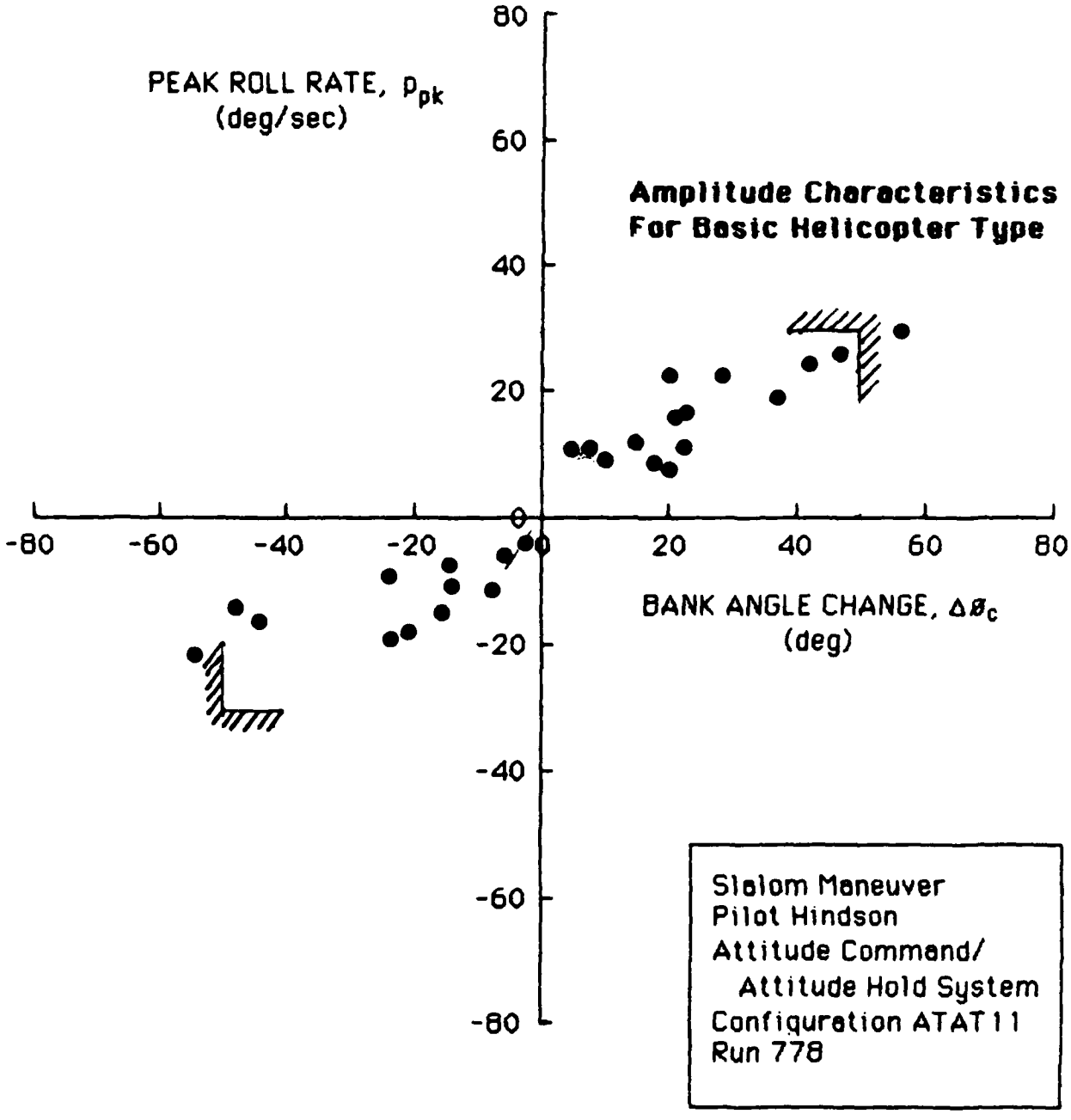

Figure 4-47. Slalom Task Performance for Attitude Command Response Type

Finding: Performance in the jink maneuver shows a slight reduction of the amplitude characteristics compared to conventional helicopter dynamics. Maximum roll rates are reduced from 40 to 30 degs/sec and commanded bank angle changes from 50 to 40 degrees.

Discussion: Figure 4-48 compares the task performance in the jink maneuver for the two vehicle response types. It is noted that the task performance differences are not associated with deficient vehicle bandwidth capability. The muted amplitude characteristics may be the result of loss of dihedral effect following augmentation of the vehicle. The outer-loop task performance metrics of minimum approach distances to the walls need to be assessed for an adequate comparison to be made.

8. IFR Heading Change Results

The IFR heading change flight task represents the lower extreme in terms of maneuver aggressiveness and amplitude.

IFR Heading Change Amplitude

Finding: The characteristic maneuver amplitude requirements are a maximum roll rate of 10 degs/sec and a maximum commanded attitude change of 25 degs.

Discussion: The task performance data are shown in Figure 4-49. The task exhibits the lowest amplitude characteristics of all the tasks simulated.

IFR Heading Change Aggressiveness

Finding: The maximum bandwidths observed in the small amplitude control are much lower than those observed in HUD and ACM tracking tasks.

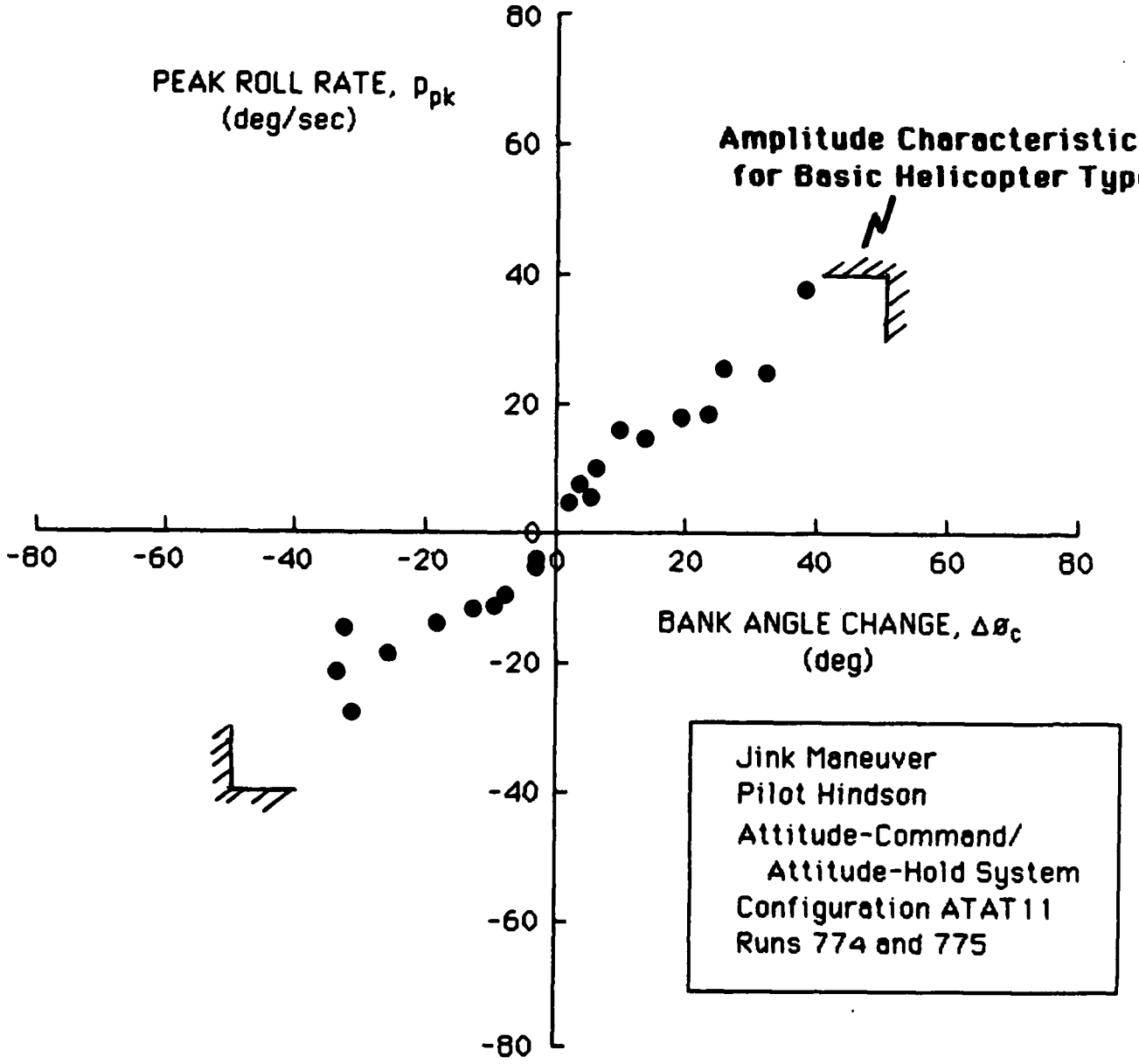

Figure 4-48. Jink Task Performance for Attitude Command Response Type

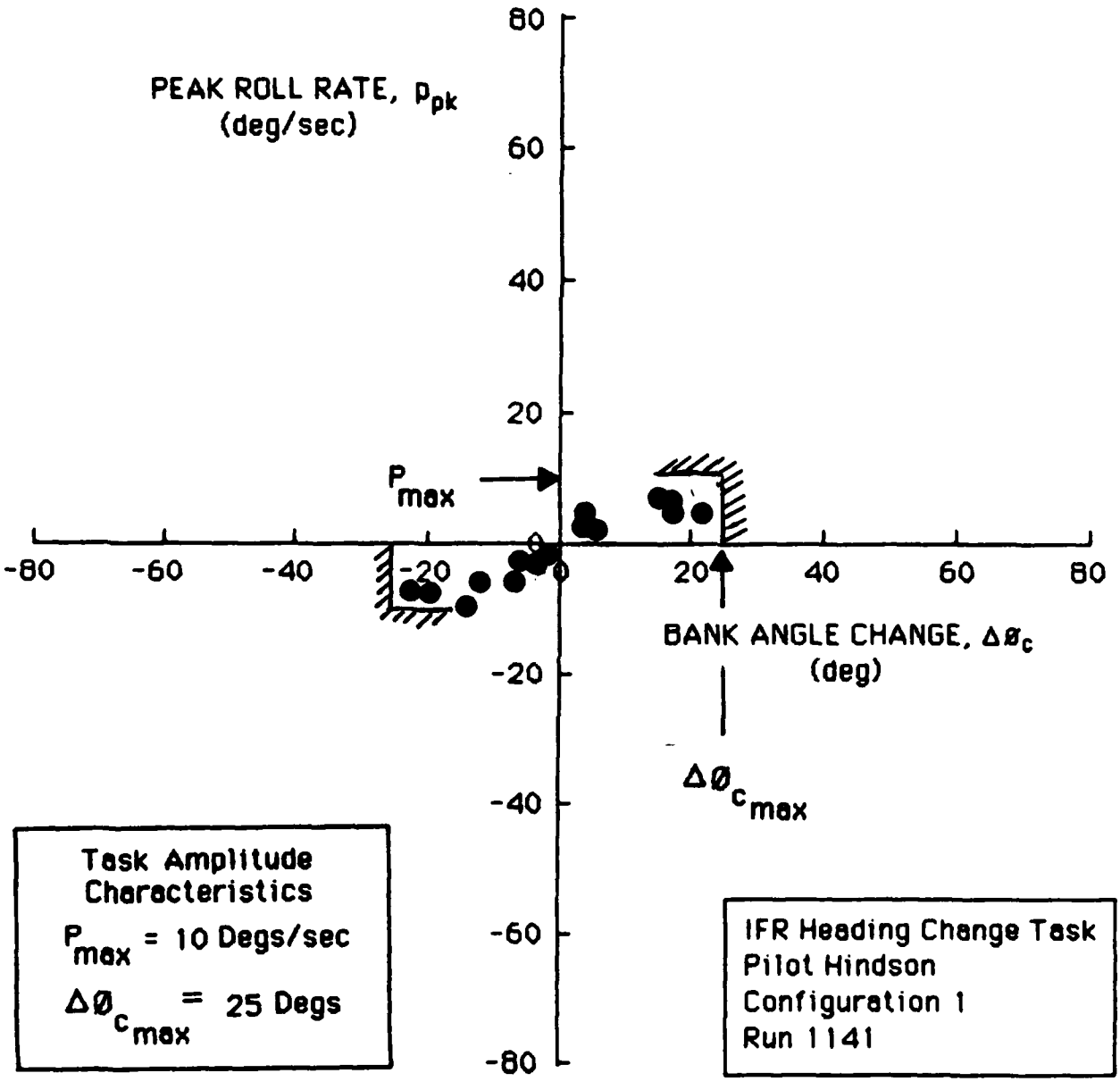

Figure 4-49. IFR Heading Change Performance Data for Basic Helicopter Response Type

Discussion: There is in fact no precision attitude control requirement for this task. The pilot basically establishes a coordinated turn and holds it until rollout.

E. Simulation Fidelity Issues

The simulator provides a controlled environment for the analysis of handling qualities issues. The validity of the results can however be compromised by fidelity deficiencies of the simulation. The following is a brief summary of fidelity issues encountered during this simulation program.

Mathematical Model Fidelity The ARMCOP mathematical model exhibited a number of response characteristics not representative of helicopter aeromechanics, and not associated with visual or motion fidelity issues.

Spurious force inputs were noted due to solution of the flapping equations in the hub-wind axis system which switches orientation rapidly with sideslip in hover. So adequate hover stabilization and control was not possible for the baseline vehicle. Solution to this problem was provided by Mr. R. L. Fortenbough of Bell Helicopter Textron by solution of the flapping equations in the hub-body axis system. This fix is documented in Volume II of this report.

The model demonstrated some uncharacteristic helicopter qualities during maneuvering. This was apparent in maneuvers such as the jink where un-coordinated flight led to uncharacteristically high lateral acceleration demands by the model. This problem was attenuated by increasing the related motion washouts. Thus motion fidelity was degraded to make-up for a mathematical modeling problem! Furthermore, the high bank angle flight, in such tasks as the HUD tracking and ACM tracking, the basic ARMCOP vehicle exhibits tendencies of airspeed loss in left turns and acceleration in right turns. With implementation of

feedback loop closures around the basic vehicle to obtain attitude response systems the severity of this asymmetry increased. Response is then typified by very abnormal airspeed loss and extreme angle-of-attack and sideslip excursions in left turns. Up to 40 kts of airspeed could be lost within a very short period. Figure 4-50 shows time histories of airspeed, slidelip, angle-of-attack and bank angle for left and right turns. This phenomenon was significantly reduced if the tail-rotor cant inherent in the UH-60 model was removed, and an improvement of Cooper-Harper rating form 6 to 3 was obtained in the HUD tracking task.

These maneuvering flight issues need to be investigated thoroughly. Comparison between in-flight maneuver and coordinated turn data from the AEFA UH-60 and ARMCOP model response would be instructive.

Throughput Time Delay The usual solution to the model fidelity issue is to increase model complexity. This however usually entails an increase in time-frame requirements which increases the overall throughput delay (control input to visual update) time. The existence of pure time delay in vehicle response has significant effect on pilot opinion. This is best seen by examination of time delay effects from in-flight investigations (Reference 51). The current MIL-F-8785C (Reference 40) criteria requires less than 100 msec for Level 1, and pilot opinion degrades about 1 Cooper-Harper per 33 msecs delay beyond this value. The estimated throughput time delays for this simulation were in the range of 180-200 msecs, so Level 2 evaluations are not suprising.

The frame-time, and overall throughput delay effects, limited the dynamic reponse characteristics that could be simulated. For the lateral axis, bandwidths above 4.0 rads/sec. could not be perceived as increased short-term response by the pilot. This severely restricted short-term response evaluations in this program. Furthermore, for higher response types augmented system bandwidths could not be increased beyond 3.5 rads/sec without encountering a stability boundary.

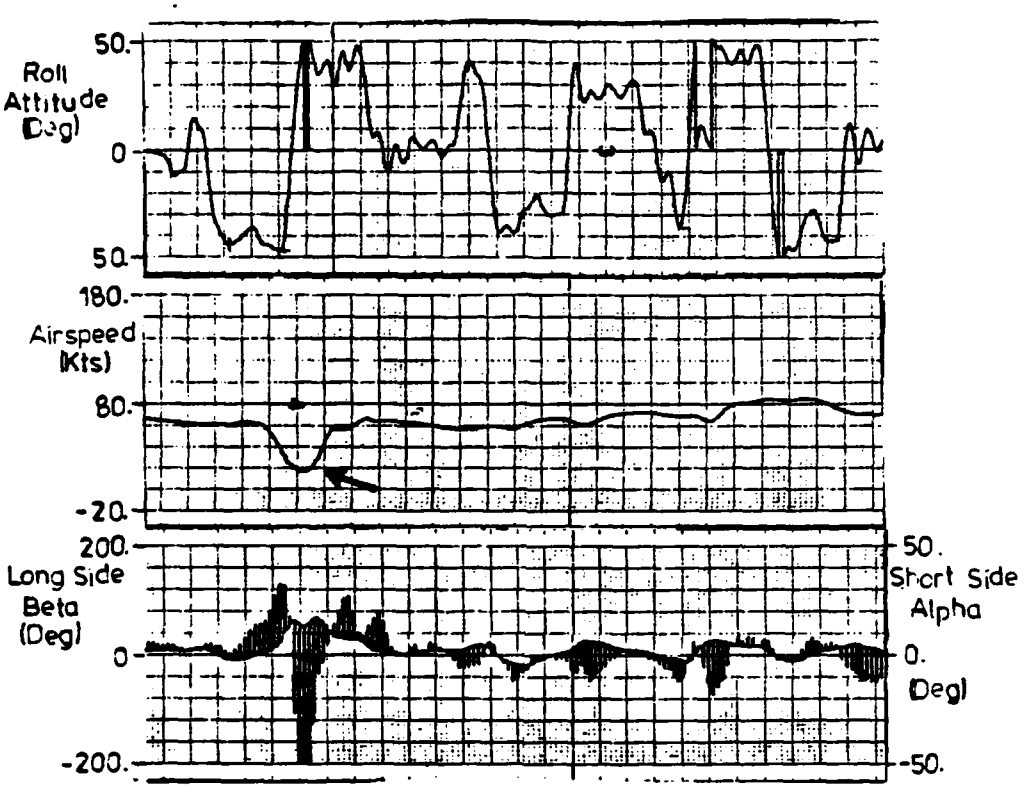

Typical State Variable Excursions in a Left Banked Turn are:

Airspeed Loss: 40 Kts in 4 Seconds
Maximum Sideslip Developed: ± 65 degs
Maximum Angle of Attack Developed: +33 degs

Figure 4-50. Anomalous Sideslip/Airspeed Response Seen in Large Amplitude Maneuvering with Attitude Command Systems

Manipulator and Motion Base Optimization Significant effort had to be expended to achieve desirable characteristics in both these areas. In maneuvering flight limb/manipulator interaction can result in pilot induced oscillations (Reference 52). Low stick damping causing limb/manipulator coupling was seen in the slalom task early in the simulation program causing very uncharacteristic lateral acceleration response.

Motion base filter gain and washout frequency assignment is still very much a cut-and-try rather than an analytical optimization approach with regard to task cues and the pilots sensory system. Motion cues were "optimized" for the up-and-away and near-earth maneuvering phases. Reductions in lateral washout frequencies were made in the near-earth phase to compensate for uncharacteristic lateral acceleration model demands.

Visual System The current generation Computer Generated Imagery (CGI) systems provide good macro texture but poor fine grained detail. This has significant effect on the pilot's control strategy and task performance in such tasks as hover and sidesteps.

In the nap-of-the-earth maneuvers such as slalom and jink the absence of a tip-path-plane resulted in the inability of the pilot to determine rotor clearance. This cue is vital to any future simulation evaluation of these tasks.

The Field-of-View (FOV) from the RCAB module is limited to approximately +-65 degress laterally, and 8 degrees up and 15 degrees down. The pitch axis view severely limits maneuvers involving substantial pitch-up e.g. air-to-air free engagements. The field-of-view can have significant effect on task execution strategy as will be discussed in the next section.

F. Task Performance Comparison between Simulator and Flight

The simulator not only suffers from fidelity issues such as motion and visual miscue, but is devoid of safety of flight considerations. The latter fact can lead to a "video-game" approach to task execution, which undermines the validity of using simulation data for handling qualities criteria development. The visual and motion system characteristics can lead to the adoption of different pilot strategies and task performance between the two environments. Flight data analysis was limited to maneuver amplitude characteristics so no comparison of aggressiveness characteristics is possible between the two environments. A number of specific examples will be discussed.

Figure 4-51 compares task performance for pilot X in the slalom and jink maneuvers. It is noted that the task amplitude characteristics are well matched between the two environments for this pilot. Figure 4-52 compares the performance for the same two manuevers for pilot Y. Two prominent features are observed:

Slalom Task Performance There has been a notable change in the strategy from flight to simulator. The pilot is no longer willing to make 90 degree roll reversals, and negotiates the course with a series of small attitude changes of about 30 degrees amplitude. This may be due to the field-of-view characteristics which limits the ability to maintain spatial awareness in large amplitude maneuvering close to the ground.

Jink Task Performance The pilot described this run as a "Yahoo maneuver with no comparison to the real world visual and motion cues". As noted the roll rates demanded were about twice that used in flight.

Comparison of the sidestep performance between flight and simulator is made in Figure 4-53. It is noted that the linear relationship

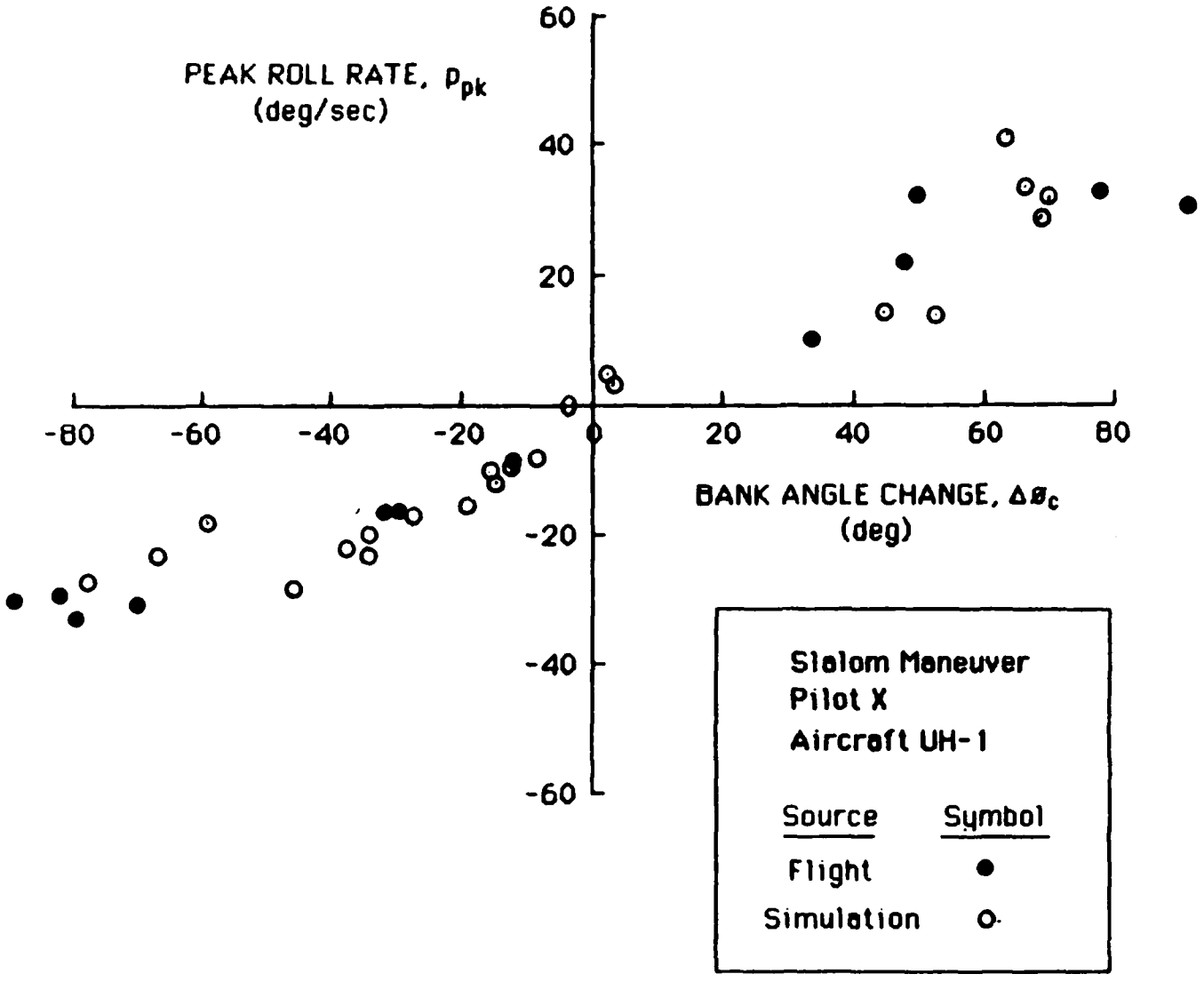

Figure 4-51a. Comparison of Flight and Simulator Performance for Pilot X in the Slalom Maneuver

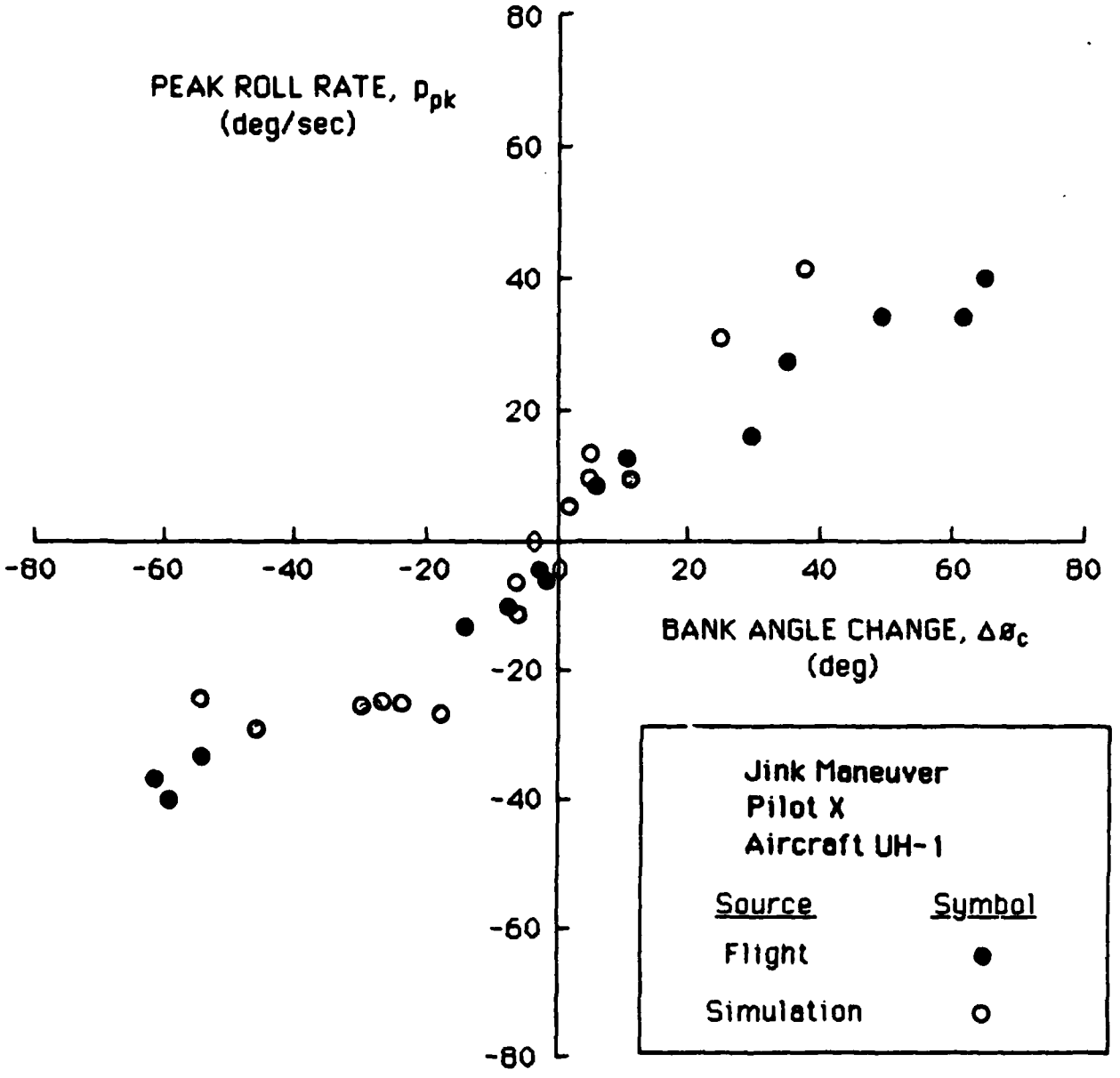

Figure 4-51b. Comparison of Flight and Simulator Performance for Pilot X in the Jink Maneuver

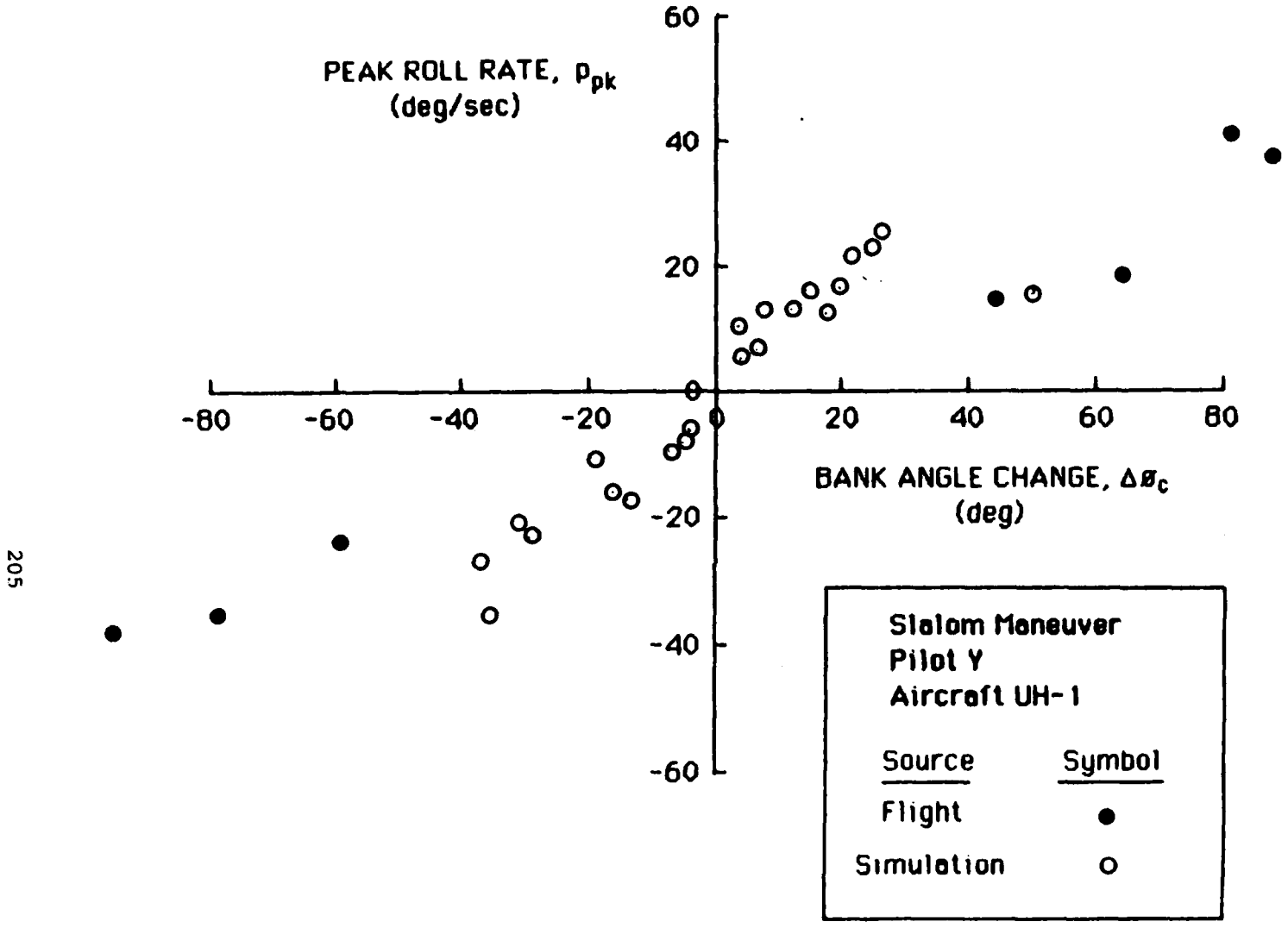

Figure 4-52a. Comparison of Flight and Simulator Performance for Pilot Y in the Slalom Maneuver

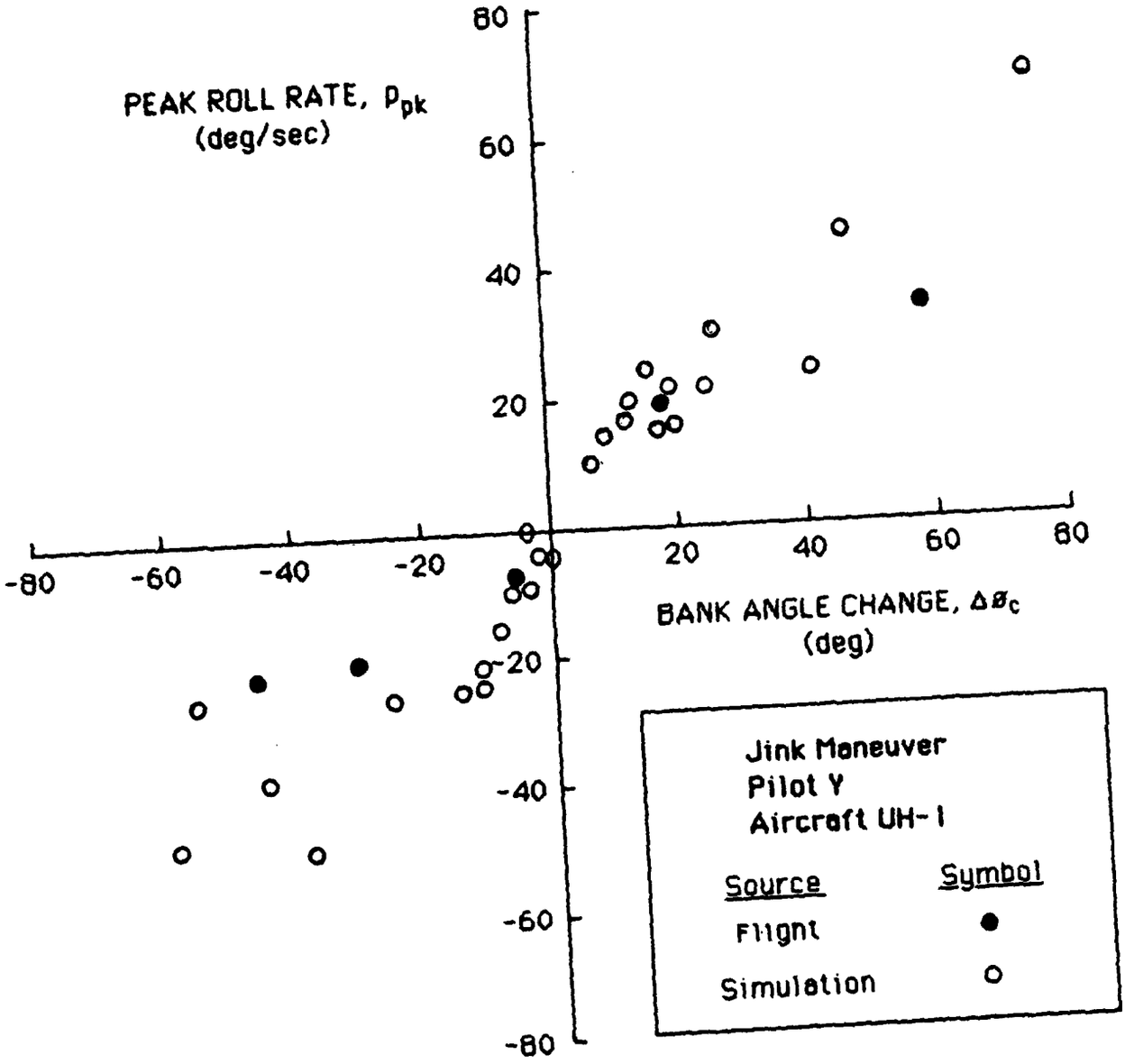

Figure 4-52b. Comparison of Flight and Simulator Performance for Pilot Y in the Jink Maneuver

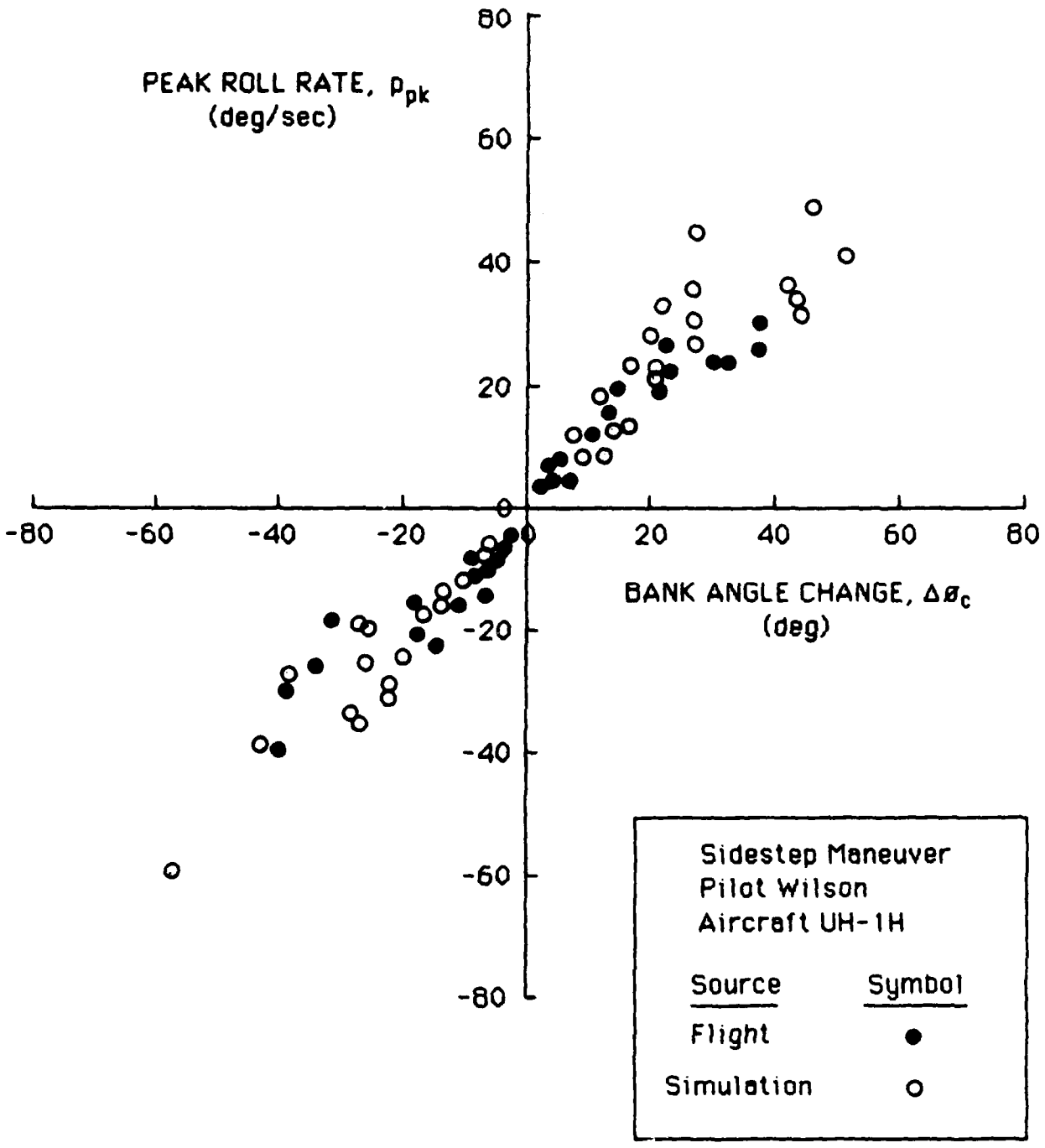

Figure 4-53. Comparison of Sidestep Performance Between Flight and Simulation

between roll rate and bank angle (i.e. constant bandwidth) is relicated in the simulator. However, there again tends to be larger roll rates and attitude changes commanded in the simulator. This may be due to the safety-of-flight fidelity problem.

For the air combat maneuvering tasks direct comparisons on a specific maneuver-by-maneuver basis is not possible. However, the data presented in Figure 4-54 compares ACM tracking data from the simulator with in-flight scissors maneuver data. Good agreement in peak roll rate demand is observed between the two. This supports the claim by the ACM qualified pilots participating in the simulation that their performance generally resembled their flight experience.

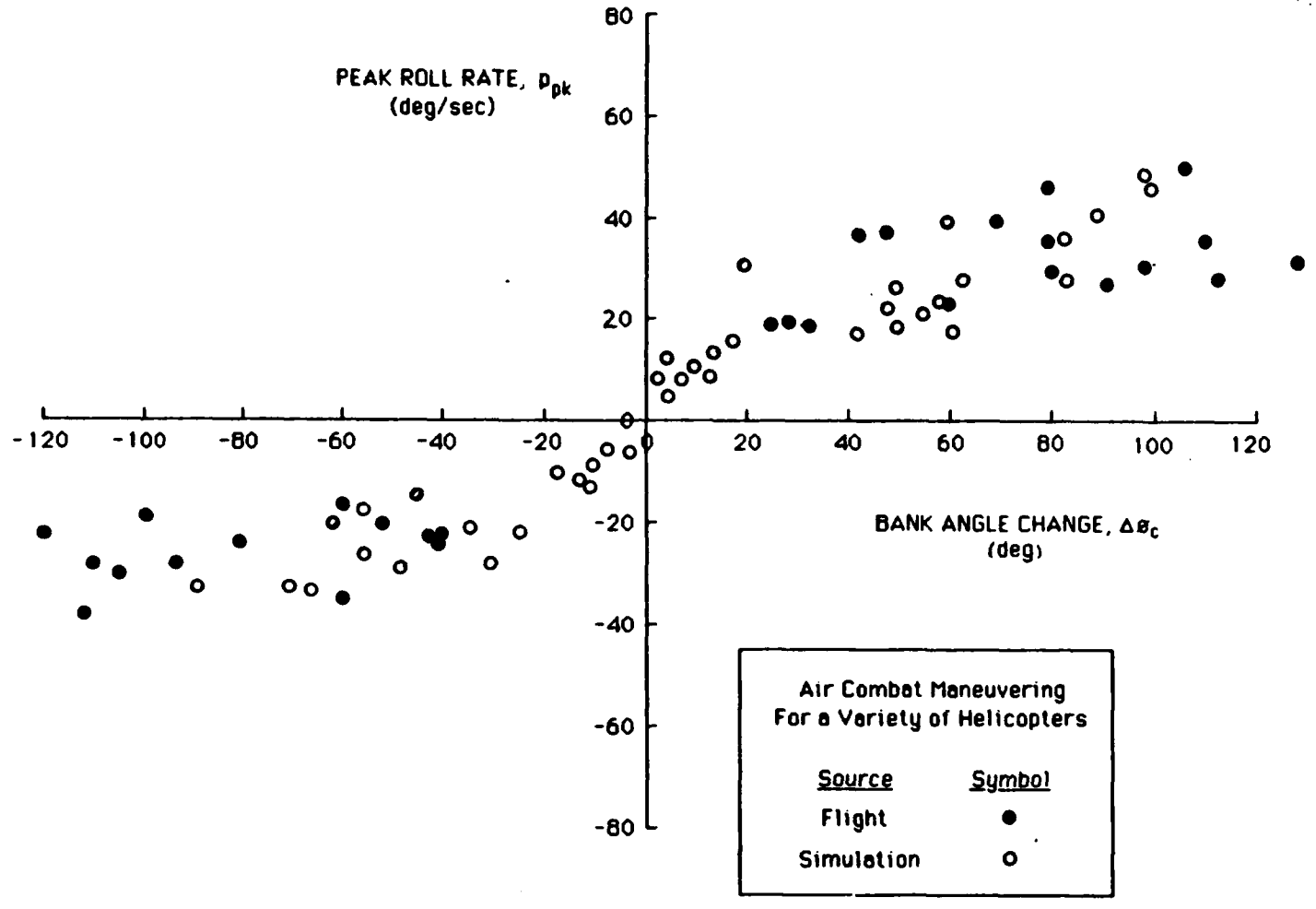

Figure 4-54. Comparison of Air Combat Maneuvering Performance between Flight and Simulator

V. Criteria Development

The objective of this section is to present a new methodology for the examination of roll control effectiveness based upon closed-loop task execution and suited for criteria specification. This approach will be supported by the theoretical development of Section II and the simulation results of Section V. The following concepts provide the foundation for this methodology:

- o Task maneuver demands can be defined quantitatively, and uniquely on a task-by-task basis

- o The relationship between key vehicle design parameters and an upper-bound on closed-loop task execution can be defined analytically.

The objectives sought in methodology development are to unify the concepts of short-term and long-term response, to clearly define the relationship between key vehicle design parameters and response characteristics, and to relate each clearly to task execution and performance.

Finally a comparison will be made between the current open-loop response based criteria and the closed-loop approach. Deficiencies in the current criteria will be identified.

A. Task Performance Modeling

Based upon the discrete maneuver analysis approach presented in section II a unique task signature can be constructed for each task evaluated in the simulation. These signatures are consistent with those of the flight tasks studied and are reasonably independent of the pilot. Furthermore, the form of the signature applies to tasks which are truly

discrete maneuvers as well as those characterized as continuous tracking tasks.

The parameters important to characterizing the closed-loop task performance are:

(1) Aggressiveness
(2) Amplitude
(3) Settling
(4) Precision
(5) Task Duration

The two prominent characteristics of the task signature are the aggressiveness and the amplitude. These were assesseed in Section V for each of the maneuvers evaluated in the simulation. These are proposed to be the two fundamental parameters governing the control effectiveness issue. The task performance catalog determined from the simulation results appears in Table 5-1, where examples of the unique task demand limits are shown for different tasks. The attributes of several of the parameters listed above will now be discussed.

1. Aggressiveness Characteristics

Aggressiveness of response reduces with the maneuver amplitude. Maximum aggressiveness is associated with precision control of attitude. As shown in Section II a metric of closed-loop bandwidth is the ratio of the peak roll rate to the bank angle change. The signature shown in Figure 5-1 is common to all maneuvers analyzed in the simulation program. The prominence of maximum aggressiveness with the precision control of attitude is clearly illustrated. Another prominent characteristic is that maximum variability or scatter in aggressiveness in bandwidth is associated with precision attitude control.

Examples of Task Demands

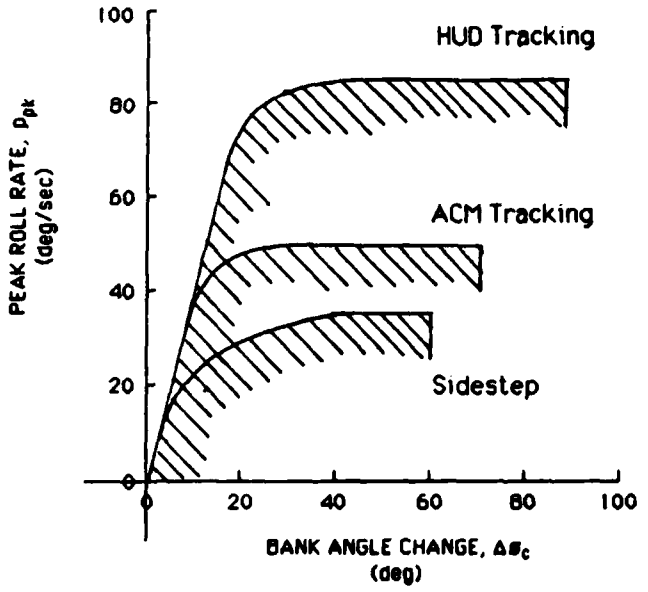

Task	Aggressiveness (natural frequency)	Settling (damping ratio)	Amplitude (max roll rate) p_{max}	Amplitude (max bank change) $\Delta\phi_{c_{max}}$
HUD Tracking	4.0 rad/sec	0.5	85 deg/sec	90 deg
ACM Tracking	2.5	0.5	40-50	110
ACM Free engagement	-	-	40	70
Sidestep	4.5	0.5	35	60
Jinking Maneuver	4.5	0.4	40	50
Slalom	2.0	0.6	30	50
Visual turn	1.5	0.45	40	40
IFR turn	-	-	10	25

Aggressiveness and settling identified for attitude changes < 10°.

Table 5-1. Catalog of Task Performance

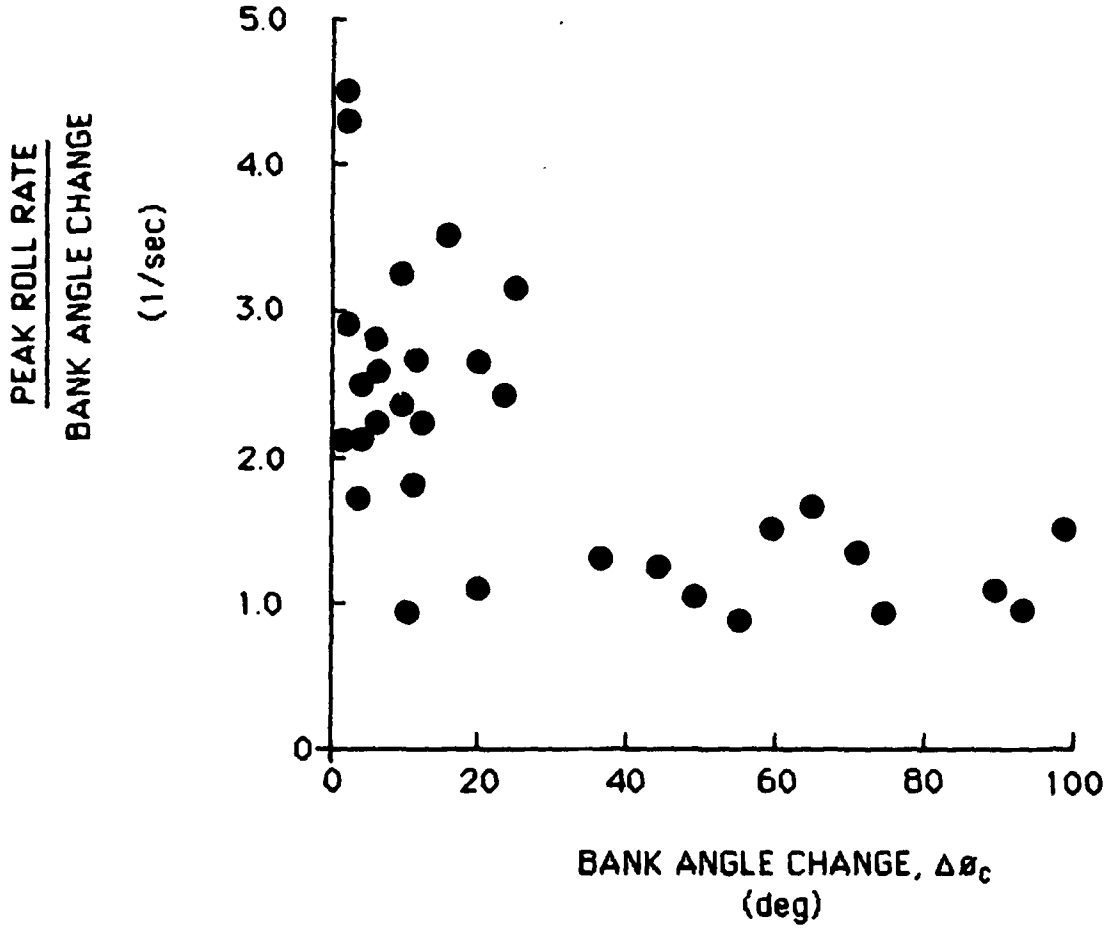

Figure 5-1. Aggressiveness versus Attitude Change for the HUD Tracking Task

The same maximum level of aggressiveness in precision attitude control has been observed for a diverse spectrum of tasks such as the HUD tracking, ACM tracking, sidestep and jinking maneuvers. These tasks represent both hover and forward flight regimes in NOE and ACM scenarios. Therefore it could be suggested that the precision attitude control requirements may be independent of the specific outer-loop involved. This hypothesis will not be supported by data from the current program. It can be expected that the disturbance environment will be the key determinant to the precision attitude control requirements.

A variety of presentation forms exist for aggressiveness. The effective bandwidth based upon the identified natural frequency and damping ratio for an equivalent second order system, or the roll rate rise-time during a discrete bank angle change could be used. However, in the analysis of test data the ratio of the peak roll rate to net bank angle change has been found to be the most convenient form. One compelling advantage of this presentation is its close connection with control characteristics of the human operator. The pilot's primary control objective is to make discrete changes in attitude to achieve desired outer-loop task performance. He controls and stabilizes attitude through roll-rate feedback from visual cues and his kinesthetic sensory system , i.e., the semi-circular canals.

2. Amplitude Characteristics

All tasks evaluated under the simulation program exhibit saturation of roll-rate demand for large amplitude maneuvers. This is clearly evidenced in the air combat tracking data of Figure 5-2.

3. Maneuver Settling

This parameter is not as easily quantifiable as aggressiveness or

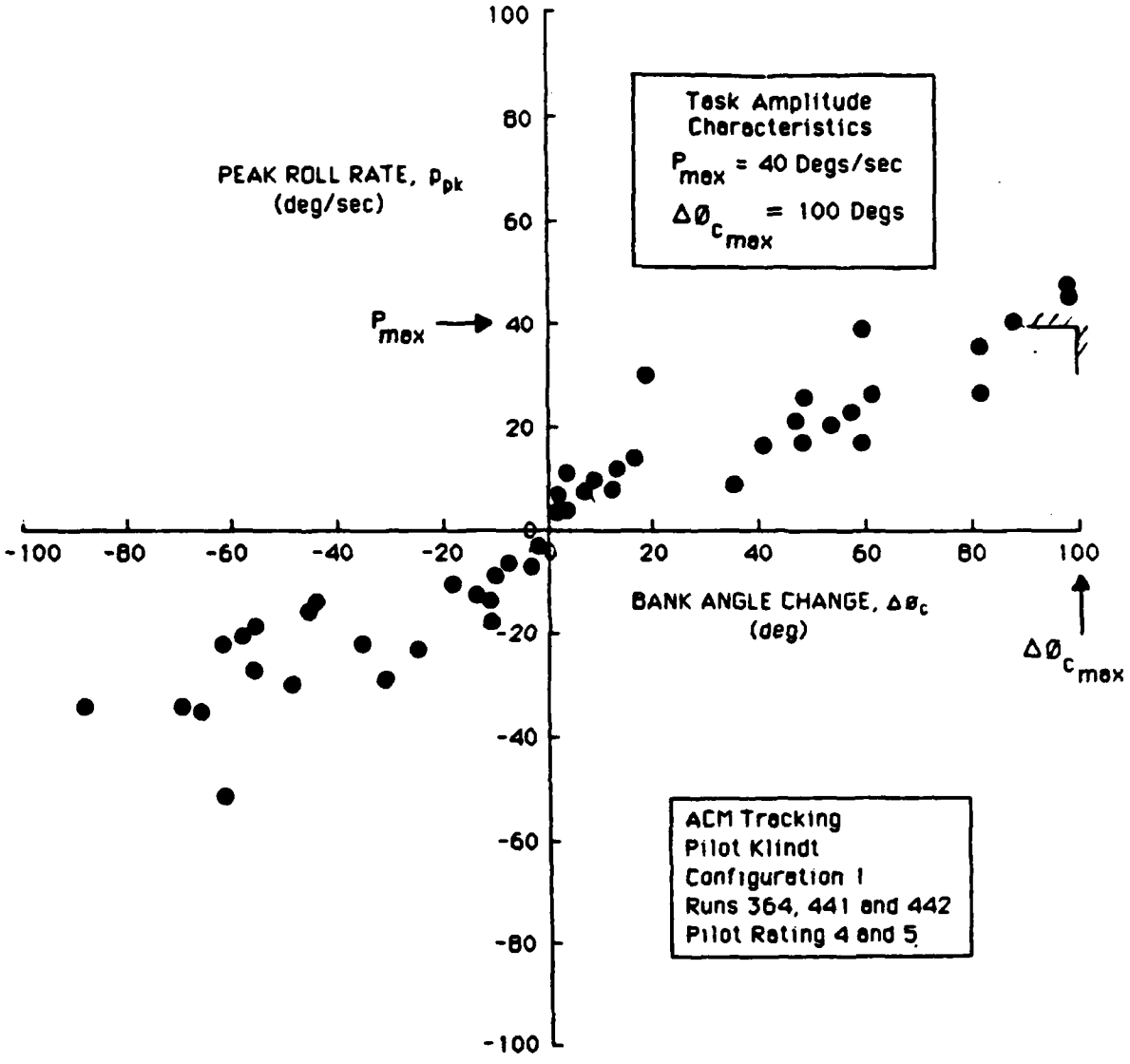

Figure 5-2. Characteristic Roll Rate Limiting for Large Amplitude Maneuvering

amplitude. This parameter is important because of its significance to response overshoot to a discrete bank angle command, and its implications for pilot compensation which is necessary to counter vehicle lag and delay. This parameter is therefore associated with pilot workload.

4. Precision

This is a secondary performance metric in large-amplitude maneuvers. This metric is paramount in such tasks as disturbance rejection or target tracking with compensatory pilot control. However, it is only important in large-amplitude maneuvering in the target tracking or weapon delivery phase for example.

B. Vehicle Capability

In section II a clear analytical relationship was developed between key vehicle design parameters and an upper-bound on closed-loop task performance. The fundamental vehicle-centered components which dictate task performance are:

(1) Short-term response
(2) Control power
(3) Control sensitivity
(4) Stability and control cross coupling

The maximum bandwidth capability for task execution was associated with a pursuit feedforward strategy on the part of the pilot. In section II a square-wave input model of this strategy was used to define the upper-bound on vehicle capability. This limit corresponds to the theoretical maximum capability without augmentation of the roll response with sideslip dynamics. This approach clearly defined the relationship between key vehicle response characteristics and closed-loop task

execution. Large amplitude control is effectively dominated by control power (i.e. maximum roll rate) characteristics, while small amplitude (precision) control is dominated by the the vehicle short-term dynamics. In the case of the lateral response characteristics of the helicopter short-term response characteristics are dictated by the flapping stiffness, while control power is defined by maximum swashplate authority.

C. Pilot-Centered Components

Pilot-centered components are more difficult to quantify than task or vehicle components. In general this requires a precise knowledge of task command, the vehicle response, and the vehicle controller movement.

The main value in quantifying the pilot-centered components is to obtain a description of the pilot control strategy used including the specific amounts of compensation and use of cueing information. For example, it has been established that the generation of significant lead compensation can be costly in terms of pilot workload and rating.

Some parameter identification was performed in the analysis of the simulator data with the objective of quantifying amounts of pilot compensation used. This effort was generally unsuccessful because of ambiguities in the command time histories (these needed to be identified also).

One approach to quantification of workload-related aspects of pilot centered performance is described in Reference 53 and involves measurement of controller deflection and rate. The approach is based on a theory of pilot rating originally presented in Reference 54 and has been used to generate pilot rating predictions relative to system bandwidth, control, sensitivity, response type, and tracking precision. This technique was considered briefly in this study but could not be

pursued because of lack of resources. Additional work should be done in this area.

D. Control Effectiveness Criteria Development

1. Definition of Task Margin

Task margin is defined as the excess vehicle capability over task demand. It is hypothesized to be a parameter appropriate for handling qualities criteria specification.

The specific means of viewing the vehicle capability versus demand in task performance is governed by the primary parameter of interest; whether it is control power or short-term response. Short-term response characteristics dominate in small-amplitude or precision attitude control tasks, while the control power effects are associated with large amplitude maneuvering. In order to address both of the above characteristics adequately the task margin forms shown in Figure 5-3 are suggested. The presentation has the attributes of defining the relationship of short-term and control power characteristics to the closed-loop performance, and it is consistent in its form of presentation of both characteristics. These characteristics are in contrast to the current control power (t_{30}, $\phi(1)$) and short term response criteria (L_p specification). These are based on open-loop response characteristics, are heterogenous in form, and do not permit quantification of their impact on closed-loop performance.

Using the discrete maneuver analysis approach has allowed definition of task performance on a task-by-task basis. Good handling qualities are associated with cases where acceptable closed-loop performance can be achieved without excessive compensation. Vehicle characteristics supporting such a condition can therefore be defined. Theoretically, the vehicle design or criteria specification

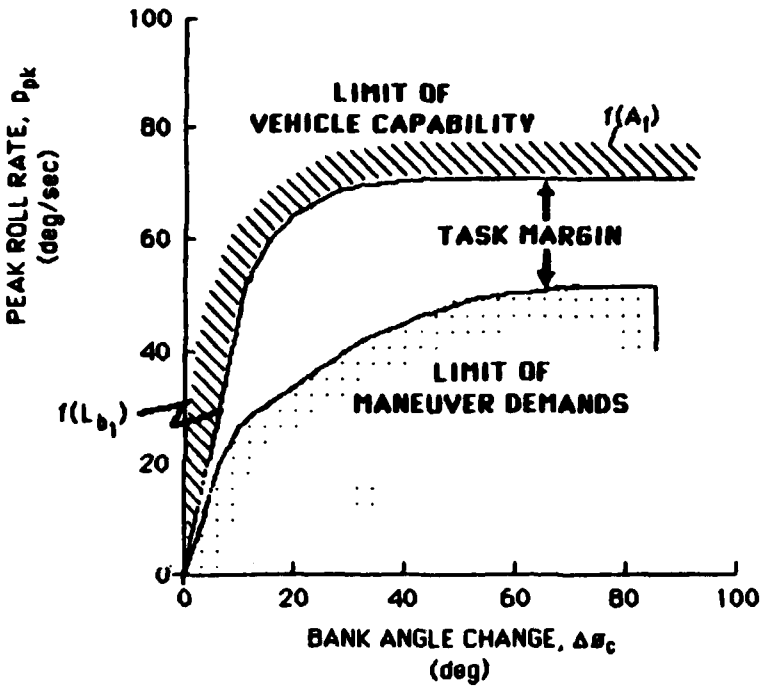

a. Control Power Analysis

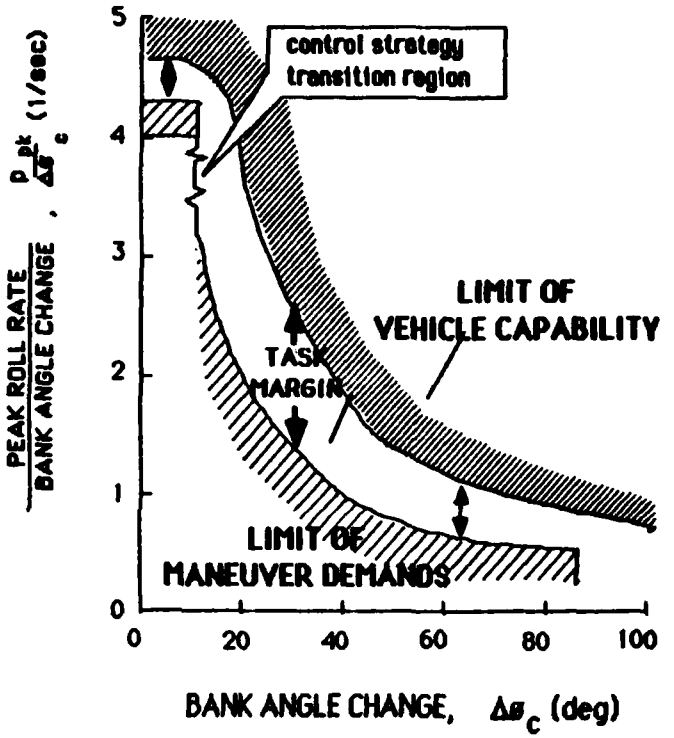

b. Short-Term Response Analysis.

Figure 5-3. Definition of Task Margin for Handling Qualities Analyses

can be presented in terms of task margin for either the short-term or control power issue. This approach will be exercised on the data obtained from the simulation.

2. Roll Axis Control Power

Task performance under degraded control power (maximum roll rate) conditions was evaluated for a diverse set of different tasks in the simulation program. These tasks include HUD tracking, ACM tracking and the sidestep task and span the nap-of-the-earth and air combat maneuvering environments. The complete set of back-up data from the simulation is shown in Figure 5-4, and summarized in Figure 5-5. As can be seen the deterioration of pilot rating due to the task dependent deficiency of control power followed a consistent trend in each case. For a control power capability of 15 degs/sec under the maximum task demand, the pilot rating was subject to an abrupt worsening. Additional saturation then produced a more gradual degradation. These data are plotted in Figure 5-6 in terms of the the control power task margin factor:

$$\eta = \frac{P_{max_{veh}}}{P_{max_{man}} - 15.0 \text{ degs/sec}} = \frac{\text{Maximum Vehicle Roll Rate Capability}}{\text{Task Demand Roll Rate - 15 degs/sec}}$$

Thus a control power criterion based upon the parameter η is maneuver independent. Note also that there is no graceful degradation from Level 1 to Level 2. Rather, the jump is essentially from Level 1 to Level 3.

C. Roll Axis Short-Term Response

Three vehicle configurations corresponding to a teetering rotor with a Bell-bar, an articulated rotor and a rigid rotor were evaluated in a number of different tasks. Figure 5-7 presents the pilot rating

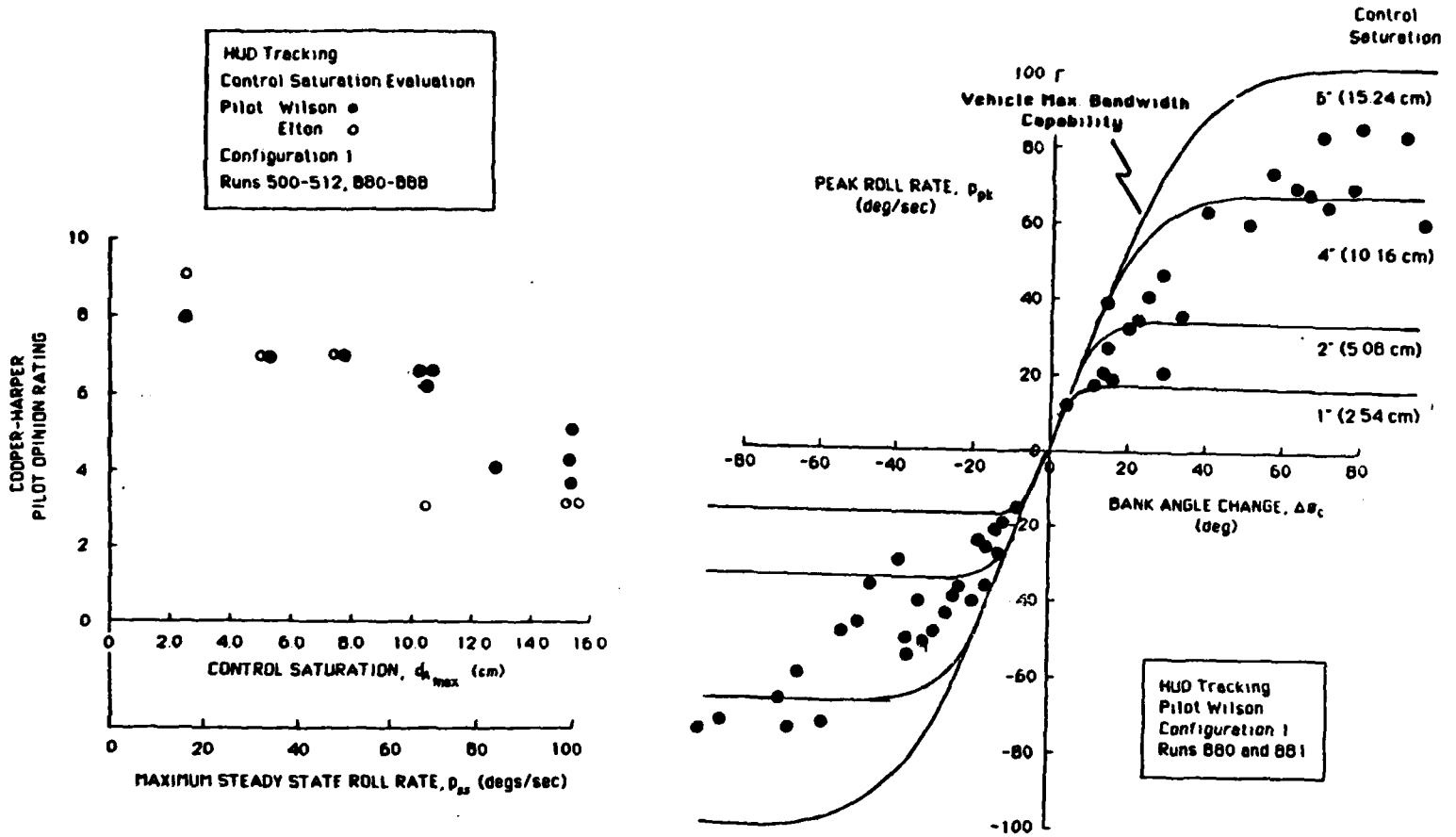

Figure 5-4a. Control Power Data for the HUD Tracking Task

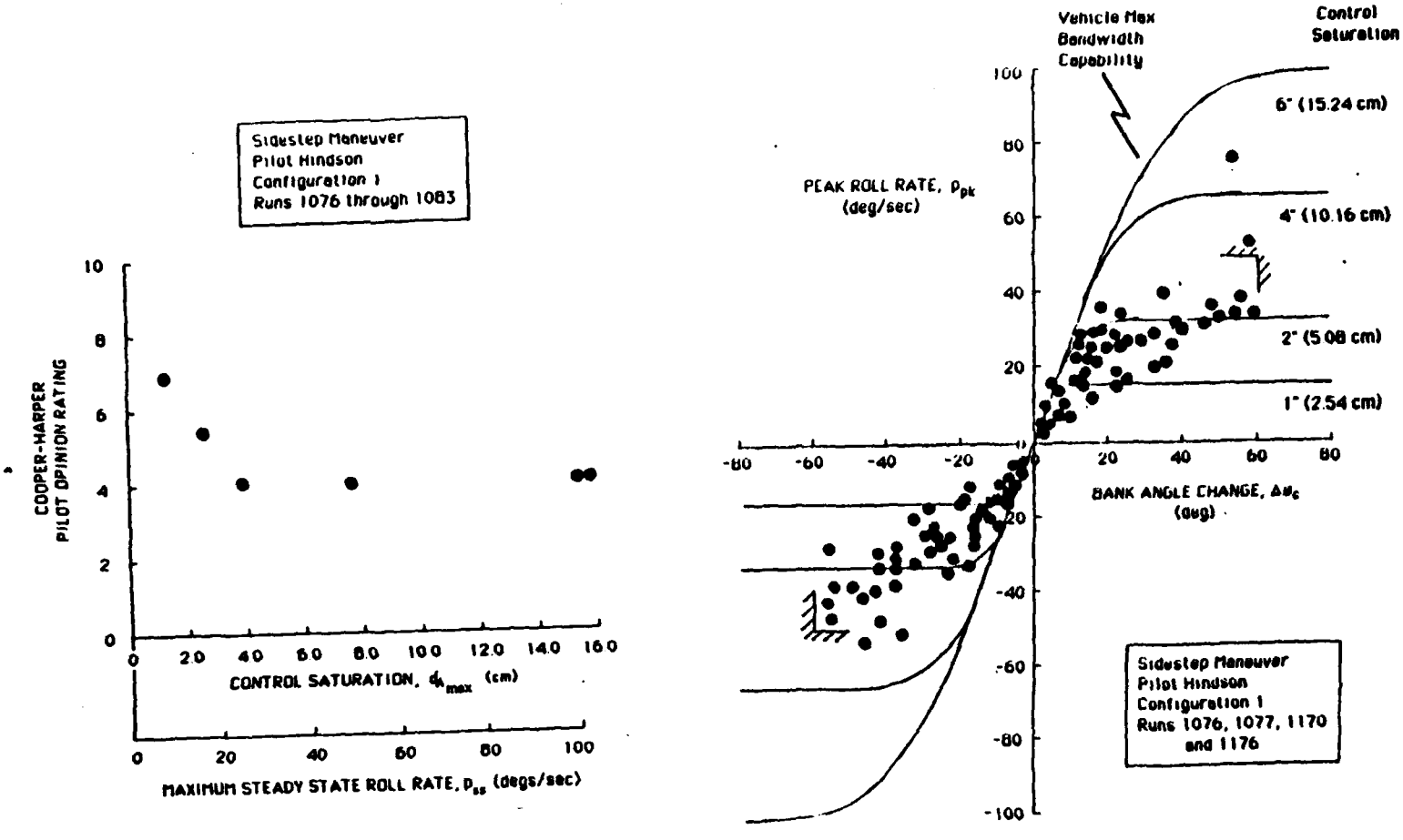

Figure 5-4b. Control Power Data for the Sidestep Maneuver

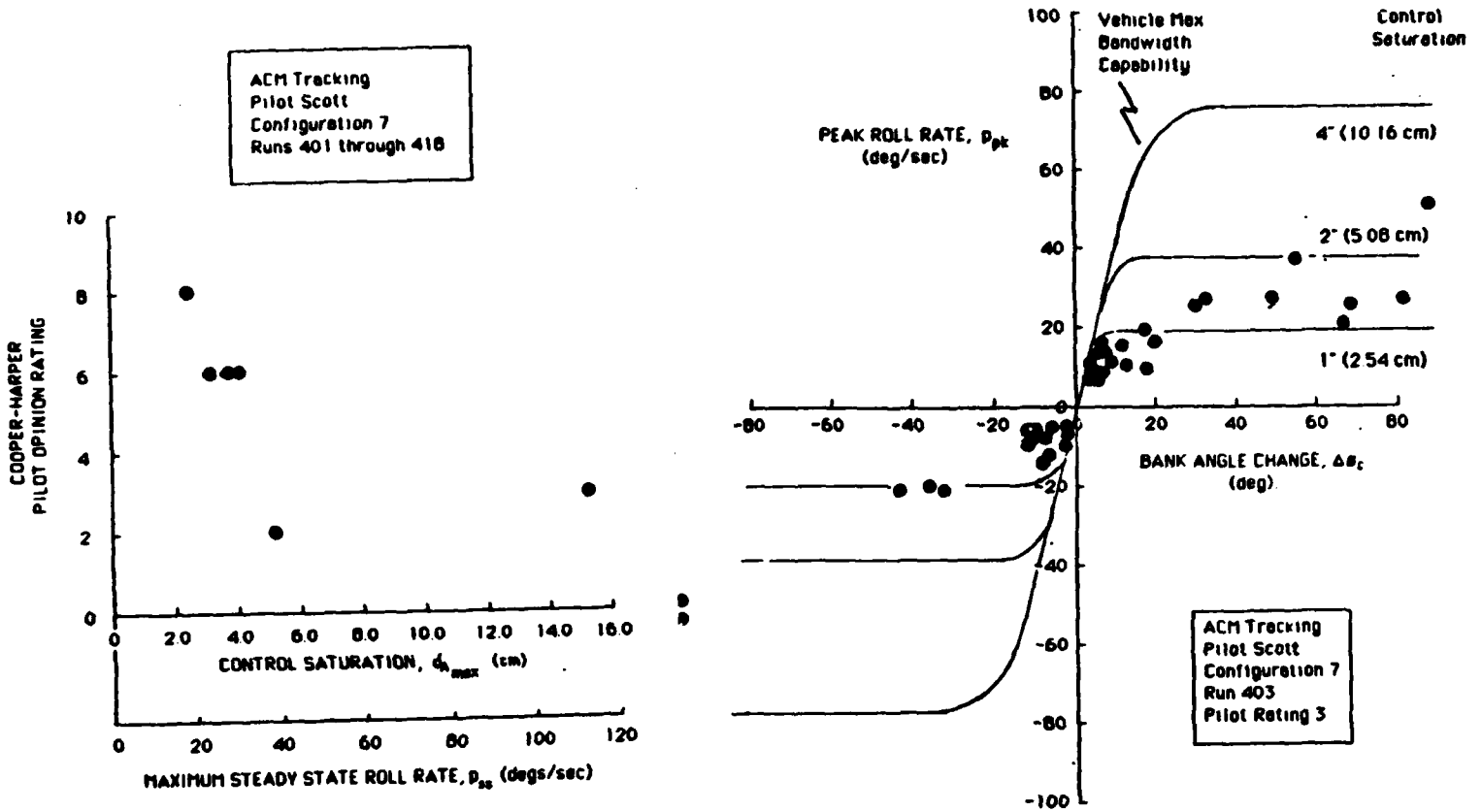

Figure 5-4c. Control Power Data for ACM Tracking for Pilot Scott

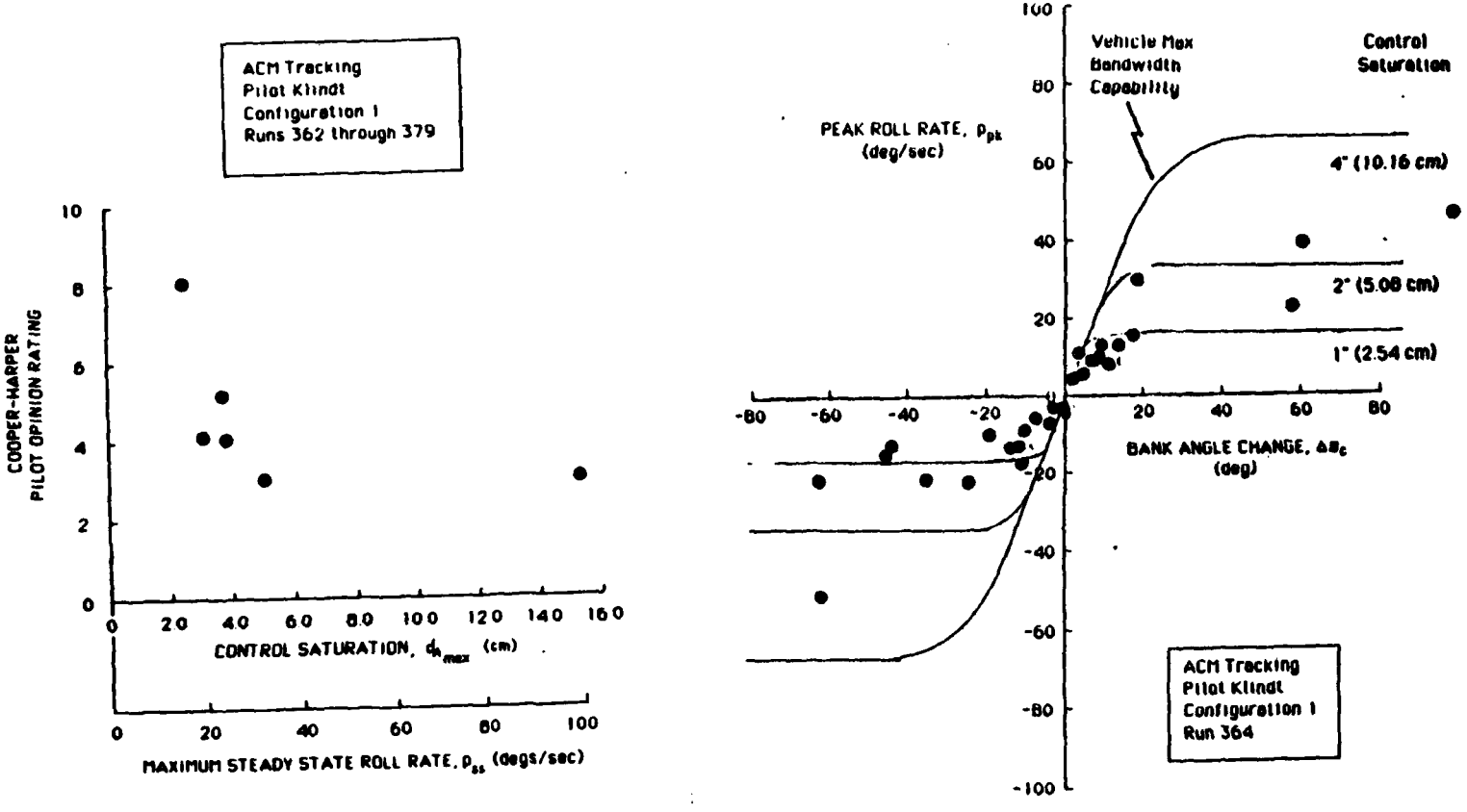

Figure 5-4d. Control Power Data for ACM Tracking for Pilot Klindt

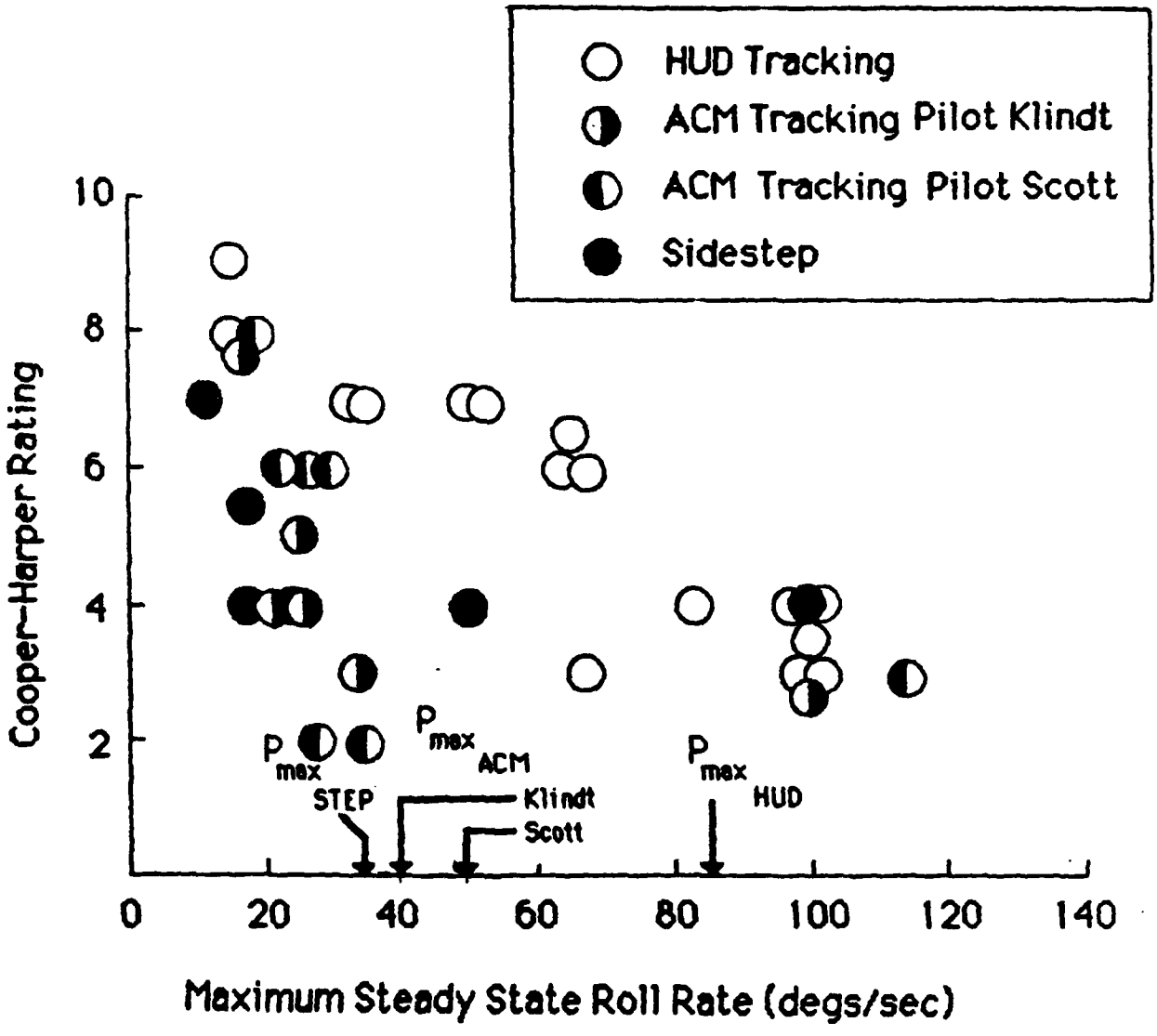

Figure 5-5. Summary of Pilot Opinion Variation with Control Power Saturation for Tasks Evaluated in the Simulation Program

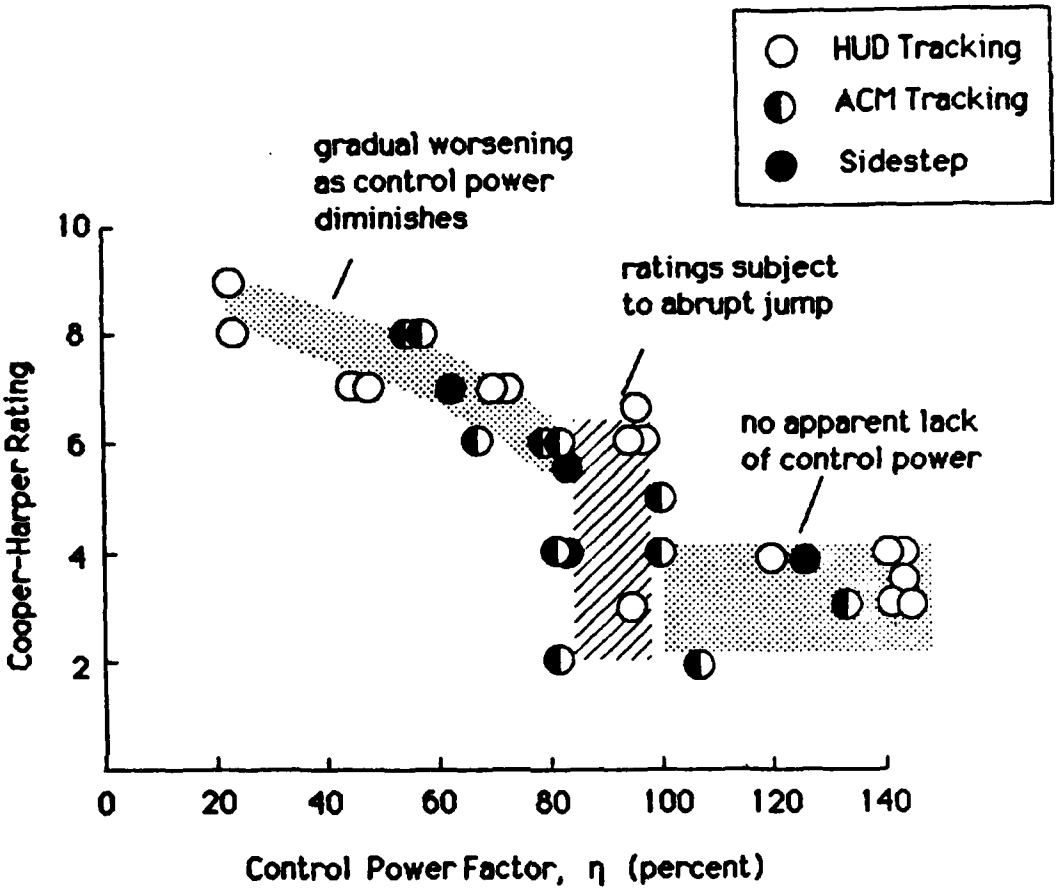

$$\eta \triangleq \frac{p_{max_{veh}}}{p_{max_{man}} \text{ -15°/sec}}$$

$p_{max_{veh}}$ = Maximum Vehicle Roll Rate Capability, degs/sec

$p_{max_{man}}$ = Maximum Roll Rate Demand for Maneuver, degs/sec

Figure 5-6. Pilot Opinion Data plotted Versus Control Power Factor

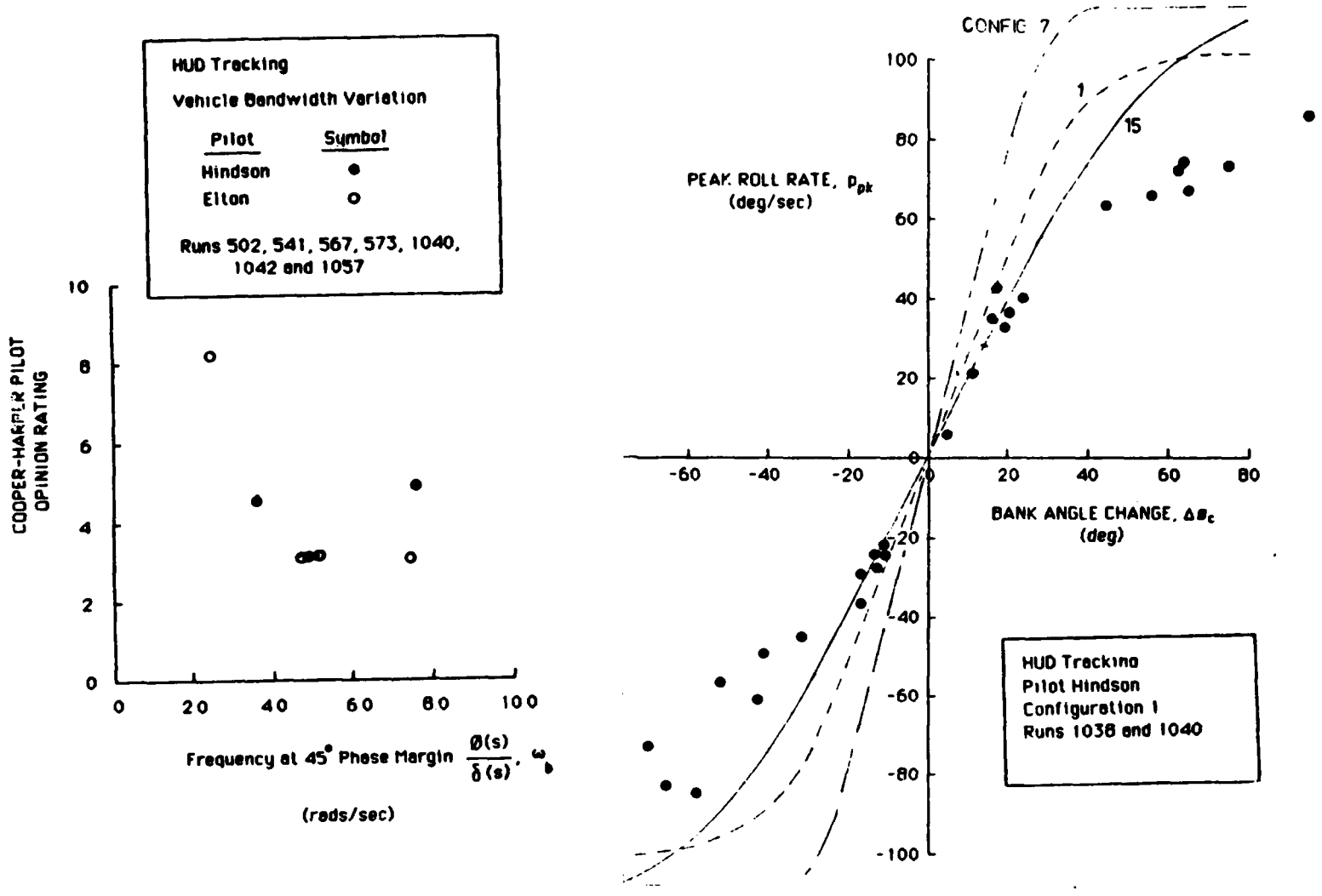

Figure 5-7. Pilot Opinion Variation with Vehicle Bandwidth for the HUD Tracking Task

data with bandwidth variation in the HUD tracking task. Maneuver performance data for these three configurations is shown in Figure 5-8. The data points shown represent maximum bandwidth data collected for the three vehicles. It is observed that the pilot exploits the increased bandwidth capability of the system in effecting the task. Furthermore, there appears to be two regions of distinctly different task execution. For small amplitude (precision attitude control) the pilot may be using a pursuit strategy, using close to the maximum bandwidth capability of the system. This region corresponds to a pulsive type control strategy. For larger attitude changes there is significant reduction in the closed-loop bandwidth sought.

Due to the task design and relatively long throughput time delay (about 200 msec) adequate pilot opinion ratings and commentary are not available to provide a criteria specification for short-term response as presented for control power. The above data however suggest that the task margin approach is appropriate to the specification of short-term response characteristics as well as control power. The definition of specific numbers for the criteria will be pursued in the future.

3. Roll Rate Sensitivity

The control sensitivity was not a variable in the simulator study. Based upon the trends indicated in other studies (e.g. References 55 and 56) and the consistency of peak roll rates observed in the analysis of flight data, there was believed to be a sound basis for maintaining a constant roll rate sensitivity. The nominal value was set in the range 17-20 degs/sec/stick inch.

Due to the nature of the experiments run, control sensitivity could not be varied over a wide range without restricting the large amplitude maneuvers or requiring excessively large manipulator movement for small-amplitude corrections. This observation itself describes natural

a. HUD Tracking Task Performance and Vehicle Characteristics from Simulator.

b. Implied Form of Short-Term Response Task and Vehicle Factors.

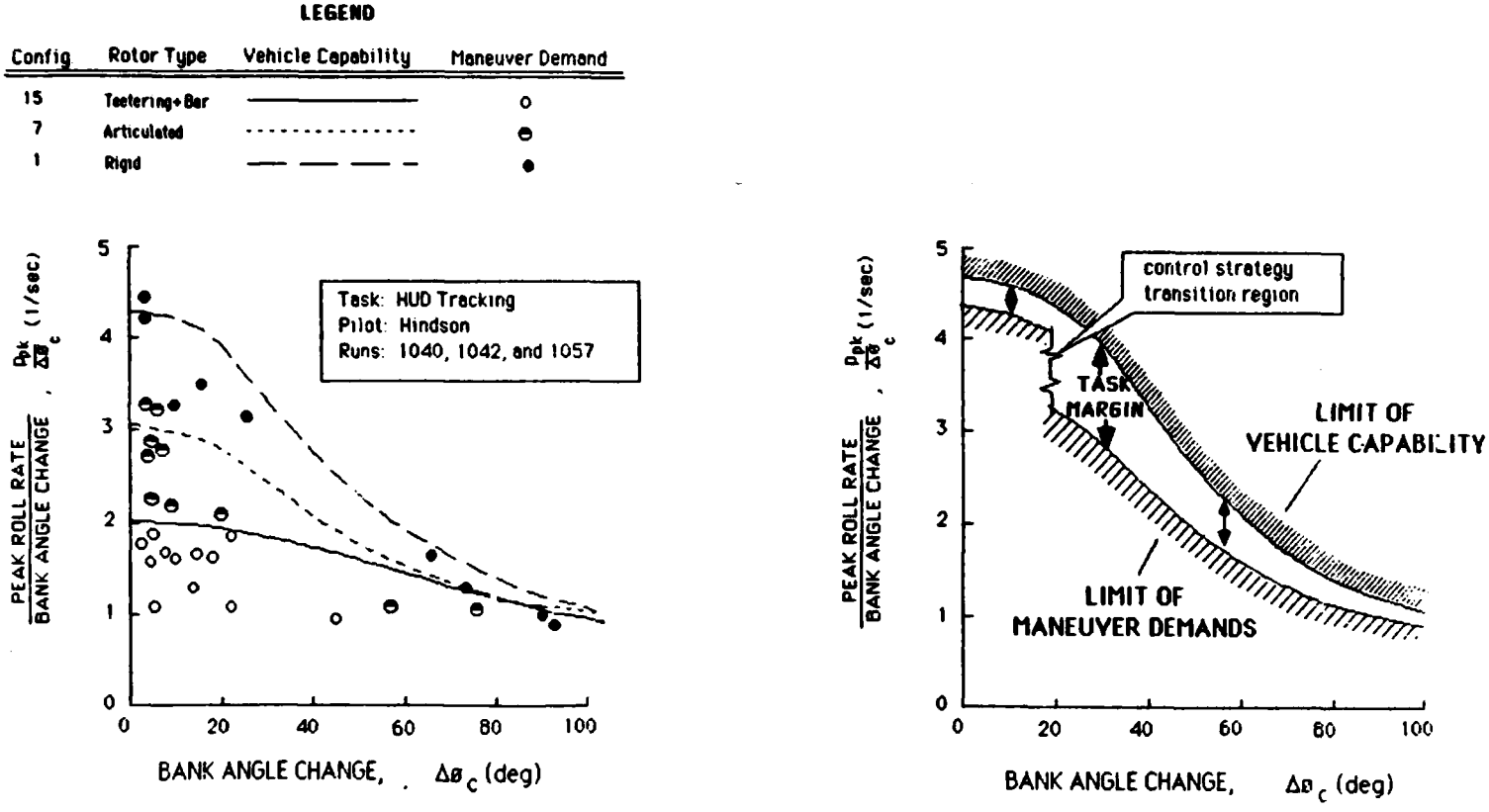

Figure 5-8. Comparison of HUD Tracking Task Performance with Variation of Vehicle Short-Term Response

design limits which make the variation in sensitivity beyond fine tuning a somewhat academic exercise.

4. Higher Augmentation System Types

Due to simulator fidelity problems no useful data in terms of control power or short-term response variations was obtained for the higher augmentation system types. The task margin can however be applied to the rate command system in exactly the same manner as the basic helicopter analysis was dealt with. The attitude command system needs further analysis to predict an upper-bound on vehicle performance due to the pilot's capability to enhance performance by overdriving the system. This approach to vehicle capability definition may also have an application in determining the control power/short-term response necessary for augmentation.

E. Comparison with Proposed Control Power Criteria for MIL-H-8501A Update

With regard to the the forward flight control power for Level 1 handling qualities under aggressive maneuvering conditions, section 3.6.8.1 of the proposed MIL-H-8501A update (Reference 3) states that:

> "The response to full lateral controller input shall result in 30 degrees of bank angle change within 1.1 seconds for aggressive maneuvering under Level 1"

It is instructive to compare response capability, $L_p = -10$ and $L_p = -0.75$ based upon the above criteria. The response is shown in phase-plane form in Figure 5-9 for the two vehicles and further compares this with the response demonstrated in a number of maneuvering tasks. The following observations can be made:

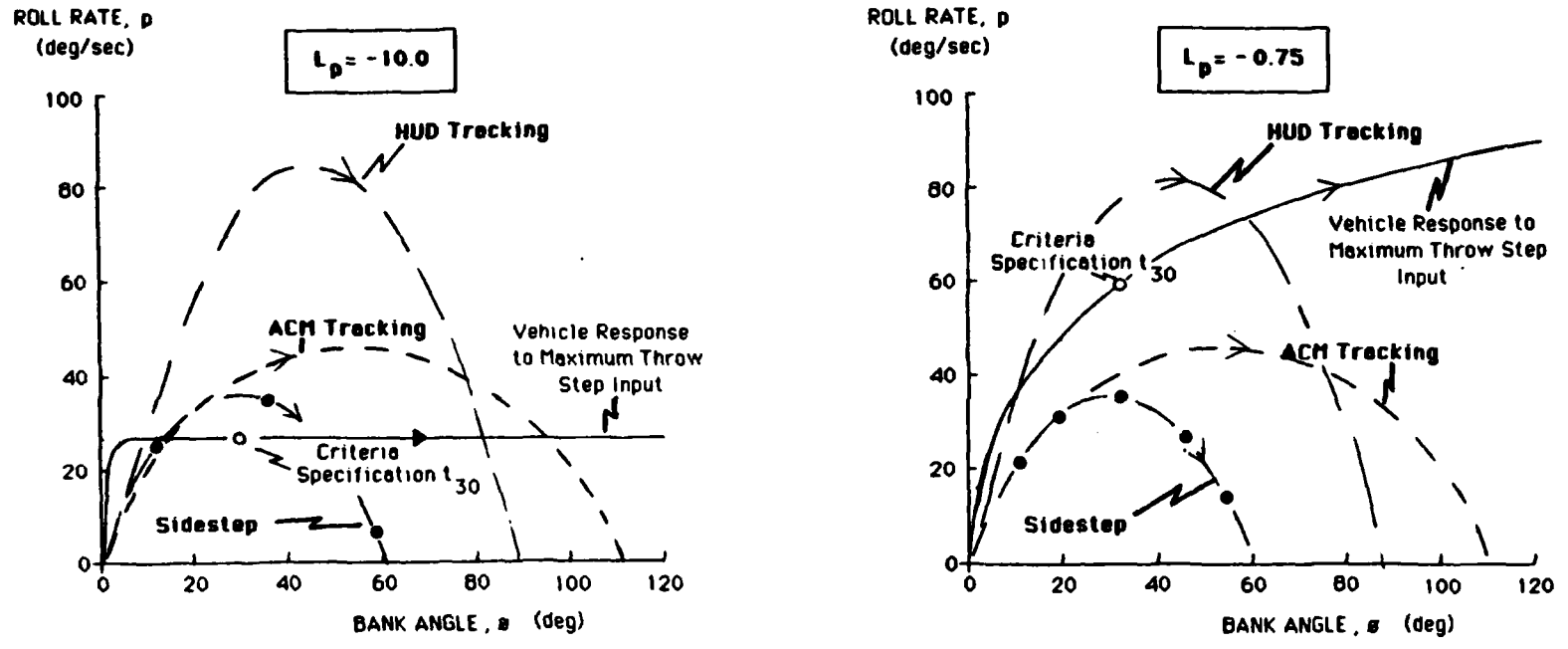

(a) L_p = -10.0

(b) L_p = -0.75

Figure 5-9. Comparison of Task Requirements and Helicopter Capability for Vehicles Satisfying the Current t_{30} Maneuvering Criteria

$\underline{L_p = -10}$ For large values of L_p , the t_{30} criterion serves to define the steady-state roll rate capability (p_{ss}=30.0/t degs/sec). The actual roll rate capability prescribed by this criterion is 27 degs/sec. From Figure 5-9 the bandwidth of the vehicle is high enough to encompass all maneuvers however the roll rate capability is clearly deficient with regard to the HUD and ACM tracking tasks. Based upon the analysis of the control power requirements (Section V-D), the vehicle would be Level 3 in these two maneuvers based upon the results of this current simulation.

$\underline{L_p = -0.75}$ The steady-state roll rate capability of this vehicle is 114 degs/sec, almost 4 times that of the vehicle above. The t_{30} criterion no longer defines steady-state roll rate capability but rather the short-term response. The required four fold increase in control power is required to make up for the short-term response deficiencies of this vehicle. Only the HUD tracking task cannot be accomodated with this vehicle. However the low value of L_p would result in probable Level 3 handling qualities due the pilot lead compensation requirements.

The physical significance of the parameter t_{30} is thus dependent upon the particular dynamics involved. The closed-loop task performance capability therefore varies significantly within the class of vehicles satisfying t_{30}. A maneuvering criteria should have the property that all vehicles satisfying it are uniformly capable of performing the same maneuver. Time to 30 degrees, as demonstrated above, does not satisfy this requirement.

A steady-state roll rate requirement is implicit in the t_{30} specification. It is believed that the data base used to define the current requirement was based upon tasks demanding only 30 degs/sec maximum roll rates. In addition, t_{30} allows for a trade-off of excess control power to make up for short-term response deficiencies. However, the short-term response area is already addressed by a specification of

roll-rate rise time (Reference 3). Thus the t_{30} specification encompasses vehicles with excessive bandwidth capability but adequate control power, and those with excessive control power but deficient bandwidth. This problem has arisen because the two fundamental, independent parameters defining closed-loop task performance, i.e., aggressiveness and maximum roll rate, have not been addressed on an independent basis.

The appropriate criteria specification parameters are:

- Maximum steady-state roll rate
- An open-loop bandwidth criteria based upon roll-rate rise time for example

Based upon the simulation results the roll control power requirement calls for at least 50 degs/sec steady-state roll rate capability. This is based upon the ACM tracking task results, neglecting the higher requirements of the single-loop HUD tracking task. The present study has not however provided an adequate basis for short-term response requirements, and this will be the focus of additional work.

F. Areas of Further Analysis

1. Theoretical

Significant advances are possible in the area of generic task performance modeling and prediction of aggressiveness requirements. The work due to Hess provides the capability for performance prediction based upon manual control theory math models. A short analysis from the Reference 57 "triple bend" maneuvers and the Reference 27 "slalom maneuvers" is given to illustrate the potential of this methodology.

Triple Bend Maneuvers This analysis is based upon the pursuit-preview tracking hypothesis using the flow-field information as discussed in Reference 58. Figure 5-10 shows the pilot loop closure for a general lateral tracking task and a diagram of the triple bend geometry from Reference 57. Note that the temporal frequencies of the bends are a simple function of the the flight speed and the curvature of the bend. Based upon the measured values from a similar lateral task reported in Reference 59, values for the outer-loop gain and lead time constant are computed for each triple bend condition. (This assumes a crossover frequency equal to twice the temporal frequency to ensure adequate outer-loop performance). The sets of pilot model values for each case are summarized in Table 5-2.

Reference 60 shows that for pursuit-preview tracking, the pilot may use $p(t)$ in the inner loop and $P(t+\tau)$ for preview. Based upon this the following equation can be used to express $p(t+\tau)$ where τ is the preview time:

$$p(t+\tau) = U K_y [(1 - T_L/\tau) \beta(S_1) + (T_L/\tau) \beta(S_2)]$$

The value of τ will be set to the effective inner-loop pilot delay and is assumed to be about 0.3 secs.

The visual field involves geometry describing the commanded groundtrack and visual streamer information. Using the above triple bend geometries, the angles $\beta(S_1)$ and $\beta(S_2)$ can be computed. The values shown correspond to points in the flight path where the roll reversals and maximum roll rates occur, i.e. going from one semi-circular arc to the other.

The resulting peak roll rate estimates are tabulated in Table 5-2. Finally, in Figure 5-11 these estimates are compared to the simulator

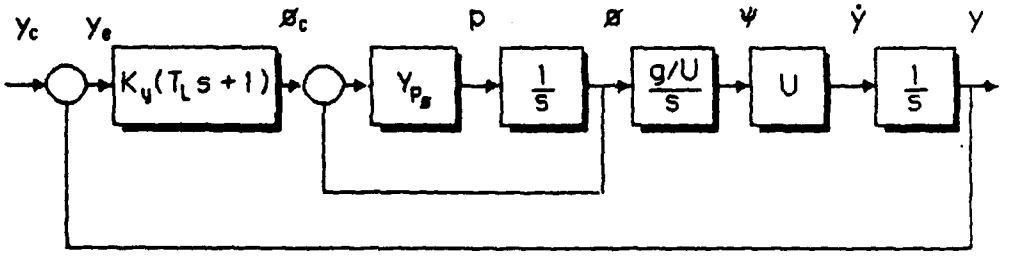

(a) Pilot Loop Closure

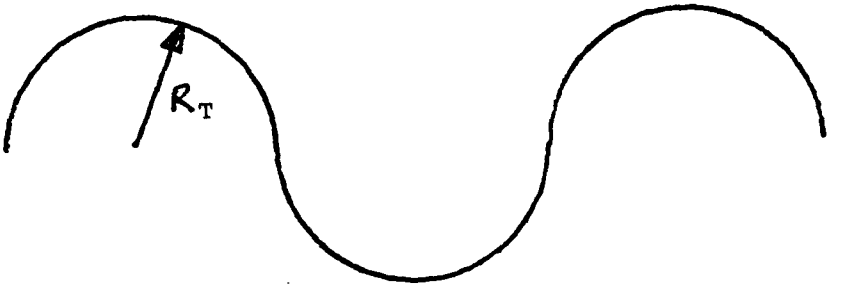

R_T = 200 feet, "Small" Triple Bend

= 500 feet, "Large" Triple Bend

(b) Triple-Bend Geometry from Reference 57

Figure 5-10. Pilot Model for the Triple Bend Maneuver

Table 5-2. Triple Bend Maneuver Model Parameters

R_T (ft)	U (kt)	ω_o (rad/s)	ω_{c_y} (rad/s)	T_L (sec)	K_y (rad/ft)	$\beta(s_1)$ (rad)	$\beta(s_2)$ (rad)	p_{pk} (deg/s)	$\Delta\phi_c$ (deg)
200	60	0.51	1.02	10	0.0025	0.30	0.59	144	115
500	40	0.13	0.26	10	0.00095	0.081	0.161	10	32
500	60	0.20	0.40	10	0.0010	0.12	0.24	24	65
500	80	0.27	0.54	10	0.0010	0.16	0.32	42	97
500	100	0.34	0.68	10	0.0018	0.20	0.40	119	121

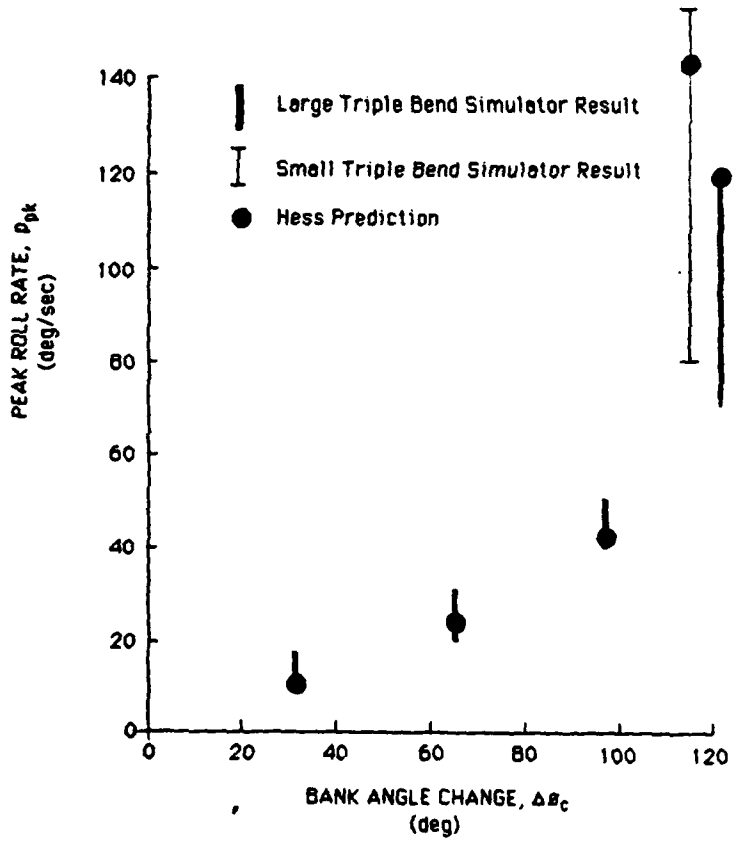

Figure 5-11. Comparison of Predicted and Simulation Data for the Triple Bend Maneuver

results reported in Reference 57. The agreement is good and suggest that at least for maneuvers where the geometry is well defined, the inner-loop maneuver performance in terms of aggressiveness and amplitude is, in turn, well defined.

Slalom Maneuvers As shown in Figure 3-18 the slalom maneuvers reported in Reference 27 are particularly representative of the roll rate limiting phenomenon. For this configuration, at least, the roll damping is high thus the attitude dynamics are rate like in the region of crossover. Based upon similar conditions Reference 59 indicated a bank angle crossover of about 2.6 rads/sec and a groundtrack (y) crossover at about 0.35 rads/sec. Referring back to the method applied to the triple bend, the peak roll rate estimate for the slalom case is about 20 degs/sec, a value close to those noted in Figure 3-18.

The above analysis shows the potential for predicting closed-loop task performance requirements based upon task definition. This approach needs to be applied to the other tasks investigated in the simulation. This method when combined with the task margin approach to handling qualities prediction has the potential to offer a closed-form analytical approach for vehicle design to handling qualities specifications.

2. Experimental

Further analysis and investigation needs to be conducted in the area of short-term response requirements. This will require further simulation, and supportive data from flight test is highly desirable. In order for simulation to provide adequate short-term response fidelity significant advances need to be made in determining the effects of computational delay and limited visual and motion cueing on task performance.

The control system type issue also needs to be addressed. No clear

indication was found in the present program for determining the appropriateness of "control response type" as a function of task. In particular the attitude-command/attitude-hold system was used for the air combat maneuvering on several occasions and was not found to be limiting. For future work, a methodology needs to be established for prescribing control response type as a function of mission. The specific topic of higher response types in unattended, high workload scenarios and in the degraded cue environment described in Reference 3 needs to be addressed.

VI. Conclusions

Closed-loop task performance can be defined in terms of the peak roll rate/ attitude change signature. Quantitative values for the maneuver amplitude and aggressiveness can be used to define the maneuver demand limits. A quantitative catalog of task performance has been compiled for a diverse set of flight tasks from nap-of-the-earth to air combat maneuvering based upon a moving base simulation program.

The fundamental dynamics governing helicopter roll response have been defined. The general response can be considered to be second order, not first order as implied by quasi-static models. A square wave input method has been used to define maximum task performance capability and clearly define the audit trail between key vehicle design parameters and closed-loop task performance. The input is suited to the demonstration of vehicle capability in the flight test environment.

The definition of task margin (the excess vehicle capability over task demand) has proven viable for integrating the concepts of short-term response and control power into a common framework. The contribution of each to closed-loop task execution has provided a unified structure for the specification of control power and short-term response handling qualities criteria. This structure is based upon closed-loop performance and is independent of the specific task involved in strict contrast to the structure proposed in the MIL-H-8501A update (Reference 3).

The simulation program allowed definition of specific numbers for the control power criteria based upon the task margin approach. For multi-loop control tasks a steady-state roll rate capability of at least 50 degs/sec is required based upon the simulation results. Simulator limitations did not provide an adequate definition of a short-term response criteria.

It has been shown that time to 30 degrees bank following full lateral control input is not a suitable maneuvering criteria. The physical significance of this parameter is dependent upon the particular dynamics involved, and the performance capability varies significantly within the class of vehicles satisfying the t_{30} requirement. The independent parameters appropriate for lateral control effectiveness criteria specification are:

- Maximum steady-state roll rate
- An open-loop bandwidth criteria based upon roll-rate rise rime for example

The theoretical work of Hess involving manual control math models, and specifically the flow-field modeling techniques for the visual scene, have potential for generic task performance modeling and aggressiveness prediction. Combination of this with the task margin approach to handling qualities prediction may offer a closed-form analytical approach for vehicle design to handling qualities specifications.

A future simulator or in-flight program is required to define the short-term response criteria. An in-flight program may be required if significant improvements cannot be made in the simulator delay effects. Additional work is also needed to address the appropriateness of control system type to task performance. The operation of higher augmentation systems in unattended, high workload scenarios and under degraded visibility conditions needs investigation.

REFERENCES

1. Anon., Military Specification, Helicopter Flying and Ground Handling Qualities; General Requirements for MIL-H-8501, 5 November 1952, (MIL-H-8501A, 7 September 1961, Amendment 1, 3 April 1962).

2. Walton, R. P. and I. L. Ashkenas, Analytical Review of Military Helicopter Flying Qualities, Systems Technology Inc., TR No. 143-1, August 1967.

3. Clement, W. F., R. H. Hoh, S. W. Ferguson, D. G. Mitchell, I. L. Ashkenas, and D. T. McRuer, Mission-Oriented Requirements for Updating MIL-H-8501, Volume 1 STI Proposed Structure, NASA CR-177331 (USAAVSCOM TR 84-A-6), January 1985.

4. Chalk, C. R. and R. C. Radford, Mission-Oriented Flying Qualities Requirements for Military Rotorcraft, Calspan Report No. 7097-F-1, January 1984.

5. Anon., Military Specification, Flying Qualities of Piloted V/STOL Aircraft, MIL-F-83300, 31 December 1970.

6. Innis, R. C., C. A. Holzhauser, and H. C. Quigley, Airworthiness Considerations for STOL Aircraft, NASA TN D-5594, January 1970.

7. Anon., Systems Specification for UTTAS, No. AMC-SS-2222-01000, December 1971.

8. Anon., Systems Specification for Advanced Attack Helicopter, No. AMC-SS-AAH-10000A, July 1973.

9. Clement, W. F. and W. F. Jewell, Piloted Simulation of Helicopter Flying Qualities in Shipboard Operations, Systems Technology Inc., TR 1198-2, forthcoming.

10. Landis, K. H. and S. I. Glusman, Development of ADOCS Controllers and Control Laws, Volume 1-3, NASA CR-177339, USAAVSCOM TR 84-A-7, March 1985.

11. Anon., Airplane Airworthiness, Civil Aeronautics Board CAR Part 04, 1 April 1941.

12. Anon., Military Specification, Flying Qualities of Piloted Airplanes, MIL-F-8785 (ASG), 1 September 1954.

13. Anon., Military Specification, Flying Qualities of Piloted Airplanes, MIL-F-8785B (ASG), 7 August 1969.

14. Hoh, Roger H., et. al., Proposed MIL Standard and Handbook - Flying Qualities of Air Vehicles. Vol II: Proposed MIL Handbook, AFWAL-TR-82-3081 Volume II, November 1982.

15. Edenborough, H. K. and K. G. Wernicke, Control and Maneuver Requirements for Armed Helicopters, Presented at the Twentieth Annual National Forum of the American Helicopter Society, Washington, D.C., May 1964.

16. McRuer, D. T. and E. S. Krendel, Mathematical Models of Human Pilot Behavior, AGARDograph No. 188, January 1974.

17. Heffley, R. K., "A Pilot-in-the-Loop Analysis of Several Kinds of Helicopter Acceleration/Deceleration Maneuvers", Helicopter Handling Qualities, NASA CP-2219, April 1982.

18. Heffley, R. K., Pilot Workload Modeling for Aircraft Flying Qualities Analysis, Manudyne Systems Inc., NADC-82094-60, 1 May 1984.

19. Key, D. L., A Critique of Handling Qualities Specifications for U.S. Military Helicopters, Paper Presented at the AIAA 7th Atmospheric Flight Mechanics Conference, Danvers, Mass., Paper No. 80-1592, August 1980.

20. Goldstein, K. W., A Preliminary Assessment of Helicopter/VSTOL Handling Qualities Specifications, NADC-81023-60, 4 November 1982.

21. Parlier, C. A., The Challenges of Maneuvering Flight Performance Testing in Modern Rotary Wing Aircraft, Presented at the 2nd Flight Testing Conference of the AIAA/AHS/IFS/SETP/SFTE/DGLR, Las Vegas, Nevada, AIAA-83-2739, November 1983.

22. Carpenter, C. G. and J. Hodgkinson, V/STOL Equivalent Systems Analysis, NADC-79141-60, May 1980.

23. Gentry, T. A., Guidance for the Use of Equivalent Systems with MIL-F-8785C, Paper presented at the AIAA 9th Atmospheric Flight Mechanics Conference, San Diego, CA, AIAA-82-1355, August 1982.

24. Pausder, H. J. and R. M. Gerdes, The Effects of Pilot Stress Factors on Handling Quality Assessments During U.S./German Helicopter Agility Flight Tests, NASA TM-84294, October, 1982.

25. Anon., AACT II Flight Test Plan, Applied Technology Laboratory, U.S. Army Research and Technology Laboratories (AVSCOM), Fort Eustis, VA, 30 June 1983.

26. Radford, R. C., D. Andrisani II, and J. L. Beilman, An Experimental Investigation of VTOL Flying Qualities Requirements for Shipboard Landings, NADC-77318-60, August 1981.

27. Corliss, L. D. and G. D. Carico, A Flight Investigation of Roll-Control Sensitivity, Damping, and Cross-Coupling in a Low-Altitude Lateral Maneuvering Task, NASA TM-84376, December 1983.

28. Wood, J. R., Comparison of Fixed-Base and In-Flight Simulation Results for Lateral High Order Systems, Paper Presented at the AIAA Atmospheric Flight Mechanics Conference, Gatlinburg, TN, MCAIR 83-021, August 1983.

29. Chen, Robert T. N., and Peter D. Talbot, An Exploratory Investigation of the Effects of Large Variations in Rotor System Dynamics Design Parameters on Helicopter Handling Characteristics in Nap-of-the-Earth Flight, Journal of the American Helicpter Society, Vol. 24, No. 3, July 1978, pp. 23-36.

30. Heffley, R. K., W. F. Clement, R. F. Ringland, W. F. Jewell, H. R. Jex, D. T. McRuer, and V. E. Carter, Determination of Motion and Visual System Requirements for Flight Training Simulators, U. S. Army Research Institute for the Behavioral and Social Sciences, TR 546, August 1981.

31. Heffley, R. K., W. F. Jewell, R. F. Whitback, and T. M. Schulman, The Analysis of Delays in Simulator Digital Computing Systems, Volume One, NASA CR-152340, February 1980.

32. Cooper, G. E. and R. P. Harper, The Use of Pilot Rating in the Evaluation of Aircraft Handling Qualities, NASA TN D-5153, April 1969.

33. Chen, R. T. N., A Simplified Rotor System Mathematical Model for Piloted Flight Dynamics Simulation, NASA TM-78575, May 1979.

34. Chen, R. T. N., Effects of Primary Rotor Parameters on Flapping Dynamics, NASA TP-1431, January 1980.

35. Talbot, P. D., B. E. Tinling, W. A. Decker and R. T. N. Chen, A Mathematical Model of a Single Main Rotor Helicopter for Piloted Simulation, NASA TM-84281, September 1982.

36. Heffley, R. K., W. F. Jewell, J. M. Lehman, and R. A. Van Winkle, A Compilation and Analysis of Helicopter Handling Qualities Data, Volume 1: Data Compilation, NASA CR-3144, August 1979.

37. Heffley, R. K., A Compilation and Analysis of Helicopter Handling Qualities Data, Volume 2: Data Analysis, NASA CR-3145, August 1979.

38. Chen R. T. N. and W. S. Hindson, Analytical and Flight Investigation of the Influence of Rotor and Other High-Order Dynamics on Helicopter Flight-Control Bandwidth, Presented at the First Annual Forum of the International Conference on Basic Rotorcraft Research, Triangle Park, NC, February 1985.

39. Heffley, R. K., T. M. Schulman, R. J. Randle, Jr., and W. F. Clement, An Analysis of Airline Landing Data Based on Flight and Training Simulator Measurements, Systems Technology, Inc., Technical Report 1172-1, July 1981.

40. Anon., Military Specification, Flying Qualities of Piloted Airplanes, MIL-F-8785C, August 1969.

41. Anon., V/STOL Handling, AGARD-R-577, June 1973.

42. Anon., Air-to-Air Combat, Headquarters Department of the Army Field Manual, FM1-107, October 1984.

43. Wolfrom, J. A., Data Presentation From Air-to-Air Combat Maneuvering Between an OH-58A and an S-76, USAAVSCOM TM-84-D-6, February 1985.

44. Monagan, S. J., R. E. Smith, and R. E. Bailey, Lateral Flying Qualities of Highly Augmented Fighter Aircraft, AFWAL-TR-81-3171, June 1982.

45. Lewis, M.S., "A Piloted Simulation of One-on-One Helicopter Air Combat at NOE Flight Levels", Proceedings of the 41st Annual Forum of the American Helicopter Society, May 1985.

46. Hilbert, K. B., A Mathematical Model of the UH-60 Helicopter, NASA TM-85890, April 1984.

47. Cooper, D. E., "YUH-60A Stability and Control", Journal of the American Helicopter Society, Vol. 24, No. 3, July 1978, pp. 2-9.

48. Hoh, R. H., and I. L. Ashkenas, Development of VTOL Flying Qualities Criteria for Low Speed and Hover, Systems Technology Inc., TR 1116-1, September 1979.

49. Paulk, C. H. Jr., D. L. Astill, and S. T. Donley, Simulation and Evaluation of the SH-2F Helicopter in a Shipboard Environment Using the Interchange Cab System, NASA TM-84387, August 1983.

50. Anon., RUNDUM, NASA-Ames Program Specification, NAPS-103, July 1982.

51. Berry, D. T., In-Flight Evaluation of Pure Time Delays in Pitch and Roll, Paper Presented at the AIAA Guidance, Navigation and Control Conference, Snowmass, CO, 85-1852, August 19-21, 1985.

52. Johnston, D. E., and D. T. McRuer, Investigation of Limb-Sidestick Dynamic Interaction with Roll Control, Paper Presented at the AIAA Guidance, Navigation and Control Conference, Snowmass, CO, 85-1853, August 19-21, 1985.

53. Smith, R. H., A Theory for Handling Qualities with Application to MIL-F-8785B, AFFDL-TR-119, 1976.

54. McDonnell, J. D., Pilot Rating Techniques for the Estimation and Evaluation of Handling Qualities, AFFDL-T-68-76, December 1968.

55. Ashkenas, I. L. and D. T. McRuer, The Determination of Lateral handling Quality Requirements from Airframe-Human Pilot System Studies, STI TR 59-135, June 1959.

56. Seckel. E, J. A. Franklin and G. E. Miller, Lateral-Directional Flying Qualities for Power Approach: Influence of Dutch Roll Frequency, Princeton University Report No. 797, September 1967.

57. Tomlinson, B. M. and G. D. Padfield, Piloted Simulation Studies of Helicopter Agility, Vertica, Vol. 4., Nos. 2-4, 1980.

58. Hess, R. A., A Model-Based Theory for Analyzing Human Control Behavior, to appear in Advances in Man-Machine Systems, Vol 2, JAI Press Inc., Greenwich, Conn., 1985.

59. Hess, R. A. and A. Beckman, An Engineering Approach to Determining Visual Information Requirements for Flight Control Tasks, IEEE Transactions on Systems, Man and Cybernetics, Vol. SMC-14, No. 2, March-April 1984, pp. 286-298.

60. Hess, R. A. and J. Sunyoto, Toward A Unifying Theory for Aircraft Handling Qualities, AIAA Paper No. 84-0236, January 1984.

A172 111

1. Report No. USAAVSCOM TR-85-A-5 NASA CR 177404	2. Government Accession No.	3. Recipient's Catalog No.
4. Title and Subtitle STUDY OF HELICOPTER ROLL CONTROL EFFECTIVENESS CRITERIA		5. Report Date April 1986 6. Performing Organization Code
7. Author(s) Robert K. Heffley, Simon M. Bourne, Howard C. Curtiss, Jr., William S. Hindson, Ronald A. Hess		8. Performing Organization Report No. Manudyne Report 83-1 10. Work Unit No.
9. Performing Organization Name and Address Manudyne Systems, Inc. 349 First Street Los Altos, CA 94022		11. Contract or Grant No. NAS2-11665
12. Sponsoring Agency Name and Address Aeroflightdynamics Directorate, U.S. Army Research and Technology Activity - AVSCOM, Ames Research Center, Moffett Field, CA 94035		13. Type of Report and Period Covered Final Report 7-83 to 7-85 14. Sponsoring Agency Code 1L162209AH76A

15. Supplementary Notes

POINT OF CONTACT: Michelle M. Eshow, Aeroflightdynamics Directorate, M.S. 211-2, Ames Research Center, Moffett Field, CA 94035 (415) 694-5272, FTS 464-5272

16. Abstract

A study of helicopter roll control effectiveness based on closed-loop task performance measurement and modeling is presented. Roll control criteria are based upon task margin, the excess of vehicle task performance capability over the pilot's task performance demand. Appropriate helicopter roll axis dynamic models are defined for use with analytic models of task performance. Both near-earth and up-and-away large-amplitude maneuvering phases are considered. The results of in-flight and moving-base simulation measurements are presented to support the roll control effectiveness criteria offered. Volume I contains the theoretical analysis, simulation results and criteria development. Volume II documents the simulation program hardware, software, protocol and data collection efforts.

17. Key Words (Suggested by Author(s))

Helicopter, rotorcraft, design criteria, stability and control, handling qualities, flying qualities, MIL-H-8501A, roll control, control effectiveness, pilot-in-the-loop, manual control, simulation.

18. Distribution Statement

Unlimited.

Subject Category 08

19. Security Classif. (of this report)	20. Security Classif. (of this page)	21. No. of Pages	22. Price*
Unclassified.	Unclassified.	257	

*For sale by the National Technical Information Service, Springfield, Virginia 22161

END

10-86

DTIC